UNIVERSIDADE FEDERAL DE SANTA CATARINA
CENTRO TECNOLÓGICO
PROGRAMA DE PÓS-GRADUAÇÃO EM ENGENHARIA CIVIL

Matheus Silva Gonçalves

Contributions to bridge weigh-in-motion systems

Florianópolis

2022

Matheus Silva Gonçalves

Contributions to bridge weigh-in-motion systems

Tese submetida ao Programa de Pós-Graduação em Engenharia Civil da Universidade Federal de Santa Catarina para a obtenção do título de Doutor em Engenharia Civil.
Orientador: Prof. Rafael Holdorf Lopez, Dr.
Coorientador: Prof. Elder Oroski, Dr.

Florianópolis
2022

Matheus Silva Gonçalves

Contributions to bridge weigh-in-motion systems

O presente trabalho em nível de doutorado foi avaliado e aprovado por banca examinadora composta pelos seguintes membros:

Prof. Túlio Nogueira Bittencourt, Dr.
Poli-USP

Prof. José Eduardo Souza de Cursi, Dr.
INSA Rouen

Prof. Tiago Morkis Siqueira, Dr.
UFSC

Prof. Paulo Junges, Dr.
UFMT

Certificamos que esta é a **versão original e final** do trabalho de conclusão que foi julgado adequado para obtenção do título de Doutor em Engenharia Civil.

_____
Coordenação do Programa de Pós-Graduação

_____
Prof. Rafael Holdorf Lopez, Dr.
Orientador

Florianópolis, 2022.

AGRADECIMENTOS

Em primeiro lugar, agradeço à minha família, por sempre me apoiar em cada passo que dou. Vocês são sempre minha maior motivação. Também deixo um agradecimento especial aos meus amigos, por estarem sempre comigo. Obrigado por, mesmo nos momentos mais difíceis, nunca terem deixado eu sentir que estava sozinho.

Agradeço aos professores, técnicos e todos os trabalhadores cuja dedicação foi essencial para que eu pudesse concluir minha formação. Afinal, tudo que conquistamos é fruto de um esforço coletivo. Nesse ponto, gostaria de fazer um agradecimento especial a todos os professores por trabalharem todos os dias, muitas vezes em situações precárias, para que avancemos como sociedade. Em particular, agradeço aos professores que fizeram parte da minha formação, desde a alfabetização até hoje. Devo grande parte do que sou hoje a vocês.

Agradeço a todos que, mesmo indiretamente, possibilitaram que eu pudesse estudar em uma universidade pública de excelência. Podem ter certeza que trabalharei para que mais pessoas tenham acesso às oportunidades que tive.

RESUMO

Pontes são estruturas importantes para possibilitar o funcionamento adequado de sistemas de transporte ao redor do mundo. Essas estruturas permanecem ao longo de toda sua vida útil sob efeito direto de condições ambientais, o que acelera sua degradação e aumenta as incertezas relacionadas ao seu desempenho. Essas incertezas são ainda maiores em cenários em que faltam informações confiáveis quanto às suas propriedades estruturais. Além disso, tanto volume quanto cargas dos veículos estão continuamente crescendo ao longo dos anos, além da presença de veículos acima do limite legal de peso. Esse contexto gera grandes desafios para pontes, principalmente aquelas mais antigas. Sistemas *Bridge weigh-in-motion* (B-WIM) são ferramentas poderosas para fornecer informações valiosas nesse tema. Sistemas B-WIM permitem estimar o peso dos eixos de veículos enquanto eles trafegam sobre a ponte em velocidade normal. Em especial, esses sistemas podem ajudar na fiscalização de limites legais de peso, o que é uma tarefa importante para controlar o nível de solicitação da estrutura. No entanto, a acurácia das estimativas reportadas por sistemas B-WIM ainda não atingiu o patamar necessário para fiscalizar diretamente os limites legais de peso, principalmente para peso por eixo, persistindo a necessidade de utilizar balanças estáticas para confirmação. O objetivo deste estudo é contribuir para a tecnologia B-WIM e a melhoria do nível de acurácia nas estimativas de peso é abordada. Primeiramente, um algoritmo B-WIM que inclui um modelo dinâmico simplificado do comportamento da ponte devido à passagem de veículos pesados é derivado. Ele difere dos métodos utilizados atualmente, que se baseiam em suposições de comportamento estático, porém mantendo um custo computacional similar. Então, um algoritmo B-WIM que inclui expectativas prévias quanto aos valores de peso por eixo a partir de uma formulação Bayesiana é proposto. Ele utiliza um modelo autoregressivo de segunda ordem (AR(2)) para modelar o erro entre respostas estimadas e medidas que evita a suposição de independência geralmente empregada. Um segundo ponto que é abordado neste trabalho é a dificuldade em se avaliar a real condição de pontes. Assim, propõe-se utilizar os dados coletados durante a calibração de um sistema B-WIM para realizar atualização de modelo para parâmetros estruturais da ponte. É importante salientar que parâmetros estruturais podem apresentar uma variabilidade inerente entre diferentes passagens de veículos de calibração devido a fatores externos, como condições climáticas. Dessa forma, visando uma melhor predição das incertezas relacionadas, um modelo Bayesiano hierárquico é aplicado. Os resultados relacionados com o processo de estimação de peso indicam que ambas as abordagens propostas foram capazes de atingir melhores resultados para as situações analisadas do que os algoritmos B-WIM estáticos geralmente empregados. Os melhores desempenhos foram observados para a estratégia Bayesiana com modelo AR(2) quando estimando peso por eixo. A estratégia de atualização de modelo Bayesiana hierárquica proposta também foi capaz de atingir seu objetivo, fornecendo estimativas semelhantes mesmo quando utilizando dados produzidos por veículos diferentes no processo de estimação. Apesar dos resultados serem obtidos para um conjunto limitado de exemplos, eles indicam que as abordagens propostas são promissoras e podem ser implementadas na prática para confirmar essas conclusões.

Palavras-chave: Pesagem em movimento em pontes. Linha de influência de pontes. Estimação de peso de veículos. Identificação de peso de veículos. Inferência Bayesiana. Fiscalização de excesso de peso. Atualização de modelo Bayesiana hierárquica.

RESUMO EXPANDIDO

Introdução
O sistema de transportes brasileiro é muito dependente do sistema rodoviário, visto que mais de 60% do transporte de cargas e 90% dos deslocamentos de passageiros são realizados por rodovias (CNT / SEST SENAT, 2018). Pontes são elementos fundamentais para o funcionamento desses sistemas, fornecendo maneiras de transpor obstáculos como rios, vales e estradas. Em um trabalho recente, Lima e Oliveira, Greco, and Bittencourt (2019) analisaram um banco de dados de milhares de pontes brasileiras, obtendo uma idade média de cerca de 40 anos para aquelas cuja idade estava disponível. Os autores também concluíram que cerca de metade das pontes analisadas estão atualmente sob alto volume de tráfego pesado. No geral, as pontes brasileiras foram projetadas em um cenário onde tanto o volume de tráfego quanto as cargas eram bastante diferentes do atual.

Veículos com sobrepeso são um dos principais pontos a serem resolvidos para melhorar a segurança do tráfego em geral (XU et al., 2016). Eles geram problemas como alto impacto na durabilidade da infraestrutura e deterioração da segurança da via (JACOB; FEYPELL-DE LA BEAUMELLE, 2010). Falando especificamente de pontes, veículos com sobrepeso foram responsáveis por mais de 40 colapsos de pontes durante o período de 1989 a 2000, apenas nos Estados Unidos (DENG; WANG, W.; YU, 2016). Logo, percebe-se que, independentemente do procedimento adotado para projetar e construir pontes, se veículos com sobrepeso não forem adequadamente controlados, a segurança da estrutura não pode ser efetivamente garantida (XU et al., 2016). A fiscalização de limites legais de peso é uma maneira reconhecidamente efetiva de diminuir os problemas induzidos por esses veículos (DENG; WANG, W.; YU, 2016). Por exemplo, o trabalho de Otto et al. (2019) mostrou que, para uma única seção monitorada, o percentual de veículos com sobrepeso cresceu 87% em apenas um ano sem fiscalização.

Outro ponto relevante é o processo de degradação ao qual pontes estão sujeitas devido à influências climáticas e ambientais durante toda sua vida útil. Esse processo é bastante complexo e envolve diversos efeitos diferentes (FRANGOPOL; LIU, 2007). Como consequência, as incertezas relacionadas ao comportamento estrutural da ponte aumentam com o passar do tempo (LANTSOGHT et al., 2017). No pior dos casos, a maior dificuldade em se avaliar a condição da estrutura pode levar a falta de manutenção, o que é uma importante causa de falhas em pontes (XU et al., 2016). É importante destacar que, para o cenário brasileiro, essa tarefa é ainda mais complexa devido a falta de informações disponíveis para muitas pontes (LIMA E OLIVEIRA; GRECO; BITTENCOURT, 2019).

Sistemas *Bridge weigh-in-motion* (B-WIM) são ferramentas importantes para ajudar na avaliação da segurança de pontes. Esses sistemas surgiram a partir do trabalho de Moses (1979), onde o peso dos veículos é obtido a partir do conhecimento das deformações induzidas e da linha de influência. Para os sistemas atuais, a linha de influência da ponte é obtida experimentalmente a partir das deformações geradas por veículos com características conhecidas. Esse processo é chamado de calibração. As informações fornecidas por esses sistemas têm muitas aplicações como seleção de veículos com sobrepeso (MANDIĆ IVANKOVIĆ et al., 2019) e avaliação de indicadores de desempenho de pontes (ŽNIDARIČ; KALIN, 2020).

Para algumas aplicações específicas, como a fiscalização direta dos limites de peso, as estimati-

vas de sistemas B-WIM ainda não atingiram o nível de acurácia necessário. Diversas instalações B-WIM atingiram desempenho suficiente apenas para pré-seleção de veículos, restando a necessidade de utilizar balanças estáticas para confirmação (RICHARDSON et al., 2014). Nesse contexto, um problema bem conhecido em sistemas B-WIM é que o nível de acurácia obtido para peso por eixo é menor quando comparado a estimativas de peso bruto total (HE et al., 2019; O'BRIEN et al., 2018; RICHARDSON et al., 2014; O'BRIEN et al., 2009). No entanto, mesmo para estimativas de peso bruto total, atingir o nível de acurácia requerido ainda é raro (ŽNIDARIČ; KALIN; KRESLIN, 2018).

Objetivos

O objetivo geral deste trabalho é contribuir para o desenvolvimento de sistemas B-WIM cada vez mais eficientes. Para atingir esse objetivo, dois pontos em específico são abordados por serem considerados os mais promissores, principalmente quando considerando o contexto brasileiro. O primeiro ponto é a melhoria do nível de acurácia das estimativas de peso feitas por sistemas B-WIM, principalmente referentes ao peso por eixo. Como a fiscalização direta dos limites legais de peso por sistemas B-WIM ainda não foi atingida em campo, este tópico permanece como um problema em aberto. O segundo ponto julgado como importante é uma combinação entre falta de informações para muitas pontes e alto nível de incertezas quanto ao desempenho de pontes devido ao processo de degradação que ocorre durante a vida útil delas. Esse ponto é especialmente importante para muitas pontes brasileiras para as quais os projetos não estão mais disponíveis.

Metodologia

O primeiro ponto a ser comentado aqui é o desenvolvimento de algoritmos para pesagem em sistemas B-WIM que busquem uma melhora na acurácia das estimativas. Foram desenvolvidas duas abordagens com esse objetivo, ambas baseadas em sugestões feitas no trabalho de Carraro et al. (2019), que proporciona uma visão geral da literatura no tema. A primeira inclui considerações da resposta dinâmica da estrutura nas predições B-WIM. Já a segunda utiliza expectativas prévias quanto aos valores de peso por eixo para auxiliar o processo de estimação.

Os algoritmos B-WIM utilizados atualmente e que foram analisados em Carraro et al. (2019) se baseiam em suposições estáticas apenas. No entanto, a resposta de uma ponte à passagem de um veículo pesado tem efeitos dinâmicos importantes e levá-los em conta é uma opção promissora para melhorar estimativas de peso. Logo, esse trabalho apresenta um algoritmo B-WIM que emprega um modelo dinâmico simplificado para o sistema veículo-ponte, que pode ser encontrado também em Gonçalves, Carraro, and Lopez (2021a). A principal contribuição desse método é a definição de um algoritmo com custo computacional similar quando comparado aos métodos estáticos atualmente utilizados (i.e., baseados apenas em poucas operações matriciais), no entanto que também inclui o efeito da resposta dinâmica. Esse algoritmo é uma extensão do trabalho de Ning-Bo Wang et al. (2017), que focou na extração da componente estática da linha de influência da ponte para um único evento de calibração. No presente trabalho, esse método foi modificado para permitir a consideração de múltiplos eventos de calibração a partir da utilização do método de maximização da verossimilhança (IENG, 2015). Ainda, a resposta dinâmica completa foi utilizada para calcular uma linha de influência paramétrica que inclui a velocidade do veículo como um parâmetro do modelo e as equações utilizadas para estimação de peso foram derivadas. Vale destacar que a velocidade é considerada constante ao longo da passagem do veículo. O método proposto fornece linhas de influência que se adequam melhor ao comportamento esperado para tais curvas (i.e., curvas contínuas ao invés de estimativas

pontuais (ŽNIDARIČ; KALIN; KRESLIN, 2018)). Essa característica deve também melhorar a capacidade de generalização do método. Como menos parâmetros são ajustados, a probabilidade de que a linha de influência extraída incorpore padrões específicos da resposta do veículo de calibração é reduzida. Ademais, a utilização da velocidade do veículo como um parâmetro do modelo é uma tentativa de modelar um efeito conhecido referente à dependência da resposta do veículo a esse parâmetro (O'BRIEN; GONZÁLEZ; DOWLING, 2010).

Outro ponto abordado referente à estimação de peso de veículos por sistemas B-WIM está relacionado à baixa acurácia geralmente reportada para previsões de peso por eixo quando comparadas as estimativas de peso bruto total. Até mesmo previsões claramente irreais, como peso por eixo negativo, podem ser observadas. Visando superar esse problema, o presente trabalho apresenta um algoritmo de pesagem Bayesiano que leva em conta expectativas prévias para os valores de peso por eixo para guiar as estimativas em direção a valores plausíveis (GONÇALVES et al., 2022). A utilização dessa expectativa prévia é justificada pelo fato de que o peso por eixo de veículos pesados não apresenta uma amplitude de variações tão extensa (i.e., é irreal imaginar peso por eixo acima de 20 toneladas ou abaixo de zero, por exemplo). A abordagem mais comum quando utilizando estratégias Bayesianas é assumir que os erros entre respostas estimadas e medidas são independentes, como no trabalho de Yoshida, Sekiya, and Mustafa (2021). Um ponto problemático importante notado ao longo da derivação do método proposto, no entanto, está relacionado à presença de resíduos fortemente autocorrelacionados. Essa autocorrelação tem um efeito indesejado para predições Bayesianas, visto que a importância da *likelihood* é artificialmente aumentada, reduzindo a importância da distribuição *prior*. Logo, em contraste com as estratégias usuais, no método proposto a suposição de independência é evitada a partir da utilização de um processo autoregressivo de segunda ordem (AR(2)) para modelar o erro supracitado.

A motivação para estudar também um tópico referente à avaliação de propriedades estruturais de pontes a partir de dados de calibração para sistemas B-WIM é a falta de informações observada para pontes brasileiras (LIMA E OLIVEIRA; GRECO; BITTENCOURT, 2019), onde mesmo parâmetros básicos (e.g., a idade exata da ponte) podem não ser conhecidos. Percebeu-se que o procedimento de calibração empregado para sistemas B-WIM gera um grande volume de informações, que pode ser utilizado para aumentar o grau de conhecimento relacionado ao comportamento estrutural da ponte. De fato, as informações coletadas durante esse processo podem ser interpretadas como testes dinâmicos para diagnóstico de pontes (OLASZEK; ŁAGODA; CASAS, 2014).

No presente trabalho, uma estratégia para atualização de modelo que utiliza os dados comentados anteriormente é proposta (GONÇALVES; LOPEZ; VALENTE, 2022). Um importante aspecto a se salientar é que esses dados provavelmente apresentam uma variabilidade inerente, em que o valor para a quantidade de interesse pode variar ao longo do processo de calibração. Essa variação pode ser melhor entendida quando relembrando que pontes estão diretamente sob influência de condições climáticas ao longo de toda sua vida útil e, então, não há controle completo sobre todas as características que afetam a resposta da ponte (e.g., temperatura, velocidade do vento) durante a calibração. Portanto, a abordagem proposta utiliza um modelo Bayesiano hierárquico que pode lidar com essa variabilidade inerente, como observado em estudos anteriores em diferentes sistemas estruturais (BEHMANESH; MOAVENI, 2016; KWAG; JU, 2020; SONG, M. et al., 2019). Essa estratégia proporciona uma melhor estimativa das incertezas totais relacionadas aos parâmetros de interesse do que aquela obtida a partir de

métodos Bayesianos clássicos (SEDEHI; PAPADIMITRIOU; KATAFYGIOTIS, 2019). Como resultado, permite-se que o procedimento de instalação e calibração de sistemas B-WIM possa ser usado para atender duas demandas distintas: efetivamente calibrar o sistema e avaliar parâmetros estruturais da ponte.

Resultados e Discussão

Para o algoritmo de pesagem com considerações quanto aos efeitos dinâmicos, três implementações distintas foram avaliadas, de acordo com as suposições feitas para o cálculo dos parâmetros do modelo: *Standard* (aproximação estática + flutuação, análogo a Ning-Bo Wang et al. (2017)), *Analytical* (quasi-estática + flutuação) e *Static* (aproximação estática apenas). As simulações numéricas utilizadas incluíram pontes com comprimentos variando de 10 a 30 metros, diferentes perfis de pavimento e veículos de teste distintos daqueles utilizados para calibração. Foram avaliados também: método da matriz (O'BRIEN; QUILLIGAN, M. J.; KAROUMI, 2006); pBWIM (O'BRIEN et al., 2018) com a implementação proposta por Gonçalves, Carraro, and Lopez (2021b); maximização da verossimilhança (IENG, 2015) e regularização (O'BRIEN et al., 2009). As estimativas para ambos os métodos *Analytical* e *Static* foram capazes de superar o erro médio absoluto reportado por todos os outros métodos avaliados. A principal diferença ocorre para pontes de 30 metros, em que o método *Analytical* apresenta um desempenho destacado. É importante notar que tais resultados ocorreram mesmo considerando que as propriedades dinâmicas da ponte não eram precisamente conhecidas previamente, indicando que a abordagem proposta é também robusta. Outro aspecto interessante de se observar é que o método *Analytical* removeu uma grande parte do enviesamento presente no erro médio absoluto devido à velocidade do veículo. Isso é um resultado direto da inclusão da velocidade do veículo como um parâmetro do modelo, que permite que um mesmo veículo induza diferentes respostas estruturais de acordo com essa velocidade. Os resultados para ambos os métodos *Static* e *Analytical* indicam que eles atingiram seus objetivos, principalmente para pontes mais longas. Apesar dos resultados para o método *Analytical* apresentarem robustez, tal método não irá desempenhar adequadamente se nenhuma estimativa para as propriedades da ponte estiver disponível. Nesse caso, pode-se empregar o método *Static* que deve ainda apresentar melhores resultados para veículos diferentes daqueles utilizados para calibração.

Já a abordagem de pesagem Bayesiana com modelo AR(2) foi avaliada tanto em sinais simulados quanto em um exemplo real de calibração de um sistema B-WIM, analisando também predições fora da amostra (i.e., veículos de teste diferentes daqueles utilizados para calibrar o sistema). Os resultados foram comparados com a solução por mínimos quadrados e por regularização com parâmetros aproximadamente ótimos. O segundo método pode ser visto com um exemplo de excelente desempenho, no entanto a estratégia aproximadamente ótima utilizada para selecionar o parâmetro de regularização não é reprodutível na prática (visto que se baseia no valor real dos pesos por eixo de cada veículo). Além disso, quatro variantes da abordagem Bayesiana proposta foram testadas, visando verificar a influência tanto da distribuição *prior* utilizada quanto do modelo para o termo de erro nos resultados. Por fim, como a definição da distribuição *prior* é em certo grau subjetiva, análises de sensibilidade também foram realizadas a partir da avaliação dos resultados para combinações diferentes de parâmetros para a distribuição *prior*. Os resultados indicaram que a abordagem proposta foi capaz de evitar estimativas espúrias como peso por eixo negativo, como pretendido. Ademais, o nível de acurácia atingido superou, no geral, aquele obtido pelos outros algoritmos analisados, mesmo considerando cenários que não se ajustam bem às expectativas iniciais definidas pela distribuição *prior* (e.g., peso por eixo claramente acima do valor médio da distribuição *prior*) e a utilização

de parâmetros de regularização obtidos a partir do conhecimento do peso real dos veículos. Os resultados são ainda melhores quando avaliamos as predições de peso por eixo, onde classes de acuracidade similares àquelas obtidas para peso bruto total foram atingidas. Além disso, as afirmações referentes à importância de modelar os erros autocorrelacionados se confirmaram. As estimativas Bayesianas sem a utilização do modelo AR(2) foram bastante similares às soluções obtidas pelo método dos mínimos quadrados, praticamente desconsiderando a informação fornecida pela distribuição *prior*. Assim, a distribuição *prior* proposta, baseada em valores esperados em aplicações práticas para o peso por eixo, necessita ser utilizado em conjunto com o modelo AR(2) para efetivamente melhorar os resultados. As análises de sensibilidade confirmaram a robustez da abordagem proposta quanto à definição da distribuição *prior*. Isso já era esperado visto que a amplitude de valores para os parâmetros dessa distribuição, capaz de cobrir pesos por eixo esperados na prática, não é tão abrangente. Isso é, de fato, a maior vantagem prática do método proposto. A distribuição *prior* tem uma clara correspondência com quantidades que são habituais para quem opera um sistema B-WIM, o que permite uma boa base para a definição dessa distribuição.

A estratégia Bayesiana hierárquica de atualização de modelo também foi avaliada utilizando sinais simulados, incluindo exemplos simplificados para ilustrar as vantagens da estratégia hierárquica, e um exemplo real de dados de calibração de um sistema B-WIM. As estimativas para sinais simulados se aproximaram bastante dos valores verdadeiros conhecidos para todos os parâmetros analisados. Em especial, o método foi capaz de estimar adequadamente as incertezas da quantidade de interesse, que é o maior objetivo em se utilizar uma estratégia hierárquica. É importante destacar que tais resultados foram confirmados utilizando uma quantidade de dados compatível com o coletado em situações práticas de calibrações de sistemas B-WIM e considerando individualmente os dados gerados por cada veículo. A última afirmação é importante visto que apenas poucos veículos são geralmente utilizados na calibração e é importante que os resultados não sejam excessivamente dependentes das características específicas de tais veículos. Quando avaliando os dados referentes ao exemplo real de calibração, os resultados também são interessantes. Nesse caso, as diferenças entre estimativas feitas utilizando dados de veículos distintos é maior do que para os sinais simulados, no entanto os resultados ainda são consistentes. Como dados reais são mais complexos, esse comportamento já era esperado. Além disso, as análises de propagação de incertezas foram capazes de prever adequadamente a resposta para os dois veículos utilizados. Todas as análises indicam que tal abordagem é promissora e capaz de fornecer informações úteis, principalmente num contexto de falta de informações básicas. Apesar do modelo simplificado utilizado, esse trabalho fornece uma fundamentação inicial para auxiliar no desenvolvimento de modelos que permitam uma melhor avaliação da segurança de estruturas.

Considerações Finais
O presente trabalho destacou a importância prática de sistemas B-WIM, indicando também possíveis caminhos para lidar com a falta de informação observada para muitas pontes brasileiras. Após discutir as abordagens propostas, é possível afirmar que o objetivo dessa tese foi atingido. Ela forneceu contribuições relevantes para aplicações de sistemas B-WIM em geral, sendo uma pequena parte na contínua evolução da tecnologia B-WIM.

Palavras-chave: Pesagem em movimento em pontes. Linha de influência de pontes. Estimação de peso de veículos. Identificação de peso de veículos. Inferência Bayesiana. Fiscalização de excesso de peso. Atualização de modelo Bayesiana hierárquica.

ABSTRACT

Bridges are important structures for the proper operation of transportation systems around the world. These structures remain over all their life-cycle under direct influence of environmental conditions, which accelerates their structural degradation and increases uncertainties related to their performance. These uncertainties are even higher for scenarios in which there is a lack of reliable information related to their structural properties. Furthermore, traffic volume and vehicle loads are continuously increasing over the last decades, which also includes the presence of vehicles over the accepted weight limits. This scenario leads to a high challenge for bridge structures, mainly the older ones. Bridge weigh-in-motion (B-WIM) systems are powerful tools for providing valuable information in this regard. B-WIM systems allow the estimation of axle weights for vehicles of the traffic flow whereas they travel over the bridge at their normal speeds. In particular, it can help in the enforcement of legal weight limits, which is important for controlling the applied loads. However, the accuracy of weight predictions reported by current B-WIM systems still has not achieved the required level for direct enforcement of legal weight limits, mainly when analyzing axle weights individually, remaining the necessity to employ static scales to check it. The goal of the present work is contributing to B-WIM technology and the improvement of accuracy level of such weight estimates is addressed. First, a B-WIM algorithm that includes simplified dynamic modeling of the bridge behavior due to the passage of heavy vehicles is derived. It differs from current employed methods, which rely on static assumptions, however keeping a similar computational cost. Then, a B-WIM algorithm that includes prior beliefs regarding the conventional values of axle weights by means of a Bayesian formulation is proposed. It utilizes a second order autoregressive (AR(2)) process for modeling the error between measured and predicted responses that avoids the usually employed independence assumption. A second issue that is addressed in the present work is the difficulty to assess real bridge conditions. Then, the data collected for calibrating the B-WIM systems is employed to perform model updating of bridge structural parameters. It is important to remark that structural parameters may present an inherent variability among the passage of each calibration vehicle due to external factors, such as environmental conditions. Therefore, in order to better predict related uncertainties, a hierarchical Bayesian framework is applied. The results related to the weight estimation process indicate that both proposed approaches are able to reach better results than the usually applied static B-WIM algorithms for the analyzed situations. The main achievements are noticed for the Bayesian strategy with AR(2) model when estimating individual axle weights. The proposed hierarchical Bayesian model updating strategy was also able to reach its goal, providing consistent estimates. Although the results were obtained for a limited set of examples, such results indicate that the proposed approaches are promising and could be implemented in practice for further assessing their effectiveness.

Keywords: Bridge weigh-in-motion. Bridge influence line. Vehicle weight estimation. Vehicle weight identification. Bayesian inference. Overweight enforcement. Hierarchical Bayesian model updating.

LIST OF SYMBOLS (CHAPTERS 1 AND 2)

$\boldsymbol{m}_g$	measured bending moment response vector of the g-th girder
E	elastic modulus of bridge girders
Z	section modulus of bridge girders
$\boldsymbol{u}_g$	measured strain vector of the g-th girder
G	total number of girders
$\boldsymbol{M}$	measured bending moment response vector
$\widehat{\boldsymbol{M}}$	theoretical bending moment response vector
J	vehicle number of axles
d_j	distance between first and j-th axle
C_j	number of scans between first and j-th axle
f	sampling frequency
v	vehicle speed
$\boldsymbol{IL}$	influence line ordinates vector
R	error function
K	total number of scans
$\boldsymbol{A}$	matrix of axle weights
$\boldsymbol{W}$	vector of axle weights
$\boldsymbol{\Lambda}$	matrix of influence line ordinates

CONTENTS

1 INTRODUCTION

The Brazilian logistic system is highly dependent on road traffic, since more than 60% of the cargo transport and 90% of passenger travels are carried out across roads (CNT / SEST SENAT, 2018). Bridges are key elements for its practical applicability, providing ways to overcome obstacles such as rivers, valleys or roads. In a recent work, Lima e Oliveira, Greco, and Bittencourt (2019) analyzed a dataset regarding hundreds of Brazilian bridges and reported an average age of about 40 years for those whose age were available (for a high number of bridges this information is not exactly known). Besides this, they also concluded that approximately half of the analyzed bridges are currently under high levels of heavy vehicles traffic. The tendency observed for the Brazilian truck fleet is also an important information in this regard, which helps to illustrate the increasing level of loads over such bridges. Figure 1 presents the number of trucks traveling across Brazilian roads, in which a continuous growth is noticed. In particular, it is seem that the number of trucks in Brazil increased by nearly 60% in 15 years. All the previously discussed indicates that the majority of Brazilian bridges was designed in a scenario where both traffic volume and truck loads were considerably distinct from what is observed nowadays.

Figure 1 – Number of trucks in Brazil from 2006 to 2020
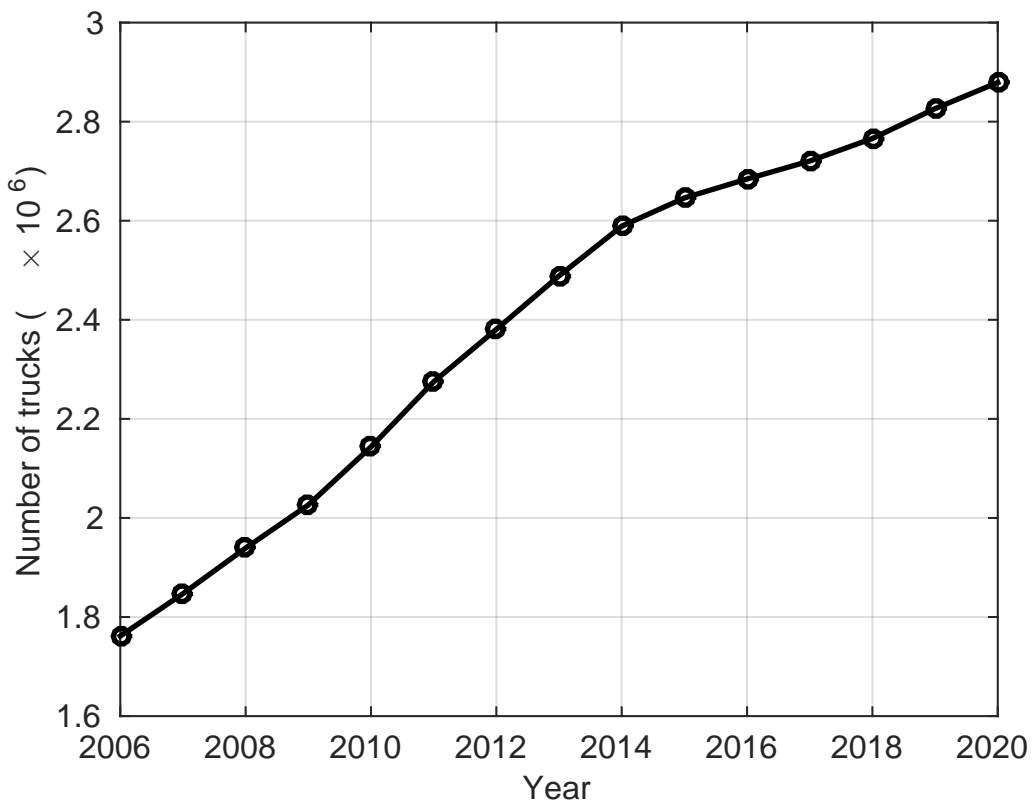
Source: IBGE (2020)

When analyzing manners to improve the safety of road traffic in general, it is noticed

Figure 2 – Bridge collapse due to overloaded vehicle

Source: Deng, Wei Wang, and Yu (2016)

that overloaded vehicles are one of the main issues to be solved (XU et al., 2016). Among the troubles induced by overloaded vehicles, one could cite the high effect on the durability of infrastructure, deterioration of road safety and increasing on risks for the own road users (JACOB; FEYPELL-DE LA BEAUMELLE, 2010). For instance, Blower and Woodrooffe (2012) reported that about 60% of trucks involved in crashes in Brazil were overloaded. This high percentage is due to more likely mechanical failures and loss of control in vehicles under such a condition. When observing the scenario for bridge structures in particular, it is noticed that overloaded vehicles were responsible for more than 40 bridge collapses during the period between 1989 and 2000 only in the United States (DENG; WANG, W.; YU, 2016). To illustrate this comment, Figure 2 shows a bridge collapse attributed to the passage of an overloaded vehicle. Therefore, independently of the procedure applied for designing and building bridges, if overloaded vehicles are not properly controlled, the safety of the structure cannot be effectively ensured (XU et al., 2016).

The enforcement of vehicle weight regulations is acknowledged as an effective way to decrease the problems induced by overloaded vehicles (DENG; WANG, W.; YU, 2016). Although the importance of respecting such limits, in many locations the usual traffic flow usually contains a considerable number of vehicles that violate these regulations. For the Brazilian context, the work of Otto et al. (2019) showed that, even with enforcement of legal weight limits, the percentage of overloaded vehicles in the usual traffic flow were about 6.5%. This same work noticed that the situation quickly worsened when this enforcement was suspended. For a single monitored section, the percentage of overloaded vehicles grew by 87% in just one year without enforcement.

Another relevant aspect to discuss regarding the safety of bridges is the occurrence of degradation processes in the structure due to the influence of environmental conditions. Indeed, civil infrastructure networks are usually subjected to aging phenomena and natural hazards during their life-cycle, which decreases the performance of the structure over time (BARONE;

FRANGOPOL, 2014). The resulting deterioration process for bridge structures is very complex and may include, for instance, alkali-silica reaction, chloride contamination, and sulfate attack (FRANGOPOL; LIU, 2007). As a consequence of such complex and important effects, the uncertainties regarding the bridge structural behavior increase over time (LANTSOGHT et al., 2017). It is an additional difficulty for the assessment of the real condition of the structure. In the worst scenario, it could lead to lack of necessary maintenance interventions, which is an important cause of bridge failures (XU et al., 2016). It is worth to remark that, for the Brazilian context, this task is even more complex due to a lack of information for many bridges (LIMA E OLIVEIRA; GRECO; BITTENCOURT, 2019). Then, it is of paramount importance that responsible authorities have reliable and accurate information regarding the safety of such structures (SCHLUNE; PLOS; GYLLTOFT, 2009). In particular, both condition of the structure and actual traffic loads are important factors to analyze when assessing bridge safety.

Bridge weigh-in-motion (B-WIM) systems arise as efficient tools for helping in bridges safety assessment. B-WIM systems work relating strains, measured by sensors underneath the bridge structure, with the axle weights of the vehicle that induced such strains. It enables real time monitoring of traffic even with vehicles travelling at their usual speeds. The information retrieved by such systems can be employed for many applications such as selection of overloaded vehicles, traffic analyses, development of traffic models and bridge design and/or assessment (MANDIĆ IVANKOVIĆ et al., 2019). In addition, some important bridge performance indicators (e.g., influence lines and load distribution factors) can be evaluated employing the measured strains (ŽNIDARIČ; KALIN, 2020). Damage detection utilizing B-WIM systems information was also addressed by some recent works (CANTERO; GONZÁLEZ, 2015; CANTERO; KAROUMI; GONZÁLEZ, 2015; O'BRIEN et al., 2021).

B-WIM systems have some interesting characteristics. Firstly, by the nothing-on-road (NOR) approach, there is no need to install sensors directly on the road surface to detect vehicle axles. It improves the durability of the overall system, since it prevents that heavy traffic damages the sensors (LYDON et al., 2016). Furthermore, it is easy to implement, since there is no need for disrupting the traffic flow during installation (YU; CAI; DENG, 2018). Hence, among traffic monitoring systems, the cost of installing and maintaining a B-WIM system is usually lower (FRØSETH et al., 2017). In addition, such systems are portable, since transducers and electronics can be easily removed from one bridge and employed on another (JACOB; FEYPELL-DE LA BEAUMELLE, 2010). Lastly, the system is not visible by truck drivers, which makes difficult for overloaded vehicles to avoid it (JACOB; FEYPELL-DE LA BEAUMELLE, 2010). Thus, B-WIM systems are able to provide unbiased traffic data (LYDON et al., 2016).

Current B-WIM systems are based on the work of Moses (1979). The main idea utilized is that measured strains can be estimated by knowing bridge influence line and axle loads. Thus, given an influence line, obtained theoretically by Moses (1979), and measured strains, it is possible to calculate the axle weights that generated it by solving an inverse problem. However,

many distinct factors affect the bridge response and increase the difficult of calculating a theoretical influence line (e.g., the rotational stiffness of the connections (ZHAO, Z.; UDDIN; O'BRIEN, 2017)). For that reason, the theoretical influence line is not suitable for B-WIM applications (QUILLIGAN, M., 2003). Thus, differently from the work of Moses (1979), current methods perform a calibration step which aims to extract an experimental influence line. In the calibration procedure, a set of vehicles with known axle weights travels the bridge at constant speed and the strains are recorded. With measured strains and known vehicle properties, the experimental bridge influence line can be estimated and applied to weigh any vehicle of the traffic flow.

Although B-WIM systems have been applied in many sites across the world, providing important information for many distinct purposes, for some specific applications the required accuracy level was not achieved. The direct enforcement of weight limits is an example of task that needs highly accurate weight predictions (JACOB; O'BRIEN; JEHAES, 2002). Several B-WIM installations achieved performance sufficient just to indicate possible overloaded vehicles, remaining the need of using static scales to effectively check it (RICHARDSON et al., 2014). Hence, the use of B-WIM data for direct enforcement of legal weight limits is limited to an accuracy level that has not been reached to date (LYDON et al., 2016). In this context, a well acknowledged issue in B-WIM systems is the lower accuracy level reported for individual axle weights when compared to gross vehicle weight (GVW) estimates (HE et al., 2019; O'BRIEN et al., 2018; RICHARDSON et al., 2014; O'BRIEN et al., 2009). An argument that helps to explain this fact is that the resulting equations are ill-conditioned, mainly for closely spaced axles crossing long span bridges (ŽNIDARIČ; KALIN; KRESLIN, 2018; O'BRIEN et al., 2018, 2009; ROWLEY et al., 2008). However, even when evaluating only GVW predictions, achieving the required accuracy classes is still rare (ŽNIDARIČ; KALIN; KRESLIN, 2018).

1.1 GOALS AND CONTRIBUTIONS

The general objective of this work is to contribute for the development of more efficient B-WIM systems. From the discussion presented so far, two specific points are selected as the most promising ones to be addressed in order to reach this goal and develop useful contributions, mainly when considering the Brazilian context. The first one is the improvement of accuracy level of B-WIM weight estimates, mainly referred to single axle predictions. As the direct enforcement of legal weight limits by B-WIM systems has not been achieved in the practical operation yet, this topic remains as an open problem. Moreover, the possibility of application of B-WIM for direct enforcement has a remarkable importance in a scenario of high volume of heavy vehicles traffic and, in particular, high occurrence of overloaded vehicles, as observed in Brazil. The second important point remarked is a combination between lack of information for many bridges and high level of uncertainties in the bridge performance due to the degradation process that occurs during their life-cycle. In this work, it is attempted to address this matter from a B-WIM perspective. The utilization of B-WIM systems rely on

performing a calibration process, which generates a considerable amount of data. In the absence of previous reliable information, the data can be utilized to improve the knowledge regarding the bridge structure. It is specially important for many Brazilian bridges for which design plans (i.e., blueprints, structural specifications) are no longer available. The two contributions addressed are summarized as:

- the improvement in accuracy of B-WIM weight estimates, mainly related to single axle estimates;

- the assessment of structural bridge properties by means of B-WIM system calibration data.

In what follows the approaches adopted for addressing both issues are further described, remarking the contributions that the present work leads to the current B-WIM technology.

1.1.1 Contributions regarding the weight estimation process

The approaches developed attempting to improve the accuracy of weight predictions address two points suggested by Carraro et al. (2019), which conducted an overview of the related literature: the consideration of dynamic response into B-WIM predictions and the utilization of prior beliefs for helping in the weight estimation. The discussions are drawn individually for each approach.

The current utilized B-WIM algorithms analyzed in Carraro et al. (2019) are based only on static assumptions. However, the response of the bridge to the passage of a heavy vehicle has important dynamic effects and accounting for them is a promising option for improving B-WIM weight estimates. Therefore, this thesis presents a B-WIM algorithm that employs a simplified dynamic model for the vehicle-bridge system, which can be found also in Gonçalves, Carraro, and Lopez (2021a). Its main contribution is the development of an algorithm whose computational cost is at a similar level when compared to the current applied static methods (i.e., based on just a few matrix operations), however which also includes the effect of the dynamic response in a simplified manner. This algorithm is an extension of the work of Ning-Bo Wang et al. (2017), which focused on extracting the static component of the bridge influence line from a single calibration run. In this study, the method was modified to allow multiple calibration runs by employing the maximum likelihood approach (IENG, 2015). Furthermore, the complete dynamic response was utilized to calculate a parametric influence line that includes the vehicle speed as a model parameter and the equations utilized for weight estimation were derived. It is worth to remark that the vehicle speed is assumed to be constant throughout its passage over the bridge. The proposed method provides influence lines that better agree with the expected behavior of such curves (i.e., continuous curves instead of pointwise estimates (ŽNIDARIČ; KALIN; KRESLIN, 2018)). This characteristic should also improve the generalization capacity of the method. As less parameters are adjusted, the probability that the extracted influence line incorporates specific patterns from the response of the calibration vehicle is reduced. Moreover,

the inclusion of the vehicle speed as a model parameter is an attempt to model a known effect (illustrated in chapter 2) referred to the dependence of vehicle response to this parameter (O'BRIEN; GONZÁLEZ; DOWLING, 2010).

A practical problem that often occurs in B-WIM weight estimation is the low accuracy for individual axle predictions. Even clearly unreal estimates, such as negative axle predictions, can be reported. In order to overcome this problem, this thesis presents a Bayesian algorithm which accounts to prior beliefs in order to guide the estimates towards more likely values (GONÇALVES et al., 2022). The prior definition was based on the values expected for axle weights of heavy vehicles, which do not have a wide range of possible values (i.e., it is unreal to expect axle weights above 20 tons or below 0). However, in order to allow that the prior distribution has the desired effect, a second order autoregressive (AR(2)) process was employed for modeling the error between measured and predicted responses. It was a necessary action, since it was noticed that the aforementioned errors were highly correlated and assuming independent errors in this scenario induces an artificially high importance to the likelihood against the prior distribution (it is illustrated in chapter 2 and detailed in chapter 4). Deriving an approach that relaxes the independence hypothesis is a clear contrast between the proposed approach and other Bayesian strategies, such as Yoshida, Sekiya, and Mustafa (2021), which was based in this independence assumption.

1.1.2 Contributions related to the assessment of structural bridge properties

The motivation for studying this topic is the lack of information noticed for Brazilian bridges (LIMA E OLIVEIRA; GRECO; BITTENCOURT, 2019), in which even basic parameters (e.g., the bridge exact age) may not be known. This aspect contributes for a higher difficult for assessing the real bridge conditions. It was realized that the calibration procedure employed for B-WIM systems generates a high amount of information (i.e., bridge response to distinct vehicles whose properties are previously known, traveling at distinct speeds and road lanes), which may be utilized for increasing the knowledge regarding the bridge structural behavior. Indeed, the information collected during this procedure can be interpreted as a dynamic diagnostic test for bridges (OLASZEK; ŁAGODA; CASAS, 2014). Furthermore, periodical in-service verifications are recommended (JACOB; O'BRIEN; JEHAES, 2002). In this case, more data from known vehicles are generated, allowing to follow the bridge structural behavior over time.

In the present work, it is proposed a model updating strategy which utilizes the aforementioned dataset (GONÇALVES; LOPEZ; VALENTE, 2022). An important aspect to remark is that this dataset likely presents an inherent variability, in which the value for the quantity of interest (QoI) may change throughout calibration events. This variation may be better understood when recalling that bridges are under direct influence of environmental conditions during all their life-cycle and, hence, there is no control over all the characteristics that affect the bridge response (e.g., temperature, wind speed) along calibration. Therefore, the proposed

approach utilized a hierarchical Bayesian framework that can deal with this inherent variability, as observed in previous studies for distinct structural systems (BEHMANESH; MOAVENI, 2016; KWAG; JU, 2020; SONG, M. et al., 2019). It provides a better estimate of the total uncertainty regarding the parameters of interest than those ones obtained from classical Bayesian methods (SEDEHI; PAPADIMITRIOU; KATAFYGIOTIS, 2019). As a result, it is allowed that the procedure of installation and calibration of B-WIM systems could be used for two distinct goals: effectively calibrate the B-WIM system and assess bridge structural parameters.

1.2 DOCUMENT ORGANIZATION

The remaining of this thesis is divided into 5 chapters. Each of the contributions just cited refers to a specific one. It results in 3 self-contained chapters, written in paper format (all such chapters have been already published). In what follows these chapters are briefly summarized:

- in chapter 2, an introductory content about B-WIM systems is presented, aiming to show the main aspects regarding such systems for readers that are not well familiarized with them. Moreover, an experimental dataset related to a field calibration of a B-WIM system that is utilized throughout this thesis is detailed. Some challenges for current B-WIM systems, including illustrative examples which give a better idea of the contributions of this work are also discussed;

- chapter 3 introduces a new algorithm for weight estimation for B-WIM systems, based on the work of Ning-Bo Wang et al. (2017). It relies on simplified dynamic considerations regarding the vehicle-bridge system response. The idea for this work was a direct result from the conclusions of the work presented in Carraro et al. (2019), in which the inclusion of dynamic modeling was considered a promising option to improve the accuracy of B-WIM systems. It is worth to mention that such considerations for B-WIM exist, however not in a computationally way that enables real-time monitoring as in the proposed approach. It is also available in Gonçalves, Carraro, and Lopez (2021a);

- the chapter 4 also focused on the weight estimation process, however it employs a Bayesian strategy to improve axle weight predictions. It is intended that this strategy eliminates spurious estimates, such as negative axle predictions, which often occurs for closely spaced axles. This approach combines a prior distribution based on the expected values of axle weights in practice and an AR(2) process for modeling the error between measured and predicted responses. It is also available in Gonçalves et al. (2022);

- chapter 5 focus on performing model updating, applying Hierarchical Bayesian modeling, for bridge structures for which some B-WIM system calibration data is available. This model updating can be useful for many applications related to the

safety of the structure, such as reliability analysis. It is also available in Gonçalves, Lopez, and Valente (2022);

- chapter 6 draws the concluding remarks and some suggestions for future works.

2 INTRODUCTION TO B-WIM SYSTEMS

Current B-WIM systems are based on the study of Moses (1979), which relates measured strains with the axle weights that generated them. Thus, the estimated axle weights are those which minimize some error function between the measured and theoretical response. It allows the real time monitoring of vehicle weights, even with such vehicles traveling at their normal speeds. Most studies and installations applying B-WIM systems employ flexural strains as quantity of interest (HELMI; TAYLOR; ANSARI, 2015). In these systems, strain sensors are attached on the bottom of bridge girders, usually at the mid-span, such as in Figure 3.

Figure 3 – Example of strain sensor placed at the mid-span of the bridge girder

(a) Lateral view of the bridge

(b) Strain sensors

In what follows, a basic model representing the general procedure regarding B-WIM systems is briefly described. For further information related to this subject, the reader is referred to Junges (2017) and Heinen (2016).

First, the strains generated by a given vehicle are collected and converted to bending moment:

$$\boldsymbol{m}_g = E_g Z_g \boldsymbol{u}_g, \tag{1}$$

in which $\boldsymbol{m}_g$, E_g, Z_g, and $\boldsymbol{u}_g$ are the measured bending moment, elastic modulus, section modulus and measured strain of the g girder, respectively.

Although some studies work with the individual response for each girder, such as Hua Zhao et al. (2014), the most common approach for calculating the structural measured response is to sum up the contribution of all girders:

$$\boldsymbol{M} = \sum_{g=1}^{G} E_g Z_g \boldsymbol{u}_g, \tag{2}$$

in which G represents the number of girders. It is worth to mention that measurements are discrete in time, at a fixed sampling rate. Thus, $\boldsymbol{M}$ is defined as a vector, where each line

Figure 4 – Example of a collected signal of measured moment
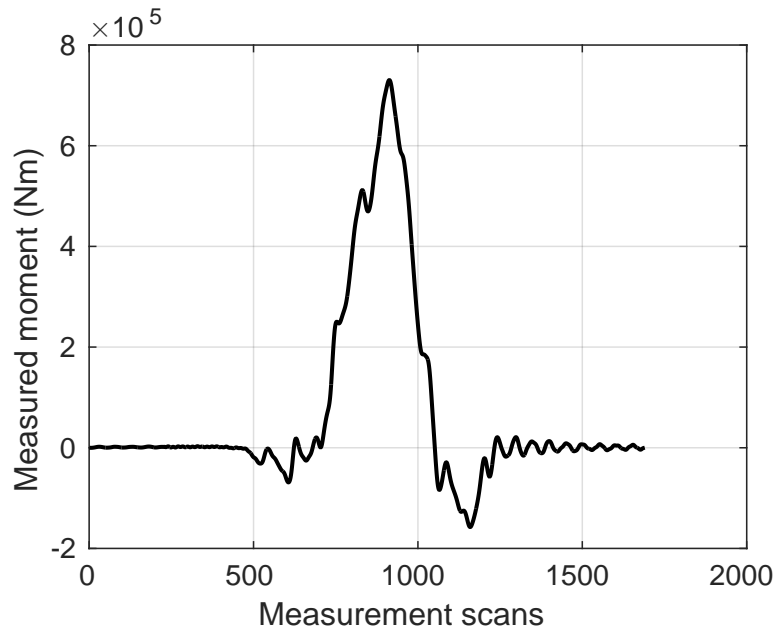
k, called here as scan, represents the measurement at a certain time. Figure 4 presents an example of the measured bending moment (**M**) for the passage of a single vehicle over a given bridge. The measurement procedure starts before the vehicle effectively enters the bridge. Hence, it could be noticed that nothing is measured at the initial phase. After the vehicle leaves the structure, however, the bridge shows its free vibration response. The effectively employed signal, therefore, is the central content, which really represents the event of a vehicle traveling over the bridge. The measurements are collected for a fixed position of the bridge, where the sensors are placed, and the measurements are a function of time (or scans). However, it is common to refer to the horizontal axis in distance unities. Since the vehicle is assumed to travel at constant speed, it is easy to convert the signal behavior from a function of the time to a function of distance. It is useful due to the more convenient physical meaning. For instance, the distance can easily relate the local that the vehicle is placed at each time step, using as reference the first wheel, with the limits of the bridge structure.

The idea behind B-WIM systems is to match this measured response with some theoretical one. For enabling the derivation of the theoretical response ($\widehat{\textbf{M}}$), the concept of influence line is employed. The influence line describes the static bending moment at the sensor position, usually the mid-span, under a unitary moving load (QUILLIGAN, M., 2003). In this case:

$$\widehat{M}_k = \sum_{j=1}^{J} W_j IL_{(k-C_j)}, \tag{3}$$

where:

$$C_j = \frac{d_j f}{v} \tag{4}$$

and J is the number of axles, W_j is the weight of the j axle, $IL_{(k-C_j)}$ is the influence ordinate at the position of the j axle, d_j is the distance between the first axle and j axle, C_j is the number of scans corresponding to d_j, f is the sampling frequency and v is the vehicle velocity. It is worthwhile to point that **IL** and $\widehat{\boldsymbol{M}}$ are defined as vectors in order to match with the discretized shape of the collected signals, whereas the index k arises as a consequence of this discretization. In addition, if $k - C_j$ results in an index that does not match an influence line ordinate, it is attributed the value of zero for $IL_{(k-C_j)}$. This last situation occurs when some vehicle axle is not over the bridge structure. Furthermore, one could observe that this theoretical response is derived based only in the static structural behavior.

The procedure for calculating the theoretical response is better presented by Figure 5. For a given scan k, the vehicle is positioned over the bridge as shown, with each axle related to a specific influence line ordinate. Thus, the total moment $(\widehat{M}_k)$ at the scan k is the sum of the contribution of each axle, resulting of the product of influence line $(IL_{(k-C_j)})$ and axle weight (W_j). It is worth to point out that d_1 and, consequently, C_1 are zero since the reference for calculating the distance is the own first axle. In addition, the relation between distances and the corresponding number of scans can be clearly observed.

One could notice that, in order to enable the proper theoretical response calculation, the vehicle speed is necessary. This parameter is usually assumed to be constant, which is a reasonable assumption for short-span highway bridges (LANSDELL; SONG, W.; DIXON, 2017). In order to calculate the vehicle velocity, some additional sensors are commonly employed. The NOR B-WIM approach, applied in the present study, provides this desired parameter without the need of traffic interruption for sensor installation (YU; CAI; DENG, 2018), also improving its durability (LYDON et al., 2016). Figure 6 presents examples of signals from such sensors, called Free-of-Axle Detector (FAD). Two distinct signals are noticed, related to sensors at the same lane, but longitudinally apart from each other. The peaks observed are related to each detected axle, indicating the number of axles. Hence, the time delay between the passage of the same axle by each sensor is used to calculate the vehicle speed, since the distance among both sensors is known. In addition, usually one sensor is placed at the center of the structure, enabling that time be converted to distance from the center in an easy way. In other words, the instant that each axle passes the sensors also is useful for working as a reference point on the structure. Such aspects are better discussed in section 2.1, in which the B-WIM calibration procedure that generated the experimental dataset utilized in the present study is detailed.

The last point to be addressed to create a functional B-WIM system is the definition of the bridge influence line, since axle weights are the unknowns calculated by such systems. In the first work in this subject, performed by Moses (1979), the bridge influence line was approached just with theoretical analysis. The theoretical influence line, however, is currently recognized as unsuitable for B-WIM applications (QUILLIGAN, M., 2003), since some simplifications are done in its derivation procedure. Thus, most of recent methods employ a calibration step in order to estimate an experimental influence line. The calibration procedure relies on performing

Figure 5 – Example of theoretical moment calculation for a four-axle truck
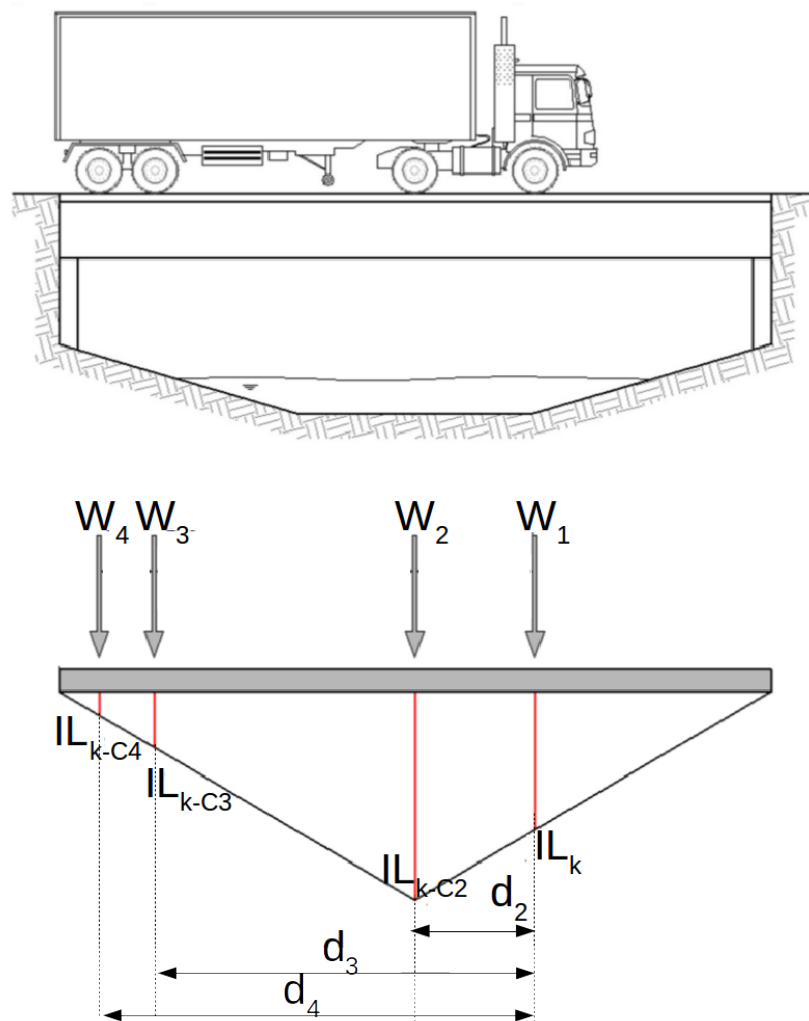
Source: Adapted from Junges (2017)

a set of runs at controlled conditions, such as constant speed and known axle weights, and recording the resulting strains. The measured strains together with the weights that generated it are enough to estimate the experimental bridge influence line, which can be applied for effectively monitoring the traffic over the bridge. More details referred to practical aspects in the calibration procedure are addressed in section 2.1.

Thus, since the axle weights are known in calibration, it is realized that the same procedure of matching theoretical and experimental responses can also be applied to calculate the experimental bridge influence line. In other words, one could select the influence line ordinates that minimize the error function R. This function usually is based on the sum of the squares of differences between the measured (M) and the theoretical ($\widehat{M}$) bending moment, which corresponds to the least squares formulation. It reads as:

Figure 6 – Example of FAD signals, considering a three-axle vehicle
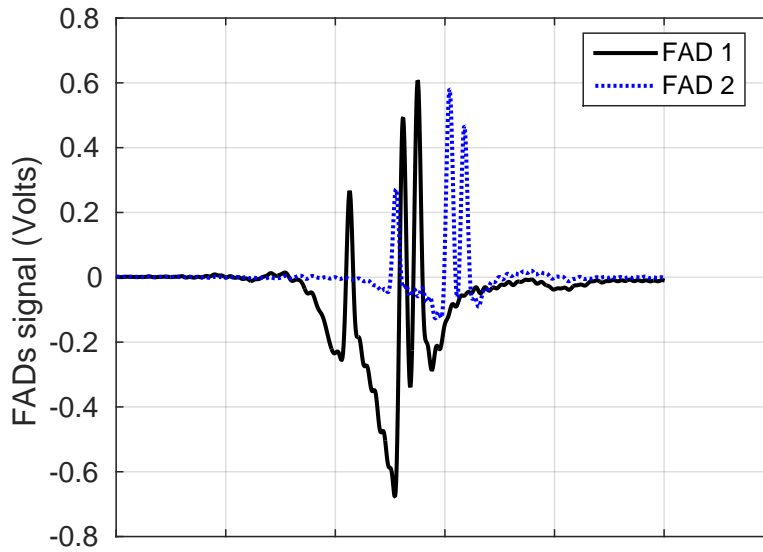
$$R = \sum_{k=1}^{K} \left(M_k - \widehat{M}_k \right)^2, \tag{5}$$

where k represents each scan and K the total number of scans. Minimizing R results in a closed-form solution for the influence line:

$$\boldsymbol{IL} = (\boldsymbol{A}^T \boldsymbol{A})^{-1}(\boldsymbol{A}^T \boldsymbol{M}), \tag{6}$$

where $\boldsymbol{A}$ is a Toeplitz matrix, employed to perform the discrete convolution related to the passage of the axle weights through the bridge. In other words, this matrix allows that the theoretical response of Equation (3) can be easily written as a function of the influence line ordinates vector:

$$\widehat{\boldsymbol{M}} = \boldsymbol{AIL}. \tag{7}$$

The matrix $\boldsymbol{A}$ is defined as:

$$A_{pq} = \begin{cases} W_j, & \text{if } p = q + C_j \\ 0, & \text{otherwise} \end{cases}. \tag{8}$$

The shape of matrix $\boldsymbol{A}$ is presented in Figure 7, where each symbol represents the respective axle weight value and all the remaining terms are zero. It can be noticed that each line is a shifted version of the previous one, which can be understood as the passage of the vehicle through the bridge, one scan at time. The first and last lines represent the instants that the first axle enters the bridge and the last axle leaves it, respectively. Moreover, the columns can

Figure 7 – Example of matrix **A** shape for a four-axle vehicle
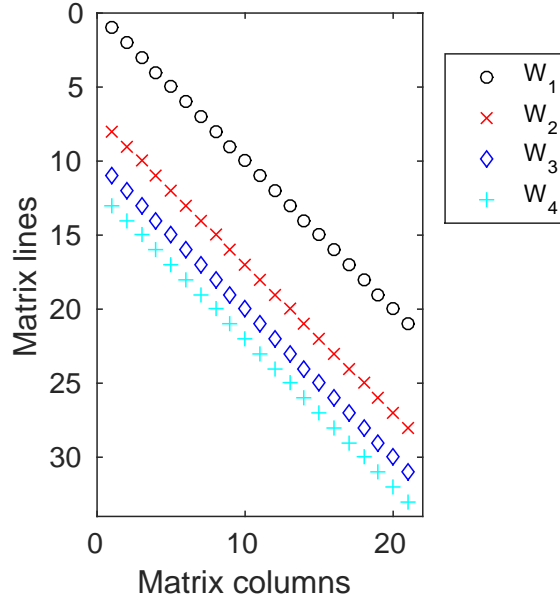
be seen as the respective positions over the bridge, with the first and last columns indicating the bridge limits.

If multiple calibration runs are available, one could proceed by averaging the resulting influence lines. However, this needs to properly take into account the vector sizes, which normally differ in distinct runs, since vehicle speed usually is not the same for all runs. As a consequence, interpolating signals is often necessary.

It could be noticed that the expression of Equation (6) results in an influence line that adjust all the discretized ordinates, without ensuring any relation among them. Distinct approaches can be applied in this step to overcome this issue, such as associating mathematical functions for the influence line and founding the parameters that define such expressions instead of the own ordinates (WANG, N.-B. et al., 2017; ŽNIDARIČ; KALIN; KRESLIN, 2018).

After the influence line based on direct measurements has been found, one can proceed similarly in order to find the unknown axle weights of the vehicles of the traffic flow. That is, the same expression of Equation (5) is minimized, however considering the axles weights as unknowns and employing the influence line just derived:

$$\boldsymbol{W} = (\boldsymbol{\Lambda}^T\boldsymbol{\Lambda})^{-1}\boldsymbol{\Lambda}^T\boldsymbol{M} \tag{9}$$

where $\boldsymbol{W}$ is the vector of predicted axle weights and $\boldsymbol{\Lambda}$ is a matrix based on the influence line ordinates, shifted according to the axle spacing, defined as:

$$\Lambda_{kj} = IL_{k-C_j}. \tag{10}$$

Thus, $\boldsymbol{\Lambda}$ is a $K \times J$ matrix. Furthermore, the same observation done for IL_{k-C_j} in Equation (3) holds here. That is, if $k - C_j$ results in an index that does not match an influence line ordinate,

Figure 8 – Example of the matrix $\boldsymbol{\Lambda}$ behavior for a four-axle vehicle
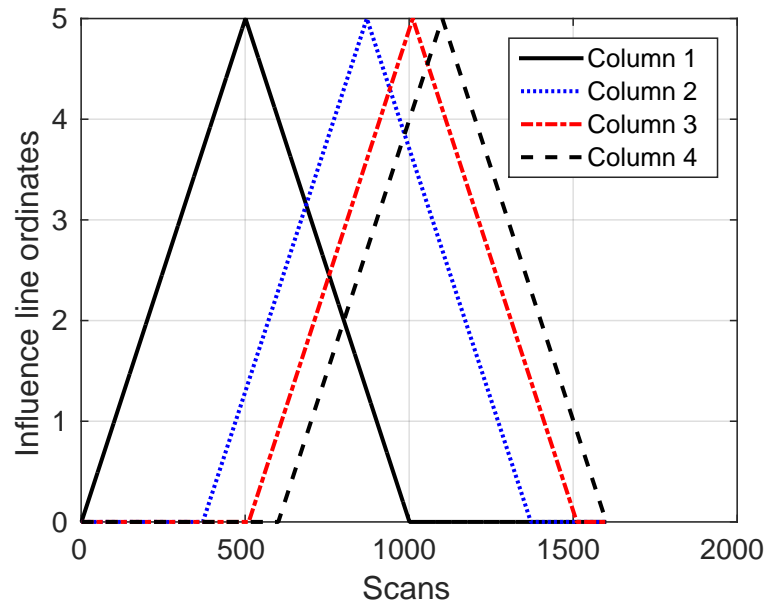
it is attributed the value of zero for IL_{k-C_j}. Figure 8 shows an example of this matrix $\boldsymbol{\Lambda}$ for a four-axle vehicle, where the horizontal axis refers to the lines of this matrix and the columns are represented by each distinct curve. Then, the shifted behavior of this matrix can be clearly seen. For each line of this matrix, the influence line ordinates related to each axle at a specific instant are represented. For instance, the only non-zero initial values (up to scan 400 approximately) are related to the first axle, since just this axle is over the bridge at such instants. As long as the vehicle moves, the contribution of other axles is also added, which is observed by the presence of more non-zero values.

It is worth to mention that the approach just described is useful for showing the main aspects regarding B-WIM systems and the way that they work. However, many distinct approaches can be conducted in each step. For instance, the weigh procedure can consider a regularization procedure instead of the simple least squares (O'BRIEN et al., 2009), the influence line extraction can consider the maximum likelihood approach, enabling the simultaneous consideration of multiple calibration vehicles (IENG, 2015), among many other possibilities.

2.1 DESCRIPTION OF THE EMPLOYED EXPERIMENTAL DATA

No matter how elaborated the model utilized for simulating a real B-WIM system application, it is not able to reproduce all the complexities inherent to the actual problem. Therefore, analyses employing experimental data are important tools for assessing the practical suitability of proposed approaches and are employed in the next chapters whenever possible. For all analyses regarding real-world signals presented in the following chapters, the data collected for the calibration procedure of a B-WIM system in the Itinguijada bridge is utilized. The Itinguijada bridge is located at BR-153, km 148, between Uruaçu and Porangatu cities, in the

Figure 9 – Itinguijada bridge

state of Goiás, Brazil. The structure is comprised of two girders and five cross beams, resulting in a total length of 29.70 meters. Figures 9, 10 and 11 present the structure, its mid-span cross section and lateral view, respectively. The calibration procedure was carried out between September 23 and 24, 2016. This same dataset was also employed in the work of Junges (2017).

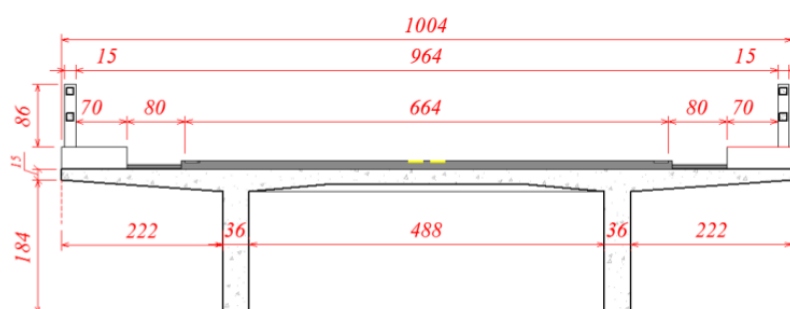Figure 10 – Mid-span cross section dimensions (values in cm)

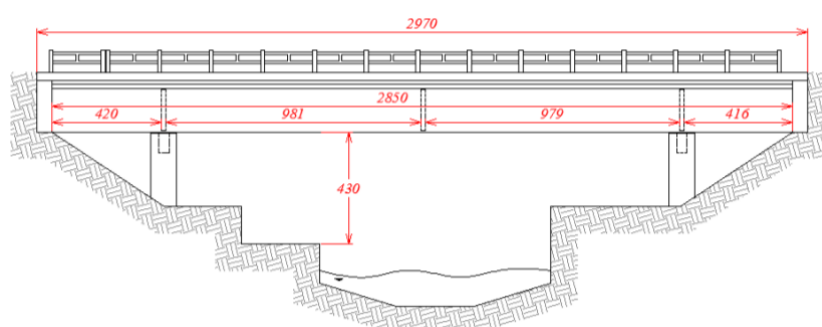Figure 11 – Lateral view dimensions (values in cm)

Table 1 – Axle weights and spacing for calibration vehicles

| Vehicle | Axle mass (kg) | | | | |
	Axle 1	Axle 2	Axle 3	Axle 4	Axle 5
Three-axle vehicle	6,900	14,900	12,900	-	-
Five-axle vehicle	7,500	14,100	13,300	11,100	9,200
Vehicle	Axle position (m)				
	Axle 1	Axle 2	Axle 3	Axle 4	Axle 5
Three-axle vehicle	0	4.78	6.07	-	-
Five-axle vehicle	0	3.57	9.16	10.43	11.66

The data was gathered at a frequency of acquisition of 512 Hz, employing a commercial system from CESTEL, named SiWIM (CESTEL, 2017). Two sets of sensors were utilized:

- Free-of-Axle Detectors (FAD): such sensors were placed under the bridge slab and were utilized for both detecting the presence of axles and calculating the vehicle speed, as previously commented. Two sensors were placed under each traffic lane: one at the mid-span and the other spaced longitudinally 4 meters from it;

- weigh sensors: such sensors were attached underneath bridge girders and measured the strains generated by passing vehicles, which are the main inputs for B-WIM purposes as already discussed. Two weigh sensors were positioned under each girder, at the mid-span of the structure since this is the region where such strains are higher. The effectively utilized signal for each girder is, then, the average from the measurements of the two sensors.

It is worth to remark that the calibration procedure took two consecutive days and, hence, no seasonality effects are present. In addition, all sensors are self-temperature-compensating transducers. Therefore, the effect of temperature variations are argued to be small in the present dataset. In what follows the measurements from weigh sensors are referred simply as strains signals, whereas the output from Free-of-Axle Detectors is called FAD signals.

Two vehicles were utilized in the calibration process, whose main characteristics are described in Table 1. The number of runs and range of vehicle velocities adopted were defined in order to follow the procedure defined by Jacob, O'Brien, and Jehaes (2002). It suggests the acquisition of signals from at least 10 valid runs per vehicle in each traffic lane. The vehicle speeds employed in each run oscillated between 40 km/h and 80 km/h, covering the expected range of speeds for the usual traffic flow. The resulting calibration dataset comprised a total of 83 runs. It is noticed that the total number of runs was somewhat higher than the minimum necessary to achieve the recommended values. This was necessary since not all runs were suitable for effectively calibrating the system, as will be discussed in what follows.

The main goal of the calibration step in B-WIM systems is to enable the calculation of the bridge influence line that provides the best agreement between measured and theoretical responses. The properties of the vehicles that induce every measured signal are necessary in the process. In this context, it is noticed that a wrong value for vehicle properties, such as

axle weights, may lead the calculation of an influence line that does not reflect the real bridge behavior. It is an important aspect to remark since the traffic flow was not closed to perform calibration due to practical limitations. Therefore, it is possible that other vehicles of the traffic flow travels the bridge at the same time than the calibration vehicle, corrupting the results. In this case, the measured response is no longer useful and such an event needs to be discarded. It is just an example of a unsuitable vehicle run. Multiple presences, troubles in signal acquisition and a time window that does not cover the whole vehicle passage are examples of issues that turn a signal useless. Thus, before any further analysis, all events were checked and those ones that do not match the desired behavior were discarded. Figure 12 depicts the FAD signals from an event in which another vehicle followed the calibration vehicle in the same traffic lane. It also presents the strains of this event in comparison with the signals from valid events of the same vehicle and traffic lane. A remarkable difference in the strains at the end of the signal is noticed, due to the contribution from the second vehicle.

Figure 12 – Example of FAD signal for an event in which two vehicles travel the bridge in sequence (above) and the comparison of the strains from this event with samples from valid signals from other events related to the same vehicle and lane (below).
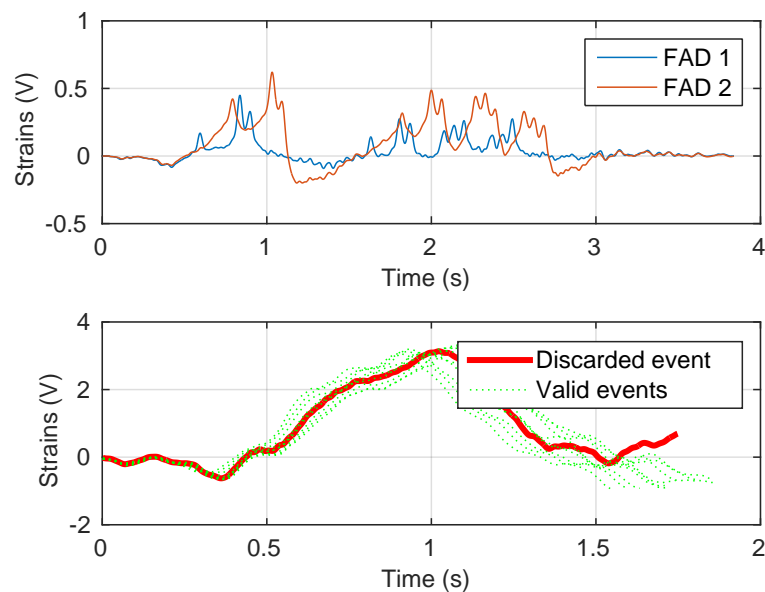
From the total of 83 initial calibration events, 49 were effectively suitable for further analyses. The next step was to identify the axles of the vehicle into FAD signals and calculate vehicle speed. This process is illustrated in Figure 13, in which signals from the two FAD sensors under the traffic lane in which the vehicle is currently travelling are presented. The response from the other two sensors under the other traffic lane were omitted since the values are negligible. It is noticed that each signal is a time-shifted version of each other and 5 axles are identified by peaks into signals. The similarity between signals from sensors under the same traffic lane is expected, since every axle will pass over both sensors and they are longitudinally

apart. The vehicle speed can be calculated as the ratio between the distance from one FAD sensor to its pair (Δx) and the time interval that the vehicle took to travel this distance (Δt).

Figure 13 – Example of FAD signals together with the parameters employed for calculating the vehicle speed.
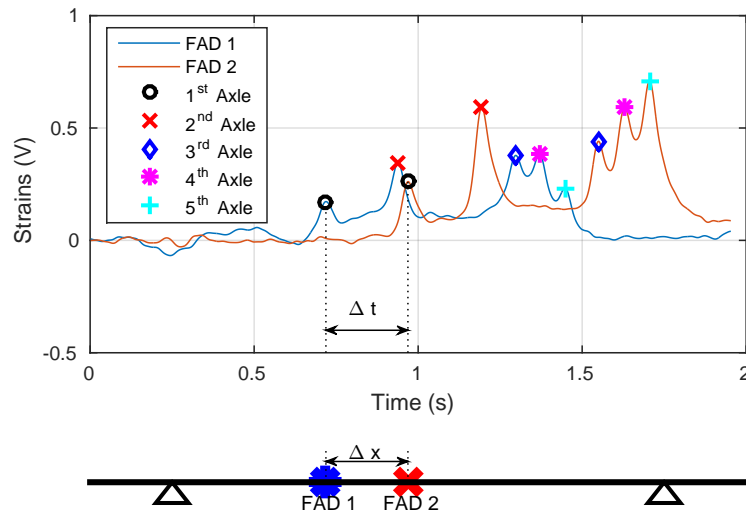
The events related to each vehicle run were previously selected from the continuously monitored signal, aiming to avoid losing any information. Then, for most events, the signal was considerably larger than the necessary for covering the passage of the calibration vehicle, including sometimes information from other vehicles of the usual traffic flow. It indicates that some splitting process is needed for separating signals related only to the passage of a single calibration vehicle over the structure. It is not a straightforward procedure since no specific sensors were utilized for measuring the time instants that a given vehicle arrives and leaves the bridge in the present study. Thus, in order to overcome this issue, the information collected by the FAD sensors was employed. First, the speed of the vehicle in each specific run was calculated as previously discussed. This velocity was assumed to be constant, as already commented. In addition, the time instant that the vehicle crosses the middle of the bridge was known, since, for the present study, a FAD sensor was located at this position. Such information together with the length of the bridge, frequency of the acquisition system and the distance between first and last vehicle axles were, then, employed for estimating the time instant that the vehicle enters and leaves the bridge. This procedure is illustrated by Figure 14 and was based in the FAD signal from the sensor positioned at the middle of the structure. It remarks the instant that the first axle passed this FAD sensor (P1). Knowing this value, the length of the bridge and the estimated velocity, the instant where this axle enters (P2) and leaves (P3) the bridge could be calculated. Such points together with the distance between first and last axle were, then, applied to calculate the instant that the last axle leaves the bridge (P4).

Figure 14 – Example of process performed for selecting the time window related to the passage of the vehicle. It presents both the FAD signal from the sensor attached to the middle of the structure (above) and the selected strains signal (below).
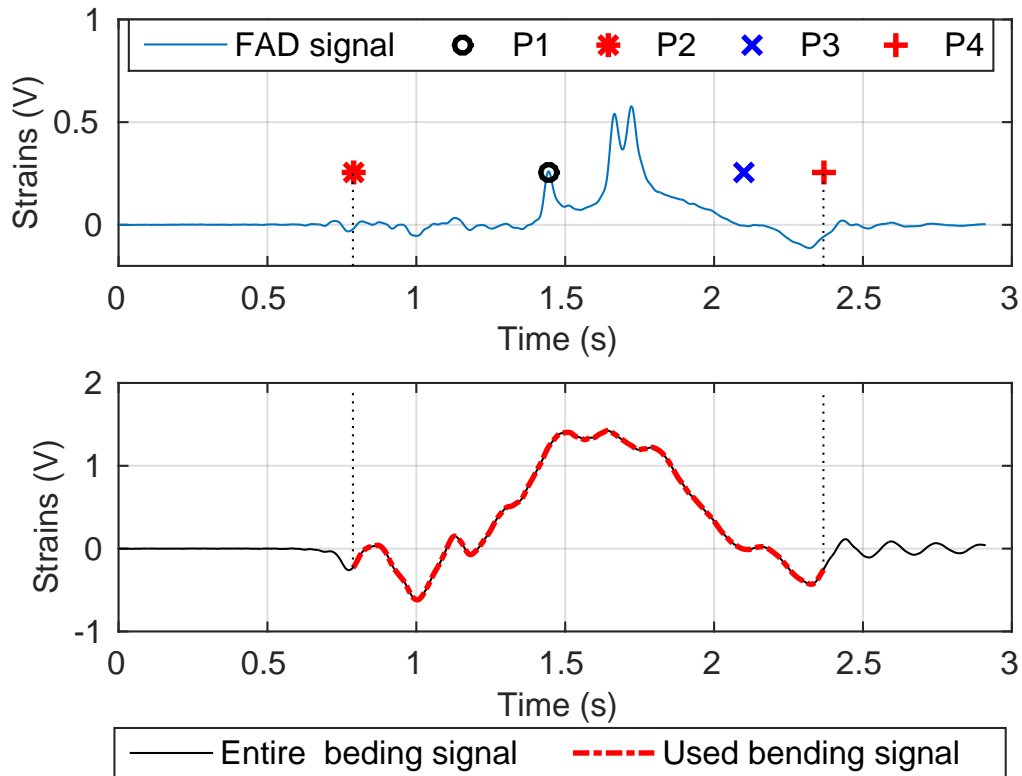
After all the discussed operations, the signals of both sensors attached to a same girder were averaged to produce a single result per girder. Those averaged signals can, then, be applied in Equation (2) for calculating the effectively monitored quantity. The dataset related to the calibration procedure is comprised of the resulting strains together with the characteristics of the vehicle which generated such strains (speed, axle weights and spacings). Further signal processing procedures, such as decimation, are not the same for all studies performed in the following chapters. Thus, they are detailed in each specific chapter.

2.2   SOME CHALLENGES IN B-WIM SYSTEMS

In previous sections both theoretical and practical aspects related to the application of B-WIM systems were briefly introduced, without many comments related to difficulties that may arise in the process. When observing the operation of such systems in more details, it is noticed that many issues may negatively affect the results provided. For instance, the weight prediction is an inverse problem in which multiple highly distinct solutions may fit similarly to the measured data. The present study was performed aiming to deal with some of such issues, intending to collaborate for the development of more efficient B-WIM systems. As a result, three distinct approaches, with different goals, were proposed. They are individually detailed

in chapter 3, chapter 4 and chapter 5, respectively. In order to improve the understanding of the present study as a whole, this section illustrates the troublesome issues that are directly addressed by the proposed approaches.

2.2.1 Response variation due to vehicle speed

Most algorithms employed for weight estimation in B-WIM systems disregard the direct influence of vehicle speed into the theoretical response, applying it only to determine the number of scans in Equation (4). However, the dynamic behavior presented by the bridge due to the passage of a heavy vehicle is dependent of such a parameter. For instance, Figure 15 presents a real example of the variation of strains response for the same three-axle vehicle due to distinct traveling speeds. It can be noticed that this variation exists and is not negligible. Furthermore, the effect of changing the velocity has a clear non-linear impact in the total response, which makes even more difficult the proper accounting of this parameter. This aspect is addressed in chapter 3, in which a B-WIM algorithm that takes the vehicle speed as a parameter is derived.

Figure 15 – Variation of measured response within vehicle speed
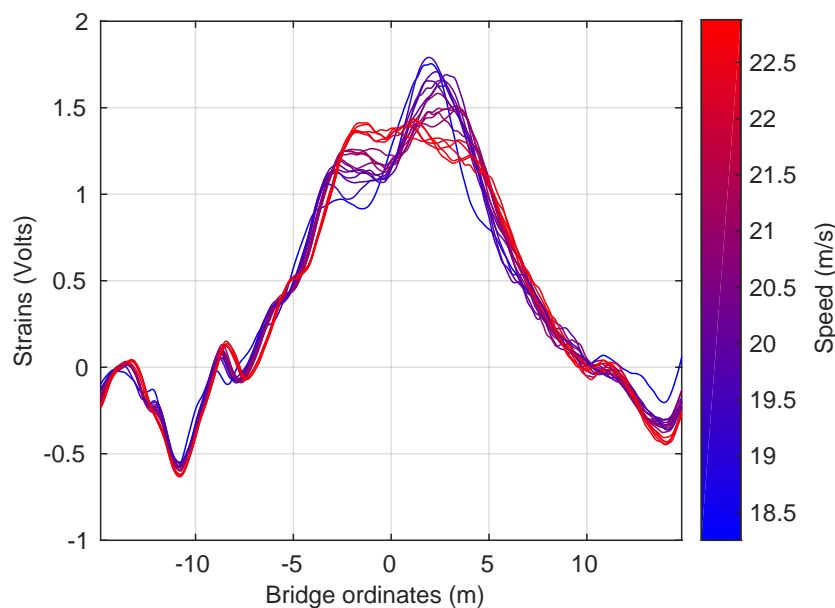
2.2.2 Influence of vehicle characteristics

The calibration procedure of B-WIM system is usually limited to a few vehicles, due to financial restrictions. However, the structural response is highly dependent on many aspects related to the vehicle applied for calibration, such as the kind of suspension system and vehicle configuration. Thus, it is already expected that the calibration procedure could not present all the possible vehicle configurations for the system. As a result, bias could be introduced into the process as a whole. For instance, Figure 16 illustrates this aspect by comparing the mean

Figure 16 – Influence lines calculated based only in one vehicle type
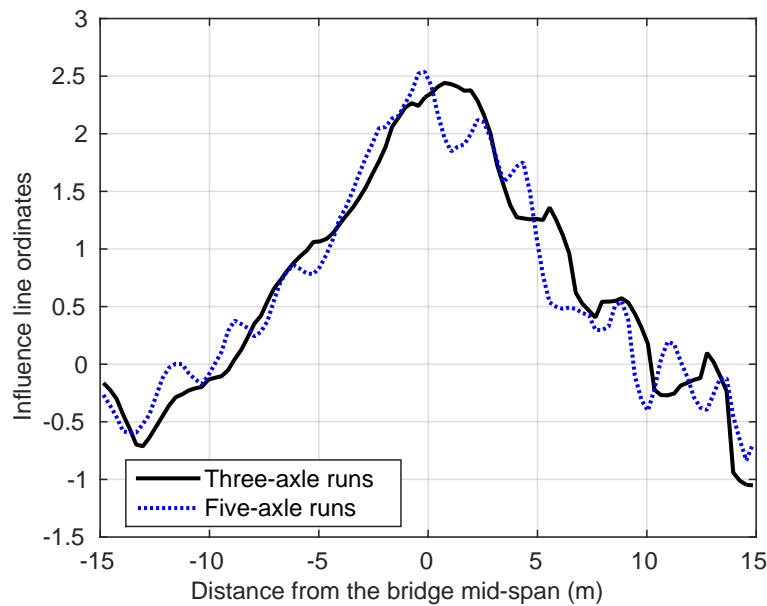
influence line, from a total of 10 distinct runs, reached when considering either the three-axle or the five-axle vehicle. It is clear that the influence line based only on the three-axle truck is considerably distinct from that one provided by the five-axle one. This is not desired, since the influence line is a bridge property and should be independent of the characteristics of calibration vehicles. It indicates that the calculated influence line, adjusted to provide the best match between theory and measurements, can represent unreal patterns. It happens since the theoretical response is not able to precisely predict the experimental results and the model is adjusted without any restriction on its shape. For instance, the dynamic response can introduce undesired oscillations in the static influence line, which appears evidently in the shape of these curves, mainly for the influence line based only in the five-axle vehicle. If one influence line is applied for weighing the other vehicle, unsuitable results may be achieved. Thus, this is another aspect that needs attention, indicating that approaches that adjust many parameters at the same time may fit just the calibration vehicles. The approach described in chapter 3 addresses this issue by employing a simplified dynamic model to extract the bridge influence line which results in a parametric curve with few parameters.

2.2.3   Multiple solutions

The process of estimating weights from measured strains can be seen as an inverse problem, susceptible to ill-posedness and ill-conditioning. Hence, the stability, uniqueness and existence of the solution is not ensured (SIMOEN; DE ROECK; LOMBAERT, 2015). In order to better understand how these points bring additional difficulties for B-WIM systems, the issue of uniqueness is better illustrated. Figure 17 presents a toy example, referred to the theoretical response generated by two largely distinct axle weight distributions. The length of the bars are

proportional to the axle weight whereas the spacing of bars is related to the axle position. The numeric values are omitted since the shape of both response and axle weights is enough to understand the overall behavior. It is noticed that the structural response is almost the same, even with the vehicle 2 presenting an axle with negative weight. As it is possible that multiple solutions equally match to the measurements, finding the right one becomes a really hard task. In addition, solutions with negative weights can also be reported, even that it is a clear physical violation. Thus, the developed methods must give special attention for the issues just cited for ensuring that accurate results be reported. The approach described in chapter 4 addresses this issue by employing a Bayesian strategy that utilizes a prior distribution, based on the expected values for axle weights and their correlations, to guide the estimation towards more plausible values, avoiding spurious predictions.

Figure 17 – Example of the similarity of response due to two quite distinct vehicle configurations
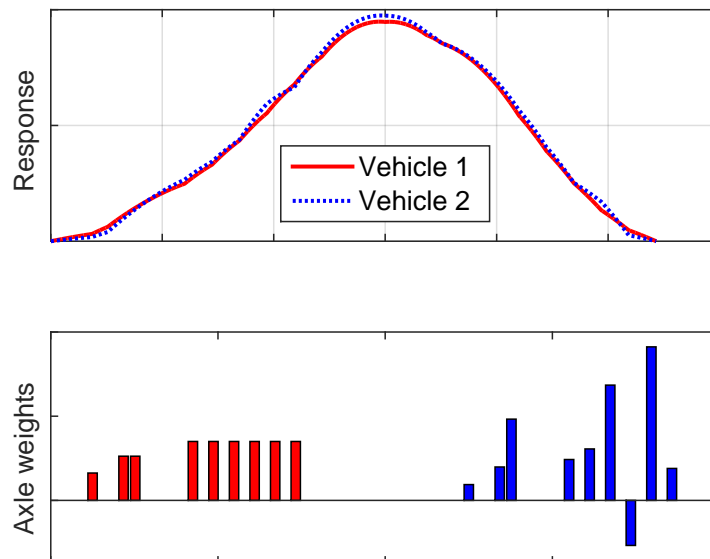
2.2.4   Serial correlation in error terms

When working with Bayesian strategies, it is often assumed that the errors between measured and theoretical responses are independent. Although it is usually a suitable option, for the present context such hypothesis does not hold. As the model employed for estimating the response induced by a given vehicle is not able to describe all the patterns present in the measured signal and the frequency of the acquisition system is usually high, the error between theoretical and measured responses is correlated. It was noticed, for instance, in the work of Yoshida, Sekiya, and Mustafa (2021). Figure 18 depicts an example of measured and theoretical responses together with the respective residuals. It could be seen that residuals show a clear pattern instead of just random fluctuations, which indicates the presence of serial correlation. A simple illustrative example is presented to show how this correlation affects estimates.

Figure 18 – Example of residuals between theoretical and measured responses.
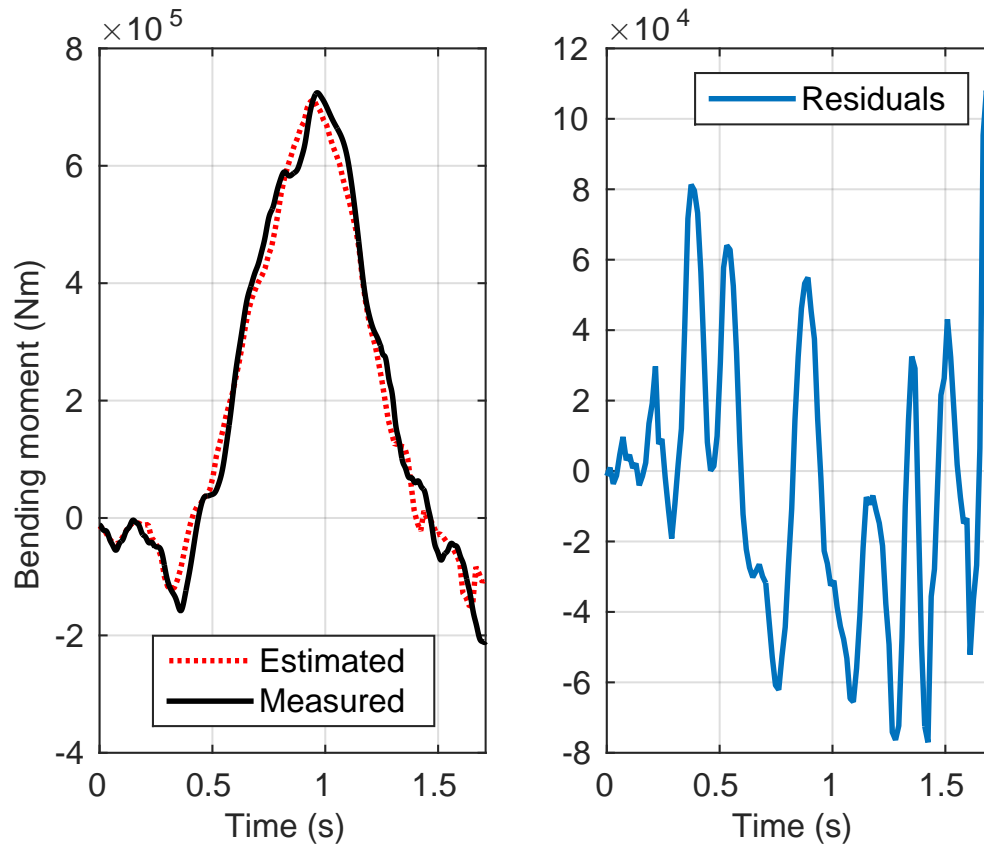
The illustrative example utilized is based on a simple two-axle vehicle, traveling over a simply supported bridge, and is better described in chapter 4. The goal is to estimate axle weights and a Bayesian framework is utilized. Two examples are analyzed, differing just by the number of data points since in example 2 the dataset is interpolated until achieve five times the dataset size employed in example 1. Hence, no additional information is introduced in example 2, it is just an artificial way of increasing the amount of data. Figure 19 depicts the probability distributions associated to the axle weights. The prior is the initial belief without observing the measurements, the likelihood reflects the most likely weights when observing just the measured data and the posterior is the effective output of the Bayesian analysis, which weighs both prior and likelihood. The point estimates related to the least squares solution and the most probable point in the Bayesian analysis are also presented. Whereas the least squares estimate does not change in the presence of the artificially generated data, the Bayesian solution is considerably shifted. The extra amount of data increases the influence of the likelihood function into the final output of the Bayesian approach, shifting the posterior distribution towards the likelihood. However, this shift is not desirable, since no extra information is really added to the model. As the independence assumption is being employed, the model interprets the extra data points added in Example 2 as new data and narrows the likelihood. Then, it is noticed that the prior distribution guides the solution of Example 1 towards the real value but has little effect in example 2. This aspect is important for chapter 4 and chapter 5. In chapter 5 the negative

effect of correlation is mitigated by the application of a decimation procedure for reducing the effective sample rate of the signal. In chapter 4, a decimation strategy is combined with the utilization of a second order autoregressive model for relaxing the assumption of independence among error terms.

Figure 19 – Resulting probability distributions and main estimates for the axle weights regarding the first and second examples
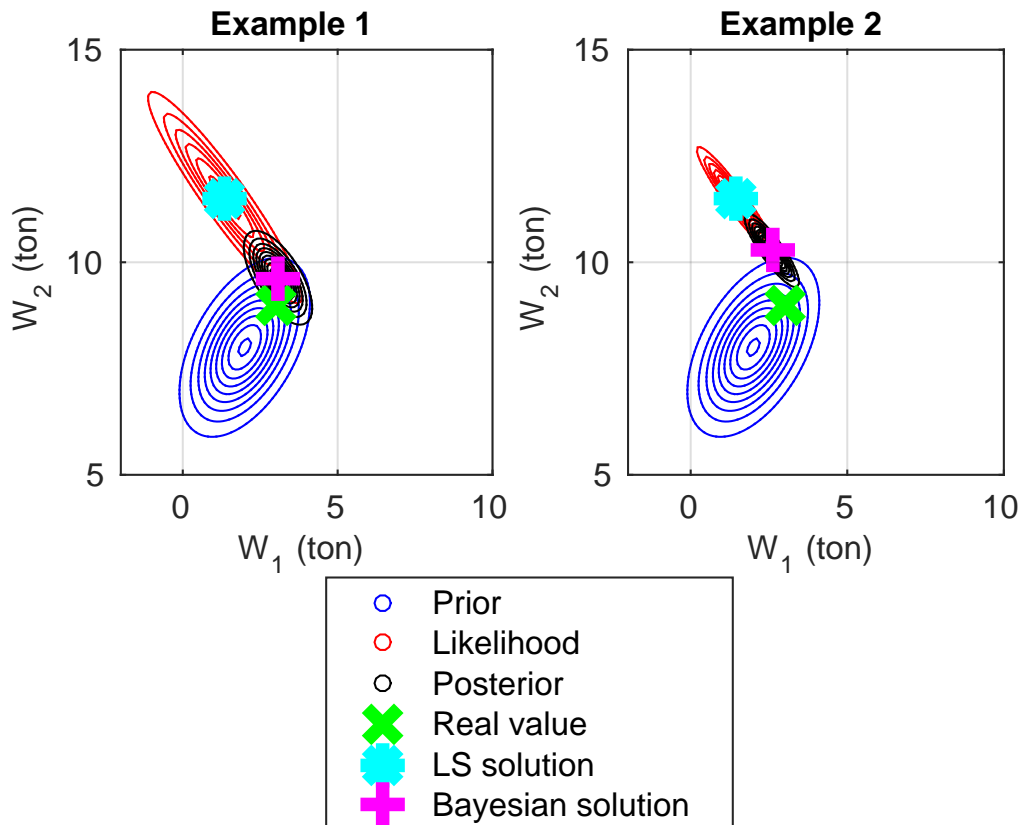
3 A B-WIM ALGORITHM CONSIDERING THE MODELING OF THE BRIDGE DYNAMIC RESPONSE

ABSTRACT

A Bridge weigh-in-motion (B-WIM) system is able to estimate vehicle weights based on data gathered by sensors underneath the bridge structure. It is a valuable tool for many applications related to the assessment of bridges safety, already operating in many sites around the world. Although the dynamic behavior of the bridge structure is a well recognized troublesome point for the improvement in B-WIM algorithm performance, most of the current employed methods rely only on static assumptions. The main goal of the present study is to adapt a simplified dynamic modeling, proposed by a recent study, to work as a B-WIM algorithm. Three main modifications are performed: the implementation of a maximum likelihood approach to perform the influence line assembly strategy for data regarding multiple runs, the derivation of a weigh procedure and the inclusion of the full analytical dynamic model. As a result, the method described is able to calculate influence lines that are both continuous curves and a direct function of the vehicle speed. Furthermore, the overall procedure needs only simple matrix operations, resulting in a computational cost similar to the static algorithms. Numerical simulations related to bridges with distinct span lengths and road roughness profiles indicated that the adapted method is able to overcome the results of the current state-of-the-art methods, specially for longer bridges.

Authors: Matheus Silva Gonçalves, Felipe Carraro, Rafael Holdorf Lopez

Note: The numbering of all figures, tables and equations has been restarted in this chapter in order to better agree with the published version of the work

LIST OF SYMBOLS (CHAPTER 3)

Z	section modulus of bridge girders
G	total number of girders
M^r	measured bending moment response vector
ε	measured strains response vector
M^t	theoretical bending moment response vector
w_j	weight of j-th axle
n	vehicle number of axles
d_j	distance between first and j-th axle
b_j	number of scans between first and j-th axle
f	sampling frequency
v	vehicle speed
L	influence line ordinates vector
x	position along the bridge span
ℓ	bridge span length
$\boldsymbol{X}$	matrix of positions
$\boldsymbol{A}$	matrix of axle weights
S	static structural response vector
λ	coefficients of the cubic polynomial
t	time
$H(.)$	Heaviside function
t_{pi}	time that axle i enters the bridge
t_{qi}	time that axle i leaves the bridge
ω_m	natural frequency of the m-th mode
ζ_m	damping ration of the m-th mode
E	elastic modulus of bridge girders
I	moment of inertia of bridge girders
F	fluctuation response vector
ψ	fitted coefficients for fluctuation response
η	theoretical vs measured difference vector
Y^t	vector comprising theoretical response and constraint conditions
Y^r	vector comprising measured response and constraint conditions
c	number of calibration events
θ	vector comprising fitted parameters
$\boldsymbol{D}$	matrix combining static and dynamic effects
W	vector of axle weights
$\boldsymbol{C}$	matrix employed to perform the weigh procedure
ρ	fitted coefficients for quasi-static response

3.1 INTRODUCTION

Bridge Weigh-in-motion (B-WIM) systems are efficient tools for providing real time monitoring of traffic, with vehicles travelling at their usual speeds. It works employing sensors located underneath the bridge to measure the strains generated by passing vehicles, aiming to estimate their weight. B-WIM systems have some interesting characteristics. Firstly, by the nothing-on-road (NOR) approach, there is no need to install sensors directly under the traffic to detect vehicle axles, which improves the durability of the overall system, since it prevents that heavy traffic damages the sensors (LYDON et al., 2016). Furthermore, it is easy to implement, since there is no need for disrupting the traffic flow during installation (YU; CAI, C.; DENG, 2018). Hence, among traffic monitoring systems, the cost of installing and maintaining a B-WIM system is usually lower (FRØSETH et al., 2017). In addition, such systems are portable, since transducers and electronics can be easily removed from one bridge and employed on another one (JACOB; FEYPELL-DE LA BEAUMELLE, 2010). Lastly, as the system is not visible by truck drivers, it makes difficult for overloaded vehicles to avoid it (JACOB; FEYPELL-DE LA BEAUMELLE, 2010). Thus, B-WIM system are able to provide unbiased traffic data (LYDON et al., 2016).

Current B-WIM systems are based on the work of Moses (1979). The main idea utilized is that measured strains can be related with the bridge influence line and axle loads. Thus, given an influence line, obtained theoretically by Moses (1979), and measured strains, it is possible to calculate the axle weights that generated it. However, the real influence line usually is between the one obtained for simply supported and fixed boundary conditions (ŽNIDARIČ; BAUMGARTNER, 1998). This is due to some factors not included in the theoretical structural model, such as the rotational stiffness of the connections (ZHAO; UDDIN; O'BRIEN, 2017). By this reason, the theoretical influence line is not suitable for B-WIM applications (QUILLIGAN, M., 2003). Thus, differently from the work of Moses, current methods perform the calibration step which aims to extract an experimental influence line. In the calibration procedure, a set of vehicles with known weight travels the bridge at constant speed and the resulting data is recorded. With the previously known axle weights together with measured strains and axle detection information, the experimental influence line of the bridge can be estimated and applied to weigh any vehicle of the traffic flow.

Although B-WIM systems are currently applied in many sites across the world, several installations achieved performance sufficient just to indicate possible overloaded vehicles, remaining the need of using static scales to effectively check it (RICHARDSON et al., 2014). Hence, the use of B-WIM data for direct enforcement of legal weight limits is limited to the accuracy level that still has not been reached to date (LYDON et al., 2016). When analyzing the difficulty to develop B-WIM systems with high accuracy level, it is widely reported in the literature that the dynamic oscillations of the vehicle and bridge are the main source of error (RICHARDSON et al., 2014). It also helps to explain why the overall accuracy of B-WIM systems are dependent of some site characteristics such as bridge span and road roughness

profile (JACOB; O'BRIEN; JEHAES, 2002), since these parameters are directly related to the vehicle-bridge dynamics.

The methods that directly employ considerations regarding dynamic effects, mainly related to moving force identification (MFI) (ROWLEY et al., 2009; FITZGERALD et al., 2017; DOWLING; O'BRIEN; GONZÁLEZ, 2012; DENG; CAI, C. S., 2010), have potential to be very accurate (YU; CAI, C. S.; DENG, 2016). However, these methods normally are too computationally expensive to be applied for real-time measurements (RICHARDSON et al., 2014). Therefore, in the current B-WIM literature most of methods are limited to static formulations, which do not make any direct consideration regarding dynamic behavior. As a consequence, previous studies observed that the results of these static methods are highly dependent on the bridge length, which could lead to undesirable performance (CARRARO et al., 2019).

Thus, it was noticed that there is a lack of B-WIM algorithms that perform approximate dynamic modeling with a computational cost close to the static methods on the current literature. In order to overcome this issue, this paper aims to adapt a recent method developed by Wang et al. (2017), which was proposed for extracting influence lines from measurements by an approximate dynamic modeling of the vehicle-bridge interaction process, to work as a B-WIM algorithm. The method of Wang et al. (2017) assumes the dynamic problem to be the passing of multiple moving forces through the bridge, applying a Euler-Bernoulli simply supported beam approximation. The analytical response of the bridge structure was divided into a fluctuation and a quasi-static parts. The former is related to the oscillation of the bridge due to the moving load, which remains after the vehicle leaves the bridge, while the latter is argued to be closely related with the static response. Hence, Wang et al. (2017) proposed to replace the quasi-static sinusoidal expression by a piece-wise cubic polynomial. Consequently, the response of the structure is considered as the superposition of the polynomial and fluctuation terms. Thus, the coefficients of the polynomial, which are extracted by least-squares, define the bridge influence line. By such an approach, the extraction of influence line requires only simple matrix operations, similarly to the current static B-WIM methods.

Although the approach proposed by Wang et al. (2017) is able to properly extract the bridge influence line, for both simulated signals and real bridge data, some of their points must be improved for it to work as a B-WIM method. Firstly, such conclusions were drawn based only on the analysis of a single vehicle run. That is, no procedure was proposed to assemble data from multiple runs, which is the usual case for the calibration step of B-WIM algorithms. As this method relies on determining the coefficients of functions, the procedure of taking the average of such coefficients does not seem to be a suitable procedure. Then, to perform the assembly strategy, in the present work, this algorithm is coupled with the maximum likelihood approach, analogously to the study of Ieng (2015). It results that the coefficients obtained are the maximum likelihood estimates for the set of all calibration runs, for the case of independent and identically distributed Gaussian error.

A second important point is the fact that the work of Wang et al. (2017) was done aiming only to extract influence lines. Then, it is still necessary the derivation of a procedure able to find the axle weights of the passing vehicle given that the influence line is known. This issue is addressed in the present paper by manipulating the expressions for influence line extraction, which also results in simple matrix operations. Thus, both influence line extraction and weigh procedure are maintained at a computational cost close to the one required by the state-of-the-art static methods.

Lastly, the formulation of Wang et al. (2017) has a clear advantage of including only continuous expressions, which are functions of the vehicle speed. Applying a continuous curve for influence line is interesting since it is the expected characteristic for a real bridge (ŽNIDARIČ; KALIN; KRESLIN, 2018). Moreover, the vehicle velocity plays a central role in B-WIM approaches, what led some authors to suggest that one influence line should be generated for each vehicle speed (O'BRIEN; GONZÁLEZ; DOWLING, 2010). However, the replacement of the quasi-static part by a polynomial could bias the solution with respect to the vehicle speed, since some part of the effect of this parameter on the bridge response is disregarded. Thus, it is proposed here that the full analytical model be applied into the B-WIM algorithm, aiming to represent as closely as possible the real dynamic behavior of the system. By this approach, the desired effect of the influence line being a function of the vehicle speed is achieved without the need of an extensive calibration procedure, based on several runs for a large set of vehicle speeds. In addition, all the equations of the proposed method are parametric, and consequently, the obtained influence lines are all continuous functions, which are in theoretical accordance with the behavior of real bridges.

The remaining of this paper is organized as follows. In Section 2, a discussion regarding some basic concepts of B-WIM systems is presented. Section 3 briefly describes the most important issues related to the approach proposed by Wang et al. (2017). In Section 4, the modifications applied in this work are detailed. The Section 5 addresses the numerical experiments performed to analyze the proposed adaptation into distinct scenarios. Section 6 presents some important remarks and suggestions for future works. At the end, Section 7 draws the main conclusions.

3.2   BASIC ASPECTS REGARDING B-WIM SYSTEMS

The usual B-WIM approach consists of transforming the bridge in a weighing mechanism. This tool enables monitoring vehicle weights at real time, providing valuable information for decision-making. It works by correlating data gathered from strain gauge sensors and the theoretical behavior of the structure, aiming to find the axle weights that provide the better agreement between theoretic and experimental results. For B-WIM applications, most studies relies on measuring flexural strains (HELMI; TAYLOR; ANSARI, 2015), which are collected by sensors attached to the bottom of bridge girders, usually at its mid-span. Hence, in this presentation, the bending moment at the cross section where the sensors are attached is

considered the monitored quantity. It is estimated from measured strains, referred to the bottom of bridge girders, through the following relation:

$$M^r = \sum_{g=1}^{G} E_g Z_g \varepsilon_g, \tag{1}$$

where E_g and Z_g are the elastic modulus and section modulus for girder g, from a total of G girders. In addition, M^r is the measured bending moment and ε_g represents the measured strain for the girder g, both defined as vectors recording the evolution of such quantities as the vehicle moves along the bridge.

The theoretical bending moment (M^t), in contrast, is usually computed considering the application of the influence line concept. The influence line represents the bending moment at the sensor position due to a unit moving load, as it travels over the bridge. Thus, the resulting bending moment could be calculated by summing up the contribution of each axle, quantified based on the influence line ordinate related to the current axle position. For a given scan k, it reads as:

$$M_k^t = \sum_{j=1}^{n} w_j L_{(k-b_j)}, \tag{2}$$

where:

$$b_j = \frac{d_j f}{v} \tag{3}$$

and w_j is the weight of the j axle, from a total of n. In addition, $L_{(k-c_j)}$ refers to the influence line ordinate at the position of the j axle, d_j is the distance between the first axle and j axle, b_j is the number of scans corresponding to d_j, f is the sampling frequency of the strain sensors and v is the vehicle speed. Parameters v and d_j are usually obtained from an axle detection system. For further details, the reader is referred to Carraro et al. (2019).

For defining the bridge influence line, one could proceed with just theoretical assumptions. However, as it is often the case, the real behavior of the bridge does not match the one resulted from a theoretical influence line, obtained from the bridge project, for example. In order to estimate a more suitable influence line, most recent methods employ a calibration procedure. In calibration, vehicles with known weight cross the bridge and the generated signals are recorded. Then, using the same principle of matching theory and experimental results, one could apply the known axle weights for obtaining a more accurate influence line estimate. Moreover, for a proper calibration procedure, it is desirable that as much data as possible be employed. It comprises distinct vehicles, traveling multiple times for a set of previously defined vehicle speeds. The passage of any single vehicle over the bridge is what is referred throughout this study as run. Therefore, it is often the case that multiple runs are necessary for calibrating the system and obtaining a more accurate influence line.

Figure 1 – Example of extracted influence line for data related to two distinct vehicles
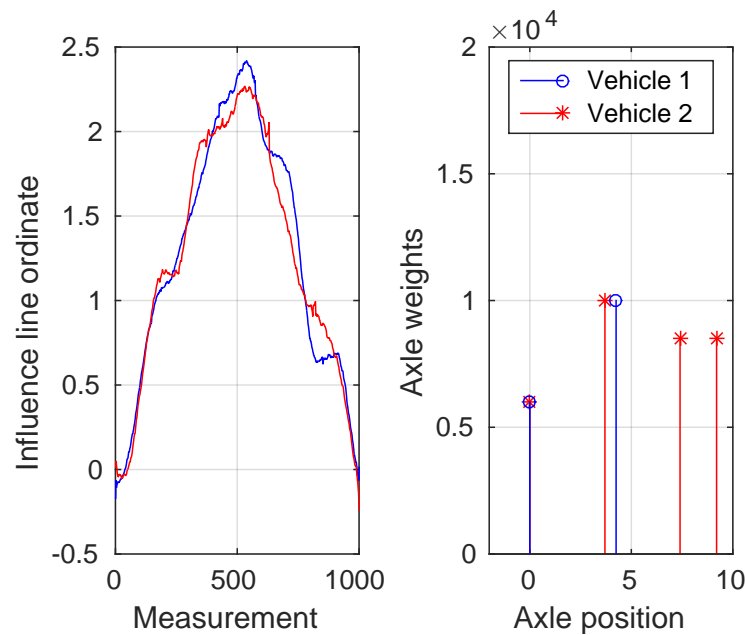
Although the calibration procedure may seem a simple concept, the proper extraction of the bridge influence line may present several practical complications. For instance, in an ideal scenario, influence lines estimated considering distinct vehicles in calibration process should represent equally well the real structure behavior. However, such an influence line could be excessively dependent of vehicle configuration, as illustrated by Figure 1. It employed numerically simulated signals for two distinct vehicles with the same velocity, available in Gonçalves, Carraro, and Lopez (2019). Each influence line was extracted utilizing the Matrix method (O'BRIEN; QUILLIGAN, M. J.; KAROUMI, 2006), considering just one specific signal for generating each curve. It could be observed that significant deviation occurs among each other. Furthermore, some dynamic oscillations seem to be incorporated in the influence lines, indicating that it was not able to distinguish among the bridge behavior and the vehicle-specific response.

The application of B-WIM systems relies on estimating the weight of passing vehicles. The weigh procedure is the methodology employed to join the influence line extracted and measured strains for reaching this goal. Then, at this step, the influence line is already known and the most likely axle weights that generated a given set of strain measurements are estimated. It is the dual problem of the calibration procedure. Thus, given that the influence line for the structure being analyzed is known, the weight of any passing vehicle can be readily calculated, for instance, from a least-squares procedure.

Summarizing, current B-WIM systems work with two clearly distinct phases. In the first, named calibration, vehicles with known weight cross the bridge structure and the recorded strains are employed to derive the bridge influence line. The second, called here weigh procedure, is the effective application of the system to weigh vehicles of the traffic flow. In this case, the influence line obtained in the calibration process is employed together with the collected

measurements to provide estimates for the weight of each travelling vehicle.

3.3   THE DYNAMIC MODEL FOR EXTRACTING THE BRIDGE INFLUENCE LINE

In what follows a brief description of the main aspects of the approach proposed by Wang et al. (2017) are discussed. Some notations and interpretations are slightly different from the original work, aiming to better relate it to B-WIM applications. For more details, including the full analytic treatment, the reader is referred to Wang et al. (2017).

The main idea behind the method is that the bridge measured response could be divided into two parts: the first one is due to the static response of the vehicle passing over the bridge, which is a function of the product of the vehicle weight and influence line ordinates, and the second one is a dynamic fluctuation response. Thus, the total response is the sum of both components, which should match the measured one.

The bridge influence line is represented as a piece-wise cubic polynomial. The reason behind such an assumption is that it is able to model the analytic static response of beams with boundary conditions ranging from simply supported to fixed at both ends, enabling also consideration of rotational stiffness. Furthermore, it is general enough to account for continuous bridges. For the case of a one span bridge, it reads as:

$$
L = \begin{cases} a_1 x^3 + a_2 x^2 + a_3 x + a_4 & 0 \le x \le \frac{\ell}{2} \\ a_5 x^3 + a_6 x^2 + a_7 x + a_8 & \frac{\ell}{2} < x \le \ell \end{cases} \tag{4}
$$

where L is the influence line ordinates, x is the respective position along the bridge span, a_i are the coefficients to be obtained through least squares and ℓ is the bridge span length. Therefore, the main goal of this method is to find the best values for the polynomial coefficients.

In order to easily perform this operation, the matrix X of the positions of the L ordinates on the bridge, is defined as:

$$
X = \begin{bmatrix} x_1^3 & x_1^2 & x_1 & 1 & 0 & 0 & 0 & 0 \\ & & \vdots & & & & \vdots & \\ \left(\frac{\ell}{2}\right)^3 & \left(\frac{\ell}{2}\right)^2 & \frac{\ell}{2} & 1 & 0 & 0 & 0 & 0 \\ 0 & 0 & 0 & 0 & \left(\frac{\ell}{2}\right)^3 & \left(\frac{\ell}{2}\right)^2 & \frac{\ell}{2} & 1 \\ & & \vdots & & & & \vdots & \\ 0 & 0 & 0 & 0 & x_o^3 & x_o^2 & x_o & 1 \end{bmatrix}_{(o \times 8)}, \tag{5}
$$

where o is the total number of influence line ordinates and x_i is the position on the bridge related to each ordinate i. The initial and final positions, x_1 and x_o, are usually defined as 0 and ℓ, respectively. It could be observed that there are two cubic polynomials in the formulation presented here, which represent the case of a one span bridge. For a continuous bridge, the number of terms increases.

In addition, the matrix of the axles weights ($\boldsymbol{A}$), applied to perform the discrete convolution related to the passage of the axles through the bridge, at each influence line ordinate, is defined as:

$$A_{pq} = \begin{cases} w_j, & \text{if } p = q + b_j \\ 0, & \text{otherwise} \end{cases},$$ (6)

where b_j is defined as in Equation (3). Therefore, the matrix $\boldsymbol{A}$ results in a Toeplitz shape. By making,

$$\boldsymbol{D}_\alpha = \boldsymbol{A}\boldsymbol{X},$$ (7)

the vector of structural response due to its static effect (S) could be written in matrix notation as:

$$S = \boldsymbol{D}_\alpha \lambda,$$ (8)

in which the vector λ is related to the coefficients that define the cubic polynomial, such as:

$$\lambda = \begin{bmatrix} a_1 & a_2 & a_3 & a_4 & a_5 & a_6 & a_7 & a_8 \end{bmatrix}^T.$$ (9)

It is worth to mention that the number of measurements collected and the number of influence line ordinates must match for the matrix operation be possible. Thus, some procedure of interpolating the collected signals should be performed and the increment value between x_i and x_{i+1} should be suitably chosen for ensuring that such dimensions match each other .

The dynamic model of the vehicle bridge system assumes that each vehicle axle is a concentrated force, equal to the axle weight. It is an extension of the work of Yang and Lin (2005), which considered a single force for the whole vehicle. As a result, it provides a closed-form solution, through modal superposition, for the multi-axle vehicle case. As commented previously, the structural response could be divided into two parts: quasi-static (u_1) and fluctuation (u_2), related to the vertical displacement of the structure. Such expressions for vertical displacement are useful to achieve the goal of deriving a formulation based on bending moment and can be derived as:

$$u_1(x,t) = \sum_m \left(\sin\left(\frac{m\pi x}{\ell}\right) \sum_{i=1}^{n} \frac{\Delta_{m,i}}{1-s_m^2} \left(H\left(t-t_{pi}\right) \sin\frac{mv\pi(t-t_{pi})}{\ell} \right.\right.$$
$$\left.\left. + H\left(t-t_{qi}\right) \sin\frac{mv\pi(t-t_{qi})}{\ell} \right)\right)$$ (10)

and

$$u_2(x,t) = \sum_m \left(\sin\left(\frac{m\pi x}{\ell}\right) \sum_{i=1}^{n} \frac{-s_m \Delta_{m,i}}{\left(1 - s_m^2\right)\sqrt{1 - \zeta_m^2}} \right.$$
$$\left. \left(\frac{H\left(t - t_{pi}\right)\sin\left(\omega_m\left(t - t_{pi}\right)\right)}{\exp\left(\zeta_m \omega_m\left(t - t_{pi}\right)\right)} + \frac{H\left(t - t_{qi}\right)\sin\left(\omega_m\left(t - t_{qi}\right)\right)}{\exp\left(\zeta_m \omega_m\left(t - t_{qi}\right)\right)} \right) \right) \tag{11}$$

where x and t are the position of the sensor and time, m is related to the modes of vibration considered, n is the number of axles, $H(.)$ is the Heaviside function, v is the vehicle speed, t_{pi} and t_{qi} are the times that the axle i enters and leaves the bridge, ω_m and ζ_m are the natural frequency and damping ratio of the m mode.

Furthermore, $\Delta_{m,i}$ is defined as:

$$\Delta_{m,i} = -\frac{2w_i \ell^3}{m^4 \pi^4 EI} \tag{12}$$

where E is the elastic modulus and I is the moment of inertia including the effect of all bridge girders, which are assumed to be constant throughout the structure. In addition, the s_m is calculated as:

$$s_m = \frac{m\pi v}{\ell \omega_m} \tag{13}$$

Recalling, for B-WIM applications usually a measure of the bending moment at the cross section is employed as quantity of interest. In order to adapt the analyzed formulation to this scenario, it is realized that for the Euler-Bernoulli beam theory the resulting moment could be written as a function of the vertical displacement:

$$M(x,t) = EI \frac{\partial^2 u(x,t)}{\partial x^2}, \tag{14}$$

again, assuming that both E and I are constant. Thus, it is allowed to represent the bending moment due to both components as:

$$M_1(x,t) = -EI \sum_m \left(\left(\frac{m\pi}{\ell}\right)^2 \sin\left(\frac{m\pi x}{\ell}\right) \sum_{i=1}^{n} \frac{\Delta_{m,i}}{1 - s_m^2} \left(H\left(t - t_{pi}\right) \sin\frac{mv\pi(t - t_{pi})}{\ell} \right. \right.$$
$$\left. \left. + H\left(t - t_{qi}\right) \sin\frac{mv\pi(t - t_{qi})}{\ell} \right) \right) \tag{15}$$

and

$$M_2(x,t) = -EI \sum_m \left(\left(\frac{m\pi}{\ell}\right)^2 \sin\left(\frac{m\pi x}{\ell}\right) \sum_{i=1}^{n} \frac{-s_m \Delta_{m,i}}{\left(1 - s_m^2\right)\sqrt{1 - \zeta_m^2}} \right.$$
$$\left. \left(\frac{H\left(t - t_{pi}\right)\sin\left(\omega_m\left(t - t_{pi}\right)\right)}{\exp\left(\zeta_m \omega_m\left(t - t_{pi}\right)\right)} + \frac{H\left(t - t_{qi}\right)\sin\left(\omega_m\left(t - t_{qi}\right)\right)}{\exp\left(\zeta_m \omega_m\left(t - t_{qi}\right)\right)} \right) \right). \tag{16}$$

The fluctuation part is applied to simulate the vibration of the structure. The quasi-static is replaced by the polynomial equations, since for low speed it is argued to be closely related with the static response of the structure. In other words, the response related to M_1 is replaced by S (Equation (8)).

Similarly to the static part, the fluctuation part could be written as a matrix operation. For this, the definition of the auxiliary matrix $\boldsymbol{D}_\beta$ is necessary:

$$D_\beta(t,m) = -\frac{2\ell s_m \sin\left(\frac{m\pi x}{\ell}\right)}{(m\pi)^2 \left(1 - s_m^2\right) \sqrt{1 - \zeta_m^2}} \sum_{i=1}^{n} w_i \left(\frac{H\left(t - t_{pi}\right) \sin\left(\omega_m\left(t - t_{pi}\right)\right)}{\exp\left(\zeta_m \omega_m \left(t - t_{pi}\right)\right)} + \frac{H\left(t - t_{qi}\right) \sin\left(\omega_m\left(t - t_{qi}\right)\right)}{\exp\left(\zeta_m \omega_m \left(t - t_{qi}\right)\right)} \right). \tag{17}$$

It is worth to mention that equations are displayed in their full form in the present work, whereas the original study opted for a slightly more simplified notation, omitting some constant terms. Both ways are equivalent since a distinct constant coefficient is fitted for each vibration mode through standard least squares and such coefficients are scale invariant when estimated by this method (JAMES et al., 2013).

Therefore, $\boldsymbol{D}_\beta$ is a matrix which has in each column the values of the fluctuation part related to the vibration mode m as a function of the time. In this matrix, each line corresponds to one discrete time step.

The vector of fluctuation response (F) is simplified by the expression:

$$F = \boldsymbol{D}_\beta \psi, \tag{18}$$

where ψ is a vector comprised of coefficients that multiply the response of each mode, analogous to the λ vector.

Thus, superposing static and fluctuation responses, the total theoretical bending moment response (M^t) could be written as:

$$\boldsymbol{D}_\alpha \lambda + \boldsymbol{D}_\beta \psi = M^t, \tag{19}$$

where $\boldsymbol{D}_\alpha$ and λ are the matrix of the cubic polynomial and its coefficients, respectively. Similarly, $\boldsymbol{D}_\beta$ and ψ are the matrix of dynamic properties and its coefficients.

This equation alone, however, does not ensure that the obtained influence line respects some conceptual characteristics expected for L, such as the continuity into the middle span and the zero value at both ends. The continuity and boundary conditions of the influence line is ensured based on a set of penalty equations:

$$\boldsymbol{D}_\gamma \lambda = 0, \tag{20}$$

where $\boldsymbol{D}_\gamma$ is a matrix containing constraint conditions, such as the zero value at both ends and the continuity of influence line values at the mid-span. This set of equations is easily added to

the matrix equation already described for the response of the structure, aiming to create only one big set of equations for the method as a whole.

The fitting parameters λ, related to the coefficients of the cubic polynomial that describes the bridge influence line, are the main variables of interest. They are extracted applying least squares technique, with a penalization parameter large enough to provide a feasible influence line ($\boldsymbol{D}_\gamma$). It is worth to point out that the method is able to deal with influence lines for both strains and displacements, since they are closely related. Including all the terms of the formulation, it results:

$$\boldsymbol{D}\theta = Y^t, \tag{21}$$

where $\boldsymbol{D}$ is the matrix including $\boldsymbol{D}_\alpha$, $\boldsymbol{D}_\beta$ and $\boldsymbol{D}_\gamma$, Y^t is the theoretical structure response vector and θ is the vector comprised of the parameters of interest λ and ψ.

Let Y^r the measured structure response vector, defined by the measured strains converted to bending moment as in Equation (1), and some zeros related to the number of constraints applied. In order to estimate θ, one could employ a least squares procedure aiming to minimize the error between Y^t and Y^r. The resulting expression for θ reads as:

$$\theta = \left(\boldsymbol{D}^T\boldsymbol{D}\right)^{-1}\left(\boldsymbol{D}^T Y^r\right) \tag{22}$$

Thus, for a given event, one could extract the static influence line by finding the λ parameters using such an equation, since λ corresponds to the first 8 terms of the vector θ.

3.4 MODIFIED APPROACH

The approach proposed by Wang et al. (2017) intended to provide a way to better extract the bridge influence line through dynamic assumptions and field measurements. Although promising results were reached, some points still have to be improved to adapt it to work as a B-WIM algorithm. Thus, the present study aims to propose some adaptations to this approach in order to generate a practical B-WIM algorithm. The main points addressed are summarized in what follows and better described in next sections:

- inclusion of assembly strategy: in the original paper, the extraction of influence line was conducted only to one vehicle at time. Thus, in the case of multiple runs, as in B-WIM system calibration, no assembly strategy was proposed. In the current work, a maximum likelihood strategy is adopted, similar to the one proposed by Ieng (2015) for the static case. By this, any number of events could be considered and all calculated parameters, including the dynamic ones, can be properly extracted;

- derivation of weigh procedure: As the work of Wang et al. (2017) was focused on influence line extraction, no weigh procedure was proposed. In the present work, the equations are rearranged in such a way that the weigh procedure is enabled.

Moreover, it results in simple matrix operations, which are easily computationally addressed;

- in the original study, a piece-wise cubic polynomial is applied to represent the quasi-static response, which is an approximation. Although it seems an useful approach when seeking for the static bridge influence line, this may not be the ideal approach to weigh vehicles. Thus, it is proposed to account for the analytic expression of both fluctuation and quasi-static response. The fitted coefficients can, then, be applied to generate the bridge influence line accounting for distinct vehicle speeds.

3.4.1 Assembly strategy

The assembly strategy is based on the approach of Ieng (2015), which applied the maximum likelihood estimate (MLE) to the influence line based on a set of distinct calibration runs. By this perspective, it is assumed that there is an error (η) between measurements and theoretical model:

$$Y_i^r = Y_i^t + \eta_i, \tag{23}$$

where Y^t and Y^r are the theoretical and measured response, respectively. The theoretical model is given by Equation (21), also including the terms related to the penalization, and the measured response is written as discussed in previous section. Furthermore, η is assumed to follow a zero mean multivariate Gaussian random distribution and i ranges from one to c, the total number of calibration events available. For further practical details of this step, the reader is referred to Carraro et al. (2019). By these assumptions, the maximum likelihood estimate for the coefficients of the method are obtained solving the following equation for θ:

$$\sum_{i=1}^{c} \mathbf{D}_i^T \mathbf{D}_i \theta = \sum_{i=1}^{c} \mathbf{D}_i^T Y_i^r, \tag{24}$$

where $\mathbf{D}$ and θ are the same quantities defined in Equation (21). However, it is interesting to remark that $\mathbf{D}_i$ is a matrix associated with the run i, which changes with each distinct calibration run since it depends on parameters such as vehicle speed, axle weights and spacing. The solution is similar to the formulation for extracting one influence line per calibration run, that is:

$$\theta = \left(\sum_{i=1}^{c} \mathbf{D}_i^T \mathbf{D}_i \right)^{-1} \left(\sum_{i=1}^{c} \mathbf{D}_i^T Y_i^r \right) \tag{25}$$

It is worth to mention that in the case of only one calibration run available, the results of this approach and the one adopted by Wang et al. (2017) are the same. However, this is a very unlikely case for B-WIM applications, since the procedure recommended is to employ, at least, 10 runs per vehicle (JACOB; O'BRIEN; JEHAES, 2002). A remarked difference among

the method presented by Ieng (2015) and the adaptation performed in the present study is the fact that in the former an influence line is derived point by point, without ensuring that a continuous curve is reached. On the other hand, the latter directly obtains the maximum likelihood estimates for the coefficients of a continuous curve.

3.4.2 Weigh procedure

As the original work intended to extract a static influence line, the fluctuation part was calculated and removed from each signal. However, the axles weights were supposed to be known in this process. Thus, the derivation of a weigh procedure is not straightforward and involves mathematical manipulations.

The main idea to overcome this issue is to develop a dynamic influence line calculation. By this approach, the parameters fitted in the calibration process are used to define an equation for influence line, which is a function of the vehicle speed. Then, it is allowed the generation of one equation for each vehicle speed. In order to make it possible, the equations for the theoretical bridge dynamic response showed in Equation (19) are rewritten as:

$$
\begin{aligned}
M^t = \sum_{i=1}^{n} w_i L(d_i) - \sum_{m} \psi_m \Bigg(&\sin\left(\frac{m\pi x}{\ell}\right) \frac{2s_m \ell}{m^2 \pi^2 \left(1 - s_m^2\right) \sqrt{1 - \zeta_m^2}} \\
\sum_{i=1}^{n} w_i \Bigg(&\frac{H\left(t - t_{pi}\right) \sin\left(\omega_m \left(t - t_{pi}\right)\right)}{\exp\left(\zeta_m \omega_m \left(t - t_{pi}\right)\right)} + \frac{H\left(t - t_{qi}\right) \sin\left(\omega_m \left(t - t_{qi}\right)\right)}{\exp\left(\zeta_m \omega_m \left(t - t_{qi}\right)\right)} \Bigg) \Bigg)
\end{aligned}
\tag{26}
$$

where both the fluctuation and static polynomial component are summed together. In addition, the influence line $L(d_i)$ refers only to the static component, remarking the fact that it is necessary to match the influence line ordinate with position of axle i. In this case, the distance among the first and i axle (d_i) is employed to properly correspond bridge influence line ordinates with the time that each individual axle enters the bridge (t_{pi}). In Equation (26), the unknowns are the axle weights w_i. The summation of the second term could be reordered, resulting in:

$$
\begin{aligned}
M^t = \sum_{i=1}^{n} w_i L(d_i) - \sum_{i=1}^{n} w_i \sum_{m} \psi_m \Bigg(&\sin\left(\frac{m\pi x}{\ell}\right) \frac{2s_m \ell}{m^2 \pi^2 \left(1 - s_m^2\right) \sqrt{1 - \zeta_m^2}} \\
\Bigg(&\frac{H\left(t - t_{pi}\right) \sin\left(\omega_m \left(t - t_{pi}\right)\right)}{\exp\left(\zeta_m \omega_m \left(t - t_{pi}\right)\right)} + \frac{H\left(t - t_{qi}\right) \sin\left(\omega_m \left(t - t_{qi}\right)\right)}{\exp\left(\zeta_m \omega_m \left(t - t_{qi}\right)\right)} \Bigg) \Bigg)
\end{aligned}
\tag{27}
$$

where the dependence of $\Delta_{m,i}$ to w_i, given by Equation (12), is written explicitly. This expression could be rewritten including both terms in the same summation:

$$M^t = \sum_{i=1}^{n} w_i \left(L(d_i) - \sum_m \psi_m \left(\sin\left(\frac{m\pi x}{\ell}\right) \frac{2s_m\ell}{m^2\pi^2 \left(1 - s_m^2\right)\sqrt{1 - \zeta_m^2}} \right.\right.$$
$$\left.\left. \left(\frac{H\left(t - t_{pi}\right)\sin\left(\omega_m\left(t - t_{pi}\right)\right)}{\exp\left(\zeta_m\omega_m\left(t - t_{pi}\right)\right)} + \frac{H\left(t - t_{qi}\right)\sin\left(\omega_m\left(t - t_{qi}\right)\right)}{\exp\left(\zeta_m\omega_m\left(t - t_{qi}\right)\right)} \right) \right) \right) \tag{28}$$

Thus, the expression can be simplified in matrix notation:

$$M^t = \boldsymbol{C}W \tag{29}$$

where W is the vector of axle weights and $\boldsymbol{C}$ is the matrix including the superposition of static and fluctuation responses, which can be written as:

$$C(t,i) = \left(L(d_i) - \sum_m \psi_m \left(\sin\left(\frac{m\pi x}{\ell}\right) \frac{2s_m\ell}{m^2\pi^2 \left(1 - s_m^2\right)\sqrt{1 - \zeta_m^2}} \right.\right.$$
$$\left.\left. \left(\frac{H\left(t - t_{pi}\right)\sin\left(\omega_m\left(t - t_{pi}\right)\right)}{\exp\left(\zeta_m\omega_m\left(t - t_{pi}\right)\right)} + \frac{H\left(t - t_{qi}\right)\sin\left(\omega_m\left(t - t_{qi}\right)\right)}{\exp\left(\zeta_m\omega_m\left(t - t_{qi}\right)\right)} \right) \right) \right) \tag{30}$$

Therefore, instead of performing the sum of the contribution of each axle at the same vibration mode, such as in calibration, here it is performed the sum of the contribution of each mode shape for the response to a single axle. Each column of the matrix $\boldsymbol{C}$ can be interpreted as the dynamic bridge influence line, shifted to coincide with the time that axle i enters and leaves the bridge. Then, one could note that the vehicle speed is a parameter for the derived influence line. Figure 2 presents an example of this influence line, as a function of vehicle speed. It may be observed that the shape differs from each other due to this dependence on vehicle velocity as an inherent parameter and, in especial, from the static one, which does not change within this parameter. Furthermore, the dynamic influence line remains affecting the response of the bridge even when the axle leaves the bridge, whereas the static one ends its effect in this case. This dependence on vehicle speed is in accordance with some works in B-WIM algorithms, which already noticed the possible improvement due to perform distinct fits for each vehicle speed (O'BRIEN; GONZÁLEZ; DOWLING, 2010). In addition, the approach derived here provides parametric equations that remark the importance of such a parameter. Thus, it is possible to provide one influence line for each vehicle speed without the need of conducting a highly expensive calibration procedure, comprised of several runs at each specific speed.

Recalling Equation (29), given the measured bending moment M^r, one could calculate the axle weights by employing the least squares method, resulting in:

$$W = \left(\boldsymbol{C}^T \boldsymbol{C} \right)^{-1} \left(\boldsymbol{C}^T M^r \right). \tag{31}$$

Figure 2 – Example of influence line as a function of speed
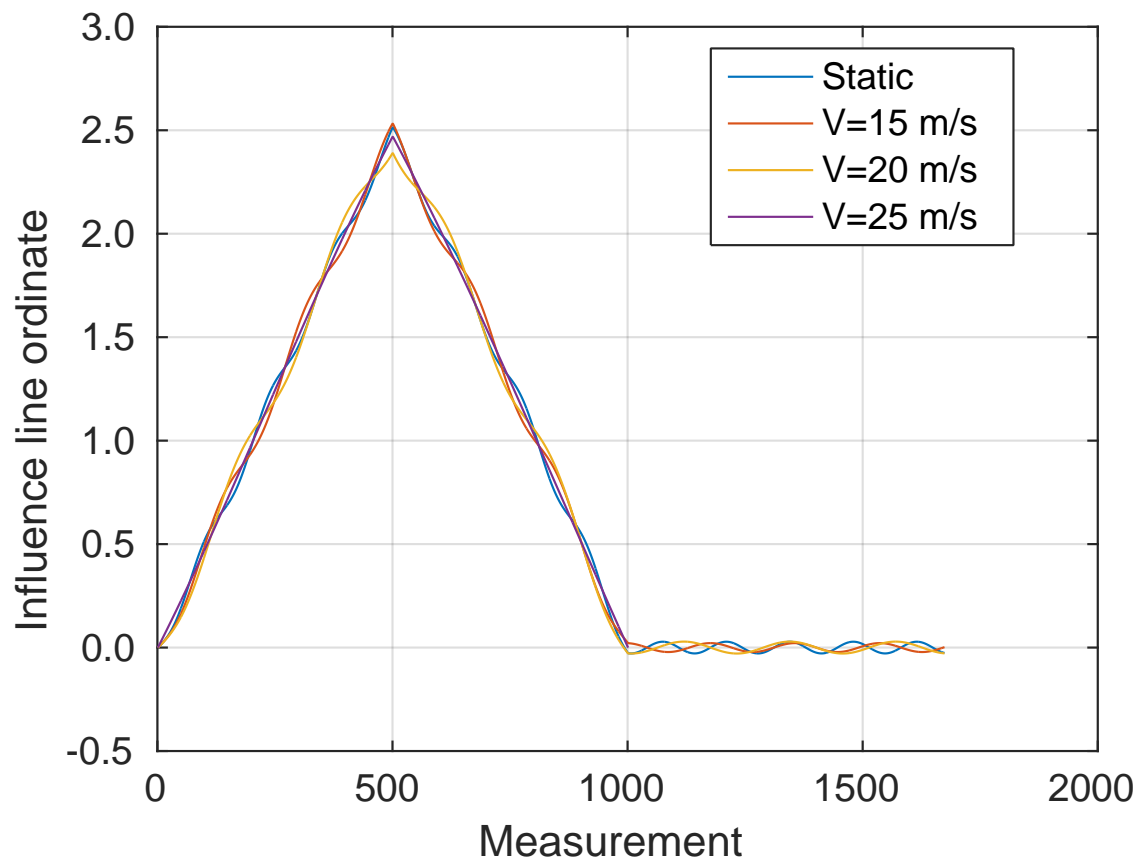
It is worth to mention that the only unknowns in this case are the axle weights, since the calibration procedure is enough to provide all the coefficients necessary to calculate the matrix **C**.

Moreover, the equations described in the present paper are slightly different from the approach proposed by Wang et al. (2017). In the present study, all parameters are included into matrix **C**, instead of disregarding the constant terms. As already discussed, this procedure does not change the estimated influence lines or weights, since those terms are just constants. The only difference is when one parameter is zero, since it removes the influence of such term from the response. This fact occurs for the even mode shapes of the simply supported Euler-Bernoulli beam model, since the sensors are located in the mid-span of the bridge in this study. Thus, instead of fitting a coefficient related to a mode shape that theoretically should not be significant to the bridge response, in the proposed adaptation, the even mode shapes are disregarded. As it is more in accordance with the behavior of the model used as approximation for the bridge response, it is expected that the generalization capacity for weighing vehicles distinct of those ones used for calibration to be improved. In addition, this interpretation also ensures that coefficients ψ derived make physical sense: the more similar to 1 they are, the more suitable the analytical response seems. In the numerical results section, the application

of even modes is tested in order to check the suitability of the affirmations stated here.

3.4.3 Full analytical response

The approach just derived is related to the fitting procedure proposed by Wang et al. (2017), which replaces the quasi-static analytical response by a polynomial term. However, as what is searched here is for a more efficient B-WIM algorithm, it is expected that including the full analytical response should be more suitable for the overall results. Therefore, the expressions for influence line extraction and weight estimate are extended to account for both the quasi-static and fluctuation parts of the analytical approach.

These modifications consist of algebraic manipulations. For the influence line extraction, the $\boldsymbol{D}_\alpha$ matrix should be replaced by:

$$
D_\alpha(t,m) = \frac{2\ell \sin\left(\frac{m\pi x}{\ell}\right)}{m^2\pi^2 \left(1 - s_m^2\right)} \sum_{i=1}^{n} w_i \left(H\left(t - t_{pi}\right) \sin\frac{mv\pi(t - t_{pi})}{\ell} + \right.
$$
$$
\left. H\left(t - t_{qi}\right) \sin\frac{mv\pi(t - t_{qi})}{\ell} \right),
$$

(32)

which was derived based on the quasi-static response presented in Equation (15), similarly to what was previously done to calculate $\boldsymbol{D}_\beta$. It is worth to remark that no constraints are necessary for the full analytical procedure, since derived curves already respect the theoretical expected behavior. For instance, they are ensured to be continuous curves at all points. Then, one could proceed as in Equation (24), considering that the matrix $\boldsymbol{D}$ is comprised just of $\boldsymbol{D}_\alpha$ and $\boldsymbol{D}_\beta$ components and $Y^r = M^r$.

In addition, the matrix $\boldsymbol{C}$ employed for weight estimation is modified to account for the inclusion of the quasi-static component instead of the simplified static one:

$$
C(t,i) = \sum_m \rho_m \left(\sin\left(\frac{m\pi x}{\ell}\right) \frac{2\ell}{m^2\pi^2 \left(1 - s_m^2\right)} \left(H\left(t - t_{pi}\right) \sin\frac{mv\pi(t - t_{pi})}{\ell} \right.\right.
$$
$$
\left.\left. + H\left(t - t_{qi}\right) \sin\frac{mv\pi(t - t_{qi})}{\ell} \right) \right) -
$$
$$
\sum_m \psi_m \left(\sin\left(\frac{m\pi x}{\ell}\right) \frac{2s_m\ell}{m^2\pi^2 \left(1 - s_m^2\right) \sqrt{1 - \zeta_m^2}} \right.
$$
$$
\left. \left(\frac{H\left(t - t_{pi}\right) \sin\left(\omega_m\left(t - t_{pi}\right)\right)}{\exp\left(\zeta_m\omega_m\left(t - t_{pi}\right)\right)} + \frac{H\left(t - t_{qi}\right) \sin\left(\omega_m\left(t - t_{qi}\right)\right)}{\exp\left(\zeta_m\omega_m\left(t - t_{qi}\right)\right)} \right) \right),
$$

(33)

where ρ_m is the fitted coefficient for the quasi-static response of each vibration mode. As, in this case, no polynomial term is available, the vector of parameters θ comprises coefficients ρ and ψ. Figure 3 shows the effect of the vehicle speed in the influence line obtained considering the full analytical treatment for the simplified vehicle-bridge interaction problem. The conclusions

Figure 3 – Example of dynamic influence line as a function of speed for the full analytical method
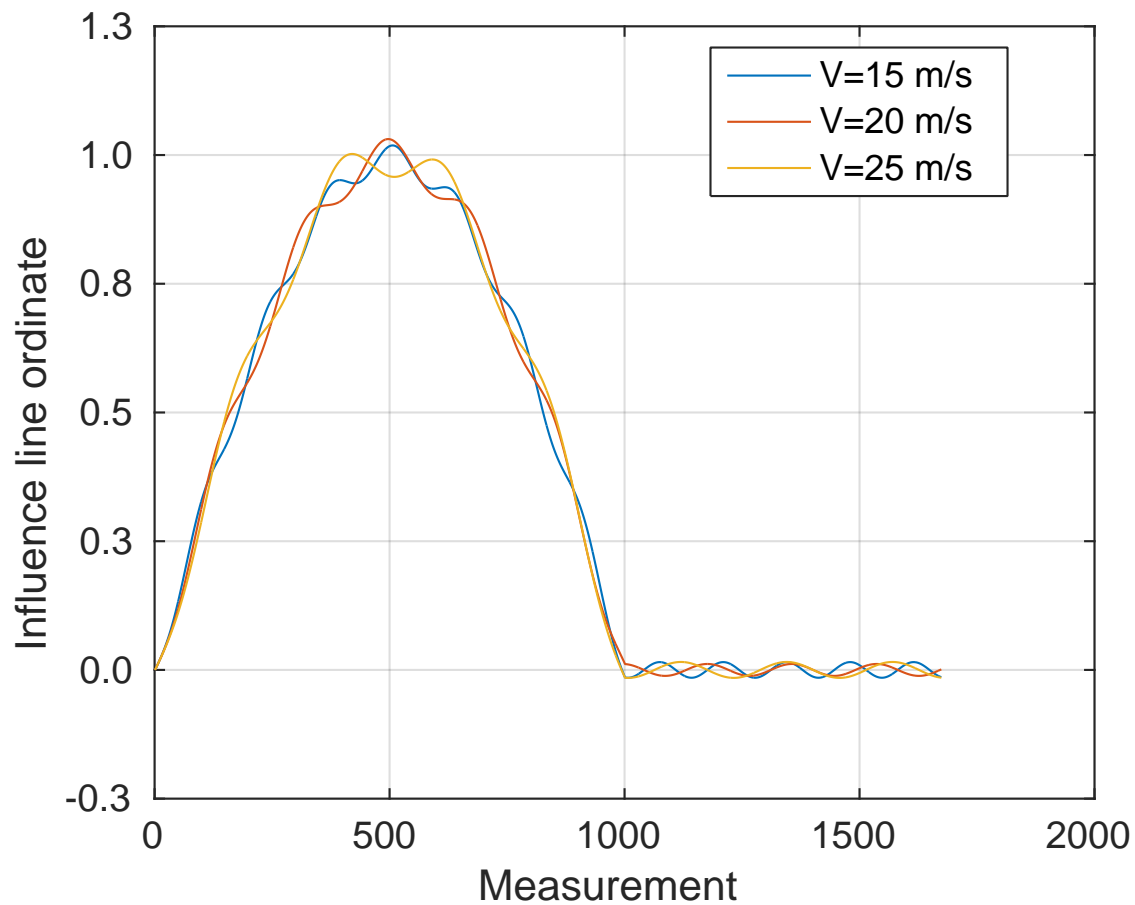
are similar to those drew from Figure 2. The main difference is that for the analytical approach no static component is available. Consequently, the influence line generated using the full analytical method at different vehicle speeds should be more distinct from each other, which is really observed in Figure 3. It is also interesting to observe that the behavior of the curve agrees with the expected one, even without necessity of utilizing the constraint term $\boldsymbol{D}_\gamma$, as previously discussed.

Although the approach using the full analytical solution for the simplified dynamic problem seems more suitable, comparisons of performance with other configurations are useful to ensure that this suitability is really confirmed. Then, for the numerical analyses performed in the next section, three distinct formulations will be compared, named as:

1. Standard: the method using the polynomial approximation for the quasi-static response, as suggested in the original work of Wang et al. (2017);

2. Analytical: the algorithm that applies the full analytical modeling for the simplified vehicle-bridge interaction model;

3. Static: the method that uses only the polynomial equation as fitting model.

Figure 4 – Example of extracted influence line for data related to two distinct vehicles
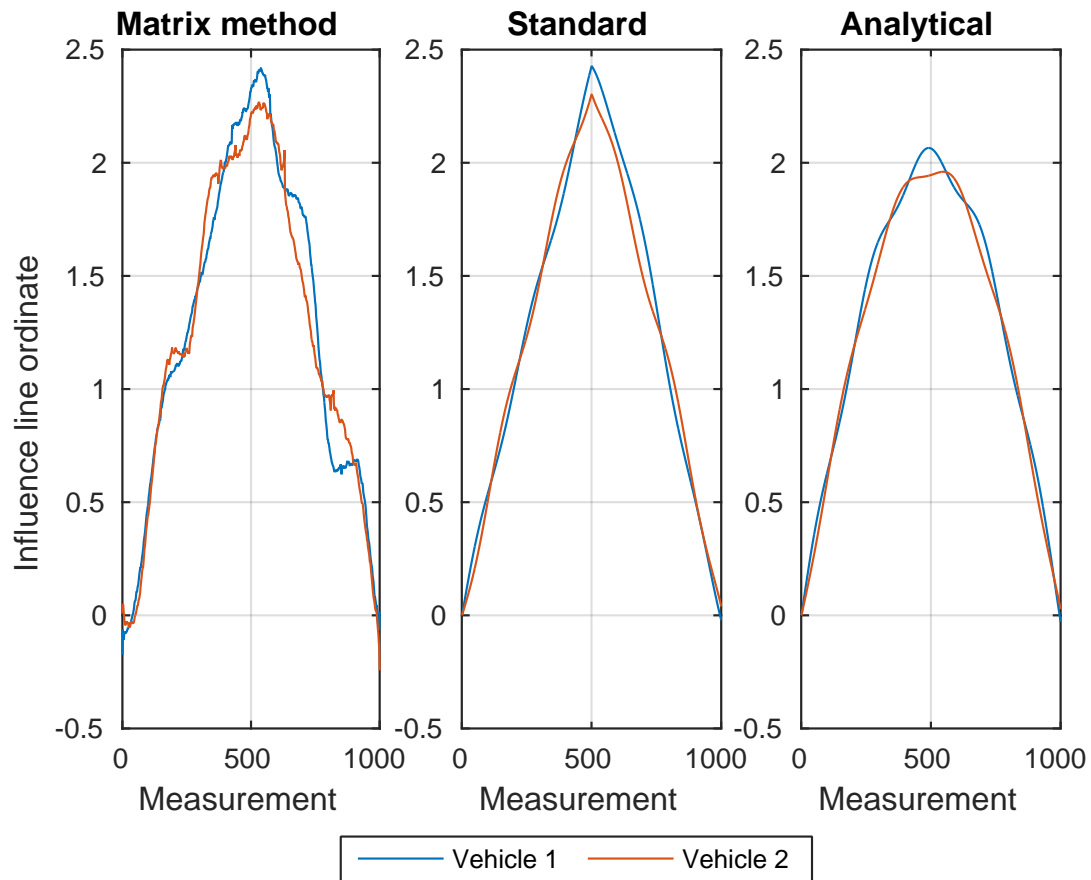
At this point, it is interesting to recall the issues related with influence line extraction previously discussed in Figure 1. In that case, distinct behavior among influence lines extracted considering data from distinct vehicles, at the same speed, was noticed. Figure 4 presents the same analysis, however considering Standard and Analytical approaches just defined. It could be seen that derived curves are more closely related for both methods. In addition, unlikely patterns such as the oscillations presented by Matrix method are not observed for Standard and Analytical cases. Indeed, fitting coefficients of continuous curves instead of each specific influence line ordinate is less susceptible to incorporate particular aspects that are not related with the real bridge behavior. For instance, the particular noise for a specific event. This is a promising first analysis for both proposed methods. More detailed numerical analyses are conducted in following section.

3.5 NUMERICAL RESULTS

In order to assess the suitability of the approaches proposed in the present study as B-WIM algorithms, a set of numerically simulated signals for the bridge response due to passing vehicles is employed. This dataset is available in Gonçalves, Carraro, and Lopez (2019). For a

more detailed description of the procedure employed for generating such signals, as well as the parameters utilized, the reader is referred to Carraro et al. (2019). In what follows, the main practical aspects of this dataset are discussed.

The dataset is comprised of simulations of the mid-span strains at the bottom of the girder generated by a set of vehicles on bridges with distinct characteristics. The bridge superstructure for all cases is comprised of a single girder, whose deck influence on bridge stiffness is disregarded. The previously cited characteristics are combinations of 3 distinct bridge span lengths and 3 road roughness profiles, considering a simply supported Euler-Bernoulli beam model. The road roughness classes are defined based on a widely used classification (ISO 8606:1995, 1995), where roughness amplitudes 0, 4 and 16 correspond to no roughness, class A and class B, respectively. Thus, a total of 9 cases are evaluated in the present study, all of them assuming values in accordance with the recommendations of Jacob, O'Brien, and Jehaes (2002), reflecting situations with practical interest:

1. bridge span length of 10m and no road roughness;

2. bridge span length of 10m and road roughness class A;

3. bridge span length of 10m and road roughness class B;

4. bridge span length of 20m and no road roughness;

5. bridge span length of 20m and road roughness class A;

6. bridge span length of 20m and road roughness class B;

7. bridge span length of 30m and no road roughness;

8. bridge span length of 30m and road roughness class A;

9. bridge span length of 30m and road roughness class B.

As the objective of this study is to evaluate the potential of the proposed methods as B-WIM algorithms, the simulated signals related to calibration vehicles are distinct from the ones applied to effectively test the algorithm. It aims to reproduce the real in-service operation of a B-WIM system, since the calibration process usually is restricted to few vehicles. For calibration, 40 runs of two distinct vehicles, with two and four axles, are applied, 20 for each of them. For testing, 200 runs are performed considering randomly generated vehicles with number of axles ranging from 2 to 9. The weight of each axle and its axle spacing are defined according to a classification often applied for Brazilian vehicles (DNIT, 2012). Table 1 presents the vehicle classes employed and their respective number of axles. The vehicle speed at each testing run is an uniform random variable ranging from 10 to 25 m/s. It is worth to mention that the damping and stiffness of the suspension of each axle is included into the model. Moreover, a Gaussian random noise with signal to noise ratio of 20 is added to every simulated signal in order to replicate some undesired effects on the measurement system. Hence, given the above described numerical model (which accounts for the vehicle damping and stiffness, rough surface, distinct bridge span lengths and noise applied to every signal), it is expected

for this numerical experiment to be representative enough to simulate the real challenges of current B-WIM systems.

Table 1 – Classes of vehicles employed

| Vehicle Class	Number of axles
2C	2
3C	3
4CD, 2S2	4
3I2, 2S3, 3S2	5
2R4, 3S3, 3D3, 3N3	6
3D4 , 3N4	7
3D5	8
3M6 , 3Q6	9

For all analyses conducted in this section, the mean absolute error in weight prediction for all testing runs is the performance criterion. Three main aspects are analyzed. Firstly, the trend in weight estimate accuracy and the number of dynamic modes employed in the model is verified. Secondly, the robustness of the methods regarding its own parameters is evaluated. Lastly, the results are compared with a set of 4 state-of-the-art static algorithms. Such aspects are useful to provide a big picture of the main characteristics of the analyzed approaches and their real potential for the practical application in B-WIM systems.

3.5.1   Effect of increasing number of modes

For both, the Standard and Analytical approaches, the number of vibration modes considered in the analysis is defined by the user. Increasing the number of mode shapes should, theoretically, improve the weight estimates. However, the dynamic models of the analyzed approaches differ from the simulated one, as well as from the real field signals. Moreover, even in the case that increasing the number of modes really results in an accuracy improvement, it also increases the number of parameters that must be provided to the algorithm. In this regard, there are two parameters, the bridge natural frequency (ω_m) and the damping ratio (ζ_m) for each vibration mode included in the model. Thus, for the first analysis, it is intended to search for the minimum number of modes necessary for each method, given that the exact model parameters are known. This verification is useful to indicate a practical initial configuration for each method.

The results of the standard method are illustrated in Figure 5a, for modes ranging from 1 to 5. Analogously, Figure 5b presents the same analysis for the Analytical method. In order to allow the evaluation of even vibration modes, the term $\sin\left(\frac{m\pi x}{\ell}\right)$ is disregarded in all equations, since it would result in zero for all even modes. The overall behavior of both methods is similar. The accuracy of the estimated weights decreases with the increase of the bridge span length, which is an already expected result. Regarding the road roughness profile, it

Figure 5 – Results for distinct number of modes

(a) Standard method

(b) Analytical method
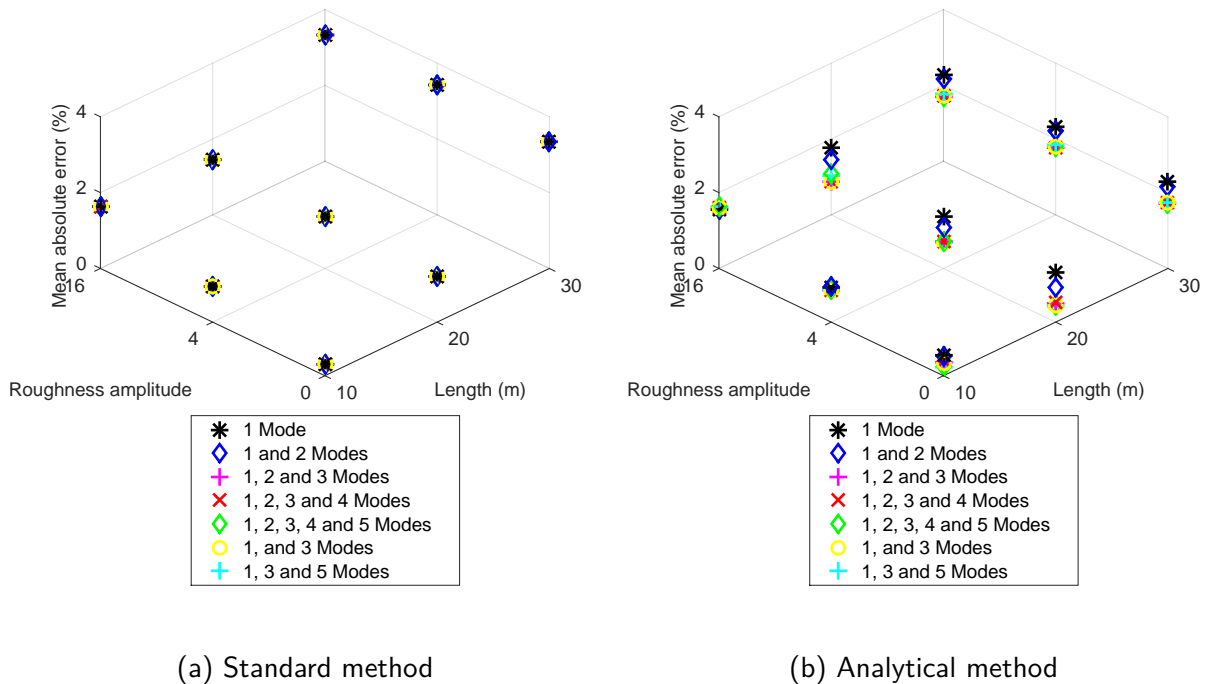
seems to be more significant for the short span bridges. Indeed, for the 30 m bridge, the results of both approach were almost independent of the road roughness class. Both behaviors are in accordance with Carraro et al. (2019), which have employed the same dataset. Furthermore, it was observed a trend in the Analytical method to perform better than the standard one, mainly when increasing the bridge span length. This last aspect is better analyzed in following sections.

Regarding the influence of number of vibration modes, the mean absolute error for the standard method presented just slight variations when changing this parameter. Hence, increasing the number of vibration modes does not significantly affect the accuracy of this method. On the other hand, for the Analytical approach, increasing the number of modes is able to improve the results for longer bridges, independently of their road roughness. A more detailed analysis indicates that the inclusion of the vibration mode 3 is the main responsible for this improvement, since the mean absolute error of the method applying only modes 1 and 3 is able to reach the best performance for all analyzed cases. The inclusion of modes 2 and 4 did not introduce valuable information to the model, only increasing the computational cost. In some cases, as the road roughness class B and the 20 m bridge, it resulted in worse estimates. As already discussed, the effect of even modes for modeling strains at the middle span of a simply supported beam should be negligible. In addition, the inclusion of the mode 5 may not affect the overall results due to the difference between the assumptions of the method and the model employed to simulate the dynamic behavior of the vehicle-bridge system.

The behavior of the Analytical and Standard methods in all analyzed cases as a function of the number of modes indicate that even modes do not contribute to performance

improvement. This last statement is in accordance with theoretical aspects already discussed in previous sections. Then, in the following analyses, only odd vibration modes are considered. Since a total of 9 cases were evaluated, and the same trend was observed, it could be suggested the use of 1 and 3 vibration modes for the Standard and Analytical methods, respectively. It is worth to point out that, by the dynamic modeling perspective, the Standard method has only one sinusoidal term per mode, whose frequency is ω_m. It occurs because the quasi-static response is replaced by a piece-wise cubic polynomial in this approach. Thus, it is not surprising that the best number of modes between both methods differs.

### 3.5.2   Effect of error in model parameters

The previous verification was performed in an ideal scenario, where all model parameters were exactly known. However, since model parameters usually are not known with high accuracy, it is interesting to verify how the results are influenced by errors in the estimation of such parameters. In other words, what is intended is checking the robustness of the analyzed approaches regarding its own model parameters. With this goal in mind, in this section, errors are introduced to both parameters, ζ_m and ω_m, and the effects on weight estimates are reported. It is desired that the performance does not be excessively corrupted by these not exact values.

The first point verified is related to the influence of the damping ratio on the weight estimates. As this parameter usually has low values, such as the 0.05 employed in this dataset, only two cases shall be evaluated: using the exact value or assuming zero for its value. It is expected that the influence does not be so expressive due to the short time that the vehicle passes through the bridge together with the low value of damping applied in this study. It is worth to mention that the value adopted for damping ratio in this study remains at a realistic level for vehicular bridges (CASTELLANOS-TORO et al., 2018).

Figure 6a and Figure 6b present the results of the Standard and Analytical methods, respectively, as a function of the damping ratio (ζ). For the analytical approach, the case with only 1 mode is included aiming to improve comparisons. For all evaluated cases of the Standard approach and the Analytical method with 3 modes, the results did not change significantly, indicating that precision in this parameter is not a central feature for these methods. The exception is the Analytical approach with only 1 mode. However, the performance reported is similar to the case adopting the exact damping ratio. Furthermore, the 3 mode case surpassed the results for all cases with 1 mode, even when disregarding damping ratio. By these results, it could be inferred that both methods are robust to the ζ parameter. Therefore, in following analysis the Analytical method is evaluated only with 3 modes and the damping ratio will be assumed zero for both Standard and Analytical approaches.

The next analysis is related to the error in the estimate of the bridge natural frequency for all vibration modes. This error was introduced in the model as an error in estimating the bridge inertia moment, by a factor ranging from 50% to 150%, where 100 % indicates that

Figure 6 – Results for two distinct values of damping ratio
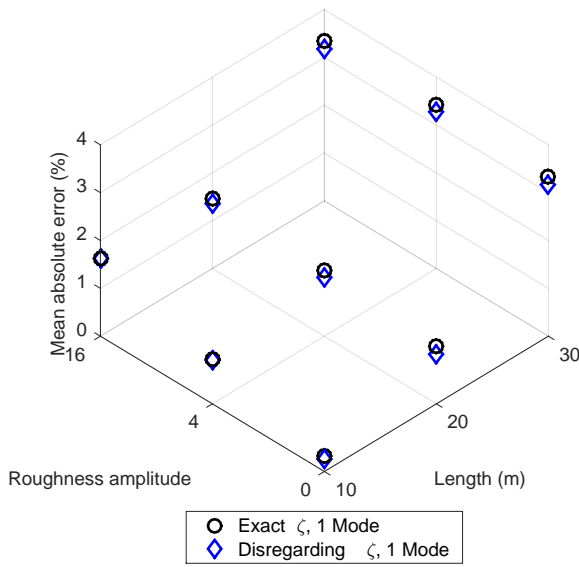
(a) Standard method
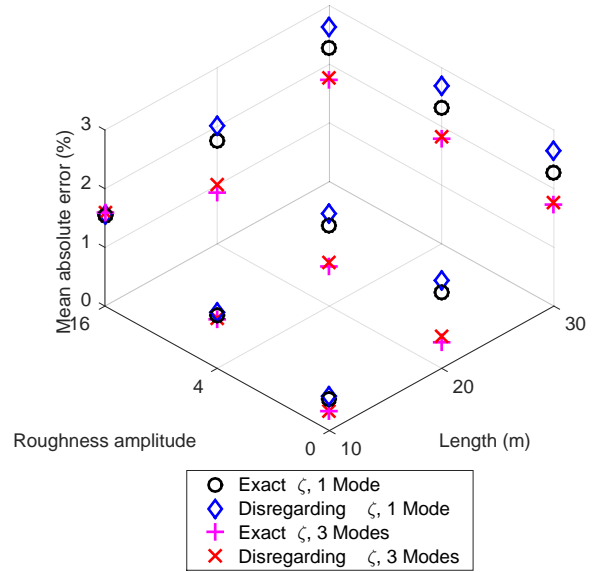
(b) Analytical method

Figure 7 – Comparison among results as a function of the error in estimating the bridge moment of inertia
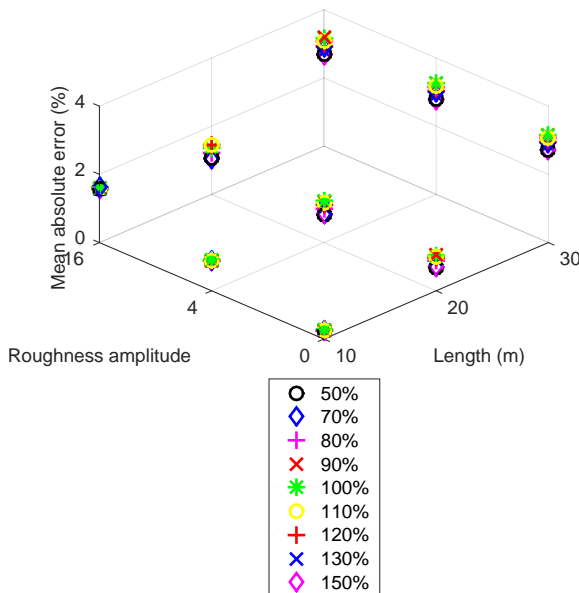
(a) Standard method
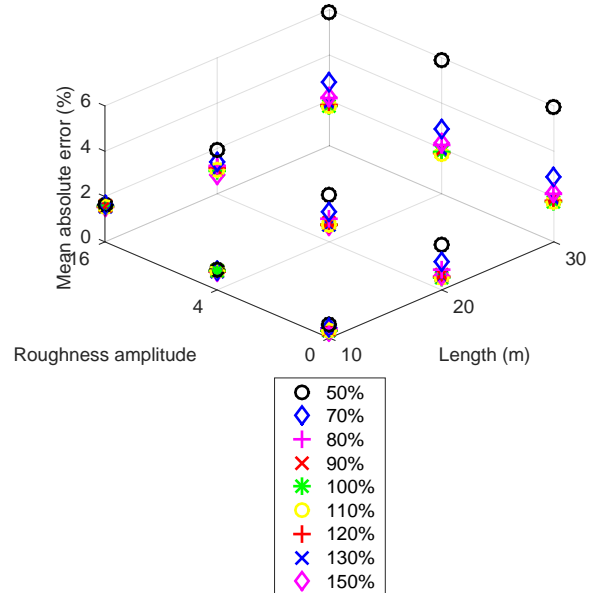
(b) Analytical method

the parameter was precisely estimated. Such a parameter is then introduced to calculate ω_m for a simply supported Euler-Bernoulli beam. Figure 7a and Figure 7b illustrate the influence of such an error in the weight estimates performed by the Standard and Analytical approaches, respectively.

The Standard approach has low variability due to errors in these model parameters. A reason that helps to explain this fact is that the major part of response for this method is due to the piece-wise cubic polynomial applied to represent the quasi-static term, which is independent of such parameters. It could be noticed that error in model parameters are able to provide better results than the model with no errors. It could be understood by the perspective of the dynamic modeling, since some information related to the quasi-static part are missing in this approach. Then, some fluctuation through the exact parameter may improve the overall result. In order to summarize the achievements of this section, the main conclusion for the Standard approach is that this algorithm is robust to variation on both model parameters: the bridge natural frequency and damping ratio.

As the Analytical approach aims to more precisely model the dynamic response of the bridge, it is expected that results be more corrupted by errors in estimating the model parameters. Consequently, the best results are obtained using the exact parameter values. An interesting aspect for the Analytical approach is that estimating ω_m lower than its exact value is considerable worse than estimating it with a higher value. This behavior was observed in cases 4 to 9, for bridges span length of 20 m and 30 m. Despite this decreasing in accuracy, most values analyzed presented reasonable results.

Thus, by the robustness perspective, the Standard method shows itself more suitable than the Analytical one. Although the Analytical method showed more variability regarding model parameters, even for the cases with higher error, which corresponds to approximately 30% of error in ω_m, the results reached an acceptable precision.

3.5.3   Comparison with state-of-the-art static algorithms

The comparison performed in this section is related to a set of state-of-the-art static B-WIM algorithms, all of them previously analyzed in the work of Carraro et al. (2019). The reason behind the consideration of solely static algorithms is to keep only computationally viable algorithms for real time monitoring. The 4 methods employed here are: matrix method (O'BRIEN; QUILLIGAN, M. J.; KAROUMI, 2006), pBWIM (O'BRIEN et al., 2018) with the modification proposed in Gonçalves, Carraro, and Lopez (2021), maximum likelihood (MLE) (IENG, 2015) and regularized approach (O'BRIEN et al., 2009).

In order to avoid biasing conclusions in this section, due to the scenario of the perfect knowledge of model parameters, the model disregarding the damping ratio and with an error of 20% on the moment of inertia was used to represent both Standard and Analytical approaches. In addition, the algorithm related with the application only of piece-wise cubic polynomial is included in the analyses. This last method is called Static, as discussed in previous section.

The results for this comparison are shown in Figure 8. As it can be seen, all presented methods have similar performance for the 10 m bridge, independently of the road roughness class. The scenario changes considerably when analyzing the longer bridges, where the methods employed in the present study show improvement. For the 30 m bridge the Analytical approach

Figure 8 – Comparison among results for Standard, Analytical and Static approaches with state-of-the-art static methods
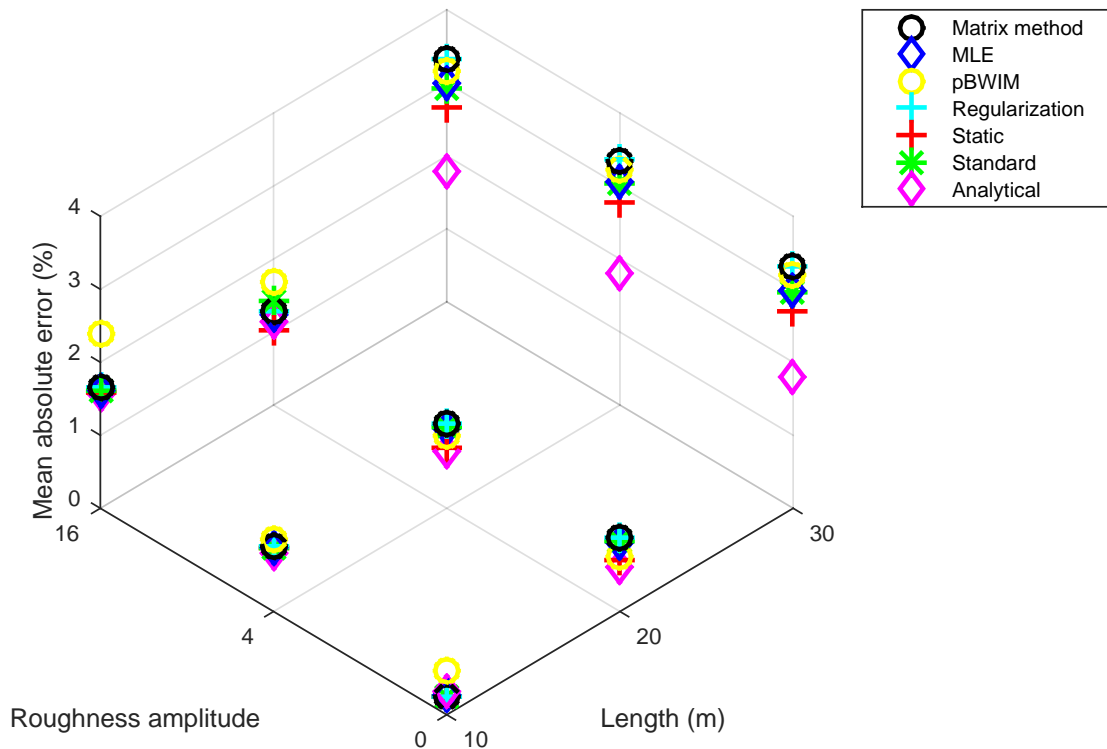
achieved a mean absolute error of almost half of the MLE result, which is the best method among the state-of-the art static methods included in this section. An additional relevant aspect is that the Static method obtained the second best results. As both Analytical and Static algorithms reached better results than the Standard one, it indicates that the inclusion of the fluctuation part is not a key feature of this model. The Static approach has an additional advantage, since it does not require any dynamic parameters, allowing an even more robust performance.

A possible reason for the performance of the Analytical and Static approaches, when compared with the 4 state-of-the-art static methods analyzed, is presented in Figure 9. It shows the mean absolute error for the calibration vehicles of the three approaches proposed in the present study compared with the MLE, the best state-of-the-art static algorithm included in this section. It could be observed that for the 30 m bridge, the results for the calibration vehicles are quite similar for Static and MLE methods. However, for the testing vehicles the Static method shows better performance. As the equations that describe the algorithms proposed in the present study represent continuous functions, the generalization capacity for these methods should be higher, since least parameters are adjusted in the fitting process, reducing the possibility of occurrence of overfitting in calibration. Table 2 presents the percentage

Figure 9 – Comparison among results for MLE, Standard, Analytical and Static approaches for calibration vehicles
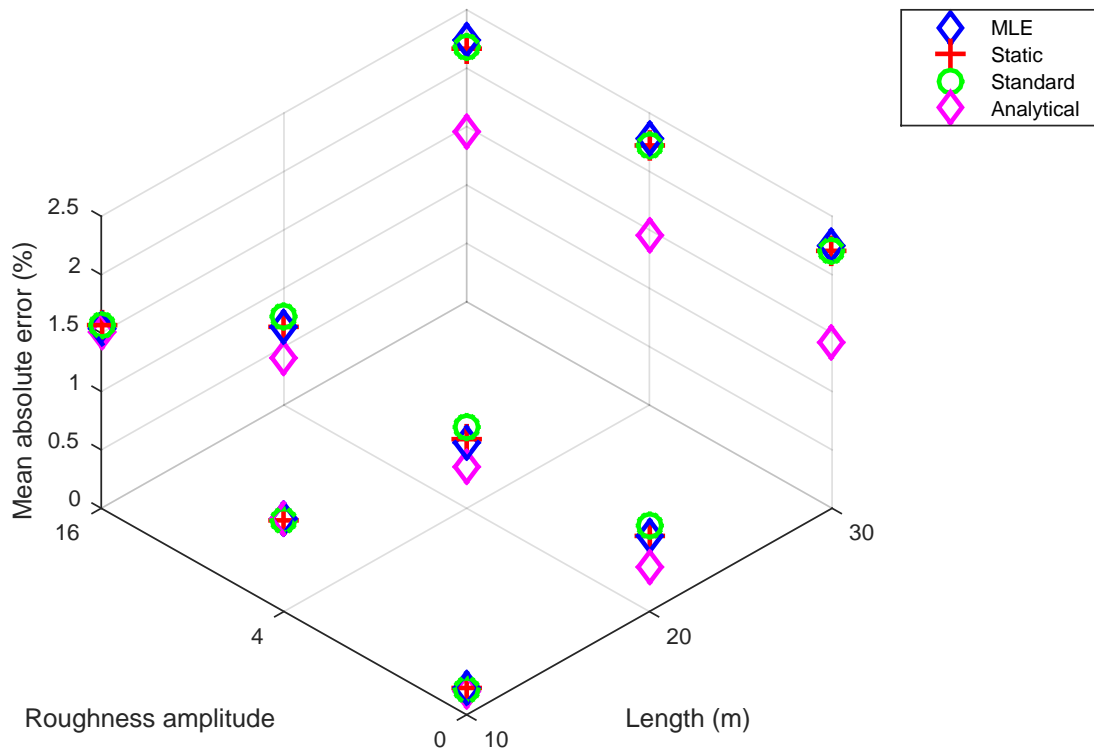
difference between mean absolute error for testing and calibration vehicles for such algorithms. It could be noticed that for Static and Analytical methods this difference is lower than for MLE, which helps to support the statement regarding overfitting. The Standard method, however, showed the same behavior of MLE. This is another fact that indicates that the fluctuation part modeling is not able to accurately predict the real measured fluctuation behavior. It is worth to recall that the algorithms proposed in this study are not able to perfectly estimate the bridge response, enabling a fair comparison with other methods.

Table 2 – Difference (%) between testing and calibration results for the 30 m bridge

Method	No road roughness	Class A	Class B
MLE	0.74	0.78	0.76
Static	0.51	0.55	0.50
Standard	0.76	0.80	0.75
Analytical	0.36	0.35	0.33

In order to better understand the difference in performance between MLE, Standard and Analytical approaches, the results of these methods are compared as a function of vehicle speed. In order to make clear comparisons, for the 9 evaluated cases, only the two extreme cases are

Figure 10 – Comparison among results for MLE, Standard and Analytical approaches as a function of the vehicle speed
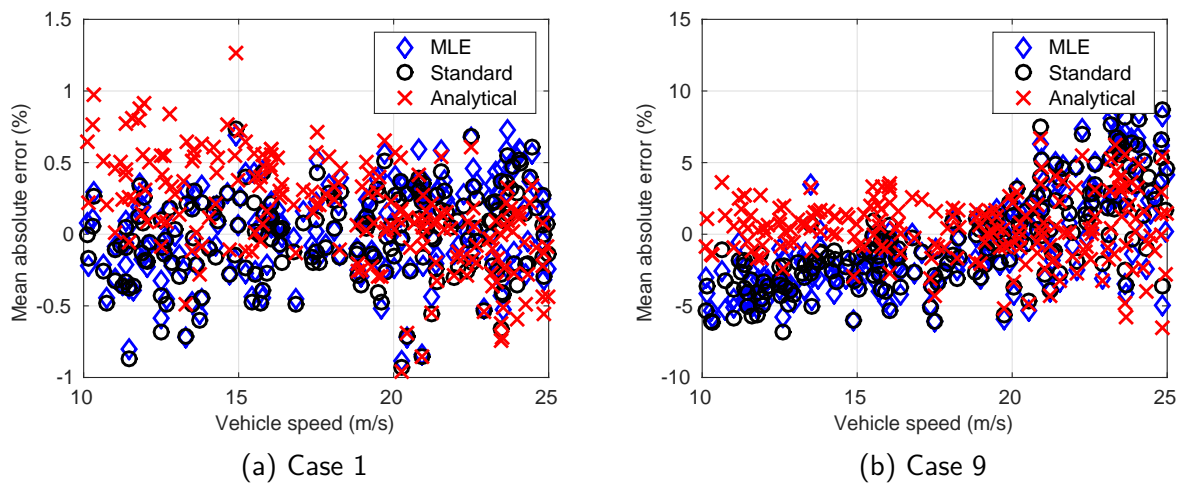
(a) Case 1

(b) Case 9

displayed: the 10 m bridge with smooth road surface (case 1) and the 30 m bridge with high road roughness (case 9). The results for these two situations are presented in Figure 10a and Figure 10b. Whereas for the case 1 results show similar characteristics, the behavior changes when bridge span is increased. It is clear that for case 9 both MLE and Standard methods have a trend in the error as a function of the vehicle speed, which is not observed for the Analytical algorithm. Recalling the dynamic assumptions of the Standard method, the quasi-static term has frequency that is a function of the vehicle speed. Hence, replacing this term by a cubic piece-wise polynomial disregarded some influence of the vehicle speed on the model. Moreover, the MLE method does not make any direct consideration regarding such parameter. On the other hand, the Analytical approach better accounts for the speed as a model parameter, which helps to remove the bias presented by the Standard and MLE algorithms. These results suggest that replacing the quasi-static response by the piecewise cubic polynomial is not the best approach for B-WIM application.

Another relevant aspect addressed here is related to analyzing the mean absolute error of MLE, Standard and Analytical algorithms as a function of the number of axles, presented in Figure 11a and Figure 11b, for the cases 1 and 9. Analogously with the speed influence evaluation, for the number of axles, the results are similar for case 1. However, it could be observed that the results for the Analytical method have a lower variance when compared with the other methods for the case 9. As the calibration process is performed only with two- and four-axle vehicles, the Analytical approach is able to better describe the process as a function of both vehicle speed and number of axles, allowing the generalization for unseen vehicles to be improved, as already discussed.

Figure 11 – Comparison among results for MLE, Standard and Analytical approaches as a function of the vehicle number of axles

(a) Case 1   (b) Case 9
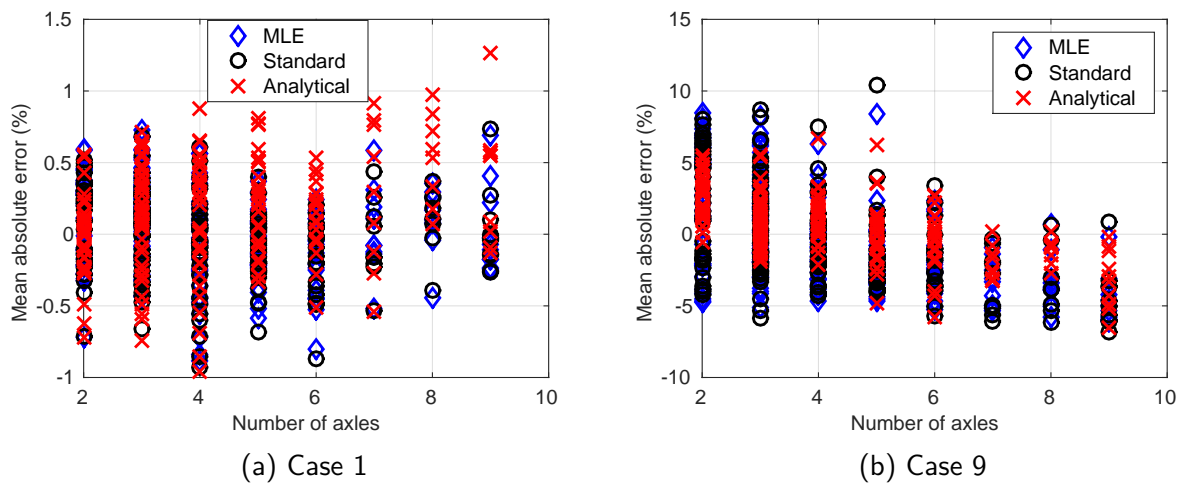
3.6 FURTHER REMARKS

All methods evaluated, independently of the static or dynamic response formulation, perform similarly for the 10 m bridge. However, for the 30 m bridge, the Analytical method outperforms all the others. An interesting aspect is that the increase on bridge span length attenuates the effect of road profile roughness, which makes the Analytical method yield almost the same mean absolute error for the three road profile cases, when evaluating longer bridges. Thus, if estimates of natural frequency of the bridge are available, the Analytical method should present better results, mainly for longer bridges.

In the case of no reliable estimates for the bridge natural frequencies, the Analytical method may suffer from performance degradation. In order to avoid it, one could apply the Standard method, which is more robust. However, the results presented by the Standard method are surpassed by the Static approach in the present study, mainly for the 30 m span bridge. Therefore, the Static algorithm shows itself more suitable for the cases where the Analytical method may not properly work. It is worth to mention that results disregarding the damping ratio parameter for both analytical and standard method were able to achieve a better level of accuracy, in comparison with the other algorithms. Thus, estimating this parameter should not be of major importance for employing proposed methods.

The comparisons among Standard, Analytical and Static algorithms indicate that the fluctuation part modeling should be the source of loss of accuracy. Some possible reasons that help to explain this statement are discussed in the following. As the long span bridge cases showed the higher potential for the application of those methods, the focus are turned to the 30 m bridge. Firstly, when comparing Static and Standard method, where the only difference relies on the inclusion or not of the fluctuation part, the capacity of generalization of the former seems higher. It indicates that some overfitting may be occurring for the Standard method. In other words, the model is fitting some information of the calibration process in such a way

that it does not represent the real behavior for unseen vehicles.

Secondly, when analyzing the robustness of the Standard method, some cases where the parameters of the model were not exactly the real bridge parameters led to better results than when applying the exact parameter value. Hence, an error in modeling the fluctuation part was able to result in better weight estimates. This suggests that the fluctuation part lacks some important information. It could be caused by the unsuitability of the simplification adopted to derive the fluctuation part, as well as the absence of the inclusion of the analytical quasi-static part.

Lastly, when comparing the Analytical and Standard approaches, results are highly improved when the exact parameters are known. Thus, the full analytical approach seems to be able to suitably model the problem, even considering noise and road roughness. This appears to indicate that the fluctuation part works better joined with the quasi-static part. Therefore, the replacement of the quasi-static part by a polynomial expression introduces modeling errors. If the quasi-static part could not be accurately predicted, the static component should be used alone.

Despite of the promising results obtained with the proposed methods, some important aspects should be addressed in order to allow their proper practical application, especially regarding the effects of distinct modeling assumptions, such as:

- vehicle velocity: numerical analyses were performed considering the maximum allowed velocity for Brazilian heavy vehicles as an upper bound for the range of vehicle speeds (BRASIL, 2016). Then, precision of such methods for vehicle speeds out of such a range was not addressed. However, by Figures 10a and 10b, there is an indicative that the analytical method removed the bias for vehicle speed, suggesting that it may still valid for higher values. In addition, the vehicle speed was supposed to be constant along each simulated run. It is considered a reasonable assumption for short-span highway bridges (LANSDELL; SONG; DIXON, 2017), usually employed in B-WIM systems. However, the presence of a non-constant speed might affect the performance of B-WIM algorithms, and is matter of future work;

- structural model: the conclusions regarding performance of analyzed methods are not necessarily extended to structures with other boundary conditions than simply supported one. Then, extending the proposed methods for other boundary conditions is a promising task for future works. In addition, in the numerical experiments, the boundary conditions of the bridge are assumed to be constant. In practice, however, it may be important to take into account the effect of seasonal changes. Moreover, the effects of the transverse load distribution on multiple girders and the influence of the deck stiffness should be investigated;

- dynamic model: although the original approach applies a polynomial able to represent situations other than simply supported bridges, the dynamic modeling is based on this assumption. This is the reason that explains why only sinusoidal terms are

present in this method. Thus, one could extend those expressions to allow modeling the dynamic behavior of bridges with other boundary conditions as well as continuous beam bridges. Such modifications will allow the proper evaluation of a broader range of bridge structures.

Finally, in the present work only simulated signals were applied. However, the real-world field measurements may present characteristics other than those analyzed here. Although a large dataset has been employed in this study, measurements for real bridges are always useful on the development of even more efficient B-WIM methods. This could also help to understand what is the most important research focus on those methods: better modeling the fluctuation part or even focusing on trying to accurately represent the quasi-static part.

3.7   CONCLUSION

The present paper proposed the adaptation of the method developed by Wang et al. (2017), originally used for extracting bridge influence lines, to work as a Bridge Weigh-in-motion (B-WIM) method. Three major modifications were performed in order to enable the application of such a method as a B-WIM algorithm:

- the implementation of an assembly strategy of multiple vehicle runs for the calibration procedure, accomplished by the use of a maximum likelihood approach;

- the derivation of a weigh procedure which requires only simple matrix operations, keeping the computational cost close to the one required by the state-of-the-art static methods;

- the inclusion of the full analytical dynamic response, aiming at increasing the method accuracy and turning the influence line into a function of vehicle speed.

As a result, the adapted method provides a way to join together the inclusion of dynamic considerations into weigh estimates and the computational cost closer to static methods, where only simple matrix operations are necessary. Furthermore, all equations are continuous and the final expression for the influence line is a direct function of the vehicle speed, which is in accordance with many studies in the same subject.

A set of numerical simulations were employed in order to evaluate the potential of application of the proposed algorithms. A total of nine cases, combining three distinct bridge span lengths and three road roughness profiles, were generated. Also, testing vehicles were distinct of those ones applied for calibration. Furthermore, three algorithms were derived: a purely static method, the Standard dynamic approach and the full Analytical approach. Results indicated that the full Analytical approach was able to surpass the performance of the other two methods and a set of 4 state-of-the-art static algorithms, especially for longer bridges. However, sensitivity analysis indicated that the Analytical method could suffer when errors are present in the dynamic model parameters, such as the bridge natural frequency. In the scenario of high error, the static method remains useful and could overcome the other methods

for the long span bridges. The Standard method led to the less precise results among the proposed approaches, which indicated that the fluctuation part might not be enough to model the dynamic behavior of the bridge. Thus, it is recommended that the Analytical method be applied when the model parameters are available. Otherwise, the Static method should be preferred. Furthermore, some improvements to the methods were suggested, such as the derivation of more general equations for distinct bridges than the simply supported ones.

ACKNOWLEDGEMENTS

REFERENCES

BRASIL. **LEI Nº 13.281, DE 4 DE MAIO DE 2016.** [S.l.: s.n.], 2016.
`http://www.planalto.gov.br/CCIVIL_03/_Ato2015-2018/2016/Lei/L13281.htm`.

CARRARO, Felipe; GONÇALVES, Matheus Silva; LOPEZ, Rafael Holdorf;
MIGUEL, Leandro Fleck Fadel; VALENTE, Amir Mattar. Weight estimation on static B-WIM
algorithms: A comparative study. **Engineering Structures**, v. 198, p. 109463, 2019. ISSN
0141-0296.

CASTELLANOS-TORO, Sebastián; MARMOLEJO, Mario; MARULANDA, Johannio;
CRUZ, Alejandro; THOMSON, Peter. Frequencies and damping ratios of bridges through
Operational Modal Analysis using smartphones. **Construction and Building Materials**,
v. 188, p. 490–504, 2018. ISSN 0950-0618.

DENG, Lu; CAI, C. S. Identification of Dynamic Vehicular Axle Loads: Theory and
Simulations. **Journal of Vibration and Control**, Sage Publications, v. 16, n. 14,
p. 2167–2194, 2010.

DNIT, Departamento Nacional de Infraestrutura de Transportes. **Quadro de fabricantes de
veículos**. Rio de Janeiro, Brazil, 2012. Available from: `https://www.gov.br/dnit/pt-
br/rodovias/operacoes-rodoviarias/pesagem/QFV2012ABRIL.pdf`.

DOWLING, Jason; O'BRIEN, Eugene J.; GONZÁLEZ, Arturo. Adaptation of Cross Entropy
optimisation to a dynamic Bridge WIM calibration problem. **Engineering Structures**, v. 44,
p. 13–22, 2012.

FITZGERALD, Paul C.; SEVILLANO, Enrique; O'BRIEN, Eugene J.;
MALEKJAFARIAN, Abdollah. Bridge weigh-in-motion using a moving force identification
algorithm. **Procedia Engineering**, v. 199, p. 2955–2960, 2017. X International Conference
on Structural Dynamics, EURODYN 2017. ISSN 1877-7058.

FRØSETH, Gunnstein T.; RØNNQUIST, Anders; CANTERO, Daniel; ØISETH, Ole.
Influence line extraction by deconvolution in the frequency domain. **Computers &
Structures**, v. 189, p. 21–30, 2017. ISSN 0045-7949.

GONÇALVES, Matheus Silva; CARRARO, Felipe; LOPEZ, Rafael Holdorf. A gradient based
optimization procedure for finding axle weights in probabilistic bridge weigh-in-motion method.
Canadian Journal of Civil Engineering, v. 48, n. 5, p. 570–574, 2021.

GONÇALVES, Matheus Silva; CARRARO, Felipe; LOPEZ, Rafael Holdorf. **Vehicle-bridge Dynamics simulation**. [S.l.: s.n.], 2019. Mendeley Data. v1. Available from: `http://dx.doi.org/10.17632/kt48wf5vjz.1`.

HELMI, Karim; TAYLOR, Todd; ANSARI, Farhad. Shear force–based method and application for real-time monitoring of moving vehicle weights on bridges. **Journal of Intelligent Material Systems and Structures**, v. 26, n. 5, p. 505–516, 2015.

IENG, Sio-Song. Bridge Influence Line Estimation for Bridge Weigh-in-Motion System. **Journal of Computing in Civil Engineering**, v. 29, n. 1, p. 06014006, 2015.

ISO 8606:1995. **Mechanical Vibration-Road Surface Profiles-Reporting of Measured Data**. [S.l.], 1995.

JACOB, Bernard; FEYPELL-DE LA BEAUMELLE, Véronique. Improving truck safety: Potential of weigh-in-motion technology. **IATSS Research**, v. 34, n. 1, p. 9–15, 2010. ISSN 0386-1112.

JACOB, Bernard; O'BRIEN, Eugene J.; JEHAES, Sophie. **Weigh-in-motion of road vehicles: final report of the COST 323 action**. Paris, 2002.

JAMES, Gareth; WITTEN, Daniela; HASTIE, Trevor; TIBSHIRANI, Robert. **An introduction to statistical learning**. [S.l.]: Springer, New York, NY, 2013.

LANSDELL, Andrew; SONG, Wei; DIXON, Brandon. Development and testing of a bridge weigh-in-motion method considering nonconstant vehicle speed. **Engineering Structures**, Elsevier, v. 152, p. 709–726, 2017. ISSN 0141-0296.

LYDON, Myra; TAYLOR, Su E.; ROBINSON, D.; MUFTI, Aftab; O'BRIEN, Eugene J. Recent developments in bridge weigh in motion (B-WIM). **Journal of Civil Structural Health Monitoring**, Springer, v. 6, n. 1, p. 69–81, 2016.

MOSES, Fred. Weigh-in-Motion System Using Instrumented Bridges. **Transportation Engineering Journal of ASCE**, v. 105, n. 3, p. 233–249, 1979.

O'BRIEN, Eugene J.; QUILLIGAN, Michael J.; KAROUMI, Raid. Calculating an influence line from direct measurements. **Proceedings of the Institution of Civil Engineers - Bridge Engineering**, v. 159, n. 1, p. 31–34, 2006.

O'BRIEN, Eugene J.; ROWLEY, Cillian W.; GONZÁLEZ, Arturo; GREEN, Mark F. A regularised solution to the bridge weigh-in-motion equations. **International Journal of Heavy Vehicle Systems**, v. 16, n. 3, p. 310–327, 2009.

O'BRIEN, Eugene J.; ZHANG, Longwei; ZHAO, Hua; HAJIALIZADEH, Donya. Probabilistic bridge weigh-in-motion. **Canadian Journal of Civil Engineering**, v. 45, n. 8, p. 667–675, 2018.

O'BRIEN, Eugene J.; GONZÁLEZ, Arturo; DOWLING, Jason. A filtered measured influence line approach to bridge weigh-in-motion. In: THE Fifth International IABMAS Conference: Bridge Maintenance, Safety Management and Life-Cycle Optimization. Philadelphia, USA: Taylor & Francis (Routledge), 2010.

QUILLIGAN, Michael. **Bridge Weigh-in-Motion Development of a 2-D Multi-Vehicle Algorithm**. 2003. Licentiate Thesis – KTH Royal Institute of Technology, Stockholm, Sweden.

RICHARDSON, Jim; JONES, Steven; BROWN, Alan; O'BRIEN, Eugene J.; HAJIALIZADEH, Donya. On the use of bridge weigh-in-motion for overweight truck enforcement. **International Journal of Heavy Vehicle Systems**, Inderscience, v. 21, n. 2, p. 83–104, 2014.

ROWLEY, Cillian; O'BRIEN, Eugene J.; GONZÁLEZ, Arturo; ŽNIDARIČ, Aleš. Experimental Testing of a Moving Force Identification Bridge Weigh-in-Motion Algorithm. **Experimental Mechanics**, v. 49, n. 5, p. 743–746, 2009.

WANG, Ning-Bo; HE, Li-Xiang; REN, Wei-Xin; HUANG, Tian-Li. Extraction of influence line through a fitting method from bridge dynamic response induced by a passing vehicle. **Engineering Structures**, Elsevier, v. 151, p. 648–664, 2017. ISSN 0141-0296.

YANG, Y.B.; LIN, C.W. Vehicle–bridge interaction dynamics and potential applications. **Journal of Sound and Vibration**, v. 284, n. 1, p. 205–226, 2005. ISSN 0022-460X.

YU, Yang; CAI, C. S.; DENG, Lu. State-of-the-art review on bridge weigh-in-motion technology. **Advances in Structural Engineering**, SAGE Publications, v. 19, n. 9, p. 1514–1530, 2016.

YU, Yang; CAI, C.S.; DENG, Lu. Nothing-on-road bridge weigh-in-motion considering the transverse position of the vehicle. **Structure and Infrastructure Engineering**, Taylor & Francis, v. 14, n. 8, p. 1108–1122, 2018.

ZHAO, Zhisong; UDDIN, Nasim; O'BRIEN, Eugene J. Bridge Weigh-in-Motion Algorithms Based on the Field Calibrated Simulation Model. **Journal of Infrastructure Systems**, v. 23, n. 1, p. 04016021, 2017.

ŽNIDARIČ, Aleš; BAUMGARTNER, W. Bridge weigh-in-motion systems-an overview. In: SECOND EUROPEAN CONFERENCE ON WEIGH-IN-MOTION OF ROAD VEHICLES. Lisbon, Portugal: [s.n.], 1998.

ŽNIDARIČ, Aleš; KALIN, Jan; KRESLIN, Maja. Improved accuracy and robustness of bridge weigh-in-motion systems. **Structure and Infrastructure Engineering**, Taylor & Francis, v. 14, n. 4, p. 412–424, 2018.

4 A BAYESIAN ALGORITHM WITH SECOND ORDER AUTOREGRESSIVE ERRORS FOR B-WIM WEIGHT ESTIMATION

ABSTRACT

Bridge weigh-in-motion (B-WIM) systems are employed for estimating axle weights of vehicles traveling over the bridge structure, providing useful information for many applications regarding structural health monitoring. In this regard, the improvement of single axle weight estimates is a major concern, since B-WIM systems in general have more difficulties with such quantities when compared to the prediction of the total weight, mainly for closely spaced axles. The main goal of the present work is to develop a weigh strategy for B-WIM systems that prevents the occurrence of spurious values, improving the overall accuracy of estimates for single axle weights. For reaching this goal, prior beliefs regarding axle weights, such as their order of magnitude and similarity for closely spaced axles, are employed. Bayesian modeling is well suited for the present problem, since it allows the suitable combination of prior beliefs and experimental data for providing proper weight estimates. In addition, a covariance matrix based on a second order autoregressive process is employed for modeling the error between theoretical and measured responses aiming to overcome the negative effects due to the presence of serial correlation in such errors. Both simulated signals and an example of B-WIM system calibration data are employed for assessing the suitability of the proposed approach. Moreover, sensitivity analyses are conducted aiming to check the robustness of the strategy to its own model parameters. For all analyses, the overall accuracy of the proposed approach, when considering both single axle as well as gross vehicle weight (GVW) estimates, outperforms the baseline algorithms. Furthermore, the sensitivity analyses indicate that the conclusions are the same for distinct prior distributions based on the same prior information.

Authors: Matheus Silva Gonçalves, Rafael Holdorf Lopez, Elder Oroski, Amir Mattar Valente

Note: The numbering of all figures, tables and equations has been restarted in this chapter in order to better agree with the published version of the work. Moreover, an illustrative example (section 4.5.1) was added to this chapter

LIST OF SYMBOLS (CHAPTER 4)

G	total number of girders
E	elastic modulus of bridge girders
Z	section modulus of bridge girders
$\boldsymbol{u}_g$	measured strain vector of the g-th girder
$\boldsymbol{y}$	measured bending moment response vector
$\widehat{\boldsymbol{y}}$	theoretical bending moment response vector
J	vehicle number of axles
d_j	distance between first and j-th axle
C_j	number of scans between first and j-th axle
v	vehicle speed
f	sampling frequency
$\boldsymbol{l}$	influence line ordinates vector
$\boldsymbol{L}$	matrix of influence line ordinates
$\boldsymbol{W}$	vector of axle weights
$\boldsymbol{\varepsilon}$	error term
$\boldsymbol{\Sigma}_\varepsilon$	covariance matrix of the error term
$\boldsymbol{\mu}_W$	mean of the prior distribution of $\boldsymbol{W}$
$\boldsymbol{\Sigma}_W$	covariance matrix of the prior distribution of $\boldsymbol{W}$
λ	regularization parameter
σ_ε^2	variance of the error term
σ_W^2	variance for the axle weight
$\boldsymbol{x}$	vector of positions over the bridge
$\boldsymbol{a}$	coefficients of the cubic polynomial related to the first half of the influence line
$\boldsymbol{b}$	coefficients of the cubic polynomial related to the second half of the influence line
x_m	position off the strain sensors
n	length of influence line vector
$\boldsymbol{X}$	matrix of positions over the bridge
$\boldsymbol{\theta}$	vector including both $\boldsymbol{a}$ and $\boldsymbol{b}$ coefficients
ρ_1	first coefficient of the second order autoregressive process
ρ_2	second coefficient of the second order autoregressive process
N	total number of scans
$\boldsymbol{A}$	matrix of axle weights
$\boldsymbol{r}$	residual vector
q^{-i}	shift operator
$\boldsymbol{B}$	matrix that represents the product between $\boldsymbol{A}$ and $\boldsymbol{X}$ matrices
$\boldsymbol{B}^*$	extended version of the $\boldsymbol{B}$ matrix

$\boldsymbol{\theta}^*$	extended version of the $\boldsymbol{\theta}$ vector
$\boldsymbol{\alpha}$	white noise vector
N_C	number of calibration runs
g	gravity acceleration
ρ_W^{ij}	correlation between the weight of axles i and j

4.1 INTRODUCTION

Bridge Weigh-in-motion (B-WIM) is a technology that uses the own bridge structure to work as a scale in order to estimate the weight of vehicles traveling over it. To accomplish this goal, the response induced by passing vehicles is measured by sensors attached under the structure. By the nothing-on-road B-WIM approach, the process is simplified since the traffic flow is not affected (YU, Y.; CAI, C.; DENG, 2018). It also results in lower costs for installation and maintenance than other systems for traffic monitoring (FRØSETH et al., 2017). In addition, as all sensors are placed under the bridge structure, overloaded vehicles are not able to identify the system and, hence, avoid it (JACOB; FEYPELL-DE LA BEAUMELLE, 2010), allowing that unbiased data be gathered (LYDON et al., 2016). For more information regarding the overall aspects of B-WIM systems, the reader is referred to Lydon et al. (2016) and Yang Yu, C. S. Cai, and Deng (2016). The information provided by B-WIM systems has many application related to structural health monitoring (SHM). For instance, it allows the calculation of important bridge performance indicators (ŽNIDARIČ; KALIN, 2020; ŽNIDARIČ; KALIN; KRESLIN, 2018; MANDIĆ IVANKOVIĆ et al., 2019). Moreover, the vehicle weight monitoring is essential for maintain bridge condition (CHEN, S.-Z. et al., 2018). When analyzing single axle weight estimates, accurate predictions can be useful for improving dynamic amplification factor (DAF) calculation (ŽNIDARIČ, 2017; O'BRIEN; GONZÁLEZ; DOWLING, 2010) and for better overweight enforcement, since axle overloading can occur as a result of redistribution of loads due to inadequate loading (ŽNIDARIČ, 2017).

Due to the wide range of applications, many efforts have been made toward the development of new strategies for improving B-WIM systems in recent years. He et al. (2019) developed a B-WIM system able to identify weight and spacing of vehicles based only on flexural strain signals from weighing sensors, which reduces the installation costs. Shi-Zhi Chen et al. (2018) presented a B-WIM system that employs a single set of long-gauge fiber Bragg grating (FBG) sensors, avoiding the need of additional devices. This idea was further applied for considering the presence of multiple vehicles (CHEN, S.-Z.; WU, G.; FENG, 2019). Žnidarič (2017) presented a procedure which varies simultaneously axles weights and spacings as well as the influence line parameters during the calibration process. Kawakatsu et al. (2019) proposed the application of a deep convolutional neural network for vehicle detection based on raw strain-signal data, employing a surveillance camera for helping in the optimization of the model parameters. Heitner et al. (2020) presented an iterative algorithm for obtaining the shape of influence lines which avoids the use of pre-weighed trucks for calibrating the system, needing only a preliminary influence line estimate. O'Brien et al. (2018) developed a probabilistic B-WIM algorithm, in which the weights of axles were calculated as the most probable ones given the probabilistic information referred to the bridge influence line. In this regard, Gonçalves, Carraro, and Lopez (2021b) proposed an alternative procedure for finding the most probable axle weights based on the gradient of the probabilistic B-WIM equations that was argued to be less time-consuming.

Most current systems, however, rely on the ideas of Moses (1979). They employ an influence line as a way of predicting the strains induced by passing vehicles, being the axle weights calculation an inverse problem. In this context, the axle weights are usually estimated by the application of least squares methods. One could cite Kawakatsu et al. (2019), Heitner et al. (2020), Gonçalves, Carraro, and Lopez (2021a) and Zhao et al. (2015, 2014) as examples of recent weigh strategies that apply least squares algorithms for axle weight estimation. For more details regarding comparison of some weigh strategies, the reader is referred to Carraro et al. (2019).

Although the recent developments on B-WIM systems, improvements regarding their performance still are needed for some applications. Richardson et al. (2014) analyzed the results reported by several B-WIM sites and concluded that the accuracy levels are not yet suitable for direct enforcement of weight limits. Even when analyzing just gross vehicle weight (GVW) estimates, such accuracy classes are still rare (ŽNIDARIČ; KALIN; KRESLIN, 2018). Issues referred to the performance of such systems are more evident when analyzing the estimates provided individually for each axle, since it is well acknowledged that B-WIM systems in general have lower accuracy for individual axles weights than for GVW estimates (HE et al., 2019; O'BRIEN et al., 2018; RICHARDSON et al., 2014; O'BRIEN et al., 2009). Indeed, authors have found that the resulting equations are ill-conditioned, mainly for closely spaced axles crossing long span bridges (ŽNIDARIČ; KALIN; KRESLIN, 2018; O'BRIEN et al., 2018, 2009; ROWLEY et al., 2008).

The limitations of least squares-based algorithms, mainly for individual axle weight estimates, motivated the investigation of other techniques. For instance, aiming to address the ill-conditioning issue for the estimation of axle weights, O'Brien et al. (2009) applied the Tikhonov regularization to the original Moses equations. To achieve this goal, the L-curve criterion for calculating the optimal regularization parameter was employed. The regularization procedure showed better results when compared to the Moses algorithm, especially for individual axles of a group (O'BRIEN et al., 2009; ROWLEY et al., 2008). However, some drawbacks prevail mainly regarding the definition of the regularization parameter of the Tikhonov method. The procedure to obtain the optimum parameter is complex and subjective (O'BRIEN et al., 2018), which has proven too difficult that prevents the practical recommendation of such a method (ŽNIDARIČ; KALIN; KRESLIN, 2018). Furthermore, it increases the required computational time of the weight estimation process (ROWLEY et al., 2008).

From the discussion presented in the previous paragraphs, it is noticed that the improvement in weight estimation, mainly for closely spaced axles, and algorithm robustness are issues in the B-WIM literature. As it was remarked in a previous work of the authors (CARRARO et al., 2019), one promising approach to overcome these issues is to include prior knowledge regarding the expected values of axle weights into the problem formulation. For example, the values of weights of axles are strictly positive, and it is expected that closely spaced axles have similar values. To include such information into the B-WIM problem formulation, the weigh

procedure may be interpreted in a Bayesian perspective. Bayesian modeling provides a formal manner of combining prior beliefs regarding some phenomenon with experimental data in order to update the current state of knowledge related to this phenomenon (PRESS, 2002).

In this context, Yoshida, Sekiya, and Mustafa (2021) recently proposed the Bayesian Bridge Weigh-in-Motion (BBWIM) method, combining Bayesian updating and B-WIM. Despite of the promising results provided by BBWIM (especially regarding the accuracy of axle weights), some important aspects of the problem still prevail, such as:

- the serial correlation of B-WIM deformation signals: although correlated noise was noticed by Yoshida, Sekiya, and Mustafa (2021), the independence assumption was employed without any corrective action. In this case, the results can be corrupted since noise correlation typically induces a false precision to Bayesian analyses due to the fact that correlated measurements carry less information than the same amount of independent data (GELMAN et al., 2013);

- prior knowledge employed: it is important to remark that the prior knowledge employed by Yoshida, Sekiya, and Mustafa (2021) was limited to the similarity among axle weights for closely spaced axles. However, it is noticed that values of axle weights are not completely unknown quantities, since they have practical limitations regarding, for instance, legal limits. Thus, more informative priors may be a better option for B-WIM purposes;

- the definition of the Bayesian approach input parameters: BBWIM requires the definition of model parameters, mainly related to the prior distribution employed. Although such parameters must be priorly chosen, no procedure for helping in their definition was suggested. Therefore, setting the configuration of this algorithm is also quite subjective. The subjectivity, by itself, may not be a problem if the robustness of the results to the model input parameters was present. However, such an aspect was not addressed either;

- limited number of examples: the conclusions are based on just a few vehicle runs, without sensitivity analyses regarding the model parameters. Then, not enough data for properly assessing the accuracy or robustness of this approach was available.

The aspects just discussed indicate that the Bayesian modeling is a promising direction for improving the accuracy of weight prediction in B-WIM systems, but that needs to be further developed. The presence of correlation among error terms has a major importance and could corrupt overall results. Furthermore, it is important for the users that results are not excessively dependent of a clever selection of model input parameters. Hence, the present work proposes a Bayesian B-WIM approach that addresses both accuracy on axle weight prediction and robustness to model parameters issues. The proposed Bayesian approach employs a second order autoregressive (AR(2)) process for modeling the error between theoretical and measured responses. This model allows to represent dependence of such errors with respect to past

values up to 2 lags, avoiding the negative effects of the independence assumption for this application. A procedure for defining both influence line and AR(2) coefficients based on the calibration data is also presented. Moreover, the present method is based on a full multivariate Gaussian distribution as prior. This allows that both mean and covariance matrix be employed for representing a more informative prior belief regarding axle weights. A procedure for defining this distribution is also presented, aiming to simplify the whole process. Although more parameters are necessary for defining this distribution, one can make a direct correspondence between this distribution and the expected values for the axle weights, reducing the subjectivity in the selection of model parameters. The results of the proposed method are compared with the Moses least squares (MOSES, 1979) and the regularization approach (O'BRIEN et al., 2009) in both numerically generated problems and an example of real-world B-WIM application. The results are also evaluated through the COST 323 accuracy classification (JACOB; O'BRIEN; JEHAES, 2002), since such classes can be assigned to possible practical applications of the system.

The remaining of this paper is organized as follows. Section 5.2 introduces the usually employed least squares solution. Section 5.3 presents the employed Bayesian approach as well as a theoretical comparison with the Tikhonov regularization. In section 5.4, the practical aspects related to the selection of the model parameters for the Bayesian algorithm are discussed, mainly those ones related to the definition of the covariance matrix of the error between theoretical and measured responses. Section 5.5 presents the main results of the paper for both numerically simulated signals and an example of real-world B-WIM data. Section 5.6 discusses some relevant aspects regarding the proposed work and suggestion for further studies. Section 5.7 presents the concluding remarks.

4.2 CONVENTIONAL B-WIM WEIGH STRATEGY

Most of B-WIM systems rely on the study of Moses (1979), which intends to provide axle weights from measured strains. By this approach, the estimated axle weights are those that minimize the sum of squared residuals between the measured and theoretical response. Most studies and installations applying B-WIM systems employ flexural strains as monitored quantity (HELMI; TAYLOR; ANSARI, 2015). In these systems, strain sensors are usually placed under the bridge girders, at the mid-span of the structure. The collected strains are converted into bending moment, summing up the contribution of each girder:

$$\boldsymbol{y} = \sum_{g=1}^{G} E_g Z_g \boldsymbol{u}_g, \tag{1}$$

where G represent the total number of girders, and E_g, Z_g, and $\boldsymbol{u}_g$ are the elastic modulus, section modulus and measured strains of the g girder, respectively. Then, $\boldsymbol{y}$ is the vector of measured structural response, comprised of the contribution of all girders.

The idea behind B-WIM systems is to match this measured response with some theoretical one. For enabling the derivation of the theoretical response $(\widehat{\boldsymbol{y}})$, the concept of influence line is employed. For B-WIM purposes, the influence line describes the bending moment response due to a unitary moving load, taking as reference the position where the sensor is placed (QUILLIGAN, M., 2003). In this case:

$$\widehat{y}_k = \sum_{j=1}^{J} W_j I_{(k-C_j)}, \tag{2}$$

where:

$$C_j = \frac{d_j f}{v}, \tag{3}$$

J is the total number of axles of the passing vehicle, W_j represents the weight of the j axle, $I_{(k-C_j)}$ is the ordinate of the bridge influence line for the location of the j axle at the scan k, d_j refers to the position of the j axle taking the first axle as reference, C_j is the respective number of scans that corresponds to d_j, v represents the velocity of the vehicle and f stands for the sampling frequency in which the acquisition system operates. In addition, the index k defines the time step related to the passage of the vehicle through the bridge. It is important to remark that if $k - C_j$ indicates an index that does not correspond to an influence line ordinate, the value of zero is set for $I_{(k-C_j)}$. This last situation occurs when some vehicle axle is not over the bridge structure. One could notice that, in order to enable the proper theoretical response calculation, vehicle speed is required. The vehicle speed is usually assumed to be constant during the vehicle passage over the bridge, which is a reasonable supposition for short-span highway bridges (LANSDELL; SONG; DIXON, 2017). In order to calculate the vehicle velocity, some additional sensors are commonly employed. The nothing-on-road B-WIM approach, applied in the present study, provides this desired parameter without the need of traffic interruption for sensor installation.

In order to simplify the further mathematical manipulations, the dependence of the theoretical structural response $\widehat{\boldsymbol{y}}$ regarding the axle weights presented in Equation (2) is rewritten in matrix notation:

$$\widehat{\boldsymbol{y}} = \boldsymbol{L}\boldsymbol{W}, \tag{4}$$

where $\boldsymbol{L}$ is the matrix of influence line ordinates and $\boldsymbol{W}$ is the vector of axle weights.

The idea behind most current B-WIM systems is to find the axle weights that result in the best match between the theoretical response of Equation (4) and the measured data in Equation (1), which is normally defined in a least squares sense. As the theoretical response is linear within the axle weights, the solution can be defined in a closed form:

$$\boldsymbol{W} = (\boldsymbol{L}^T\boldsymbol{L})^{-1}(\boldsymbol{L}^T\boldsymbol{y}), \tag{5}$$

where $\boldsymbol{y}$ is calculated as in Equation (1).

4.3   THE EMPLOYED BAYESIAN WEIGH STRATEGY

The least squares solution, usually employed in B-WIM systems, does not make use of any prior knowledge regarding the axle weights. Indeed, the solution takes into account just the vector of measured bending moment and the matrix of influence line ordinates. In this case, even the clear physical limitation related to the non-negativity of such a quantity is not taken into account. Thus, by the least squares approach, even negative axle weights may be reported, mainly for closely spaced axles in a group. The non-negativity is just an example of how the prior knowledge can be applied in the B-WIM context. In the present work, it is realized that axle weights are quantities that are not allowed to assume a wide range of values, since they are usually restricted to a few tons due to legal purposes. In addition, the weight of axles from the same vehicle have the tendency of presenting correlation, mainly for closely spaced ones. All those aspects represent prior knowledge that can be exploited for improving the weight estimates for B-WIM systems.

In order to allow the proper consideration of prior knowledge regarding axle weights, it is employed a Bayesian formulation. By the Bayesian perspective, the degree of knowledge regarding some parameters is represented by probability distributions and this prior knowledge is updated based on the measured data (BEHMANESH; MOAVENI, 2016). The idea is that previous beliefs regarding some phenomenon are modified due to new observations in order to obtain a posterior belief (PRESS, 2002). Thus, the probabilities for the updated parameters are assumed to reflect the degree of belief on their values, given the information collected by the experimental procedure (SIMOEN; DE ROECK; LOMBAERT, 2015).

The main idea of Bayesian methods is based on the Bayes theorem, which, for the present work, is defined as:

$$p(\boldsymbol{W}|\boldsymbol{y}) \propto p(\boldsymbol{y}|\boldsymbol{W})p(\boldsymbol{W}), \tag{6}$$

where $p(\boldsymbol{W})$ is the prior probability distribution for the axle weights, $p(\boldsymbol{y}|\boldsymbol{W})$ is the likelihood function and $p(\boldsymbol{W}|\boldsymbol{y})$ is the posterior probability distribution.

The prior distribution $p(\boldsymbol{W})$ is related to the knowledge prior to the experimental results. This can reflect some known bounds for the variable, such as the just discussed non-negativity of the axle weights. In addition, the prior distribution can be seen as a regularizer, which may improve the well-posedness of the problem (YUEN, 2010). The likelihood function $p(\boldsymbol{y}|\boldsymbol{W})$ reflects the probability of observing the measurements given some fixed set of parameters. In this context, it is directly related with the distribution assumed for the error between theoretical and measured data. Finally, the posterior distribution $p(\boldsymbol{W}|\boldsymbol{y})$ is the description of uncertainties for the updated parameter, reflecting the current state of knowledge due to the contribution of both the measured data and the prior knowledge. Thus, it is the effective output of the Bayesian methodology, which allows a better understanding with respect to the analyzed parameters.

For defining the likelihood function, it is assumed that the difference between theoretical

$(\widehat{\boldsymbol{y}})$ and experimental $(\boldsymbol{y})$ responses is defined as:

$$\boldsymbol{y} = \widehat{\boldsymbol{y}} + \boldsymbol{\varepsilon}, \tag{7}$$

where $\boldsymbol{\varepsilon}$ is the error term, which is assumed to follow a zero-mean multivariate normal distribution, whose covariance matrix is $\boldsymbol{\Sigma}_\varepsilon$.

Then, by including the known expression for the probability density function (pdf) of a multivariate normal distribution and replacing the expression for the theoretical response of the bending moment $\widehat{\boldsymbol{y}}$ (Equation (4)), the likelihood function $p(\boldsymbol{y}|\boldsymbol{W})$ can be defined as:

$$p(\boldsymbol{y}|\boldsymbol{W}) \propto |\boldsymbol{\Sigma}_\varepsilon|^{-\frac{1}{2}} \exp\left(-\frac{1}{2}\left(\boldsymbol{y}-\boldsymbol{L}\boldsymbol{W}\right)^T \boldsymbol{\Sigma}_\varepsilon^{-1}\left(\boldsymbol{y}-\boldsymbol{L}\boldsymbol{W}\right)\right), \tag{8}$$

where $|.|$ stands for matrix determinant.

In order to simplify the following mathematical derivations, it is employed a multivariate normal distribution for the prior distribution of the axle weights, which reads as:

$$p(\boldsymbol{W}) \propto |\boldsymbol{\Sigma}_W|^{-\frac{1}{2}} \exp\left(-\frac{1}{2}\left(\boldsymbol{W}-\boldsymbol{\mu}_W\right)^T \boldsymbol{\Sigma}_W^{-1}\left(\boldsymbol{W}-\boldsymbol{\mu}_W\right)\right), \tag{9}$$

where $\boldsymbol{\mu}_W$ and $\boldsymbol{\Sigma}_W$ are the mean and covariance matrix for the prior distribution of $\boldsymbol{W}$.

Including both Eqs. (8) and (9) into (6):

$$p(\boldsymbol{W}|\boldsymbol{y}) \propto \left(|\boldsymbol{\Sigma}_W||\boldsymbol{\Sigma}_\varepsilon|\right)^{-\frac{1}{2}}$$

$$\exp\left(-\frac{1}{2}\left(\left(\boldsymbol{W}-\boldsymbol{\mu}_W\right)^T \boldsymbol{\Sigma}_W^{-1}\left(\boldsymbol{W}-\boldsymbol{\mu}_W\right) + \left(\boldsymbol{y}-\boldsymbol{L}\boldsymbol{W}\right)^T \boldsymbol{\Sigma}_\varepsilon^{-1}\left(\boldsymbol{y}-\boldsymbol{L}\boldsymbol{W}\right)\right)\right). \tag{10}$$

This expression includes the whole probabilistic content regarding the posterior distribution of the axle weights given the measured data and the prior belief on their values. Therefore, it is possible to assess the uncertainties regarding the prediction of the axle weights. For B-WIM systems purpose, however, it is necessary that a point estimate for the quantities of interest be available. In order to obtain a single estimate for the axle weights from the posterior distribution, it could be used the maximum a posteriori (MAP) estimate. The MAP is the set of axles weights whose posterior probability distribution achieves a maximum value, being the most probable values.

Hence, the procedure for calculating this value is based on finding $\boldsymbol{W}$ which maximizes Equation (10). For this purpose, the logarithm of such an expression is maximized. As the logarithm is a monotonically increasing function, employing such an artifice does not change the MAP estimate. Therefore, the expression of Equation (10) is modified to:

$$\log\left(p(\boldsymbol{W}|\boldsymbol{y})\right) \propto -\frac{1}{2}\log\left(|\boldsymbol{\Sigma}_W||\boldsymbol{\Sigma}_\varepsilon|\right)$$

$$-\frac{1}{2}\left(\left(\boldsymbol{W}-\boldsymbol{\mu}_W\right)^T \boldsymbol{\Sigma}_W^{-1}\left(\boldsymbol{W}-\boldsymbol{\mu}_W\right) + \left(\boldsymbol{y}-\boldsymbol{L}\boldsymbol{W}\right)^T \boldsymbol{\Sigma}_\varepsilon^{-1}\left(\boldsymbol{y}-\boldsymbol{L}\boldsymbol{W}\right)\right). \tag{11}$$

It is noticed that some logarithm properties were employed. For maximizing such an expression, it is necessary to take its first derivative with respect to $\boldsymbol{W}$. It is worth to remark that the first part of the expression is zero, since, for the employed approach, no dependence among the covariance matrices $\boldsymbol{\Sigma}_\varepsilon$ and $\boldsymbol{\Sigma}_W$ with respect to $\boldsymbol{W}$ is assumed. Hence:

$$\frac{\partial \log\left(p(\boldsymbol{W}|\boldsymbol{y})\right)}{\partial \boldsymbol{W}} = -\frac{1}{2}\frac{\partial}{\partial \boldsymbol{W}}\left(\left(\boldsymbol{W}-\boldsymbol{\mu}_W\right)^T\boldsymbol{\Sigma}_W^{-1}\left(\boldsymbol{W}-\boldsymbol{\mu}_W\right) + (\boldsymbol{y}-\boldsymbol{L}\boldsymbol{W})^T\boldsymbol{\Sigma}_\varepsilon^{-1}\left(\boldsymbol{y}-\boldsymbol{L}\boldsymbol{W}\right)\right). \tag{12}$$

Performing the derivatives of the right hand side of Equation (12) one obtains:

$$\frac{\partial \log\left(p(\boldsymbol{W}|\boldsymbol{y})\right)}{\partial \boldsymbol{W}} = -\boldsymbol{\Sigma}_W^{-1}\left(\boldsymbol{W}-\boldsymbol{\mu}_W\right) + \boldsymbol{L}^T\boldsymbol{\Sigma}_\varepsilon^{-1}\left(\boldsymbol{y}-\boldsymbol{L}\boldsymbol{W}\right), \tag{13}$$

making the above expression equal to zero and after some algebraic manipulations, the MAP solution for the Bayesian weigh is:

$$\boldsymbol{W} = \left(\boldsymbol{\Sigma}_W^{-1} + \boldsymbol{L}^T\boldsymbol{\Sigma}_\varepsilon^{-1}\boldsymbol{L}\right)^{-1}\left(\boldsymbol{\Sigma}_W^{-1}\boldsymbol{\mu}_W + \boldsymbol{L}^T\boldsymbol{\Sigma}_\varepsilon^{-1}\boldsymbol{y}\right). \tag{14}$$

Therefore, it is worth pointing out that the Bayesian solution for the axle weights can be calculated by performing just some matrix operations, analogously to the least squares solution. Consequently, it requires a similar computational time. It is worth to remark that, when compared with the method of Yoshida, Sekiya, and Mustafa (2021), it is noticed that both approaches rely on a similar Bayesian formulation. Indeed, both methods assume Gaussian prior and likelihood together with a linear theoretical model. As stated in the introductory section, the most remarkable improvements proposed in the present study are the procedure for defining the prior distribution and the model for accounting to the serial correlation among error terms. Such aspects are addressed in following sections.

4.3.1   The Tikhonov regularization by the Bayesian perspective

The just described Bayesian approach represents a quite general framework for the weigh procedure performed by B-WIM systems. Indeed, the parameters $\boldsymbol{\Sigma}_\varepsilon$, $\boldsymbol{\Sigma}_W$ and $\boldsymbol{\mu}_W$ can cover a wide range of approaches. In this regard, it is interesting to analyze the Tikhonov regularization proposed by O'Brien et al. (2009). The main goal of this method also was to better represent the weights of closely spaced axles. The solution of this method is defined as:

$$\boldsymbol{W} = \left(\boldsymbol{L}^T\boldsymbol{L} + \lambda \boldsymbol{I}\right)^{-1}\boldsymbol{L}^T\boldsymbol{y}, \tag{15}$$

where λ is the regularization parameter. The goal of the present analysis is to show that the Tikhonov regularization solution is not an alternative approach to the Bayesian one. Conversely, it is a special case of the Bayesian approach, resulting of a specific set of parameters. Let $\boldsymbol{\mu}_W = \boldsymbol{0}$ and:

$$\Sigma_\varepsilon = \sigma_\varepsilon^2 I, \tag{16}$$

$$\Sigma_W = \sigma_W^2 I, \tag{17}$$

where I is the identity matrix, σ_ε^2 is the value of variance for the error vector ε, and σ_W^2 is the variance for the weight of each axle. Including Equation (16) and Equation (17) into Equation (14) and manipulating the parameter σ_ε^2, one has:

$$W = \left(L^T L + \frac{\sigma_\varepsilon^2}{\sigma_W^2} I \right)^{-1} \left(L^T y \right). \tag{18}$$

It could be noticed that the expression of Equation (18) is rigorously the same as stated in the work of O'Brien et al. (2009) and represented in Equation (15). By the Bayesian point of view, however, the parameter λ appears as the ratio between the variance of the error and the prior distribution. Thus, the Bayesian approach is also able to model the situation related to the Tikhonov regularization. Furthermore, it gives a practical interpretation for the parameter λ, which may avoid the necessity of employing additional and somewhat subjective procedures for finding a suitable value of λ.

4.4 PROPOSED PROCEDURE FOR DEFINING THE MODEL PARAMETERS

For employing the described Bayesian method, it is necessary to provide 4 parameters, namely: L, Σ_ε, Σ_W and μ_W. The proper implementation of the method relies on a suitable definition of these model parameters. Hence, in the present section, a procedure is presented for helping the user to define them.

4.4.1   Influence line definition

A main issue for creating a functional B-WIM system is the definition of the bridge influence line and, consequently, the L matrix. In the first work in this subject, performed by Moses (1979), the bridge influence line was approached only with theoretical analysis. The theoretical influence line, however, is currently recognized as unsuitable for B-WIM applications (QUIL-LIGAN, M., 2003), since some simplifications are required in its derivation procedure. Hence, recent works have addressed the influence line extraction for bridge structures, considering many distinct approaches. For instance, influence lines were modeled as cubic splines (ŽNIDARIČ; KALIN, 2020), based on B-splines after the elimination of dynamic fluctuation (ZHENG et al., 2020) and B-splines basis employing sparse regularization (CHEN, Z. et al., 2019). In addition, calculation strategies also involved least squares (O'BRIEN; QUILLIGAN, M. J.; KAROUMI, 2006), regularized least-squares QR decomposition method (ZHENG et al., 2019b), maximum likelihood (IENG, 2015), considering simplified models for the dynamic response of the bridge due to a passing vehicle (GONÇALVES; CARRARO; LOPEZ, 2021a; WANG et al., 2017), to

name just a few examples. Some methods for influence line identification were also analyzed by Carraro et al. (2019) and Zheng et al. (2019a).

For the present study, a piecewise cubic polynomial is used for representing the bridge influence line. This model relies on a small number of parameters and is theoretically able to describe the influence line for both single and multi-span continuous beams (WANG et al., 2017). In what follows the procedure is derived for a single-span bridge, employing two distinct cubic polynomials for representing each half of the influence line. However, the procedure can be straightforwardly extended for multi-span continuous bridges. Let $\boldsymbol{x} = x_1, \ldots, x_n$ be a set of longitudinally spaced points representing the positions over the bridge where the influence line is calculated. In this formulation, x_1 and x_n are the points that characterize the starting and ending points of the structure, respectively. Hence:

$$I = \begin{cases} a_1 x_i^3 + a_2 x_i^2 + a_3 x_i + a_4, & \text{if } x_i \leq x_m \\ b_1 x_i^3 + b_2 x_i^2 + b_3 x_i + b_4, & \text{otherwise} \end{cases}, \tag{19}$$

in which $\boldsymbol{a} = [a_1, a_2, a_3, a_4]$ and $\boldsymbol{b} = [b_1, b_2, b_3, b_4]$ are the coefficients that define each cubic polynomial, x_m is the point referred to the position where the strain sensors are placed and $1 \leq i \leq n$. Lets define $x_m = 0$ without loss of generality. In order to enforce the continuity of the curve, let $a_4 = b_4$. We may then define the $\boldsymbol{X}$ matrix as:

$$\boldsymbol{X} = \begin{bmatrix} x_1^3 & x_1^2 & x_1 & 0 & 0 & 0 & 1 \\ \vdots & \vdots & \vdots & \vdots & \vdots & \vdots & \vdots \\ x_{m-1}^3 & x_{m-1}^2 & x_{m-1} & 0 & 0 & 0 & 1 \\ 0 & 0 & 0 & 0 & 0 & 0 & 1 \\ 0 & 0 & 0 & x_{m+1}^3 & x_{m+1}^2 & x_{m+1} & 1 \\ \vdots & \vdots & \vdots & \vdots & \vdots & \vdots & \vdots \\ 0 & 0 & 0 & x_n^3 & x_n^2 & x_n & 1 \end{bmatrix}_{(n \times 7)}. \tag{20}$$

Then, the bridge influence line can be written as:

$$I = \boldsymbol{X}\boldsymbol{\theta}, \tag{21}$$

in which $\boldsymbol{\theta}$ is:

$$\boldsymbol{\theta} = \begin{bmatrix} a_1 & a_2 & a_3 & b_1 & b_2 & b_3 & b_4 \end{bmatrix}^T. \tag{22}$$

4.4.2 Covariance matrix for the error term

The covariance matrix $\boldsymbol{\Sigma_\varepsilon}$ is a parameter required in the process. The most common approach is to assume independence among measurements from distinct scans and homoscedasticity. It highly simplifies the whole process, since the resulting covariance matrix is diagonal and can be defined by a single parameter. For the present context, however, such a hypothesis

may not be enough. The reason is that dynamic fluctuations are present in the collected signals and they hardly are precisely captured by the theoretical model. Then, the difference between theoretical and experimental responses may show some patterns and, hence, present autocorrelation. It was noticed, for instance, in the work of Yoshida, Sekiya, and Mustafa (2021).

In order to relax the independence hypothesis and allow the presence of autocorrelation in the model, it is assumed that the error term is described by a second order autoregressive process (AR(2)) (BOX et al., 2015):

$$\varepsilon_k = \rho_1 \varepsilon_{k-1} + \rho_2 \varepsilon_{k-2} + \alpha_k, \tag{23}$$

in which ρ_1 and ρ_2 are the coefficients of the AR(2) process, k is the measurement scan and α_k is a zero-mean random variable such that $\alpha_k \sim \mathcal{N}\left(0, \sigma_\varepsilon^2\right)$. Then, the error observed at scan i is a function of the errors at the two previous scans.

The AR(2) error assumption results in a specific covariance matrix structure. This matrix has a closed-form solution for its inverse, which is necessary for further steps. According to Congdon (2007), $\boldsymbol{\Sigma}_\varepsilon^{-1}$ can be written as:

$$\boldsymbol{\Sigma}_\varepsilon^{-1} = \frac{1}{\sigma_\varepsilon^2} \begin{bmatrix} 1 & -\rho_1 & -\rho_2 & 0 & & & & \\ -\rho_1 & 1+\rho_1^2 & -\rho_1(1-\rho_2) & -\rho_2 & & & & \\ -\rho_2 & -\rho_1(1-\rho_2) & 1+\rho_1^2+\rho_2^2 & -\rho_1(1-\rho_2) & & & & \\ 0 & -\rho_2 & -\rho_1(1-\rho_2) & 1+\rho_1^2+\rho_2^2 & & & & \\ & & & & \ddots & & & \\ & & & & & -\rho_1(1-\rho_2) & 1+\rho_1^2 & -\rho_1 \\ & & & & & -\rho_2 & -\rho_1 & 1 \end{bmatrix}_{(N \times N)}, \tag{24}$$

being N the number of scans for the measured signal. Notice that just three parameters are required for representing $\boldsymbol{\Sigma}_\varepsilon$ and its inverse: σ_ε^2, ρ_1 and ρ_2. It is, hence, a computationally interesting approach that addresses the important aspect of correlation among error terms. In addition, it was opted to limit the order of the model to 2 since models of such an order are frequently adequate for representing stationary time series (BOX et al., 2015).

4.4.3 Parameter estimation from calibration data

Both influence line and coefficients of the AR(2) model are calculated from the calibration data. The procedure adopted for estimating such coefficients is an adaptation of the extended least squares method (ISERMANN; MÜNCHHOF, 2011). To allow this procedure, it is necessary to write the theoretical response in a different manner:

$$\hat{\boldsymbol{y}} = \boldsymbol{AX\theta}, \tag{25}$$

where $\boldsymbol{A}$ is a Toeplitz matrix created from the vector of axle weights of a given vehicle:

$$\left[A_{ij}\right]_{N \times n} = \begin{cases} W_k, & \text{if } i = j + \frac{d_k f}{v} \\ 0, & \text{otherwise} \end{cases} , \tag{26}$$

in which N is the total number of measurement scans, n is the number of influence line ordinates and the remaining parameters are the same as in Equation (2) and Equation (3). Moreover, it is important to define the residuals vector:

$$\boldsymbol{r}_i = \boldsymbol{y}_i - \widehat{\boldsymbol{y}}_i, \tag{27}$$

being $\boldsymbol{r}_i$ the residuals vector for the calibration run i. By combining Equation (23) and Equation (7), one could write:

$$y_k = \widehat{y}_k + \rho_1 \varepsilon_{k-1} + \rho_2 \varepsilon_{k-2} + \alpha_k, \tag{28}$$

being k the referred measurement scan. Then, if one applies the residuals $\boldsymbol{r}$ as estimates of $\boldsymbol{\varepsilon}$, the effect of correlation may be included into the model. It could be accomplished by defining an extended system of equations based on replacing Equation (25) into Equation (28):

$$\boldsymbol{y} = \boldsymbol{B}\boldsymbol{\theta} + \boldsymbol{r}q^{-1}\rho_1 + \boldsymbol{r}q^{-2}\rho_2 + \boldsymbol{\alpha}, \tag{29}$$

in which the operator q^{-i} is such that, for every element r_k in $\boldsymbol{r}$, $r_k q^{-i} = r_{k-i}$. Hence, q^{-i} is a shift operator employed for matching the autoregressive components of the model with the residuals elements related to their respective lags. For the shifted values whose residuals index are lower than 1, the value of zero is assigned since it represents the expected value of the random variable α_k. Furthermore, $\boldsymbol{B}$ is utilized to represent the product between $\boldsymbol{A}$ and $\boldsymbol{X}$ matrices. Notice that each calibration run has its own $\boldsymbol{B}$ and $\boldsymbol{r}$ parameters and their indices were omitted for sake of clarity.

The system of equations in Equation (29) can be written in a more compact manner:

$$\boldsymbol{y} = \boldsymbol{B}^*\boldsymbol{\theta}^* + \boldsymbol{\alpha}, \tag{30}$$

in which:

$$\boldsymbol{B}^* = \begin{bmatrix} B_{11} & \dots & B_{17} & 0 & 0 \\ B_{21} & \dots & B_{27} & r_1 & 0 \\ B_{31} & \dots & B_{37} & r_2 & r_1 \\ \vdots & \ddots & \vdots & \vdots & \vdots \\ B_{N1} & \dots & B_{N7} & r_{N-1} & r_{N-2} \end{bmatrix}, \boldsymbol{\theta}^* = \begin{bmatrix} \theta_1 \\ \vdots \\ \theta_7 \\ \rho_1 \\ \rho_2 \end{bmatrix}. \tag{31}$$

Hence, the number of extra columns added is equal to the order of the AR model. In this regard, by employing the extended matrix $\boldsymbol{B}^*$ and vector $\boldsymbol{\theta}^*$, the difference between theoretical and measured responses is converted to just the white noise component $\boldsymbol{\alpha}$.

As the error term of the extended system is now the conventional white noise, the usual methods for parameter estimation can be employed for calculating $\boldsymbol{\theta}^*$. In this regard, the MLE strategy, proposed by Ieng (2015), is employed. It reads as:

$$\boldsymbol{\theta}^* = \left(\sum_{i=1}^{N_C} \left(\left(\boldsymbol{B}_i^* \right)^T \boldsymbol{B}_i^* \right) \right)^{-1} \sum_{i=1}^{N_C} \left(\left(\boldsymbol{B}_i^* \right)^T \boldsymbol{y}_i \right), \tag{32}$$

being N_C the number of calibration runs.

It is noticed that the extended matrix and, thus, the estimated parameters are dependent of the residuals values and vice-versa. Therefore, an iterative approach is adopted. An initial random guess for the residuals of each calibration run is utilized for calculating the first estimate of $\boldsymbol{\theta}^*$. With such an estimate, the residuals are calculated and, hence, employed for generating a new $\boldsymbol{B}^*$ matrix. The procedure continues until the differences between estimates in successive runs are smaller than a defined threshold. It is suggested that the values of ρ_1 and ρ_2 be monitored for convergence since it is expected that the magnitude of such parameters stays at a same level regardless the structure being analyzed. In the present work, a threshold of 0.0001 in the variation of both ρ_1 and ρ_2 was utilized as convergence criteria. Such an approach can be summarized as:

Result: $\boldsymbol{\theta},\rho_1,\rho_2,\sigma_\varepsilon^2$;

Set a random initial value for the residuals vector for every run ($\boldsymbol{r}_i$);

Define the convergence criteria (e_{Max});

while $e \geq e_{Max}$ **do**

Set as zero two variables to account for each summation in Equation (32);

for $i = 1$ **to** N_C **do**

Calculate $\boldsymbol{B}_i^*$ as in Equation (31);

Update the summations variables as in Equation (32);

end

Calculate $\boldsymbol{\theta}^*$ employing Equation (32);

Calculate every $\boldsymbol{r}_i$ vector employing the new $\boldsymbol{\theta}^*$ estimate;

Calculate e;

end

Pick $\boldsymbol{\theta}$, ρ_1 and ρ_2 from the $\boldsymbol{\theta}^*$ vector;

Calculate $\boldsymbol{\alpha}$ for each calibration run and applies such values for estimating σ_ε^2

return $\boldsymbol{\theta},\rho_1,\rho_2,\sigma_\varepsilon^2$.

Algorithm 1: Procedure to estimate $\boldsymbol{\theta},\rho_1,\rho_2,\sigma_\varepsilon^2$.

The convergence of the method is fast, where usually up to 10 iterations are enough for the difference between successive values of ρ_1 and ρ_2 be at the third decimal digit.

It is important to remark that measurements from B-WIM systems are usually collected at a high sampling frequency. This frequency may affect the estimation results related to the

AR(2) process. For instance, in the work of SMAIL, THOMAS, and LAKIS (1999) the results of the model were significantly affected for sampling frequencies higher than 10 times the highest frequency of interest. Then, in the present study, the signals are first decimated to stay at an effective sampling frequency bellow 10 times the maximum frequency where significant response is observed in the frequency domain representation of signals from the calibration runs. Moreover, it is important to check if calculated coefficients are related to a stationary AR process since unreliable results may arise otherwise. Such conditions are (BOX et al., 2015):

$$\rho_2 + \rho_1 < 1 \tag{33}$$

$$\rho_2 - \rho_1 < 1 \tag{34}$$

$$-1 < \rho_2 < 1. \tag{35}$$

The non-stationarity may also occur due to the presence of an unit root, which results in the sum of coefficients close to 1. In the case of coefficients indicating a non-stationary process, higher decimation factors may be evaluated. If non-stationarity still is present, it is suggested that the usual diagonal covariance matrix be employed.

4.4.4 Prior distribution

The definition of prior distribution parameters is based on the information available for the bridge under analysis. In the presence of recent data collected by static scales near the B-WIM system, the parameters can be directly estimated from this database. If no data is available, some legal regulations can work as a reference, since it is expected that most vehicles respect such limits. In the worst scenario, one could just enforce the lower bound due to the non-negativity of axle weights by assigning a low probability of occurrence of negative values. It is worth to remark that the main goal of the prior distribution is to cover what is really expected regarding the problem at hand, avoiding to include wrong beliefs into the model. In this context, it is important to ensure that non-zero probability be assigned to all possible values for the quantity of interest (PRESS, 2002). Consequently, a common approach is to employ weakly informative priors, which are distributions that intentionally reflect weaker information than what is currently known (GELMAN et al., 2013). It also indicates that there is no reason for concern regarding fine-tuning prior parameters.

In the present work, the prior parameters are defined based on the Brazilian heavy vehicles classification (DNIT, 2012). In this classification, single axle weights for common vehicle types are usually limited to 10 ton for all axles except the first, which is limited to 6 ton. Such values are, then, defined as an upper reference. As a lower reference, it is adopted the value of 2 ton for all axles to account for empty vehicles. Both values together imply that:

$$\mu_W^j = \begin{cases} 4g, & \text{if } j = 1 \\ 6g, & \text{otherwise,} \end{cases} \tag{36}$$

where the index j refers to the axle number and g is the gravity acceleration.

For defining the covariance matrix $\boldsymbol{\Sigma}_W$, it is employed the relation among such a matrix and the correlation matrix:

$$\Sigma_W^{ij} = \rho_W^{ij} \sigma_W^i \sigma_W^j, \tag{37}$$

where ρ_W^{ij} is the correlation between the weight of axles i and j. In addition, σ_W^i and σ_W^j are the standard deviation of the axle weights i and j, respectively.

The value of σ_W^j is calculated aiming to have 1 standard deviation from the mean to the lower and upper references previously defined, in order not to overly constrain the Bayesian procedure:

$$\sigma_W^j = \begin{cases} 2g, & \text{if } j = 1 \\ 4g, & \text{otherwise.} \end{cases} \tag{38}$$

As no database of axle weights is available for this study, a set of vehicles employed in other works related to B-WIM (YU, Y.; CAI, C.; DENG, 2018; ZHAO et al., 2015, 2014; CARRARO et al., 2019; YOSHIDA; SEKIYA; MUSTAFA, 2021; ZHENG et al., 2019a; HAO; XIE; YU, M., 2019; WU, H. et al., 2020; MAKI et al., 2019; LECHNER et al., 2010) are analyzed in order to help in the definition of ρ_W^{ij}. It is excluded just those vehicles where axles of the same group have exactly the same value, since it is an indicator that the group was weighed together and the results averaged for the contribution of each axle. Figure 1 presents the relation among axle weights from a same vehicle, where the distinction among those ones belonging to a same group is remarked. The criterion for belonging to a same group employed here is the axle stay at 2.4 meters or less from any other axle of the group, since it is the value employed in the Brazilian classification. Based on the Pearson correlation coefficient calculated from such a set of vehicles, two distinct values of correlation are employed:

$$\rho_W^{ij} = \begin{cases} 0.9, & \text{if } i \text{ and } j \text{ belong to a same group} \\ 0.5, & \text{otherwise.} \end{cases} \tag{39}$$

It is worth to remark that the prior distribution employed does not mathematically ensure non-negative axle predictions. However, in the practical scenario, negative estimates are effectively avoided. In order to understand the reason, it is important to recall that for B-WIM systems the total weight is usually predicted with suitable precision whereas the contribution of each axle is difficult to distinguish. Then, a negative value occurs together with a considerable overestimation of the weight of other axles, providing high discrepancies. Hence, not only the marginal axle weight distribution is relevant to prevent negative estimates, but also the correlation among them since it includes a tendency for the estimates to stay at a similar level. Thus, the combination of both correlation among axle weights and marginal distributions for the weight of each axle in the proposed approach are enough to ensure proper predictions in the practical scenario. Moreover, the proposed prior distribution also avoids an excessive

Figure 1 – Correlation of axles weight from a same vehicle
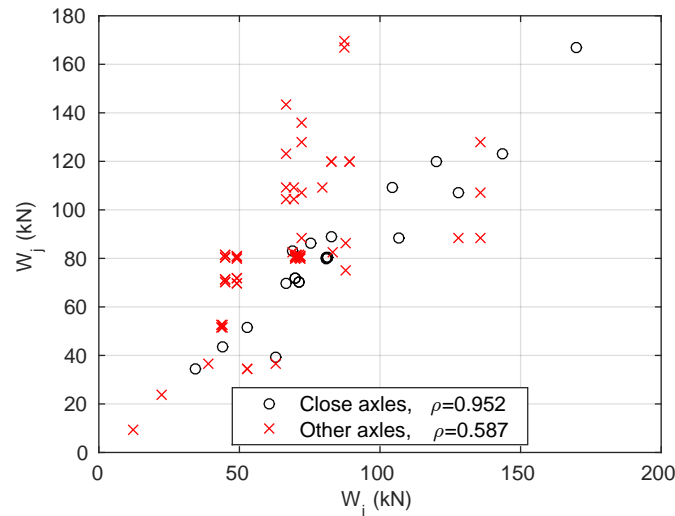
bias toward median weights, which would jeopardize the predictions for overweight axles. It is important to notice that the AR(2) model for the error between theoretical and measured responses is important to ensure that the prior distribution be properly accounted for. Such statements are assessed in the Section 4.5.

It could be noticed that the selection of prior distribution parameters may be somewhat subjective. Indeed, it is a common criticism to Bayesian methods (SIMOEN; DE ROECK; LOMBAERT, 2015). In the present work, however, it is argued that subjectivity is not a problem itself. Indeed, inference from observational data involves some subjective judgement, in such a way that several scientists analyzing the same dataset will often develop distinct interpretations (PRESS, 2002). Conversely, the main drawback with subjective procedures is related to their robustness. Or, in other words, the sensitivity of the results regarding the model inputs (INSUA; RUGGERI, 2000). When lack of robustness is observed, some feasible model parameters for the prior distribution can lead to highly distinct results and potentially poor weight predictions. In this regard, the clear correspondence of the prior distribution with the axle weights expected by the user helps to mitigate the possible negative effects of the subjectivity. For practical purposes, such a range of suitable values should span just a few tons and, hence, the values adopted by distinct users could not deviate excessively from each other. Therefore, it is expected that the consequences of the subjectivity in choosing the prior parameters be reduced in this context. Such aspect is further analyzed in Section 4.5.

4.5   RESULTS

This section presents some numerical experiments to evaluate the proposed Bayesian approach. The first analysis to be conducted is an illustrative example, aiming to better present the main aspects related to the Bayesian approach and how its features can contribute to more reliable axle estimates. Then, numerical models are created for simulating the vehicle-bridge

system, allowing that the capacity of the method to provide reliable weight estimates for vehicles highly distinct of those ones employed for calibrating the system be assessed. Next, a real-world B-WIM system example is analyzed, employing the calibration information collected at a bridge in Brazil. For both numerical simulations and the real-world B-WIM system example, a set of distinct algorithm configurations is analyzed to assess the improvements provided by each feature added to the proposed approach as well as the robustness to its own model parameters.

4.5.1 Illustrative examples

In this section, a simple illustrative example is presented in order to better remark some theoretical aspects previously discussed. In this context, it is employed a two-axle vehicle, since it allows a graphical representation of the probabilities related to each set of axle weights. It is worth to mention that this example does not intend to simulate a real-world B-WIM application. Otherwise, the main goal is to create an example that clearly shows the theoretical aspects regarding the Bayesian approach that are more relevant to the purpose of the present study. With this goal in mind, the remaining parameters of this example were defined. In Table 1, it is presented some of the main parameters employed. Notice that the spacing between both axles is set to a quite small value. This short spacing was chosen to assess the capability of the algorithms for estimating the axle weights in this challenging situation. Indeed, they have more difficulties to distinguish the contribution of each individual axle in such a situation. Consequently, the advantages of the Bayesian strategy may be easily observed. In practical applications, larger vehicles with more axles are more susceptible to such kind of instability, as will be presented in the next subsections.

Table 1 – Parameters for the illustrative example

Vehicle speed (m/s)	20
bridge length (m)	5
Axle spacing (m)	0.5
First axle weight (ton)	3
Second axle weight (ton)	9

Other relevant aspect to be discussed is the fact that theoretical models are not able to perfectly predict the behavior of the system. In this example, the bending moment induced by the vehicle is simulated based on a noisy influence line. The influence line is calculated by perturbing the theoretical influence line of a simply supported bridge with a zero mean Additive White Gaussian Noise (AWGN) with standard deviation of 0.05, i.e., $\mathcal{N}(0,0.05^2)$. Furthermore, a zero mean AWGN, with standard deviation of 10000, i.e., $\mathcal{N}(0,10000^2)$, is also applied to the resulting bending moment. Figure 2 illustrates this process. The influence lines are shown at the left hand side, including both the theoretically calculated and the perturbed one, which remarks that the added noise does not excessively corrupt its shape. On the other hand, the

calculated bending moment is presented for three cases. The theoretical one is calculated by employing the theoretical influence line and the exact axle weights for the analyzed vehicle. The perturbed bending moment results from employing the known axle weights and the perturbed influence line just described. Finally, the effectively utilized signal is the one resulted from the application of an extra AWGN to the perturbed curve. By comparing these figures, it is clear that the shape of the signal is considerably changed by each process, however keeping the main behavior of the curve. Regarding the proposed procedure, the theoretical curves are employed for predicting the bridge response and the resulting curve after adding noise to the data is employed to simulate the experimental one. As no set of axle weights is able to precisely match the measured response, the solution process should not provide the exact solution.

Figure 2 – Influence lines and resulting bending moment
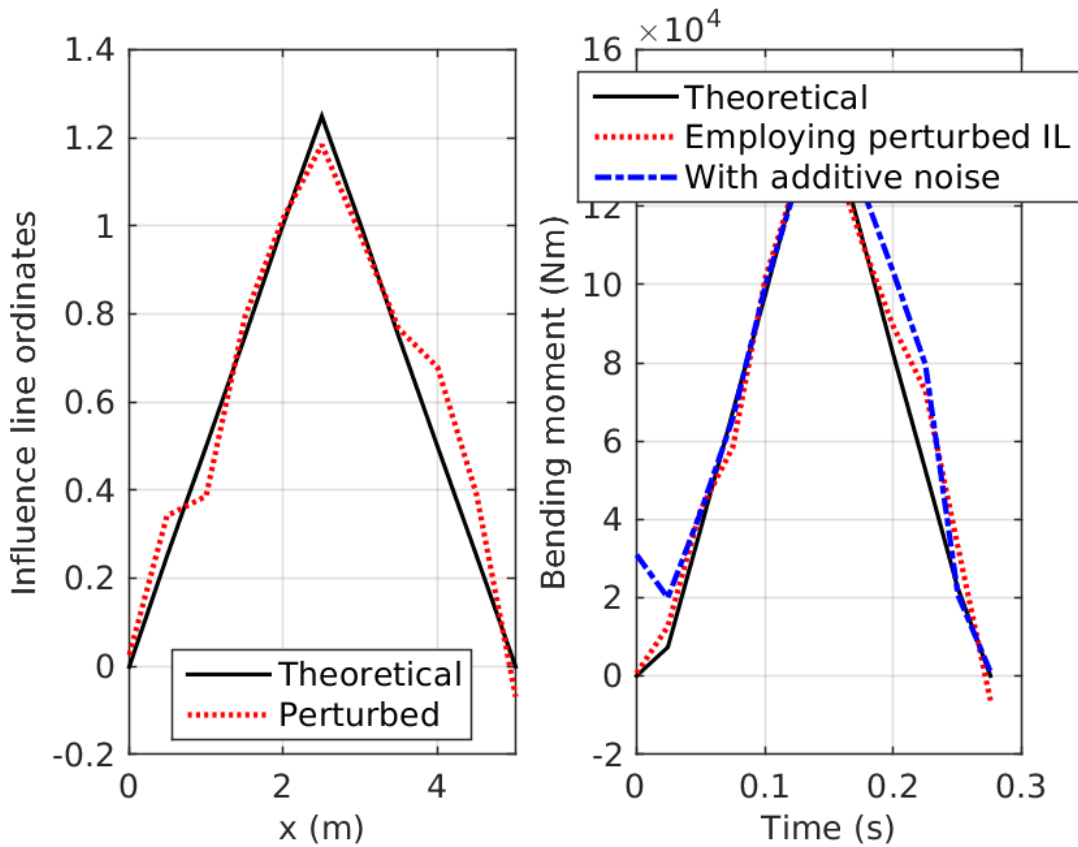
In this example, a Gaussian prior distribution is employed, also including the correlation among weights of both axles, whose parameters are:

$$\boldsymbol{\mu}_W = \begin{bmatrix} 2 \\ 8 \end{bmatrix}, \tag{40}$$

$$\boldsymbol{\Sigma}_W = \begin{bmatrix} 1 & 0.5 \\ 0.5 & 1 \end{bmatrix}. \tag{41}$$

In order to estimate the axle weights from the simulated data, one could employ procedures such as the least squares approach. A closed-form least squares solution can be obtained maximizing a particular likelihood function for this example. Suppose that the deviation among each entry of the theoretical and experimental response vector, i.e., the error ε, follows a Gaussian distribution such that $\varepsilon \sim \mathcal{N}\left(0, \sigma_\varepsilon^2\right)$:

$$y_i = \hat{y}_i(\boldsymbol{W}) + \varepsilon, \tag{42}$$

where $\boldsymbol{y}$ and $\hat{\boldsymbol{y}}$ are experimental and theoretical responses, respectively, i is the related index of the response vector and $\boldsymbol{W}$ is the vector of axle weights. The dependence of $\hat{y}_i$ regarding $\boldsymbol{W}$ was discussed in Equation (4). In addition, the realization of each random variable ε is independent of all the others. Or, in other words, ε is an iid variable (independent and identically distributed). In this case, the likelihood function can be expressed as:

$$\mathcal{L} = \prod_{i=1}^{N} p\left(y_i | \hat{y}_i(\boldsymbol{W}), \sigma_\varepsilon^2\right), \tag{43}$$

where N is the total number of scans of the response vector. It is worth to remark that the probabilities assigned to Equation (43) can be easily calculated by the known expression of the pdf of a Gaussian distribution since the error follows such a distribution.

This likelihood function can then be used to graphically show the probability associated to each set of axle weights. Indeed, it provides additional information when compared just with the least squares solution: instead of presenting only a punctual estimate for the parameters of interest, the whole likelihood function enables the visualization of equally probable solutions. It is useful to indicate some trends, mainly referred to the range of weight combinations that have similar probability.

For obtaining the well known least squares solution, it is necessary some further steps. Recall that the least squares solution is the set of axle weights that maximize the likelihood function. The usual approach is, however, maximizing the logarithm of the likelihood. It allows to simplify the mathematical operations without changing the maximum point, since the logarithm is a monotonically increasing function. It reads as, also including the expression for the Gaussian pdf:

$$\log\left(\mathcal{L}\right) = \log\left(\prod_{i=1}^{N} \frac{1}{\sigma_\varepsilon \sqrt{2\pi}} \exp\left(-\frac{1}{2}\left(\frac{y_i - \hat{y}_i(\boldsymbol{W})}{\sigma_\varepsilon}\right)^2\right)\right). \tag{44}$$

Applying some logarithm properties:

$$\log\left(\mathcal{L}\right) = \sum_{i=1}^{N}\left(\log\left(\frac{1}{\sigma_\varepsilon \sqrt{2\pi}}\right) - \frac{1}{2}\left(\frac{y_i - \hat{y}_i(\boldsymbol{W})}{\sigma_\varepsilon}\right)^2\right). \tag{45}$$

In order to maximize such an expression, it is necessary make the first derivative of this expression with respect to the axle weights equal to zero:

$$\frac{\partial \log(\mathcal{L})}{\partial \boldsymbol{W}} = -\sum_{i=1}^{N} \frac{1}{2} \frac{\partial}{\partial \boldsymbol{W}} \left(\frac{y_i - \hat{y}_i(\boldsymbol{W})}{\sigma_\varepsilon} \right)^2 = 0. \tag{46}$$

The derivative of such an expression results in:

$$\sum_{i=1}^{N} \frac{\partial \hat{y}_i(\boldsymbol{W})}{\partial \boldsymbol{W}} \left(\frac{y_i - \hat{y}_i(\boldsymbol{W})}{\sigma_\varepsilon^2} \right) = 0. \tag{47}$$

Thus, employing matrix notation and recalling that the relation between theoretical moment ($\hat{\boldsymbol{y}}$) and the vector of axle weights ($\boldsymbol{W}$) is defined by Equation (4):

$$\left(\frac{1}{\sigma_\varepsilon^2} \right) \boldsymbol{L}^T (\boldsymbol{y} - \boldsymbol{L}\boldsymbol{W}) = 0. \tag{48}$$

It is clear that the parameter σ_ε does not have influence in this process. Rearranging the expression:

$$\boldsymbol{L}^T \boldsymbol{L} \boldsymbol{W} = \boldsymbol{L}^T \boldsymbol{y}. \tag{49}$$

Finally, the least squares solution for the vector of axle weights can be written as:

$$\boldsymbol{W} = \left(\boldsymbol{L}^T \boldsymbol{L} \right)^{-1} \boldsymbol{L}^T \boldsymbol{y}. \tag{50}$$

As discussed along the derivation of the least squares solution, the parameter σ_ε is not important for the punctual weight estimate. However, this parameter is relevant when combining both prior and likelihood for generating Bayesian estimates. In this section, σ_ε is set to 10000, which is equal to the standard deviation of the additive noise directly applied to the bending moment. In the sequel, two examples are analyzed to highlight the effects of the likelihood function and serial correlation.

4.5.1.1 Example 1: likelihood function

The previously discussed likelihood function is useful for showing not just the most probable axle weights but also the assigned probabilities for other sets of axle weights. In the left hand side of Figure 3, it is presented the likelihood function of the analyzed example for a sampling rate of 40 Hz. In addition, the least squares solution and the real values of the axle weights are also shown. As already discussed, the least squares solution is the most probable point of the likelihood function. This example is interesting since it graphically shows some problematic aspects in the least squares process. Notice that the probabilities associated with the likelihood function are highly negatively correlated. As both axles are considerably close, it is difficult for the likelihood function to distinguish among the real contribution of each axle. Thus, similar probabilities are assigned to pairs of axle weights whose sum are at a same level, even that, individually, the value of each axle weight is unrealistic. It explains the observed negative correlation: an increasing in the weight of one axle must be balanced

with the decreasing of the weight of the remaining one in order to keep the likelihood function at the same level. However, regarding the practical point of view, even this simple example shows that the current likelihood function assigns high probability to some combinations of axle weights including negative values, higher than the probability of the real values. The tendency is that for larger vehicles, with more axles, a higher number of spurious combinations may have high probability and, in some cases, resulting as the most probable ones. It helps to explain why negative values may be reported for individual axles in a group of closely spaced axles in B-WIM systems.

The aspects just analyzed do not indicate that the likelihood function has some problem itself. Otherwise, it makes clear that some prior knowledge is missing from the formulation: for instance, as it is known that axle weights are non-negative quantities, it is an interesting approach to include this consideration into the formulation. It can be useful for helping in the process of choosing among a set of highly probable axle weights those ones that best match the expected behavior. In this context, the proposed Bayesian approach arises as an effective alternative to include prior knowledge into the formulation. The right hand side of Figure 3 presents the results when including the prior distribution defined for this example. It shows that the prior correlation among axle weights is important for the process, since it opposes the trend presented by the likelihood function in such a way that it concentrates the resulting posterior in a much more tight range of axle weights. Hence, the application of the prior distribution decreases the probability of occurrence of spurious results for individual axles. Furthermore, for this example, the most probable posterior axle weights have a more befitting behavior when compared with the practical expected values. It results, for this simple example, in better axle estimates than just employing the least squares approach. Summarizing, by employing a prior knowledge regarding the most probable combination of axle weights, it is possible to guide the process to more suitable results.

4.5.1.2 Example 2: serial correlation

The second aspect to be addressed here is the correlation that might occur in time series data. In the Example 2, this effect is simulated by interpolating the data until the number of measures is equal to the expected value for a sampling rate of 200 Hz. It is clear that this process does not generate additional data. Otherwise, it is just an artificial way of increasing the amount of data. The remaining parameters of the problem are all kept the same, including the parameters related to the prior and likelihood.

In the left hand side of Figure 4, it is presented the comparison among the likelihood obtained in the Example 1 and the likelihood of the current example. As this likelihood function is based on the independence assumption, the model interprets the extra data as reliable information, assigning to the interpolation points the same importance of the other points. Then, with more data, the confidence of the model referred to the reported estimates increases. This is the reason behind the narrowing of the level curves of the likelihood of

Figure 3 – Resulting probability distributions and main estimates for the axle weights regarding the first example
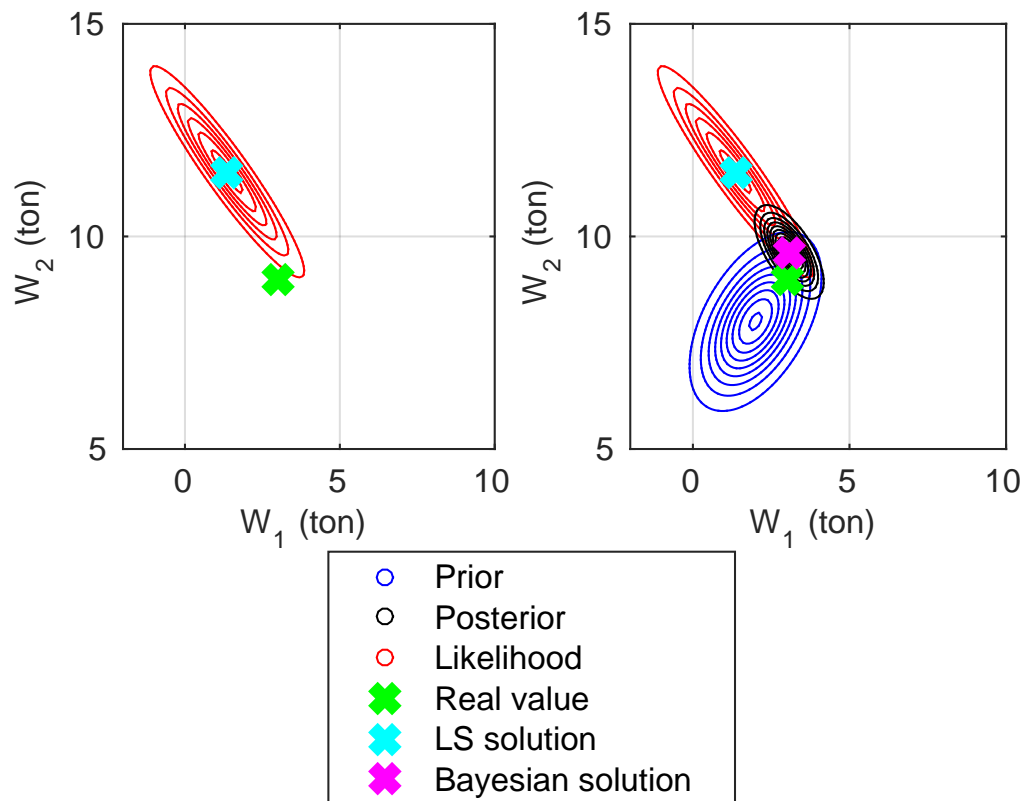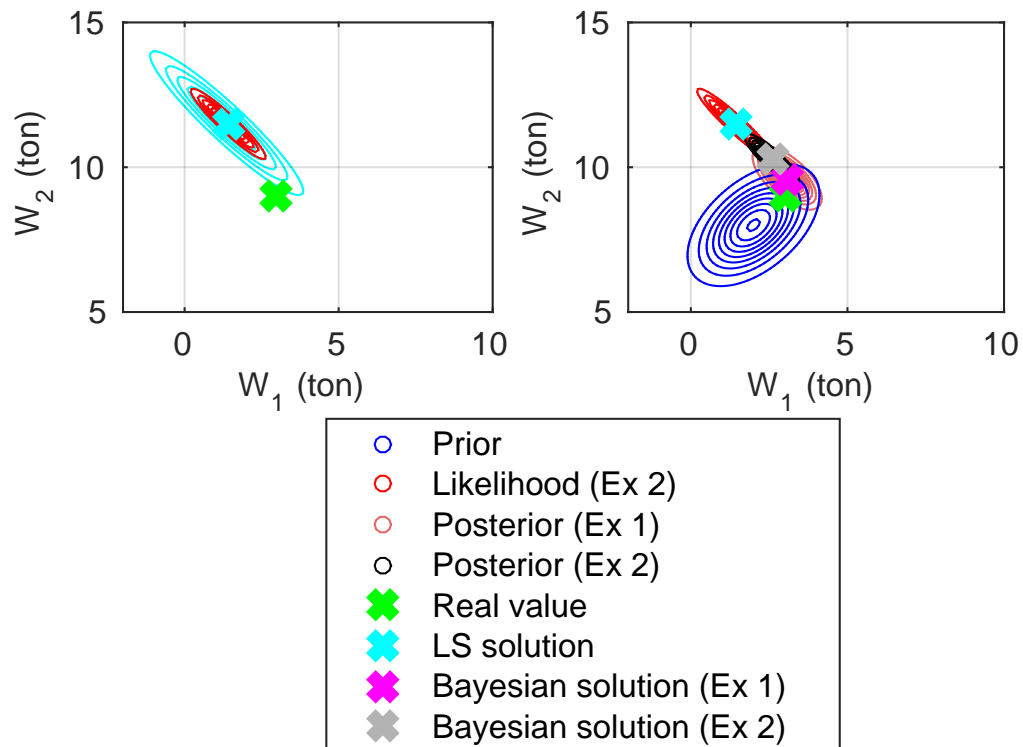

Example 2 when compared to Example 1. However, it is perceived that the artificial data added in this example clearly violates the independence assumption and, hence, the level curves of example 2 mislead the analysis. It is worth to mention that the least squares solution remains the same as in Example 1, which intuitively is the expected behavior, since no real additional information is provided to the model.

The right hand side of Figure 4 depicts the posterior distributions for both examples. Whereas the least squares estimate does not change in the presence of the artificially generated data, the Bayesian solution is considerably shifted. The extra amount of data increases the influence of the likelihood function into the final output of the Bayesian approach, shifting the posterior distribution towards the likelihood. However, this shift is not desirable, since no extra information is really added to the model. Therefore, Example 2 indicates that the correlation that may arise from experimental time series data should be properly addressed to avoid the corruption of the Bayesian process as a whole.

4.5.2 Numerical simulations

Two examples of bridge structures are evaluated. The only distinction between them is the bridge span length, which is 10 m for the first example and 20 m for the second one. Both bridges are modeled as simply supported single girder bridges, employing the Euler-Bernoulli

Figure 4 – Resulting probability distributions and main estimates for the axle weights regarding the second example.

○	Prior
○	Likelihood (Ex 2)
○	Posterior (Ex 1)
○	Posterior (Ex 2)
✖	Real value
✖	LS solution
✖	Bayesian solution (Ex 1)
✖	Bayesian solution (Ex 2)

beam model. For both bridges, all structural parameters are assumed to be constant in the structure. Table 2 presents the parameters employed for the simulations for both structures. The vehicles are modeled as a system of sprung masses where the damping and stiffness of the suspension of each axle are included into the model. The procedure employed for performing the numerical simulations is the same as detailed in Carraro et al. (2019). The dataset comprising all the simulations utilized in this paper is available in Gonçalves (2021).

Table 2 – Bridge parameters

| Property	Value (Units)
Bridge modulus of elasticity	10^{10} (Pa)
Bridge damping coefficient	0.05 (–)
Bridge moment of inertia	0.5 (m^4)
Bridge mass per unit length	$10^4 (kg/m)$

In order to provide more robust information for assessing the suitability of the Bayesian strategy, an in service accuracy check is simulated as defined in the COST 323 specification (JACOB; O'BRIEN; JEHAES, 2002). Hence, the simulated signals related to calibrating and testing the system are distinct from each other. It is an attempt to model a situation as close as possible to a B-WIM system practical operation, since calibration is performed usually with

a few vehicles. Thus, for calibrating the system, two vehicles, with two and four axles, are considered and each of them performs 20 runs over the bridge: 4 runs at 13.33 m/s, 12 runs at 16.67 m/s and 4 runs at 20 m/s.

For testing the system, vehicles with 2 to 9 axles are simulated. A set with 200 randomly selected vehicle configurations is employed, where both axle weights and spacing are determined based on a Brazilian vehicles classification (DNIT, 2012). The vehicles are assumed to have axle weights corresponding to a distinct percentage of the maximum value legally allowed in such a classification. The value for each axle is independent from each other and is randomly chosen based on a uniform distribution ranging from 40% to 120%. This scenario represents a situation where no pattern among axles is present. Thus, it is possible to check the robustness of the Bayesian strategy regarding the prior belief related to the similarity among axle weights. Furthermore, some vehicles with axle weights above the maximum limit are intentionally simulated. Such vehicles are utilized for evaluating the capacity of the methods related to overweight identification.

The vehicle speed at each testing run is a uniformly distributed random variable bounded by 10 and 20 m/s, i.e., $\mathcal{U}(10,20)$. The vehicles are assumed to travel the bridge at a constant speed on every run, an assumption generally applied in B-WIM systems (GONÇALVES; CARRARO; LOPEZ, 2021a; LANSDELL; SONG; DIXON, 2017). In addition, aiming to better represent the real behavior of experimental procedures, each simulated signal is contaminated by adding a Gaussian random noise with Signal to Noise Ratio (SNR) of 20. Finally, a roughness profile related to class B (ISO 8606:1995, 1995) is assumed for the whole structure, where for each run a distinct profile is generated. The sampling rate is 1000 Hz for all simulations. Figure 5 presents one example of strain signal for each modeled bridge.

Figure 5 – Example of simulated strains for both modeled bridges due to a two-axle vehicle.


(a) 10 m bridge

(b) 20 m bridge
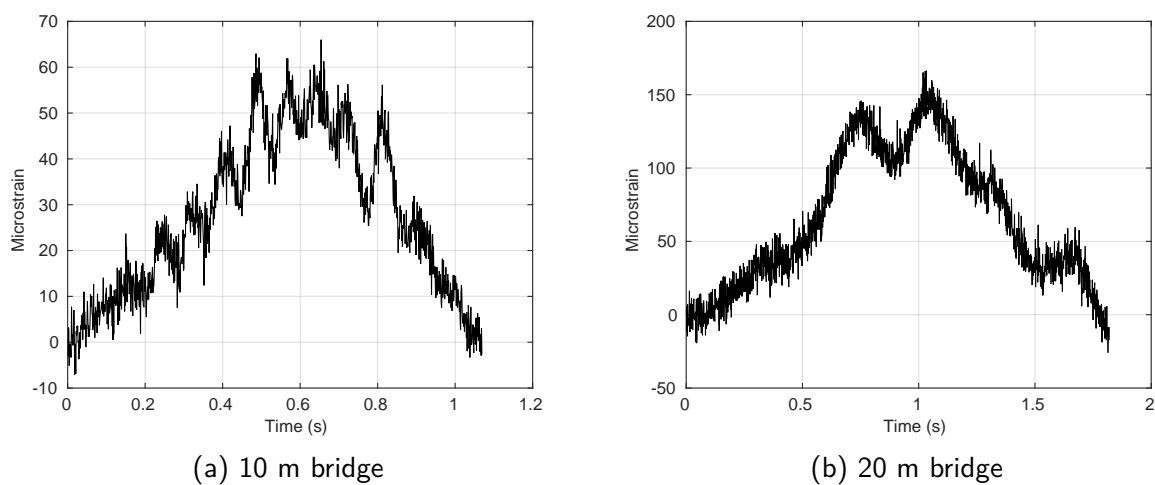
In order to assess the effect of both the prior distribution of axle weights and the second order autoregressive covariance matrix for the error between model and system response, four distinct Bayesian strategies are evaluated:

1. B1: Including prior knowledge, but zero correlation among axle weights and without any strategy for modeling serial correlation;

2. B2: Including complete prior knowledge and without any strategy for modeling serial correlation;

3. B3: Including the same prior knowledge as in B1 and the proposed AR(2) model for the error term;

4. B4: Including the same prior knowledge as in B2 and the proposed AR(2) model for the error term. It is the strategy that addresses all the modeling aspects discussed in the present study.

Aiming to provide a more practical comparison criterion, it is also evaluated the performance of two algorithms from the current literature. The first one is the least squares solution (LS) for the axle weights, as previously discussed. It is the simplest way to proceed and works as a baseline performance. The second one is based on an algorithm already discussed in the present work, the Regularized approach (O'BRIEN et al., 2009). It is a method developed focusing specifically on improving the predictions of individual axles, as in the present work. Thus, it is a natural candidate to be added to the pool of algorithms. However, the application of the regularization approach relies on the definition of the regularization coefficient, which is not an easy task (O'BRIEN et al., 2018; ŽNIDARIČ; KALIN; KRESLIN, 2018). Indeed, as in a previous work (CARRARO et al., 2019), a preliminary implementation of the regularization approach reported weight predictions quite similar to the LS algorithm, since low regularization parameters were being estimated. In order to provide a useful threshold performance and mitigating the effects of subjectivity on parameter definition, an alternative strategy was adopted. Instead of simulating a practical scenario, where the parameter is obtained without knowledge related to the real weights of the vehicle, in the present implementation it is simulated a nearly optimal performance for the regularization approach. A pre-defined set of candidate parameters, comprised of 1000 points logarithmically spaced ranging from 10^{-90} to 10^5 (the same order of the bounds employed in the work of O'Brien et al. (2009)), is tested and it is chosen the one that results in the minimum sum of squared residuals between predicted and real axle weights. Notice that this strategy does not have any practical relevance, since, obviously, the exact weights of passing vehicles are not previously known for real B-WIM applications. Then, the relevance of this strategy is just to represent what could be seen as an excellent performance, mainly for closely spaced axles. This modified regularization strategy is named here as Reg.

Two criteria are employed for assessing the suitability of the algorithms. The first one is the COST 323 accuracy classification for weigh-in-motion systems (JACOB; O'BRIEN; JEHAES, 2002). It is a measure of quality employed by many works in the B-WIM subject (ŽNIDARIČ; KALIN; KRESLIN, 2018; ŽNIDARIČ, 2017; O'BRIEN; GONZÁLEZ; DOWLING, 2010; RICHARDSON et al., 2014), where B-WIM systems can be assigned to classes ranging from A(5) to D(25), but that could be extended to E(50). The simulations performed in this

Figure 6 – Frequency domain representation of all calibration signals before decimation for the 10 m bridge.
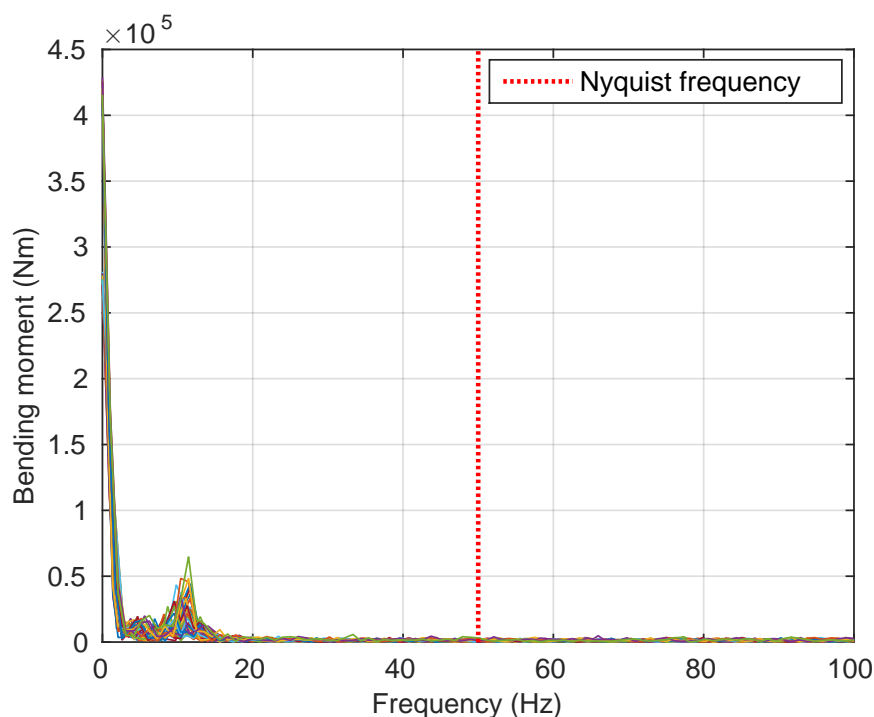
study are considered under environmental repeatability (I) and full reproducibility test condition (R2). The second tool employed is the boxplot of the errors obtained for each vehicle run. In the boxplots, the red line indicates the median of the data and the central box represents the 25th and 75th percentiles. The whiskers are extended to include all the elements that are not considered outliers. Such outliers are individually marked by red points. It enables a better visualization of the behavior of the error obtained by each method, making the comparison easier. Both accuracy classes and boxplot of errors are reported for gross vehicle weight (GVW), group of axle, single axle, and axle of a group, based on the definitions stated by the COST 323 specification (JACOB; O'BRIEN; JEHAES, 2002).

4.5.2.1 10 m span bridge

Figure 6 depicts the frequency domain representation of all calibration signals grouped together. It can be noticed that the most important frequencies are concentrated around 15 Hz. Then, a decimation factor of 10 is utilized, resulting in an effective sampling frequency of 100 Hz. The 50 Hz threshold also presented in the figure represents the Nyquist frequency for the decimated signals.

Table 3 and Figure 7 present, respectively, the accuracy classes and boxplot of errors for the analyzed algorithms. It is opted to include the number of events with negative axle predictions in the table since eliminating such spurious estimates is one of the main goals of the present work. In addition, it is called class F the algorithm that could not reach the class E(50). For all methods, it is observed that the errors are small for GVW and axle group, and

they consistently increase for single axle and axle of a group. Regarding the Bayesian methods, a tendency of increasing the accuracy when moving from B1 to B4 is observed in this example, mainly for single axle and axle of a group. It also happens with the number of negative axles reported, which moves from 3 to 0. This trend indicates that both the inclusion of a prior distribution of axle weights and the utilization of the AR(2) covariance matrix for modeling the serial correlation are important for a proper weigh procedure. When compared to LS, it is noticed that B4, the Bayesian algorithm with best performance, improves results for group of axles, single axle and axle of a group quantities without affecting the GVW estimates. When compared to the Reg version with nearly optimal regularization parameters, it is noticed that B4 strategy reaches similar performance. For almost all quantities the accuracy classes are the same. The only exception is axle of a group, where Reg presents a better classification. Then, even for an unlike scenario where all regularization parameters are chosen as the best possible, the Bayesian strategy B4 performance is equivalent to the one of the Reg algorithm, and clearly outperforms LS.

Table 3 – Accuracy classes and number of negative axle events for the algorithms analyzed for simulated vehicles in the 10 m bridge.

|	LS	Reg	B1	B2	B3	B4
GVW	A(5)	A(5)	A(5)	A(5)	A(5)	A(5)
Axle group	B+(7)	A(5)	B+(7)	B+(7)	B+(7)	A(5)
Single axle	C(15)	B(10)	C(15)	C(15)	B(10)	B(10)
Axle of a group	E(40)	C(15)	E(40)	E(35)	E(30)	D(25)
Negative axle events	3	0	3	3	0	0

It is interesting to recall that this dataset was created including some vehicles with axle weights above the legal limits. Therefore, these limits are utilized for overweight definition and the performance of the algorithms for correctly classifying every axle with regard to respecting or not the limits is evaluated. Table 4 depicts the results for LS, Reg and B4 algorithms. It is noticed that all methods, in general, show similar performance, where mostly of predictions are correct. Just a minor difference is perceived for false positive percentage referred to LS, which is slightly higher.

As the definition of the prior distribution is somewhat subjective, it is also employed an informal sensitivity analysis, where the magnitude of changes in the output due to variations in

Table 4 – Results for the classification of every vehicle axle as overweight or not for LS, Reg and B4 algorithms. A total of 220 overweight axles and 633 not overweight are present in this dataset.

	LS	Reg	B4
True overweight	184	177	169
True not overweight	591	620	609
False overweight	42	13	24
False not overweight	36	43	51

Figure 7 – Boxplots for the errors of each analyzed quantity of interest for simulated vehicles and the 10 m bridge.
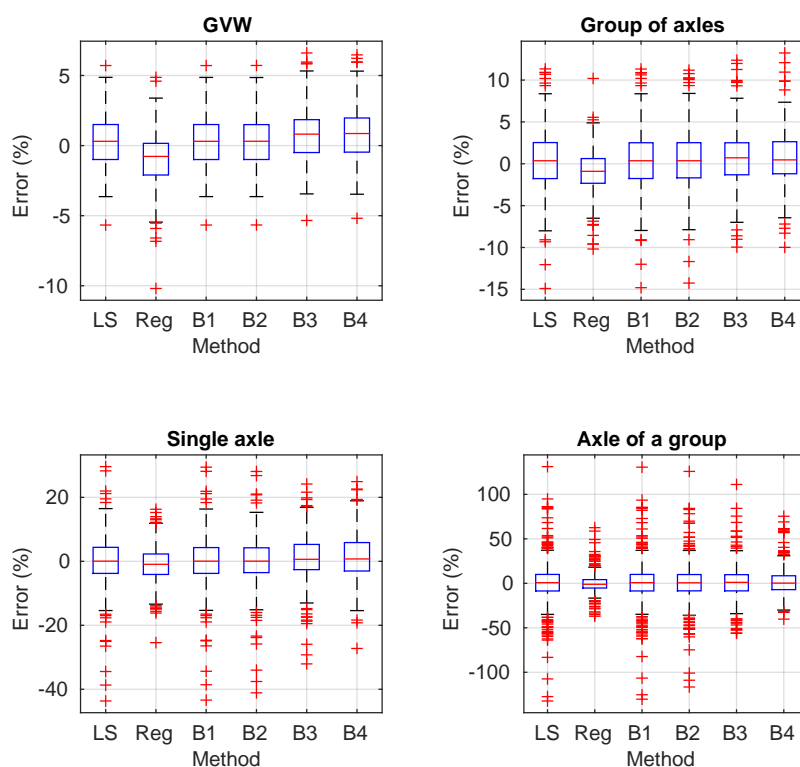
the input parameters is evaluated. It is a simplified procedure, with some limitations. However, it is an important tool for robustness assessment, far better than ignoring it (INSUA; RUGGERI, 2000). The main goal of such analyses is to show that the change in reported results due to deviations in the prior parameters is not significant. It is useful to indicate that the results of the Bayesian method are not attributed just to the application of a clever set of parameters, which is an indicator of the robustness of the proposed strategy.

For assessing such a robustness, the accuracy reported by a set of variants of the best method in the previous analyses, the B4 algorithm, is evaluated. The variants are defined by changing some parameters of the prior distribution, following the same prior information discussed in subsection 4.4.4. As the definition of such parameters is subjective, many distinct priors can be developed from the same prior information. The values are chosen in order to represent distinct practical scenarios, always respecting what seems reasonable from the initial information. In Table 5, it is presented the parameters employed in this analysis. Aiming to better illustrate the employed distributions, Figure 8 depicts the marginal prior distributions for the weights of each axle. The algorithms are named according to Table 5. Three options of variance are defined, based on keeping 0.5, 1 or 2 standard deviations from the mean to both reference values (2 and 10 tons). On the other hand, two distinct mean values are defined, calculated by modifying the lower reference from 2 to 0 tons. It is worth to remark that the

prior marginal distributions from B5 and B6 are the same of B1 to B4 since what is modified among them is just the correlation among axle weights, which is not represented in the picture. The main goal is to show that even considering highly distinct prior distributions, the results are kept at a similar level.

Table 5 – Parameters employed on the sensitivity analysis regarding the B4 approach

	B5	B6	B7	B8	B9	B10
$\mu_W^{(1)}$ (kN)	4g	4g	4g	4g	3g	5g
$\mu_W^{(2 \text{ to } J)}$ (kN)	6g	6g	6g	6g	5g	7g
$\rho_W^{(\text{Not same group})}$	0.70	0.00	0.50	0.50	0.50	0.50
$\rho_W^{(\text{Same group})}$	0.95	0.75	0.90	0.90	0.90	0.90
$\sigma_W^{(1)}$ (kN)	2g	2g	4g	1g	2g	2g
$\sigma_W^{(2 \text{ to } J)}$ (kN)	4g	4g	8g	2g	4g	4g

Figure 8 – Comparison of the marginal prior distributions for the weight of each axle related to each algorithm evaluated. LR and UR stands for the lower and upper references defined in subsection 4.4.4, respectively, whereas ZR indicates the axis corresponding to zero ton.
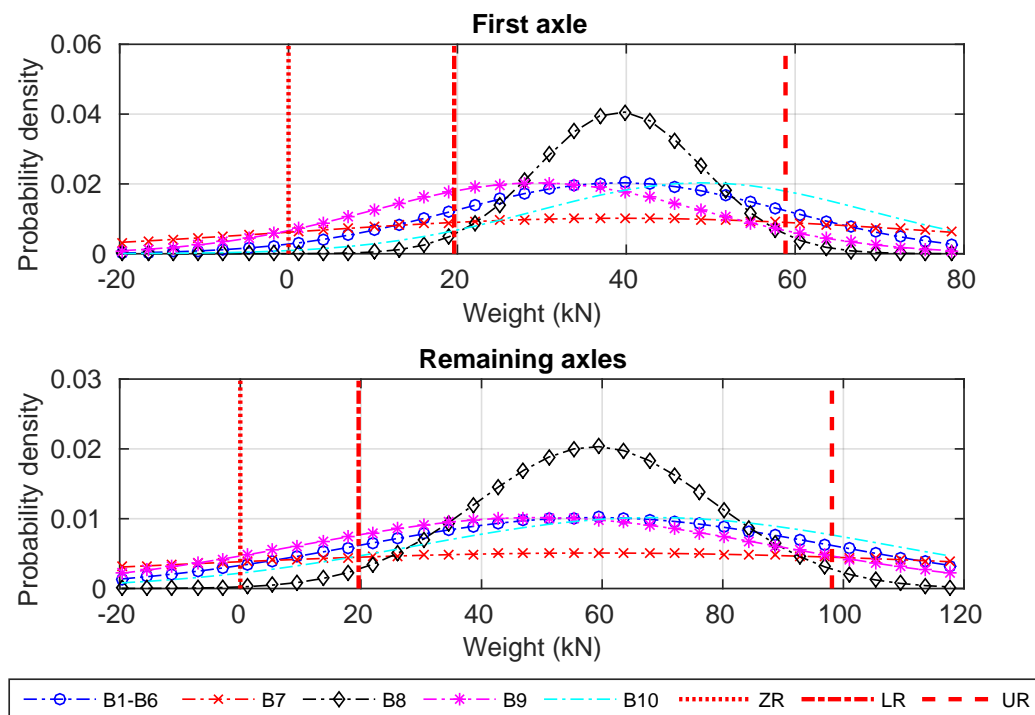

Table 6 and Figure 9 depict both accuracy classes, with the number of negative axle events, and boxplot of errors for all variants of the B4 approach as well as the LS algorithm. In general, the difference among all variants of the Bayesian approach are quite small. Indeed, the accuracy classes for almost all methods and quantities reproduced the same results as for B4 algorithm. In addition, the accuracy classes of the Bayesian methods were always better

or equal to the ones reported by LS. The most significant improvements occur for the axle of a group quantity. Moreover, it is clear that the proposed strategy was able to avoid negative axle predictions since it did not occur for any event or algorithm. Thus, it could be concluded that the results of the Bayesian strategy are robust to the prior parameters for this example.

Table 6 – Accuracy classes and number of negative axle events for the sensitivity analysis for simulated vehicles and the 10 m bridge.

	LS	B4	B5	B6	B7	B8	B9	B10
GVW	A(5)	A(5)	A(5)	A(5)	A(5)	A(5)	A(5)	A(5)
Axle group	B+(7)	A(5)	A(5)	B+(7)	B+(7)	A(5)	A(5)	A(5)
Single axle	C(15)	B(10)	C(15)	B(10)	B(10)	C(15)	B(10)	C(15)
Axle of a group	E(40)	D(25)	D(25)	D(25)	D(25)	E(30)	D(25)	D(25)
Negative axle events	3	0	0	0	0	0	0	0

Figure 9 – Boxplots for the errors of each analyzed quantity of interest for simulated vehicles and the 10 meter bridge.
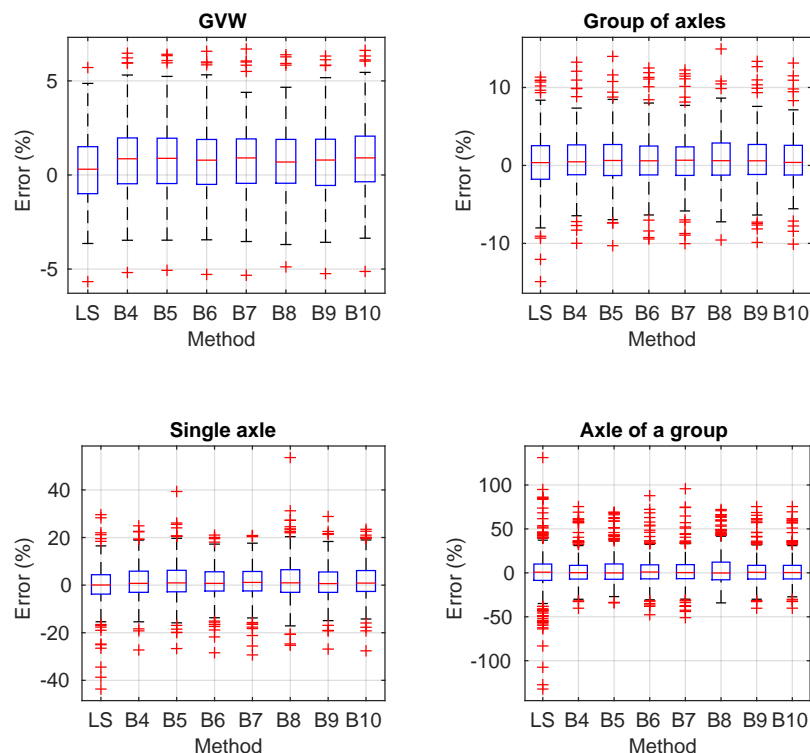
4.5.2.2   20 m span bridge

For this second example a distinct decimation factor is applied. The reason is that the most important range of frequencies is significantly lower for this example when compared to the previous one. The frequency domain representation of all calibration signals is presented in

Figure 10 – Frequency domain representation of all calibration signals before decimation for the 20 m bridge.
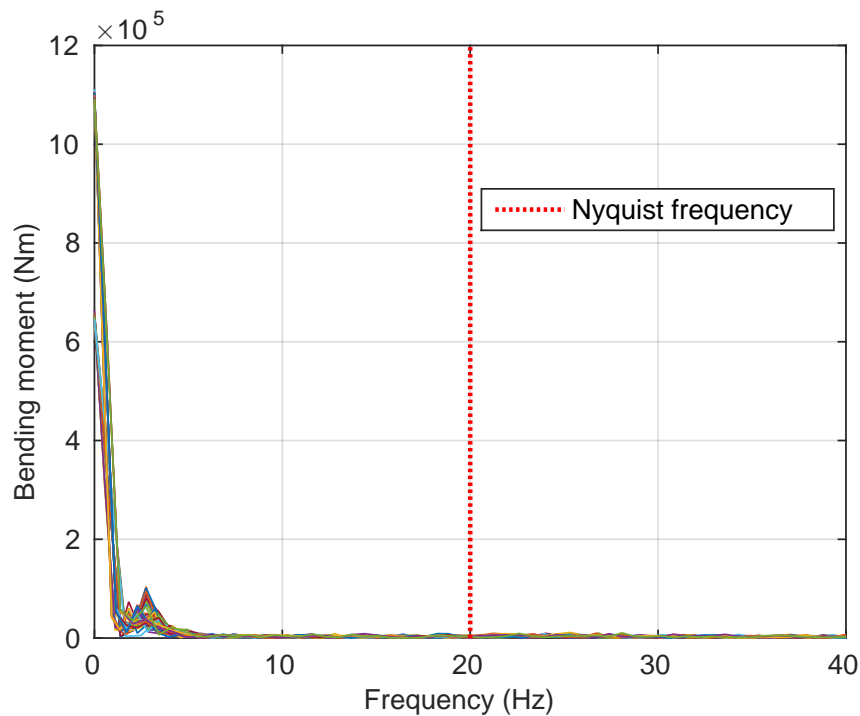

Figure 10, in which it is perceived that the frequency content is limited to about 5 Hz. Thus, the decimation factor of 25 is adopted, resulting in an effective sampling frequency of 40 Hz.

Table 7 and Figure 11 depict the accuracy classes, including the number of negative axle events, and the boxplot of errors for the analyzed algorithms, respectively. The first issue that is clearly noticed for this example is that results for all methods and quantities are significantly deteriorated when compared to the first example. The reduction in accuracy for B-WIM algorithms for longer bridges is already well known in literature as reported, for instance, in Gonçalves, Carraro, and Lopez (2021a). Moreover, longer bridges increase the difficult to distinguish among the individual contribution of closely spaced axles. Therefore, worse results in this example were already expected. For all methods, it is observed a high contrast among results for GVW and the other quantities of interest. Whereas the errors are kept small for GVW, they increase by a high amount for the remaining quantities. When comparing the results of each method, the conclusions are the same as for the first example. Some of then are even more evident. Regarding the Bayesian methods, an even more pronounced tendency of increasing the accuracy when moving from B1 to B4 is observed in this example, mainly for single axle, axle of a group and the number of negative axles reported. In this example, however, a high performance jump from B2 to B3 is noticed. It indicates that for this longer bridge example the impact of modeling the error correlation is even more significant. This result is in accordance with the last example and shows that both the prior distribution and the error term assumptions are suitable for this application. More importantly, it also indicates that the AR(2) model for the error term is of paramount importance to enable that the prior

knowledge be effectively utilized in the Bayesian context.

It can be seen that B4 outperforms LS by a even larger margin than for the shorter bridge of the previous example. Such a margin includes many accuracy classes of distance from B4 to LS for Axle group, Single axle and Axle of a group together with the elimination of negative axle events. When comparing B4 to the Reg version with nearly optimal regularization parameters, it is noticed that B4 outperforms the latter for GVW and axle group, although it has a slightly worse performance for Single axle. It is an interesting aspect, since it shows that even in the case where the best regularization parameter is calculated from previously knowing the vehicle weight, B4 shows a better overall performance than Reg. As the regularization approach can be seen as a simplified version of the Bayesian strategy, as discussed in Section 4.3.1, even the optimal regularization parameters may not be enough to outperform the more complete B4 strategy. Then, for this more challenging dataset, the B4 method clearly outperforms LS. Regarding Reg algorithm, even for an unlikely scenario where all regularization parameters are chosen based on the real vehicle weights, the B4 strategy presents a better performance in the whole picture.

Table 7 – Accuracy classes and number of negative axle events for the algorithms analyzed for simulated vehicles and the 20 m bridge.

	LS	Reg	B1	B2	B3	B4
GVW	A(5)	B(10)	A(5)	A(5)	A(5)	A(5)
Axle group	F	C(15)	F	F	C(15)	B(10)
Single axle	F	D+(20)	F	F	E(40)	D(25)
Axle of a group	F	E(35)	F	F	F	E(35)
Negative axle events	73	0	73	70	4	0

Similarly to the previous example, it is also evaluated the performance of the algorithms for overweight classification, and the results are in Table 8. In this case, it is clearly noticed that the overweight classification of the LS method is not reliable since it reported almost 200 false positives. The results for Reg and B4 are also worse when compared to the shorter bridge example, mainly for properly identifying overweight axles. The false positives, however, still are kept at a low level for both. It is interesting to notice that the maximum overweight allowed for all axles is 20%, and both B4 and Reg are able to properly identify overweight axles for roughly 50% of the cases. Such results are particularly interesting to show that the prior distribution employed for B4, with mean values significantly below the overweight limit, does not prevent the prediction of weights above such limits.

Table 9 and Figure 12 shows accuracy classes, with the number of negative axle events, and boxplot of errors for all variants of the B4 approach, as well as the LS algorithm. In this example, the difference among all variants of the Bayesian approach are quite small when compared to the results of the LS approach. For Group of axle, single axle and axle of a group all Bayesian variants largely outperforms LS. Furthermore, negative axles are avoided for all events and for all Bayesian methods, which is in contrast with the 73 events where such

Figure 11 – Boxplots for the errors of each analyzed quantity of interest for simulated vehicles and the 20 m bridge.
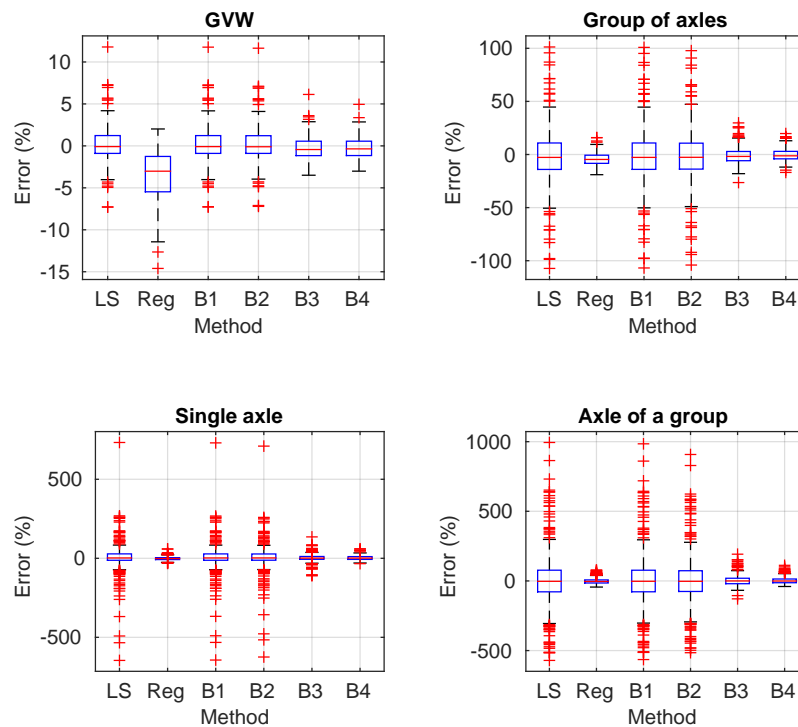

Table 8 – Results for the classification of every vehicle axle as overweight or not for LS, Reg and B4 algorithms. A total of 220 overweight axles and 633 not overweight are present in this dataset.

	LS	Reg	B4
True overweight	127	108	103
True not overweight	434	623	606
False overweight	199	10	27
False not overweight	93	112	117

a spurious prediction occurred for the LS method. Thus, the results are robust to the prior parameters for this more complex example.

Table 9 – Accuracy classes and number of negative axle events for the sensitivity analysis for simulated vehicles and the 20 m bridge.

	LS	B4	B5	B6	B7	B8	B9	B10
GVW	A(5)	A(5)	A(5)	A(5)	A(5)	A(5)	A(5)	A(5)
Axle group	F	B(10)	B(10)	B(10)	C(15)	C(15)	B(10)	B(10)
Single axle	F	D(25)	D(25)	E(30)	E(35)	E(30)	D(25)	E(30)
Axle of a group	F	E(35)	E(35)	E(40)	E(45)	E(35)	E(40)	E(35)
Negative axle events	73	0	0	0	0	0	0	0

Figure 12 – Boxplots for the errors of each analyzed quantity of interest for simulated vehicles and the 20 m bridge.
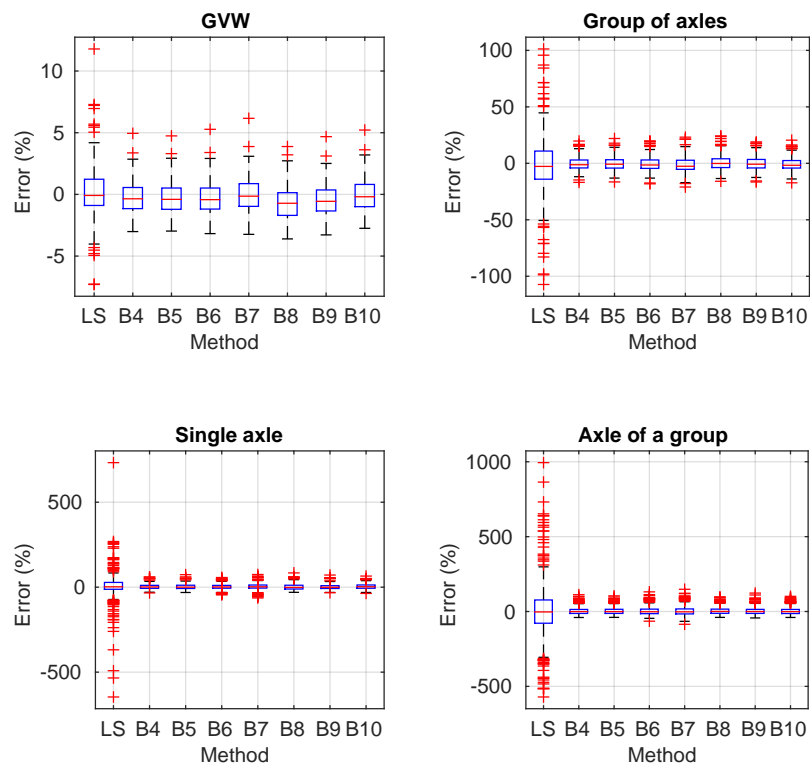
4.5.3 Real-world B-WIM system calibration data

The data collected during the calibration procedure for the Itinguijada bridge is employed as an example of real-world B-WIM application. The Itinguijada bridge is located at the km 147 of the BR 153, state of Goiás, Brazil. This structure has a total of 29 meters, with two girders and five cross beams. Each girder of the structure was monitored by two strain sensors attached at its bottom, longitudinally positioned at the mid-span. Figure 13 depicts the bridge structure and the placement of strain sensors. One pair of free-of-axle detectors (FAD) sensors was installed at the bridge slab underneath each traffic lane, from a total of 2 lanes. One sensor was attached at the mid-span of the bridge and the other was positioned 4 meters longitudinally from it. The sampling rate of the system is 512 Hz.

Two trucks were employed in the calibration procedure, where axle spacing and weight distribution are presented in Table 10. The dataset is comprised of 49 strains and FAD signals, 29 for the three-axle vehicle and 20 for the five-axle one. In this regard, at least 10 runs are referred to each possible combination of vehicle and lane. For each run, a distinct velocity was employed. The value of each vehicle speed was obtained by the FAD sensors located underneath the bridge slab. The dataset is divided according to the lane where the vehicle traveled and one influence line is calculated for each lane. The results for runs related to both lanes are combined in order to provide an overall picture regarding the system accuracy.

Table 10 – Axle weights and spacing for the calibration vehicles

	Axle weight (ton)				
	Axle 1	Axle 2	Axle 3	Axle 4	Axle 5
Three-axle vehicle	6.900	14.900	12.900	-	-
Five-axle vehicle	7.500	14.100	13.300	11.100	9.200
	Axle position (m)				
	Axle 1	Axle 2	Axle 3	Axle 4	Axle 5
Three-axle vehicle	0	4.78	6.07	-	-
Five-axle vehicle	0	3.57	9.16	10.43	11.66

As only the calibration runs data are available, the accuracy classes are calculated considering an initial verification case as defined in the COST 323 specification (JACOB; O'BRIEN; JEHAES, 2002). In addition, the number of vehicles is limited, hence, an extended repeatability condition (r2) is adopted. The same general procedure utilized in Section 4.5.2 is employed for this example. Thus, it is important to remark that, according to Table 10, both vehicles are considerably heavier than what was assumed by the adopted prior distributions. It is, again, an interesting analysis to check the suitability of the results of the proposed Bayesian approach when the prior belief is not so accurate.

Figure 14 presents the frequency domain representation of all signals prior to decimation, where it could be perceived that the maximum significant frequency content is around 8 Hz. Although a decimation factor equal to 8 could be enough to ensure that the effective sampling frequency stays below 10 times the maximum frequency, it is adopted here a decimation factor of 16. It is done to avoid that the sum of model coefficients for the autoregressive process be close to 1, as previously discussed in Section 4.4.3. It results in an effective sampling rate of 32 Hz and a Nyquist frequency of 16 Hz.

The accuracy classes obtained by each method, as well as the number of negative axle events are presented in Table 11, while the boxplots of the errors are depicted in Figure 15. A

Figure 13 – Example of strain sensors placement and bridge lateral view.
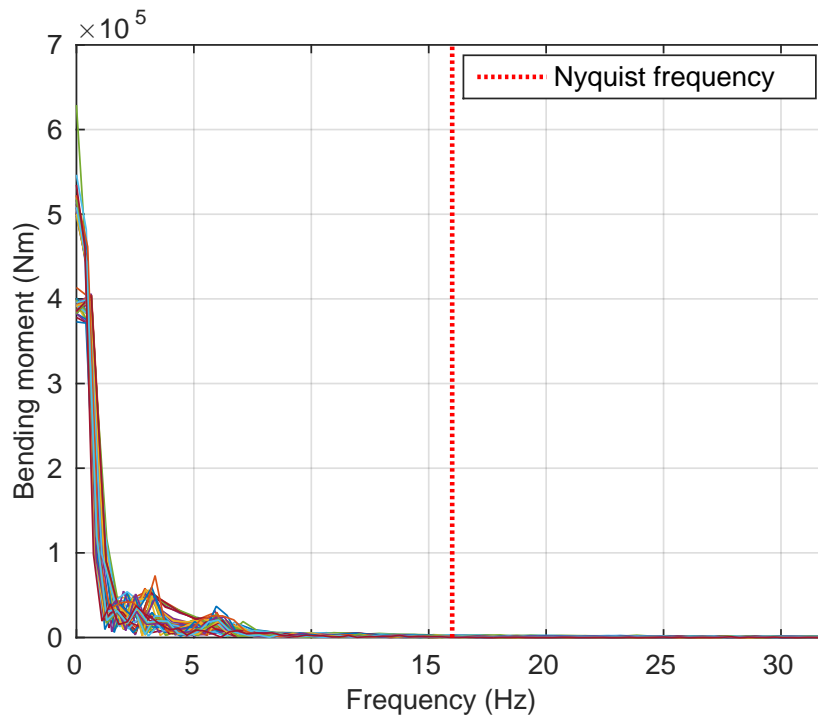

(a) Lateral view of the bridge

(b) Strain sensors

Figure 14 – Frequency domain representation of all real data signals before decimation.

first point to remark is that the errors for quantities other than GVW are lower when compared to the analysis of Section 4.5.2.2, even considering that it is a real engineering application, subject to many complexities beyond those modeled in the numerical simulation. Two main issues explain this fact. First, the same dataset is employed for both calibrating the influence lines and testing the algorithms' performance. By this way, the influence lines are able to better predict the response generated by the vehicles in the present case. Second, the number of vehicles is limited in this case, which implies a more homogeneous dataset and, hence, less susceptible to produce outliers.

When analyzing the performance of each method, conclusions similar to the ones of the previous section may be drawn. When compared to LS, B1 and B2 provide some improvements, however the absence of the AR(2) model for the error term seems to excessively limit them. The number of negative axle events is also reduced from 4 in the LS algorithm to 0 for B3 and B4. At the end, B4 appears again as the algorithm with the best performance when observing the overall picture, performing better or equal to LS for all quantities of interest. It indicates that all issues addressed in the present study are important to obtain better weight predictions, mainly the utilization of the AR(2) model for the error term. When compared to the version of the Reg algorithm with nearly optimal regularization parameters, B4 presents better or equal accuracy classes for almost all quantities of interest. The only exception is for axle of a group quantity, where the analyzed configuration of Reg algorithm shows a better performance. Thus, the inclusion of some prior knowledge together with the AR(2) model for the error term is able to outperform the solutions of Reg method for axle group and GVW. Such results are even more significant when it is noticed that the vehicles employed in this example are considerably

heavier than the mean values informed to the prior distribution and, even in this case, results of the B4 approach are very promising.

Table 11 – Accuracy classes and number of negative axle events for the algorithms analyzed for the real B-WIM system example.

	LS	Reg	B1	B2	B3	B4
GVW	C(15)	C(15)	C(15)	C(15)	C(15)	B(10)
Axle group	C(15)	C(15)	C(15)	C(15)	C(15)	C(15)
Single axle	E(45)	D(25)	E(45)	E(40)	D(25)	C(15)
Axle of a group	F	D(25)	F	F	F	E(35)
Negative axle events	3	0	3	1	0	0

Figure 15 – Boxplots for the errors related to each analyzed quantity of interest for the real B-WIM system example.
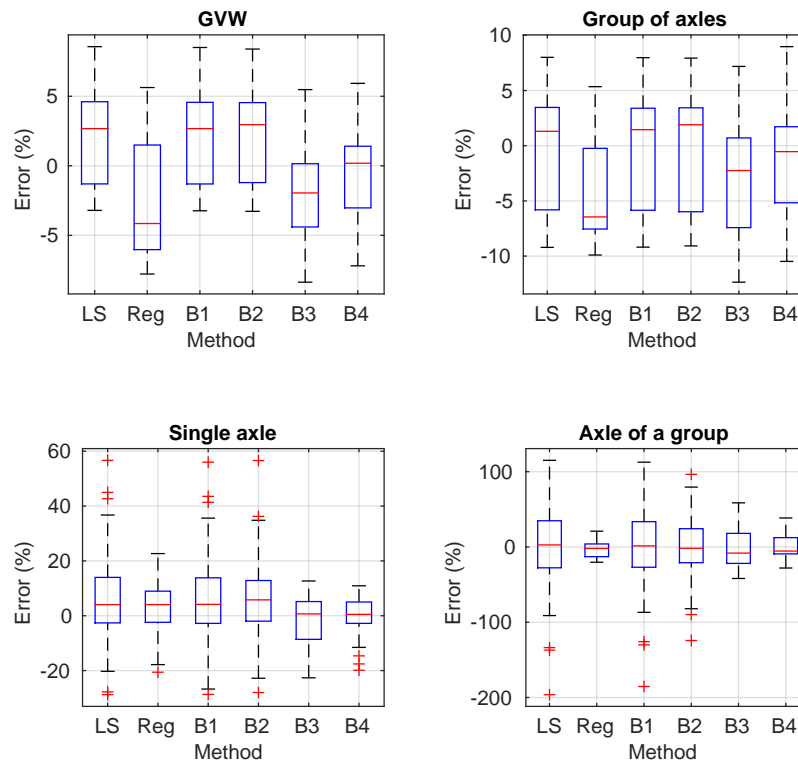

In order to make the conclusions more robust, sensitivity analyses are also conducted for this example, considering the same variants of the B4 algorithm applied in subsection 4.5.2. Table 12 and Figure 16 present both the table with the accuracy classes, including also the number of negative axle events, and the boxplot of the errors for all variants of the B4 strategy, respectively. The results for GVW and Group of axles show low variations among the seven evaluated configurations. For Single axle and Axle of a group, the difference is slightly higher, however all Bayesian algorithms still provide a performance far better than the LS for such quantities. When evaluating the number of negative axle events, it is noticed its occurrence

in 3 of 49 events in the LS algorithm. Again, all Bayesian variants avoided such a spurious estimate. In general, all variants of the B4 method outperform the LS method in all quantities of interest, mainly when the weight of the axles are individually evaluated. Such results indicate that the Bayesian algorithm defined by strategy B4 is robust to its model parameters even for a real-world B-WIM system example, whose vehicle properties do not fit precisely to the prior beliefs.

Table 12 – Accuracy classes and number of negative axle events for the sensitivity analysis for the real B-WIM system example.

	LS	B4	B5	B6	B7	B8	B9	B10
GVW	C(15)	B(10)	B(10)	B(10)	B(10)	C(15)	B(10)	B(10)
Axle group	C(15)	C(15)	B(10)	C(15)	C(15)	B(10)	C(15)	C(15)
Single axle	E(45)	C(15)	C(15)	D(25)	E(30)	C(15)	D+(20)	D+(20)
Axle of a group	F	E(35)	E(30)	E(40)	E(50)	E(30)	E(35)	E(35)
Negative axle events	3	0	0	0	0	0	0	0

Figure 16 – Boxplots for the errors related to each analyzed quantity of interest for the real B-WIM system example.
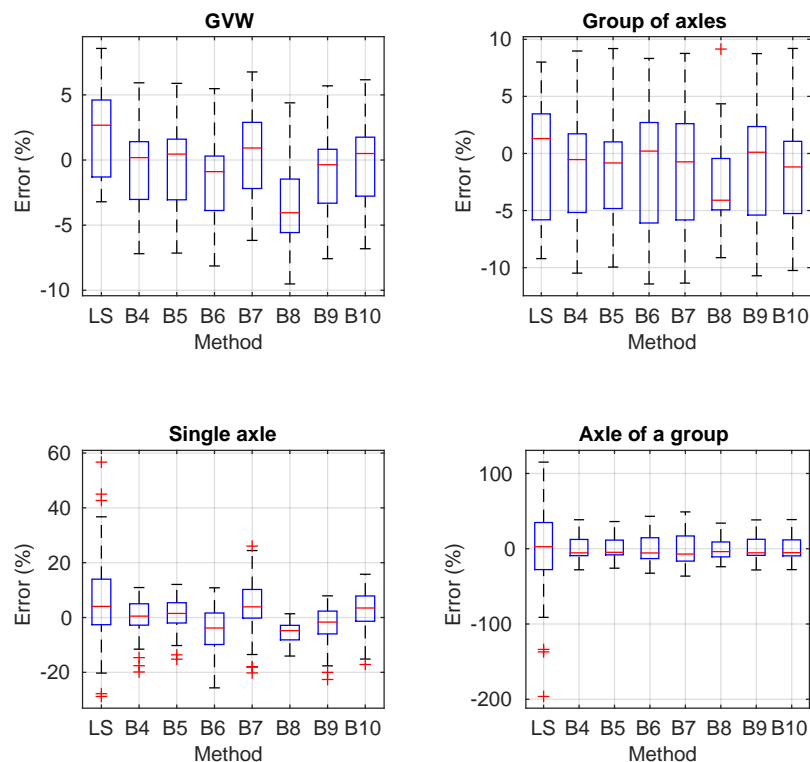
The previous analyses in this example were based on the same dataset for both calibrating the system and testing the performance of the methods. It happened due to the limited amount of information that was collected during the calibration procedure of the B-WIM system. However, as two vehicles were employed in this procedure, some out-of-sample analyses

are possible to be conducted. Therefore, it is performed two cross-validation analyses, where one type of vehicle is employed to calculate the model parameters, while the remaining one is utilized to assess the model accuracy. For sake of space just the results of the accuracy classes and the boxplot of GVW for LS, Reg and B4 are presented, considering both situations. For both scenarios, a full repeatability condition (r1) is assumed, since just one vehicle and load is being employed. In addition, as calibration and test vehicles are distinct, an in service accuracy check is assumed. For the next analysis, cases 1 and 2 refer to testing the system with the three- and the five-axle vehicles, respectively.

The boxplots in Figure 17 show that all methods are biased for both scenarios, where the first case estimates heavier weights than the true values, while the opposite occurs for the second case. In order to allow an out-of-sample analysis, the dataset utilized for calibration purposes did not reach the quantities of vehicles recommended by the COST 323 specification (JACOB; O'BRIEN; JEHAES, 2002). Then, it is expected that results be negatively affected. When comparing the accuracy classes of LS, Reg and B4 methods, in Table 13, the overall results for this cross validation analysis are also favorable to B4. The performance of B4 is better or equal to LS for all quantities and scenarios. When compared to Reg, the solution of B4 algorithm is better or equal for almost all quantities of interest and scenarios. The only exception is for axle of a group. Moreover, both algorithms completely prevent the occurrence of negative axle weight predictions. Thus, even in this complex situation, with few calibration runs and for out-of-sample predictions, the B4 algorithm is able to provide better overall results when compared to Reg and LS.

Table 13 – Accuracy classes and number of negative axle events for the algorithms analyzed for the real B-WIM system example considering out-of-sample predictions.

	Case 1			Case 2		
	LS	Reg	B4	LS	Reg	B4
GVW	C(15)	C(15)	B+(7)	C(15)	C(15)	C(15)
Axle group	C(15)	B(10)	B+(7)	D+(20)	D+(20)	D+(20)
Single axle	E(45)	E(30)	D(25)	E(40)	E(30)	C(15)
Axle of a group	F	C(15)	D(25)	F	D(25)	E(40)
Negative axle events	0	0	0	3	0	0

4.6   FURTHER REMARKS

Considering the numerically simulated signals and the real B-WIM system calibration, the Bayesian approach proposed in the present study clearly outperformed LS. When compared to the version of Reg algorithm with nearly optimal regularization parameters, the overall results are also favorable to the proposed Bayesian strategy. Sensitivity analyses showed that the obtained results were robust to variations in model parameter values. The aspects discussed confirm that the proposed approach is robust to its model parameters and able to reach its

Figure 17 – Boxplots for the GVW errors related to each cross validation case for the real B-WIM system example.
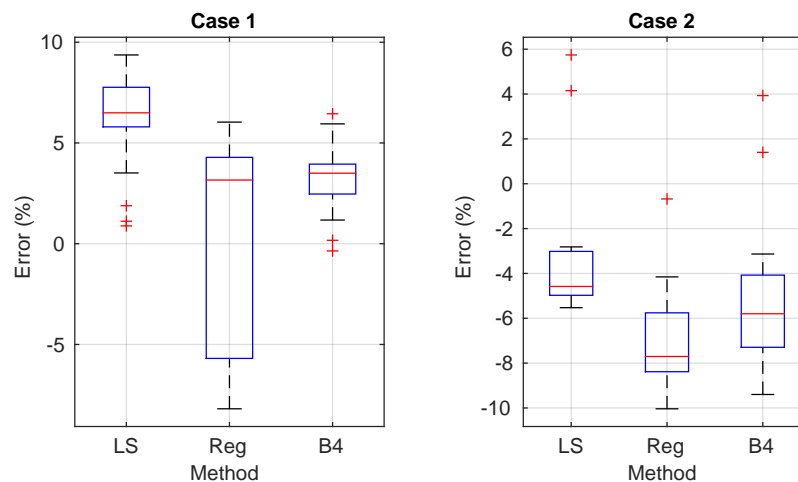
goal of improving the weight estimate for individual axles without corrupting the predictions for GVW.

A relevant aspect to further comment is related to the prior distribution. As already discussed, a common criticism to Bayesian models is related to the subjectivity of the selection of prior distributions. This subjectivity is not disregarded in the present study. Conversely, it is clearly recognized in the process of selection for the prior parameters. However, the axle weights of heavy vehicles are quantities for which good initial guesses are available. In this context, the negative effects of the subjectivity of prior definition are mitigated: as a not so wide range of values is suitable for practical purposes, the differences for distinct selections are not so high. The sensitivity analyses are performed for effectively checking this statement. As the results are robust to variations of such parameters, the present work shows that the inclusion of prior knowledge in the proposed Bayesian approach is a suitable action even recognizing the subjectivity related to the selection of the prior distribution.

The examples also indicated that the proposed strategy is robust regarding violations in its own prior assumptions. Even considering numerical simulations where axle weights were independent and allowing weights significantly above the mean of the prior distribution, the errors were kept at a level clearly below what was obtained by LS and, in the overall picture, better than the Reg algorithm with nearly optimal parameters. The real B-WIM system calibration data also employed vehicles whose weight of axles were considerably above the prior belief. In this case, the results of the Bayesian approach were even better, since accuracy classes of this strategy were equal or outperformed LS and Reg for almost all quantities of interest. The only exception was the axle of a group quantity for the Reg algorithm. It is important to remark that no negative axle event was reported for any example and variant of the B4 algorithm, even that negative weights constraints were not rigorously enforced. Indeed, the combination of correlation among axle weights and the employed marginal prior distributions were sufficient to avoid negative values. One possible reason is that negative axles arise usually

for closely spaced axles, where it is difficult to quantify the contribution of each of them for the bridge response. In this context, many combinations of axle weights present similar fitting to the data and even a weak bias toward positive ones may suffice to avoid spurious values. Then, the present strategy provides information enough to avoid negative weight predictions without corrupting estimates for heavy vehicles. Such results are quite encouraging, since they increase the confidence of the users into the suitability of the weight predictions for real traffic applications, where vehicle properties may differ from what is previously expected. In addition, the overall system accuracy class obtained, related to the worse class among all evaluated quantities of interest, significantly improved. It changed from a system with a class worse than E(50) for LS to a E(35) system. If the axle in a group quantity is disregarded, which is usual for B-WIM systems, the new overall system accuracy class is C(15). It means that, by employing the proposed Bayesian approach, even the single axle estimates can achieve an accuracy level similar to the GVW. This achievement is far to be reached by LS. It is an important practical consequence of the improvements allowed by the Bayesian strategy, which extends the range of proper applications by just modifying some computational implementation.

The comparison with the Reg method demands a special discussion. The first attempt was to provide a comparison with a practical version of the Reg algorithm, whose performance would be reproduced in real applications. However, the results initially obtained were quite similar to the LS method due to low values for the regularization parameters reported by the implemented strategy for automatically selecting it. It is important to remark that the difficult in selecting proper regularization parameters is recognized in literature (ŽNIDARIČ; KALIN; KRESLIN, 2018; O'BRIEN et al., 2018; CARRARO et al., 2019) and the performance of the regularization approach relies on such a parameter. As such an additional result would not improve the comparisons, an alternative point of view was utilized. Instead of trying a practical implementation of the method, whose results would be subjective, it was implemented a version of the method that avoids the subjectivity in the selection of such a parameter. It was reached by selecting the best parameter possible for each event. In this regard, the sum of squared residuals between predicted and true axle weights was utilized as the optimality criterion. It was possible in this study since all true vehicle weights are known, which is not the practical case evidently. Moreover, the nearly optimal term was employed since a finite set of regularization parameters was applied, even that a thinner grid had been evaluated and no improvement in the results was noticed. Hence, the cost for removing the subjectivity on the definition of the regularization parameter was to eliminate the practical relevance of the reported results since they are not reproducible in real field tests. At the end, as it is known that the Reg method is able to improve results mainly for closely spaced axles, the results from the adopted approach work as a threshold for a excellent performance level. And, even in this unbalanced comparison, the B4 strategy presented a better overall performance. Thus, when taking into account also the practical issues, conclusions are clearly favorable to B4, the algorithm including both proposed prior distribution and second order autoregressive error

model.

The serial correlation issue is another aspect that deserves a particular discussion. The serial correlation could be reduced by including more modeling issues, such as the dynamic behavior of the structure. However, due to the high sampling frequency, some correlation among sequential measurements hardly would be completely avoided. Thus, in the present work, it was adopted a model to represent such a correlation based on a second order autoregressive process. In order to improve its performance, the signals were first decimated. This step is important since it reduces the order of the autoregressive model necessary to represent the correlation. Hence, as previously discussed, it may avoid some undesired model parameters, such as non-stationary AR models. The results, mainly when increasing the bridge span length, indicated that modeling such a correlation has a fundamental importance to allow that the prior information be effectively utilized in the problem. The reason is that the likelihood function is excessively weighed by the false independence assumption, which, in turn, results in ignoring the prior distribution for the Bayesian prediction. It is noticed by the minor differences between B1 and LS algorithms, in contrast with the large improvements presented by B4. Despite the proposed error model, the overall procedure still keeps what is one of the most important aspect of the present strategy: the correspondence with the practical experience. The parameters in this proposed Bayesian model are not just numbers, but are linked to physical quantities whose estimates are available. Thus, one could provide good guesses for such parameters without the necessity of performing further steps. It is in contrast, for instance, with the definition of the regularization parameter for the Reg algorithm. In this case, the parameter value can assume virtually any positive number and additional procedures are necessary for finding a good parameter value. Summarizing, the proposed Bayesian strategy is not developed just aiming to improve weight estimates, it also attempts to be well suited for practical applications. For this, the model parameters are defined to keep a clear correspondence with quantities that are usual for who operates a B-WIM system.

Despite the promising results presented in this work, some issues still could be improved:

- the prior distribution was defined using information of just a few vehicles, since no database of axle weights was available. Therefore, one could compile information from an existing database and apply the obtained estimates of the mean ($\boldsymbol{\mu}_W$) and covariance matrix ($\boldsymbol{\Sigma}_W$) for the axle weights into the proposed Bayesian approach;

- the influence line employed works as a proof of concept for the Bayesian strategy, since the focus of the study was not on the method to obtain this curve. As bridge influence line extraction is an active research subject, utilizing influence lines calculated by other methods may present even better results;

- in the present work, just point estimates for axle weights were considered. However, the full posterior probability density function can be useful for further applications. For instance, one could calculate the probability of overloading of a given truck;

- the proposed model accounts for correlation among error terms, however other aspects still could be included in order to obtain even better results. For instance, one could check if relaxing the hypothesis of homoscedasticity could improve the predictions.

4.7 CONCLUSION

The present study proposed a Bayesian approach for performing the weight estimation for B-WIM systems aiming to improve the prediction for individual axle weights. It employed previous knowledge regarding the expected values of axle weights, such as the correlation among them, for avoiding spurious solutions that may arise when applying the least squares method. In addition, a second order autoregressive process for modeling the error term correlation was proposed.

The results for both numerically simulated signals and an example of real-world B-WIM system calibration indicated that the proposed approach was able to considerably improve the prediction of individual axle weights without loosing precision in the GVW estimates. In addition, sensitivity analyses showed that results were robust regarding variation of the model parameters. The presented results indicated that the proposed Bayesian approach is a feasible option for practical applications regarding B-WIM systems, mainly for improving individual axle weight estimates.

ACKNOWLEDGMENTS

REFERENCES

BEHMANESH, Iman; MOAVENI, Babak. Accounting for environmental variability, modeling errors, and parameter estimation uncertainties in structural identification. **Journal of Sound and Vibration**, v. 374, p. 92–110, 2016. ISSN 0022-460X.

BOX, George E. P.; JENKINS, Gwilym M.; REINSEL, Gregory C.; LJUNG, Greta M. **Time Series Analysis: Forecasting and Control**. Fifth. [S.l.]: John Wiley & Sons, 2015. ISBN 978-1-118-67502-1.

CARRARO, Felipe; GONÇALVES, Matheus Silva; LOPEZ, Rafael Holdorf; MIGUEL, Leandro Fleck Fadel; VALENTE, Amir Mattar. Weight estimation on static B-WIM algorithms: A comparative study. **Engineering Structures**, v. 198, p. 109463, 2019. ISSN 0141-0296.

CHEN, Shi-Zhi; WU, Gang; FENG, De-Cheng. Development of a bridge weigh-in-motion method considering the presence of multiple vehicles. **Engineering Structures**, v. 191, p. 724–739, 2019. ISSN 0141-0296.

CHEN, Shi-Zhi; WU, Gang; FENG, De-Cheng; ZHANG, Lu. Development of a Bridge Weigh-in-Motion System Based on Long-Gauge Fiber Bragg Grating Sensors. **Journal of Bridge Engineering**, v. 23, n. 9, p. 04018063, 2018.

CHEN, Zhiwei; YANG, Weibiao; LI, Jun; YI, Tinghua; WU, Junchao; WANG, Dongdong. Bridge influence line identification based on adaptive B-spline basis dictionary and sparse regularization. **Structural Control and Health Monitoring**, v. 26, n. 6, e2355, 2019.

CONGDON, Peter. **Bayesian statistical modelling**. [S.l.]: John Wiley & Sons, 2007. ISBN 978-0-470-01875-0.

DNIT, Departamento Nacional de Infraestrutura de Transportes. **Quadro de fabricantes de veículos**. Rio de Janeiro, Brazil, 2012. Available from: `https://www.gov.br/dnit/pt-br/rodovias/operacoes-rodoviarias/pesagem/QFV2012ABRIL.pdf`.

FRØSETH, Gunnstein T.; RØNNQUIST, Anders; CANTERO, Daniel; ØISETH, Ole. Influence line extraction by deconvolution in the frequency domain. **Computers & Structures**, v. 189, p. 21–30, 2017. ISSN 0045-7949.

GELMAN, Andrew; CARLIN, John B.; STERN, Hal S.; DUNSON, David B.; VEHTARI, Aki; RUBIN, Donald B. **Bayesian Data Analysis**. Third. [S.l.]: Chapman and Hall/CRC, 2013. ISBN 9781439840955.

GONÇALVES, Matheus Silva. **Vehicle-bridge Dynamics simulation for B-WIM analyses**. [S.l.: s.n.], 2021. Mendeley Data. v1. Available from: `http://dx.doi.org/10.17632/4wvrwb6bzg.1`.

GONÇALVES, Matheus Silva; CARRARO, Felipe; LOPEZ, Rafael Holdorf. A B-WIM algorithm considering the modeling of the bridge dynamic response. **Engineering Structures**, v. 228, p. 111533, 2021. ISSN 0141-0296.

GONÇALVES, Matheus Silva; CARRARO, Felipe; LOPEZ, Rafael Holdorf. A gradient based optimization procedure for finding axle weights in probabilistic bridge weigh-in-motion method. **Canadian Journal of Civil Engineering**, v. 48, n. 5, p. 570–574, 2021.

HAO, Tianzhi; XIE, Zhengyuan; YU, Mengsheng. The identification technology of vehicle weight based on bridge strain time-history curve. **Advances in Structural Engineering**, v. 22, n. 7, p. 1606–1616, 2019.

HE, Wei; LING, Tianyang; O'BRIEN, Eugene J.; DENG, Lu. Virtual Axle Method for Bridge Weigh-in-Motion Systems Requiring No Axle Detector. **Journal of Bridge Engineering**, v. 24, n. 9, p. 04019086, 2019.

HEITNER, Barbara; SCHOEFS, Franck; O'BRIEN, Eugene J.; ŽNIDARIČ, Aleš; YALAMAS, Thierry. Using the unit influence line of a bridge to track changes in its condition. **Journal of Civil Structural Health Monitoring**, v. 10, n. 4, p. 667–678, 2020.

HELMI, Karim; TAYLOR, Todd; ANSARI, Farhad. Shear force–based method and application for real-time monitoring of moving vehicle weights on bridges. **Journal of Intelligent Material Systems and Structures**, v. 26, n. 5, p. 505–516, 2015.

IENG, Sio-Song. Bridge Influence Line Estimation for Bridge Weigh-in-Motion System. **Journal of Computing in Civil Engineering**, v. 29, n. 1, p. 06014006, 2015.

INSUA, David Ríos; RUGGERI, Fabrizio. **Robust Bayesian Analysis**. [S.l.]: Springer, New York, NY, 2000. v. 152. ISBN 978-1-4612-1306-2.

ISERMANN, Rolf; MÜNCHHOF, Marco. **Identification of dynamic systems: an introduction with applications**. [S.l.]: Springer, Berlin, Heidelberg, 2011. ISBN 978-3-540-78879-9.

ISO 8606:1995. **Mechanical Vibration-Road Surface Profiles-Reporting of Measured Data**. [S.l.], 1995.

JACOB, Bernard; FEYPELL-DE LA BEAUMELLE, Véronique. Improving truck safety: Potential of weigh-in-motion technology. **IATSS Research**, v. 34, n. 1, p. 9–15, 2010. ISSN 0386-1112.

JACOB, Bernard; O'BRIEN, Eugene J.; JEHAES, Sophie. **Weigh-in-motion of road vehicles: final report of the COST 323 action**. Paris, 2002.

KAWAKATSU, Takaya; AIHARA, Kenro; TAKASU, Atsuhiro; ADACHI, Jun. Deep Sensing Approach to Single-Sensor Vehicle Weighing System on Bridges. **IEEE Sensors Journal**, v. 19, n. 1, p. 243–256, 2019.

LANSDELL, Andrew; SONG, Wei; DIXON, Brandon. Development and testing of a bridge weigh-in-motion method considering nonconstant vehicle speed. **Engineering Structures**, Elsevier, v. 152, p. 709–726, 2017. ISSN 0141-0296.

LECHNER, B.; LIESCHNEGG, M.; MARIANI, O.; PIRCHER, M.; FUCHS, A. A Wavelet-Based Bridge Weigh-In-Motion System. **International Journal on Smart Sensing and Intelligent Systems**, v. 3, n. 4, p. 573–591, 2010.

LYDON, Myra; TAYLOR, Su E.; ROBINSON, D.; MUFTI, Aftab; O'BRIEN, Eugene J. Recent developments in bridge weigh in motion (B-WIM). **Journal of Civil Structural Health Monitoring**, Springer, v. 6, n. 1, p. 69–81, 2016.

MAKI, Yuji; HA, Tuan Minh; FUKADA, Saiji; TORII, Kazuyuki; ONO, Ryohei. Stiffness Evaluation and Current Status of a Degraded Road Bridge Slab Located in a Mountainous Area. **Journal of Advanced Concrete Technology**, v. 17, n. 1, p. 62–78, 2019.

MANDIĆ IVANKOVIĆ, Ana; SKOKANDIĆ, Dominik; ŽNIDARIČ, Aleš; KRESLIN, Maja. Bridge performance indicators based on traffic load monitoring. **Structure and Infrastructure Engineering**, Taylor & Francis, v. 15, n. 7, p. 899–911, 2019.

MOSES, Fred. Weigh-in-Motion System Using Instrumented Bridges. **Transportation Engineering Journal of ASCE**, v. 105, n. 3, p. 233–249, 1979.

O'BRIEN, Eugene J.; QUILLIGAN, Michael J.; KAROUMI, Raid. Calculating an influence line from direct measurements. **Proceedings of the Institution of Civil Engineers - Bridge Engineering**, v. 159, n. 1, p. 31–34, 2006.

O'BRIEN, Eugene J.; ROWLEY, Cillian W.; GONZÁLEZ, Arturo; GREEN, Mark F. A regularised solution to the bridge weigh-in-motion equations. **International Journal of Heavy Vehicle Systems**, v. 16, n. 3, p. 310–327, 2009.

O'BRIEN, Eugene J.; ZHANG, Longwei; ZHAO, Hua; HAJIALIZADEH, Donya. Probabilistic bridge weigh-in-motion. **Canadian Journal of Civil Engineering**, v. 45, n. 8, p. 667–675, 2018.

O'BRIEN, Eugene J.; GONZÁLEZ, Arturo; DOWLING, Jason. A filtered measured influence line approach to bridge weigh-in-motion. In: THE Fifth International IABMAS Conference: Bridge Maintenance, Safety Management and Life-Cycle Optimization. Philadelphia, USA: Taylor & Francis (Routledge), 2010.

PRESS, S. James. **Subjective and Objective Bayesian Statistics: Principles, Models, and Applications**. Second. [S.l.]: John Wiley & Sons, 2002. ISBN 978-0-471-34843-6.

QUILLIGAN, Michael. **Bridge Weigh-in-Motion Development of a 2-D Multi-Vehicle Algorithm**. 2003. Licentiate Thesis – KTH Royal Institute of Technology, Stockholm, Sweden.

RICHARDSON, Jim; JONES, Steven; BROWN, Alan; O'BRIEN, Eugene J.; HAJIALIZADEH, Donya. On the use of bridge weigh-in-motion for overweight truck enforcement. **International Journal of Heavy Vehicle Systems**, Inderscience, v. 21, n. 2, p. 83–104, 2014.

ROWLEY, Cillian; GONZÁLEZ, Arturo; O'BRIEN, Eugene J.; ŽNIDARIČ, Aleš. Comparison of conventional and regularized bridge weigh-in-motion algorithms. In: PROCEEDINGS of the international conference on heavy vehicles. [S.l.: s.n.], 2008. P. 221–230.

SIMOEN, Ellen; DE ROECK, Guido; LOMBAERT, Geert. Dealing with uncertainty in model updating for damage assessment: A review. **Mechanical Systems and Signal Processing**, v. 56-57, p. 123–149, 2015. ISSN 0888-3270.

SMAIL, M.; THOMAS, M.; LAKIS, A. ARMA MODELS FOR MODAL ANALYSIS: EFFECT OF MODEL ORDERS AND SAMPLING FREQUENCY. **Mechanical Systems and Signal Processing**, v. 13, n. 6, p. 925–941, 1999. ISSN 0888-3270.

WANG, Ning-Bo; HE, Li-Xiang; REN, Wei-Xin; HUANG, Tian-Li. Extraction of influence line through a fitting method from bridge dynamic response induced by a passing vehicle. **Engineering Structures**, Elsevier, v. 151, p. 648–664, 2017. ISSN 0141-0296.

WU, Hanli; ZHAO, Hua; LIU, Jenny; HU, Zhentao. A filtering-based bridge weigh-in-motion system on a continuous multi-girder bridge considering the influence lines of different lanes. **Frontiers of Structural and Civil Engineering**, v. 14, n. 5, p. 1232–1246, 2020.

YOSHIDA, Ikumasa; SEKIYA, Hidehiko; MUSTAFA, Samim. Bayesian Bridge Weigh-in-Motion and Uncertainty Estimation. **ASCE-ASME Journal of Risk and Uncertainty in Engineering Systems, Part A: Civil Engineering**, v. 7, n. 1, p. 04021001, 2021.

YU, Yang; CAI, C. S.; DENG, Lu. State-of-the-art review on bridge weigh-in-motion technology. **Advances in Structural Engineering**, SAGE Publications, v. 19, n. 9, p. 1514–1530, 2016.

YU, Yang; CAI, C.S.; DENG, Lu. Nothing-on-road bridge weigh-in-motion considering the transverse position of the vehicle. **Structure and Infrastructure Engineering**, Taylor & Francis, v. 14, n. 8, p. 1108–1122, 2018.

YUEN, Ka-Veng. **Bayesian Methods for Structural Dynamics and Civil Engineering**. [S.l.]: John Wiley & Sons, 2010. ISBN 9780470824566.

ZHAO, Hua; UDDIN, Nasim; O'BRIEN, Eugene J.; SHAO, Xudong; ZHU, Ping. Identification of Vehicular Axle Weights with a Bridge Weigh-in-Motion System Considering Transverse Distribution of Wheel Loads. **Journal of Bridge Engineering**, v. 19, n. 3, p. 04013008, 2014.

ZHAO, Hua; UDDIN, Nasim; SHAO, Xudong; ZHU, Ping; TAN, Chengjun. Field-calibrated influence lines for improved axle weight identification with a bridge weigh-in-motion system. **Structure and Infrastructure Engineering**, Taylor & Francis, v. 11, n. 6, p. 721–743, 2015.

ZHENG, Xu; YANG, Dong-Hui; YI, Ting-Hua; LI, Hong-Nan. Bridge influence line identification from structural dynamic responses induced by a high-speed vehicle. **Structural Control and Health Monitoring**, v. 27, n. 7, e2544, 2020.

ZHENG, Xu; YANG, Dong-Hui; YI, Ting-Hua; LI, Hong-Nan. Development of bridge influence line identification methods based on direct measurement data: A comprehensive review and comparison. **Engineering Structures**, v. 198, p. 109539, 2019. ISSN 0141-0296.

ZHENG, Xu; YANG, Dong-Hui; YI, Ting-Hua; LI, Hong-Nan; CHEN, Zhi-Wei. Bridge Influence Line Identification Based on Regularized Least-Squares QR Decomposition Method. **Journal of Bridge Engineering**, v. 24, n. 8, p. 06019004, 2019.

ŽNIDARIČ, Aleš. **Influence of number and quality of weigh-in-motion data on evaluation of load effects on bridges**. 2017. Doctoral Thesis – University of Ljubljana, Ljubljana, Slovenia.

ŽNIDARIČ, Aleš; KALIN, Jan. Using bridge weigh-in-motion systems to monitor single-span bridge influence lines. **Journal of Civil Structural Health Monitoring**, v. 10, n. 5, p. 743–756, 2020.

ŽNIDARIČ, Aleš; KALIN, Jan; KRESLIN, Maja. Improved accuracy and robustness of bridge weigh-in-motion systems. **Structure and Infrastructure Engineering**, Taylor & Francis, v. 14, n. 4, p. 412–424, 2018.

5 MODEL UPDATING USING HIERARCHICAL BAYESIAN STRATEGY EMPLOYING B-WIM CALIBRATION DATA

ABSTRACT

Bridge weigh-in-motion (B-WIM) systems are employed for monitoring traffic weights, providing useful information for management decisions. Many applications were proposed based on the information collected, such as calculation of influence lines and damage detection. In this work, an additional application is addressed, to perform model updating of structural parameters from information collected during the calibration of B-WIM systems. The goal of model updating techniques is to adjust the model parameters in order to achieve better agreement between predicted and experimental responses. Therefore, the resulting updated model is able to provide valuable information for decision makers. For many civil engineering applications, the updated parameters may have an inherent variability during the execution of the experimental procedure, since some external effects, such as environmental conditions, may change considerably along the process. To account for this inherent variability properly, a hierarchical Bayesian strategy is adopted. Results for both numerically simulated signals and a real engineering calibration procedure indicate that the proposed hierarchical Bayesian model updating approach is able to perform suitable estimates.

Authors: Matheus Silva Gonçalves, Rafael Holdorf Lopez, Amir Mattar Valente

Note: The numbering of all figures, tables and equations has been restarted in this chapter in order to better agree with the published version of the work

LIST OF SYMBOLS (CHAPTER 5)

$\boldsymbol{m}_g$	measured bending moment response vector of the g-th girder
Z	section modulus of bridge girders
E	elastic modulus of bridge girders
$\boldsymbol{u}_g$	measured strain vector of the g-th girder
$\boldsymbol{M}$	measured bending moment response vector
G	total number of girders
$\widehat{\boldsymbol{M}}$	theoretical bending moment response vector
J	vehicle number of axles
W_j	weight of the j-th axle
l	influence line ordinate
d_j	distance between first and j-th axle
C_j	number of scans between first and j-th axle
f	sampling frequency
v	vehicle speed
$\boldsymbol{y}$	monitored quantity vector
$\widehat{\boldsymbol{y}}$	theoretical response vector
ε	error between theoretical model and experimental results
$\boldsymbol{\theta}$	vector of quantities of interest for all calibration runs
N	number of runs
μ_θ	mean of logarithmic values of the distribution of θ
σ_θ	standard deviation of logarithmic values of the distribution of θ
$\boldsymbol{Y}$	set comprising all measurements
σ_ε^2	variance of the Gaussian additive error
K	total number of scans
$\widehat{\theta}$	mode of the full conditional distribution of θ
α_θ	shape parameter of the inverse gamma distribution employed as prior for σ_θ^2
α_ε	shape parameter of the inverse gamma distribution employed as prior for σ_ε^2
β_θ	scale parameter of the inverse gamma distribution employed as prior for σ_θ^2
β_ε	scale parameter of the inverse gamma distribution employed as prior for σ_ε^2
μ_θ^*	mean of the posterior distribution of θ
σ_θ^*	standard deviation of the posterior distribution of θ

5.1 INTRODUCTION

Bridges are essential elements for allowing the proper operation of transportation systems around the world. A high number of these structures were built decades ago, for traffic conditions remarkably different from those presented nowadays. Over all their life time, bridges remain under the direct effects of environmental conditions. Therefore, the increasing traffic loads, aging infrastructure, and adverse environmental conditions have led many bridges to present a considerable deterioration (LYDON et al., 2016). Moreover, old structures might also present an additional challenge regarding lack of information, such as design drawings (KHAN et al., 2022). Even the bridge's exact age might not be precisely known in some cases, as is commonly noticed for Brazilian bridges (LIMA E OLIVEIRA; GRECO; BITTENCOURT, 2019). Such aspects, together with the presence of high uncertainties related to the deterioration of materials, such as reinforced concrete, indicate the need of monitoring of some structures (HEITNER et al., 2020). In this context, structural health monitoring (SHM) procedures have been employed (ŽNIDARIČ; KALIN, 2020). SHM involves collecting information related to the response of a structure from specific sensors with the goal of providing objective information for decision-making regarding its safety and serviceability (CATBAS et al., 2012).

Bridge weigh-in-motion (B-WIM) systems are able to provide useful information for SHM purposes (YU; CAI, C. S.; DENG, 2016). B-WIM systems are based on the ideas of Moses (1979); they utilize strains measured at the bottom of the structure and the concept of influence lines to estimate the weight of vehicles traveling over the bridge. Among the advantages of B-WIM systems, one could cite the low costs for installation and maintenance, the acquisition of unbiased data and the possibility of not affecting the usual traffic flow (LYDON et al., 2016; FRØSETH et al., 2017; YU; CAI, C.; DENG, 2018). Data provided by B-WIM systems can be employed, for instance, for the selection of overloaded vehicles, development of traffic load models, traffic analyses, and bridge design or assessment (MANDIĆ IVANKOVIĆ et al., 2019). Furthermore, the measured strains could be utilized to evaluate some important bridge performance indicators, such as influence lines and loading distribution factors (ŽNIDARIČ; KALIN, 2020). Recently, some works also addressed the utilization of B-WIM systems for damage detection (CANTERO; GONZÁLEZ, 2015; CANTERO; KAROUMI; GONZÁLEZ, 2015; O'BRIEN et al., 2021). Currently applied B-WIM systems perform a calibration step, where strains resulting from the passage of trucks with known properties are monitored. Then, experimental influence lines are calculated to better predict the bridge behavior due to moving loads. It is noticed that, as a number of vehicles are recommended for this procedure (JACOB; O'BRIEN; JEHAES, 2002), a considerable amount of data is usually generated during the calibration process.

This work intends to address an additional application for B-WIM systems. It is proposed to perform model updating of bridge structural parameters based on the information collected during the calibration procedure. Model updating is a technique that aims to adjust the parameters of a given model in order to match the predicted response with the experimental

system behavior. The updated structural model is able to provide valuable information for helping in management decisions (SCHLUNE; PLOS; GYLLTOFT, 2009). For instance, one could employ the updated model to estimate a better lifetime reliability for the structure (OKASHA; FRANGOPOL; ORCESI, 2012), improve the remaining bridge strength prediction (MA et al., 2014), check whether corrective interventions are working as expected (BROWNJOHN et al., 2003), and perform nondestructive damage assessment (SIMOEN; DE ROECK; LOMBAERT, 2015).

Many different strategies are available for performing model updating. Authors working in structural engineering have given special attention to Bayesian model updating approaches (MA et al., 2014). The main idea of Bayesian methods is that new measurements can modify prior beliefs related to some phenomenon, resulting in a posterior belief (PRESS, 2002). In this context, a parameter is assumed to be an unknown fixed value and the uncertainty related to its value is reduced when increasing the quantity of data. Therefore, as no inherent variability is assumed, the classical Bayesian modeling might underestimate the total uncertainties (SEDEHI; PAPADIMITRIOU; KATAFYGIOTIS, 2019), assuming that the uncertainty vanishes for the hypothetical scenario of an infinity dataset. This issue might not be suitable for civil engineering structures, where some structural parameters have an inherent variability regarding different sources of uncertainty (BEHMANESH et al., 2015). In this case, many external factors, such as wind speed and ambient temperature, can modify the value of the updated parameter during different realizations of the experiment. Furthermore, many simplifications and idealizations are often needed to model such structures, introducing more uncertainties to the model.

Owing to the drawbacks discussed for the classical Bayesian strategy, a hierarchical Bayesian approach is adopted in this work. The hierarchical framework differs from the classical Bayesian strategies mainly by the inclusion of an extra layer of variables between the prior information and measured data. Therefore, the parameters that define probability distributions of both the error term and the quantity of interest can be updated based on the collected experimental data (BEHMANESH; MOAVENI, 2016), allowing better estimation of the total uncertainty of updating parameters. Although this is a relatively new approach in the structural engineering field (KWAG; JU, 2020), it was successfully applied in recent works, mainly regarding dynamic models and modal parameters (BEHMANESH et al., 2015; SONG, M. et al., 2019; BEHMANESH; MOAVENI, 2016; SEDEHI; PAPADIMITRIOU; KATAFYGIOTIS, 2019, 2020).

In this work, therefore, a hierarchical Bayesian approach is proposed to perform model updating of structural parameters from a set of strain measurements related to the response of a bridge structure to the passage of heavy vehicles with known properties. Such data are available as the result of the calibration process of B-WIM systems. In particular, the proposed approach is formulated to be well suited for bridges where no reliable previous information on the structural parameters is available, as, for instance, when considering old bridges for which design plans (i.e., blueprints or structural specifications) are no longer available. In addition, it

is noticed that the assumption of independence between error terms from a same vehicle run might be violated in this context. Hence, a downsampling procedure is employed, aiming to mitigate this effect. Two different steps for validation are performed. In the first, numerically simulated signals, which allow for complete knowledge about the target values of updated parameters, are employed to assess the suitability of results. For the second analysis, a dataset related to a real B-WIM system calibration procedure is utilized and the provided estimates are evaluated. By these analyses, it is expected to properly assess the suitability of the proposed approach.

The remainder of the work is organized as follows. The next section presents an introductory discussion regarding B-WIM systems, as well as the modeling strategy employed to relate the quantities of interest (QoI) with the monitored response. After this, the hierarchical Bayesian model is described, as well as the sampling procedure employed for effectively performing the updating procedure. Then the results of the proposed approach are presented for both numerically generated signals and an example of real-world B-WIM calibration procedure. After this, some additional remarks and suggestions for future works are made, and some conclusions are presented.

5.2 B-WIM SYSTEMS AND THE APPLICATION OF CALIBRATION DATA FOR MODEL UPDATING

Most B-WIM systems in operation nowadays are based on the ideas first established by Moses (1979), who proposed a procedure for estimating axle weights from the strains induced by passing vehicles. By this approach, the axle weights are estimated as those weights that minimize the error between measured and theoretical responses, applying the concept of an influence line to calculate the latter. The bridge flexural response is employed by most B-WIM systems (HELMI; TAYLOR; ANSARI, 2015), where sensors are usually located at the bridge mid-span to record the strains at the bottom of the girders.

The collected strains are, therefore, converted to bending moment:

$$\boldsymbol{m}_g = E_g Z_g \boldsymbol{u}_g, \tag{1}$$

where $\boldsymbol{m}_g$ = measured bending moment; Z_g = section modulus; E_g = elastic modulus; and $\boldsymbol{u}_g$ = measured strain of the g girder.

The effective structural response is, then, the sum of the bending moment calculated for every girder:

$$\boldsymbol{M} = \sum_{g=1}^{G} E_g Z_g \boldsymbol{u}_g, \tag{2}$$

where $\boldsymbol{M}$ is the structural response vector, including the contribution of the measured bending moment of every girder, from a total of G girders.

B-WIM systems calculate axle weights by minimizing some error function between theoretical ($\widehat{\boldsymbol{M}}$) and experimental ($\boldsymbol{M}$) responses. The theoretical response vector is calculated by employing the concept of an influence line. In this regard, the influence line is defined as the total bending moment of all the girders at the sensor location that is induced by a unitary load as it moves throughout the bridge (QUILLIGAN, M., 2003). Hence, the theoretical response referred to the scan k is:

$$\widehat{M}_k = \sum_{j=1}^{J} W_j I_{(k-C_j)}, \tag{3}$$

where:

$$C_j = \frac{d_j f}{v} \tag{4}$$

and J = vehicle's number of axles; W_j = weight of the jth axle; $I_{(k-C_j)}$ = bridge influence line ordinate at the position of the jth axle, related to the scan k, d_j = distance between the first and jth axles; C_j = number of scans corresponding to d_j; f = sampling rate; and v = vehicle speed. It is worth pointing out that, for the situation where a specific vehicle axle is outside the bridge structure, the value of $I_{(k-C_j)}$ is set to zero. Moreover, the vehicle speed is assumed to be constant along the passage of the vehicle. This constant speed assumption is considered reasonable for short-span highway bridges (LANSDELL; SONG, W.; DIXON, 2017). In this study, this desired parameter is obtained by means of free-of-axle detectors (FADs), avoiding the need for traffic interruption to install the FADs.

A main issue for creating a functional B-WIM system is the definition of the bridge influence line. In the first work in this subject, performed by Moses (1979), the bridge influence line was approached just with theoretical analysis. The theoretical influence line, however, is currently recognized as unsuitable for B-WIM applications (QUILLIGAN, M., 2003), since some simplifications are made in its derivation procedure. Thus, most recent methods apply a calibration procedure to estimate an experimental influence line. In the calibration, several runs are conducted for vehicles with known configuration and at controlled speed and the resulting strains are recorded. Therefore, the influence line that generates the best agreement between measured strains and axle weights is calculated. The works of O'Brien, Michael J. Quilligan, and Karoumi (2006), Ieng (2015) and Gonçalves, Carraro, and Lopez (2021) present examples of methods for performing such a task for B-WIM systems. Both the amount and diversity of information gathered during the calibration procedure are important factors for the proper operation of B-WIM systems. In this regard, it is intended to perform several calibration runs with a number of vehicles and travel velocities (JACOB; O'BRIEN; JEHAES, 2002). For a practical scenario, it is expected that dozens of runs would be performed, with, at least, two different vehicles.

For this work, instead of employing the collected dataset just to calculate the bridge influence line as usual, a model updating approach is proposed, regarding a key structural

parameter for the bridge under analysis. Thus, proceeding in this way, one could perform a single calibration procedure for both obtaining an influence line for B-WIM purposes and updating the knowledge regarding bridge structural parameters. The updated model could be useful, for instance, to predict the response that would be induced by any vehicle, including confidence bounds. The QoI for this study, denoted θ, is defined as the product of the elastic and section modulus, presented in Equation (1), considering that all girders have the same properties:

$$\theta = EZ. \tag{5}$$

In selecting a single parameter to be updated, the aim is to provide simple and practical information regarding the structure. Then, the derivation of the strategy is simplified, while at the same time providing a parameter that can be compared with the expected value given, for example, by the design information.

To properly complete the definition of the proposed model updating strategy, it is necessary to define the forward model employed to relate the QoI and the monitored output. As already discussed, in B-WIM applications, usually the strains at the bottom of the bridge girders are monitored. Thus, for the proposed model updating strategy, the effective system response and forward model are defined by rearranging Equation (2) and Equation (3), considering that all girders have the same properties. This results in the following expression for the monitored quantity vector ($\boldsymbol{y}$):

$$\boldsymbol{y} = \sum_{g=1}^{G} \boldsymbol{u}_g. \tag{6}$$

The QoI (θ), which is disregarded in Equation (6), is included in the proposed forward model, which is analogous to Equation (3):

$$\widehat{y_k} = \frac{1}{\theta} \sum_{j=1}^{J} W_j I_{(k-C_j)}, \tag{7}$$

where $\widehat{y_k}$ represents the theoretical response for the scan k, and $\widehat{\boldsymbol{y}}$ is the theoretical response vector.

In this work, a theoretical influence line is employed in the forward model, with the scale constant, defined by θ, being updated by the model updating process. Although it was previously discussed that theoretical influence lines are unsuitable for B-WIM applications, this does not necessarily imply that the shape of this theoretical response cannot be useful for model updating of the bridge structural parameters, since both strategies have clearly distinct goals. For the former, the precision on the predicted weights is analyzed. This usually results in an ill-conditioned problem, mainly for closely spaced axles (O'BRIEN et al., 2018, 2009; ROWLEY et al., 2008), where many different combinations of axle weights can generate a quite similar strain pattern. Conversely, in the latter approach, the focus is turned to the bridge structural

response itself. As the QoI adopted in this study is a single scale parameter, the presence of major ill-conditioning issues is avoided. The utilization of a theoretical influence line can simplify the practical application of the whole model updating process, being a natural choice for a first evaluation of the proposed procedure. A set of examples, including a real calibration procedure, is further analyzed in order to assess the suitability of the adopted strategy.

As mathematical models are just approximations of the real behavior of the monitored system, it is expected that deviations between theoretical and measured responses will occur. This relation is defined by:

$$y_{k,i} = \widehat{y}_{k,i} + \varepsilon_{k,i}, \tag{8}$$

where $y_{k,i}$ = monitored quantity; $\widehat{y}_{k,i}$ = theoretical response; and $\varepsilon_{k,i}$ = error between theoretical model and experimental results for scan k and calibration run i. In this work, an independent and identically distributed zero-mean Gaussian error is assumed.

5.3 THE PROPOSED HIERARCHICAL BAYESIAN FRAMEWORK

A relevant aspect to be noticed before further modeling steps is that the bridge response is affected by many external effects, which are not controlled by the person conducting the calibration procedure. The influence of such external effects in model updating can be observed from both the direct modification in the QoI value for each vehicle run and the induction of a secondary effect that changes the perception of the model to the QoI. The former is clearly noticed when observing, for instance, how variations in temperature across different calibration runs have an impact on the value of the elastic modulus and, hence, on the QoI of this study. The latter is exemplified by any factor that also has an influence on the measured strains, but that is not included into the model. For instance, in this study, the transverse position of the vehicle is not employed to estimate the bridge response. However, according to the transverse position where the vehicle travels, different responses can be induced even when all other conditions are kept exactly the same. In this case, different QoI values may generate the best fit with the experimental data for each vehicle run.

For the previously discussed reasons, it is expected that the QoI presents an inherent variability among different runs. Then, assuming that the QoI is represented by a fixed value, as in the classical Bayesian method, does not seem the best approach. Indeed, classical approaches might underestimate uncertainties, resulting in unrealistically narrow uncertainty bounds for system output predictions (SEDEHI; PAPADIMITRIOU; KATAFYGIOTIS, 2019). To perform model updating properly in this context, it is proposed to employ a hierarchical Bayesian strategy. The hierarchical framework allows a more flexible consideration regarding the QoI, including, for instance, an unknown mean and covariance matrix. This modeling strategy assumes that a different parameter value can be associated to each experiment. Thus, it enables estimation of the inherent variability of the QoI (BEHMANESH; MOAVENI, 2016).

In addition, it is possible to propagate the uncertainties to predictions of some other QoI (BALLESTEROS et al., 2014). As a result, reliable uncertainty bounds for the system output can be predicted (SEDEHI; PAPADIMITRIOU; KATAFYGIOTIS, 2019). In this framework, the theoretical structural responses are functions of variables that follow probabilistic distributions defined by hyperparameters (GELMAN et al., 2013). These hyperparameters are considered unknowns and are computed utilizing the experimental data (BALLESTEROS et al., 2014). This approach can be seen as an inclusion of an extra layer of variables between prior information and measured data, respecting a hierarchical framework. Although this is a relatively new approach in the structural engineering field (KWAG; JU, 2020), it was successfully applied in recent works to different structural systems, such as a two-story reinforced concrete building (SONG, M. et al., 2019), a footbridge (BEHMANESH; MOAVENI, 2016), and a soil-slope structure under earthquakes (KWAG; JU, 2020).

The proposed hierarchical Bayesian framework can be illustrated as follows. Let $\boldsymbol{\theta}$ be the set of θ_i values for every calibration run i, from a total of N runs. All θ_i values are assumed to follow a log-normal distribution, with parameters μ_θ and $\sigma_\theta{}^2$. The choice of a log-normal distribution is based on the fact that the QoI defined for this study is a nonnegative quantity. Thus, including this information in the model should help to avoid improper convergence of sampling strategies. In addition, let $\boldsymbol{Y} = \{\boldsymbol{y}_i, i = 1, \ldots, N\}$ be the set comprising all measurements, where each time history $\boldsymbol{y}_i$ can be calculated by Equation (6). The theoretical model, defined by Equation (7), is assumed to deviate from the measurements by a zero-mean independent Gaussian additive error with variance σ_ε^2. Each time history $\boldsymbol{y}_i$ is sampled at a constant frequency f. Hence, the kth value of Equation (7) is defined as an integer value, ranging from 1 to K_i, where K_i is the number of collected measurements for the calibration run i.

Applying the Bayes theorem, the posterior distribution of the parameters μ_θ, σ_ε^2, σ_θ^2, and the set of parameters $\boldsymbol{\theta}$, given all the measured data $\boldsymbol{Y}$, can be written as:

$$\underbrace{p\left(\mu_\theta, \sigma_\theta^2, \boldsymbol{\theta}, \sigma_\varepsilon^2 | \boldsymbol{Y}\right)}_{\text{Posterior}} \propto \underbrace{p\left(\boldsymbol{Y} | \boldsymbol{\theta}, \sigma_\varepsilon^2\right)}_{\text{Likelihood}} \underbrace{p\left(\boldsymbol{\theta} | \mu_\theta, \sigma_\theta^2\right)}_{\text{Prior}} \underbrace{p\left(\mu_\theta, \sigma_\theta^2, \sigma_\varepsilon^2\right)}_{\text{Hyperprior}}. \tag{9}$$

The parameters for the hyperprior are assumed to be independent of each other:

$$p\left(\mu_\theta, \sigma_\theta^2, \sigma_\varepsilon^2\right) = p\left(\mu_\theta\right) p\left(\sigma_\theta^2\right) p\left(\sigma_\varepsilon^2\right). \tag{10}$$

In this study, such hyperprior distributions are defined as:

$$p(\mu_\theta) \propto 1, \tag{11}$$

$$p\left(\sigma_\theta^2\right) \sim \text{Inverse Gamma}\left(\alpha_\theta, \beta_\theta\right) \propto \left(\frac{1}{\sigma_\theta^2}\right)^{\alpha_\theta+1} \exp\left(\frac{-\beta_\theta}{\sigma_\theta^2}\right), \tag{12}$$

$$p\left(\sigma_\varepsilon^2\right) \sim \text{Inverse Gamma}\left(\alpha_\varepsilon, \beta_\varepsilon\right) \propto \left(\frac{1}{\sigma_\varepsilon^2}\right)^{\alpha_\varepsilon+1} \exp\left(\frac{-\beta_\varepsilon}{\sigma_\varepsilon^2}\right). \tag{13}$$

Equation (11) indicates that no previous knowledge is assumed for μ_θ. Conversely, Equation (12) and Equation (13) are chosen since they are strictly positive and correspond to conjugate distributions when the likelihood is Gaussian. The latter makes sampling strategies such as the Gibbs sampler procedure easier, since it results in standard distributions for the full conditional distribution of both variances (GELMAN et al., 2013).

The expression for $p\left(\boldsymbol{\theta}|\mu_\theta, \sigma_\theta^2\right)$ in Equation (9) can be calculated straightforwardly since each θ_i is assumed to be drawn from the same log-normal distribution. Considering that each θ_i is independent of the others, it reads as

$$p\left(\boldsymbol{\theta}|\mu_\theta, \sigma_\theta^2\right) \propto \frac{1}{\left(\sigma_\theta^2\right)^{\frac{N}{2}} \prod_{i=1}^{N} \theta_i} \exp\left(-\frac{1}{2}\sum_{i=1}^{N}\left(\frac{\log(\theta_i)-\mu_\theta}{\sigma_\theta}\right)^2\right). \tag{14}$$

Finally, the probability of $p\left(\boldsymbol{Y}|\boldsymbol{\theta}, \sigma_\varepsilon^2\right)$ in Equation (9) can be computed, recalling that the error term for this work is assumed to follow a zero-mean Gaussian distribution and its value for every measurement is independent from the others:

$$p\left(\boldsymbol{Y}|\boldsymbol{\theta}, \sigma_\varepsilon^2\right) \propto \frac{1}{\left(\sigma_\varepsilon^2\right)^{\sum_{i=1}^{N}\frac{K_i}{2}}} \exp\left(-\frac{1}{2}\sum_{i=1}^{N}\sum_{k=1}^{K_i}\left(\frac{y_{i,k}-\widehat{y}_{i,k}(\theta_i)}{\sigma_\varepsilon}\right)^2\right), \tag{15}$$

where the dependence of $\widehat{y}_{i,k}$ with respect to θ_i is remarked.

Therefore, the posterior distribution of Equation (9) can be defined as:

$$p\left(\boldsymbol{\theta}, \mu_\theta, \sigma_\theta^2, \sigma_\varepsilon^2|\boldsymbol{Y}\right) \propto \overbrace{\frac{1}{\left(\sigma_\varepsilon^2\right)^{\sum_{i=1}^{N}\frac{K_i}{2}}} \exp\left(-\frac{1}{2}\sum_{i=1}^{N}\sum_{k=1}^{K_i}\left(\frac{y_{i,k}-\widehat{y}_{i,k}(\theta_i)}{\sigma_\varepsilon}\right)^2\right)}^{p(\boldsymbol{Y}|\boldsymbol{\theta},\sigma_\varepsilon^2)}$$

$$\overbrace{\frac{1}{\left(\sigma_\theta^2\right)^{\frac{N}{2}} \prod_{i=1}^{N} \theta_i} \exp\left(-\frac{1}{2}\sum_{i=1}^{N}\left(\frac{\log(\theta_i)-\mu_\theta}{\sigma_\theta}\right)^2\right)}^{p(\boldsymbol{\theta}|\mu_\theta,\sigma_\theta^2)} \underbrace{\left(\frac{1}{\sigma_\theta^2}\right)^{\alpha_\theta+1}\exp\left(\frac{-\beta_\theta}{\sigma_\theta^2}\right)}_{p(\sigma_\theta^2)} \underbrace{\left(\frac{1}{\sigma_\varepsilon^2}\right)^{\alpha_\varepsilon+1}\exp\left(\frac{-\beta_\varepsilon}{\sigma_\varepsilon^2}\right)}_{p(\sigma_\varepsilon^2)}. \tag{16}$$

Rearranging the expression:

$$p(\boldsymbol{\theta},\mu_\theta,\sigma_\theta^2,\sigma_\varepsilon^2|\boldsymbol{Y}) \propto \frac{1}{\left(\prod_{i=1}^N \theta_i\right)\left(\sigma_\varepsilon^2\right)^{\sum_{i=1}^N \frac{K_i}{2}+\alpha_\varepsilon+1}}\frac{1}{\left(\sigma_\theta^2\right)^{\frac{N}{2}+\alpha_\theta+1}}$$

$$\exp\left(-\frac{1}{2}\left(\frac{\sum_{i=1}^N \sum_{k=1}^{K_i}\left(y_{i,k}-\widehat{y}_{i,k}\left(\theta_i\right)\right)^2+2\beta_\varepsilon}{\sigma_\varepsilon^2}+\frac{\sum_{i=1}^N\left(\log\left(\theta_i\right)-\mu_\theta\right)^2+2\beta_\theta}{\sigma_\theta^2}\right)\right). \quad (17)$$

Equation (17) provides the posterior distribution of the hyperparameters, given the whole dataset of calibration runs defined by $\boldsymbol{Y}$. In what follows, a sampling strategy is derived in order to effectively provide the updated parameters from the hierarchical Bayesian model.

5.3.1 Sampling strategy

In this work, a Gibbs sampler is adopted for sampling from the posterior distribution defined by the hierarchical Bayesian model in Equation (17). The Gibbs sampler is a special case of the more general Markov chain Monte Carlo (MCMC) algorithm, named Metropolis-Hastings. It is an iterative process, which works by generating a sample for every parameter from its full conditional distribution, keeping the remaining parameters at their previous sampled values. The full conditional distributions for this study can be inferred from Equation (17):

$$p(\mu_\theta|.) \sim \mathcal{N}\left(\sum_{i=1}^N \frac{\log\left(\theta_i\right)}{N},\frac{\sigma_\theta^2}{N}\right), \quad (18)$$

$$p\left(\sigma_\theta^2|.\right) \sim \text{Inverse Gamma}\left(\frac{N}{2}+\alpha_\theta,\frac{\sum_{i=1}^N\left(\log\left(\theta_i\right)-\mu_\theta\right)^2+2\beta_\theta}{2}\right), \quad (19)$$

$$p\left(\sigma_\varepsilon^2|.\right) \sim \text{Inverse Gamma}\left(\sum_{i=1}^N \frac{K_i}{2}+\alpha_\varepsilon,\frac{\sum_{i=1}^N \sum_{k=1}^{K_i}\left(y_{i,k}-\widehat{y}_{i,k}\left(\theta_i\right)\right)^2+2\beta_\varepsilon}{2}\right), \quad (20)$$

$$p(\theta_i|.) \propto \frac{1}{\theta_i}\exp\left(-\frac{1}{2}\left(\frac{\sum_{k=1}^{K_i}\left(y_{i,k}-\widehat{y}_{i,k}\left(\theta_i\right)\right)^2}{\sigma_\varepsilon^2}+\frac{\left(\log\left(\theta_i\right)-\mu_\theta\right)^2}{\sigma_\theta^2}\right)\right). \quad (21)$$

As the distributions employed in this work are conjugate distributions with respect to the likelihood function, the full conditional distributions of most parameters result in standard distributions and are easy to sample. The only exception is $p(\theta_i|.)$. In order for the Gibbs sampler to work properly, a strategy needs to be adopted to enable easier sampling of this distribution. Here, the normal approximation of this distribution is adopted, based on Gelman et al. (2013). This is a convenient approach for unimodal and roughly symmetric distributions, where the logarithm of the density is approximated by a quadratic function of the parameter θ_i, centered at its mode. This approximation can be defined as

$$p(\theta_i|.) \approx \mathcal{N}\left(\widehat{\theta}_i,\left(\boldsymbol{I}(\widehat{\theta}_i)\right)^{-1}\right), \quad (22)$$

where $\widehat{\theta}_i$ is the mode of the full conditional distribution of θ_i and $I(\theta_i)$ is defined as

$$I(\theta_i) = -\frac{d^2}{d\theta_i^2} \log\left(p\left(\theta_i|.\right)\right). \tag{23}$$

The mode of the full conditional distribution presented in Equation (21) can be obtained by solving the following expression for θ_i, derived making the gradient of the logarithm of this distribution equal to zero:

$$\frac{1}{\sigma_\varepsilon^2} \sum_{k=1}^{K_i} \left(y_{i,k} - \widehat{y}_{i,k}(\theta_i)\right) \frac{\partial \widehat{y}_{i,k}(\theta_i)}{\partial \theta_i} - \frac{1}{\theta_i \sigma_\theta^2}\left(\log(\theta_i) - \mu_\theta\right) - \frac{1}{\theta_i} = 0 \tag{24}$$

Finally, the function $I(\theta_i)$ is derived as

$$I(\theta_i) = -\frac{1}{\theta_i^2} + \frac{1}{\sigma_\theta^2}\left(\frac{1 + \mu_\theta - \log(\theta_i)}{\theta_i^2}\right) +$$

$$\frac{1}{\sigma_\varepsilon^2} \sum_{k=1}^{K_i} \left(\left(\frac{\partial \widehat{y}_{i,k}(\theta_i)}{\partial \theta_i}\right)^2 - \frac{\partial^2 \widehat{y}_{i,k}(\theta_i)}{\partial \theta_i^2}\left(y_{i,k} - \widehat{y}_{i,k}(\theta_i)\right)\right) \tag{25}$$

This approximation allows easy and direct sampling for the full conditional distribution $p(\theta_i|.)$. It is worth mentioning that, as the mathematical model employed for relating QoI and monitored quantity is an expression previously known (Equation (7)), its derivatives may be easily calculated.

5.4 RESULTS

To evaluate the suitability of employing a hierarchical Bayesian model updating approach based on the information collected during the calibration procedure of a B-WIM system, a set of examples is addressed in this section. The first two examples are generated by simplified models, where numerical simulations are in perfect accordance with all assumptions stated in this study. In addition, all parameters utilized for generating the dataset are previously known. Such examples are useful for validation purposes, as well as for clearly presenting the drawbacks related to the underestimation of the total uncertainty for the classical Bayesian approach. In a second step, more elaborate numerical simulations are performed, aiming to better represent the response of a bridge structure to a heavy vehicle traveling over it. In this case, the dynamic response of a simply supported Euler-Bernoulli beam under moving sprung mass systems is employed. Some additional issues are modeled to reproduce practical aspects, while keeping the computational time tractable to allow a large number of analyses. Among the modeled issues could be cited the effect of the road roughness profile, the inclusion of noise for all measurements and the presence of uncertainty on both estimated vehicle speed and the exact instants that the vehicle enters and leaves the bridge. The numerical simulation allows the

analysis of as many vehicles as intended, but without all the aspects that may affect the real behavior of the measured signal. The last problem is referred to a real case of B-WIM system calibration, which includes many other levels of complexities, inherent from real-world civil engineering systems. However, as it is a real calibration procedure, the number of vehicles employed is limited and the real values of the QoI are not previously known. For all performed analyses, the Gibbs sampler is executed for 10,000 iterations, considering a burn-in phase of 20%. Furthermore, prior distribution parameters are the same, regardless of the example analyzed. For the classical model, $\alpha_\varepsilon = 0.5$ and $\beta_\varepsilon = 0$, whereas μ_θ and σ_θ^2 are calculated to ensure that the mean and standard deviation of the log-normal prior distribution are 4×10^9 and 4×10^{10} Nm, respectively. This gives $\mu_\theta = 19.802$ and $\sigma_\theta = 2.148$ as the prior parameters for the classical approach. It is worth pointing out that the magnitude of the parameters is considerably different from the expected values of θ, owing to the parameterization of the log-normal distribution employed as a prior. For the hierarchical models, $\alpha_\theta = \alpha_\varepsilon = 0.5$, $\beta_\theta = 10^{-3}$ and $\beta_\varepsilon = 0$.

5.4.1 Numerical simulations: initial validation

The main idea for this first analysis is to employ a model simple enough to exactly match all assumptions performed in the model updating strategy. In other words, the signals are generated from the product of precisely known axle weights and a static influence line for a simply supported single girder bridge, with a total length of 10 m. All structural parameters are assumed to be constant throughout the structure and a sample rate of 100 Hz is adopted. A single vehicle configuration is employed in this first step, as described in Figure 1.

Figure 1 – Vehicle configuration for validation examples.
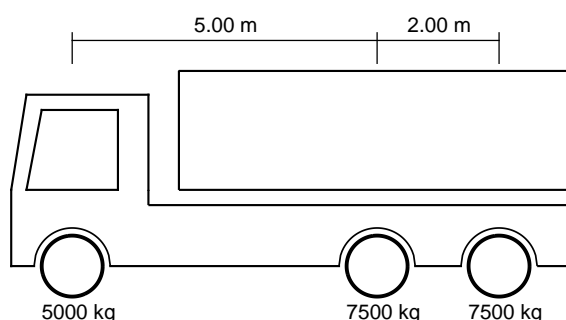
The vehicle is assumed to cross the bridge at a constant speed on every run. A total of 100 runs are simulated, considering three different vehicle speeds: 60 runs at 20 m/s, 20 runs at 24 m/s, and 20 runs at 16 m/s. Furthermore, the simulations also include the effect

Table 1 – Exact values for the parameters that define θ_i and ε probability distributions

Example	μ_θ	σ_θ	Distribution of θ	μ_ε	σ_ε	Distribution of ε
Example 1	22	0.005	Log-normal	0	2×10^{-6}	Gaussian
Example 2	22	0.05	Log-normal	0	2×10^{-6}	Gaussian

of an independent zero-mean additive Gaussian random noise for every signal and scan, such that $\varepsilon_{i,k} \sim \mathcal{N}\left(0,(2 \times 10^{-6})^2\right)$.

For each simulation, a different value of θ_i is sampled from a log-normal distribution, such that $\theta_i \sim \mathcal{LN}\left(\mu_\theta,\sigma_\theta^2\right)$. A total of two examples are addressed in this validation section, considering different values for σ_θ^2. The first example assigns a quite low variance, in such a way that the classical Bayesian approach may provide suitable results. For the second example, the variance is increased to a level where the practical distinction between classical and hierarchical approaches can be clearly observed. The exact values for characterizing θ_i and $\varepsilon_{i,k}$ in both examples are given in Table 1. Notice that, owing to the parameterization of the log-normal distribution, the values of μ_θ and σ_θ are not directly comparable to the magnitude of the variable θ. To allow such a comparison, the mean and standard deviation of θ are analyzed in the following sections. Both the mean value (μ_θ^*) and standard deviation (σ_θ^*) of θ are straightforwardly calculated from the provided parameters as $\mu_\theta^* = \exp(\mu_\theta + \frac{\sigma_\theta^2}{2})$ and $\sigma_\theta^* = \sqrt{(\exp(\sigma_\theta^2) - 1)\exp(2\mu_\theta + \sigma_\theta^2)}$. Figure 2 depicts the simulated strains for both examples. It could be noticed that a higher variability is present for Example 2, where a higher variance is defined for θ. All information related to both examples can be found in Gonçalves (2021).

Figure 2 – Simulated strains for both examples in initial validation.
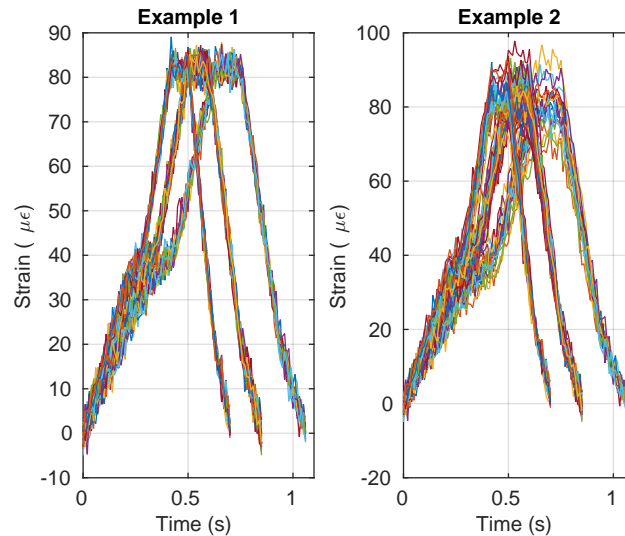

5.4.1.1   Example 1

Both classical and hierarchical methods are employed for the first example, which also evaluates the influence of the dataset size on the estimated uncertainties. It is worth remarking

that the proportion of runs at each vehicle speed is kept the same for all datasets. The results for the classical approach are summarized in Figure 3, which presents histograms for both θ and σ_ε. The parameter N indicates the dataset size related to each result, which is a notation that is also adopted for following analyses. Recall that, for the classical approach, the QoI is assumed to be constant for all calibration runs. Thus, it is noticed that the uncertainties continuously decrease as the amount of information provided to the model increases. As the classical approach assumes that the QoI is a fixed value, the model is not able to represent the inherent variability of the QoI and the underestimation of total uncertainty is clearly noticed. Therefore, in a hypothetical scenario, the classical approach admits that the uncertainties regarding the parameter of interest vanish when employing a infinitely large dataset. Conversely, the histograms for σ_ε clearly show that the classical approach, even disregarding the inherent variability of the QoI, is able to estimate σ_ε precisely for this example. As the variability of the QoI is defined by a coefficient of variation of just 0.5% and estimates for σ_ε are in accordance with the real values, the classical approach may be able to provide suitable results in this simple case.

Figure 3 – Estimates of analyzed parameters for the classical approach applied to Example 1.
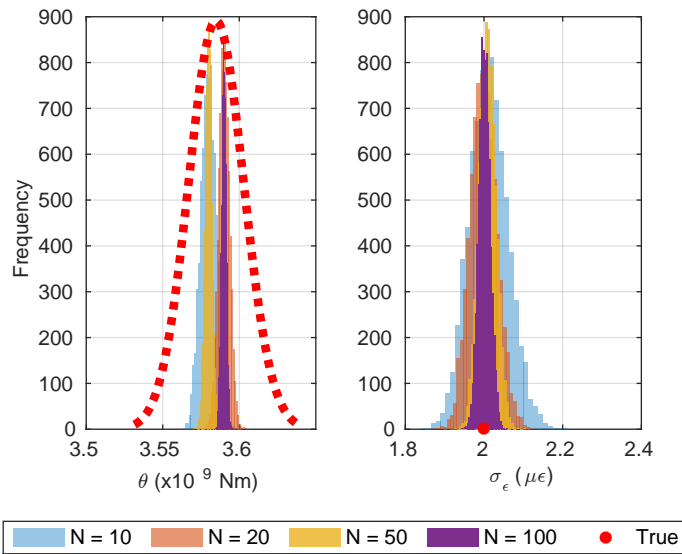
The results obtained using the hierarchical strategy are shown in Figure 4, which presents the mean (μ_θ^*) and standard deviation (σ_θ^*) of the QoI instead of the parameter values for the log-normal distribution of θ (since the former parameters are more straightforwardly interpreted from a practical perspective). This presentation issue is adopted for all the following hierarchical model results. The histograms for μ_θ^* and σ_ε are centered with respect to the true values employed in the simulations, even for the smallest dataset available. The same could not be said for σ_θ^*; however, a clear convergence toward the expected value is noticed when the amount of information is increased. Indeed, this convergence is perceived for all evaluated parameters. Therefore, the hierarchical strategy is able to provide proper estimates for the QoI

in this case, including the variability of θ. For this simple example, it was already expected that both classical and hierarchical methods were able to properly estimate both θ and ε, since inherent variance in θ was intentionally kept at a low level.

Figure 4 – Estimates of analyzed parameters for the hierarchical approach applied to Example 1.
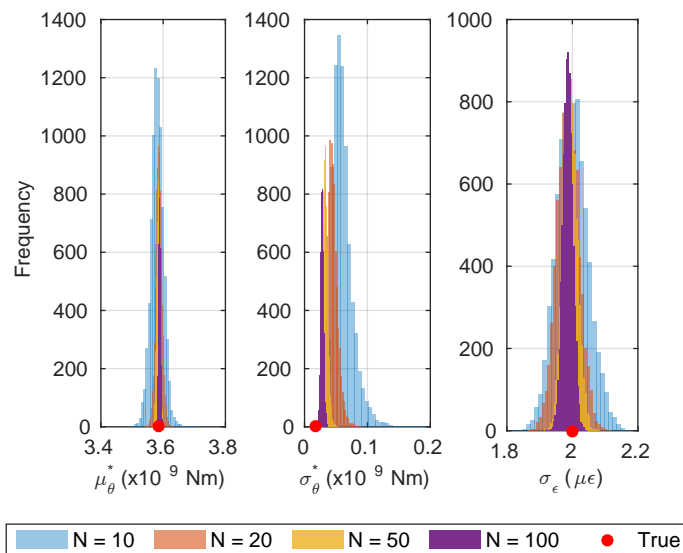
5.4.1.2 Example 2

The second example introduces a troublesome issue for the classical strategy: a significant inherent variability of the QoI for different experiments. The unsuitability of the classical Bayesian approach in this scenario is clearly noticed in Figure 5, which shows the histograms for both θ and σ_ε as a function of the number of vehicle runs employed in the model updating process. The provided estimates for θ are almost point estimates of the mean value of the real distribution, disregarding almost entirely the uncertainty associated with such a parameter. Furthermore, it is possible to observe that, by ignoring the inherent uncertainty in the QoI, the classical model is forced to assign all the uncertainty to the error parameter σ_ε. Hence, the updated values of σ_ε are overestimated.

The histograms for all updated parameters regarding the hierarchical approach are presented in Figure 6. Similarly to what was observed in Example 1, the results for the hierarchical approach also properly converge to the exact values for all parameters. Indeed, both examples are defined in such a manner that the assumptions made in the hierarchical strategy are exact. Therefore, it is already expected that such a convergence easily occurs. However, even this simple example is enough to show the possible drawbacks in employing the classical strategy.

The unsuitability of the classical approach for this example is even more remarkable when analyzing Figure 7, which presents the estimated distribution for the QoI reported by

Figure 5 – Estimates of analyzed parameters for the classical approach applied to Example 2.
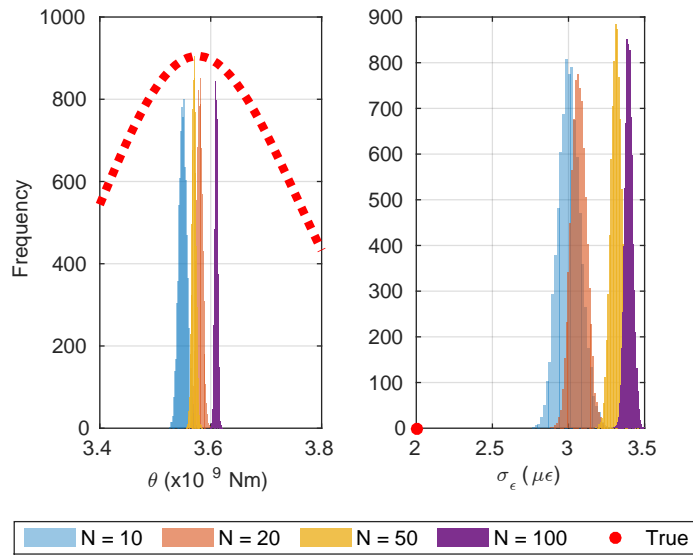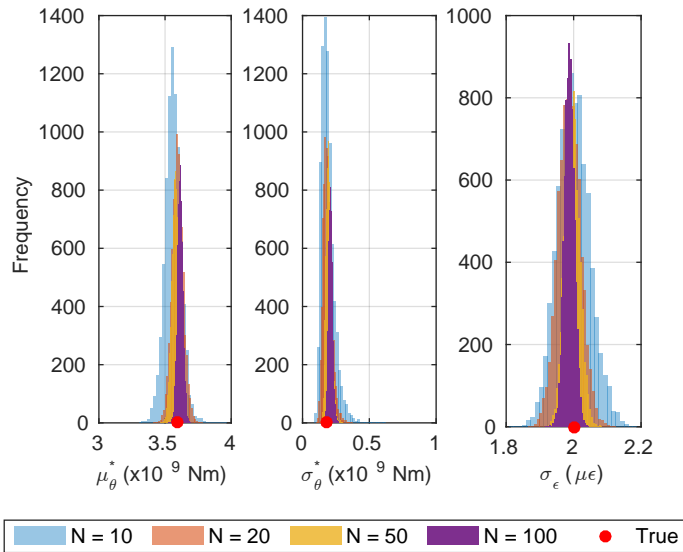

Figure 6 – Estimates of analyzed parameters for the hierarchical approach applied to Example 2.

both classical and hierarchical models, in comparison with the known real distribution. The samples for the classical strategy are straightfordwardly obtained from the MCMC samples. For the hierarchical approach, however, the maximum a posteriori (MAP) values for μ_θ and σ_θ^2 are employed in calculating the values of the probability density function (pdf) of the log-normal distribution for θ. It could be noticed that the uncertainty estimated by the classical approach is highly underestimated, resulting in almost a point estimate for θ. This is a concerning issue, mainly when employing such estimates for further safety analyses, where uncertainty in the QoI may play an important role. In this example, a coefficient of variation of 5% is disregarded when employing the classical strategy. Conversely, the hierarchical approach is able to provide more

reliable estimates of the total uncertainty regarding the QoI. Indeed, for this example, where all modeling assumptions are in perfect agreement with the simulated signals, the estimates clearly agree with the true distribution for the QoI.

Figure 7 – Estimates of the pdf of θ for Example 2: (a) classical approach; and (b) hierarchical approach.
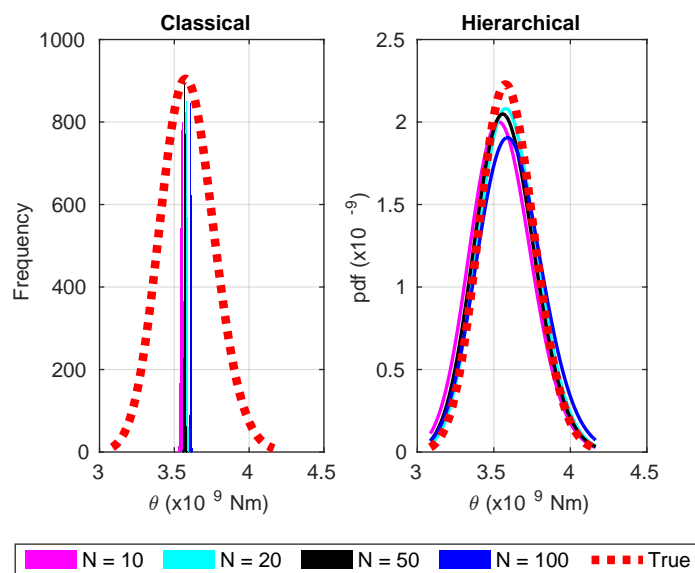
Both analyzed examples are relatively simple but quite informative. They indicate that the hierarchical strategy is more robust and reliable, since it is able to properly account for the inherent variability of the QoI. Hence, if no significant variability is present, it will perform as well as a classical Bayesian strategy. However, in the presence of such a variability, the hierarchical approach clearly outperforms the classical one. Then, for further analyses, just the hierarchical approach is evaluated.

The analyses just performed are useful for illustrating some issues related to the classical approach when inherent variability is present in the QoI and demonstrating that the hierarchical approach should be preferred in this case. However, such examples are unrealistically in accordance with the modeling assumptions. Therefore, it is important that more representative examples be addressed to show that the hierarchical strategy is effectively well suited for the proposed application. In the following examples, more elaborate models are employed, aiming to represent a real B-WIM system calibration procedure.

5.4.2   Numerical simulations: simplified dynamic model

Numerical simulations are conducted, employing the Euler-Bernoulli beam model for a simply supported single girder bridge. The bridge total length is set to 15 m, assuming also that all structural properties are constant along the structure. Eight different vehicles are employed, aiming to represent a wide range of practical vehicle configurations, based on a vehicle classification from Brazil (DNIT, 2012). Each vehicle is modeled as a system of sprung

Table 2 – Main characteristics of vehicles for numerical simulations

Vehicle ID	Total mass (kg)	Total length (m)	Number of axles
1	16,000	4.25	2
2	23,000	5.50	3
3	33,000	9.20	4
4	43,000	12.90	5
5	53,000	16.60	6
6	57,000	16.50	7
7	67,000	20.20	8
8	74,000	20.10	9

Table 3 – Number of runs performed with defined speed by each analyzed vehicle

| Vehicle ID	Speed (m/s)	Number of runs
1, 2, 3, 4, 5, 6, 7, 8	16	10
1, 2, 3, 4, 5, 6, 7, 8	20	30
1, 2, 3, 4, 5, 6, 7, 8	24	10

masses, as detailed in Carraro et al. (2019). The main characteristics of the vehicles are defined in Table 2, while a detailed description of all parameters employed in the numerical simulations is given in the Appendix .1.

A total of 400 signals are simulated, 50 for each vehicle. For every vehicle run, a constant speed is assumed, which is the usual approach in B-WIM systems (GONÇALVES; CARRARO; LOPEZ, 2021), where three different speeds are considered: 16, 20 and 24 m/s. The division of total runs between different vehicles and velocities is given in Table 3. These values of speed are chosen to reproduce a typical scenario of B-WIM system calibration (JACOB; O'BRIEN; JEHAES, 2002). Although the speed is defined to be constant throughout the passage of the vehicle, it is considered that this parameter is not exactly known. Indeed, a multiplicative Gaussian error, with unitary mean and 5% as coefficient of variation, is applied to every speed before the model updating procedure. This error is employed to simulate the inherent uncertainty related to estimating the vehicle speed from collected signals in a real-world application. The fact that the vehicle speed is not precisely known also implies an uncertainty regarding the prediction of the time interval related to the passage of the vehicle over the bridge. This occurs because the exact time instants that the vehicle enters or leaves the bridge are not directly measured in this study. Thus, the vehicle speed and the time instant that the vehicle crosses some FAD, whose position is known, are employed to estimate the total length of signal related to the passage of the vehicle over the bridge.

Three additional features are modeled, aiming to better simulate the real behavior expected for bridge structures, as well as some practical difficulties that should arise in this context. First of all, a roughness road profile referred to class B (ISO 8606:1995, 1995)

is assumed, considering a different profile for each run. Second, a white Gaussian noise, such that the signal to noise ratio is set to 20, is added to every signal. Finally, for each simulation, a different value of θ_i is sampled based on a Gaussian distribution, such that $\theta_i \sim \mathcal{N}\left(5 \times 10^9, \left(5 \times 10^8\right)^2\right)$. Notice that this distribution for the QoI is different from the log-normal distribution adopted in the definition of the hierarchical model. It aims to reproduce the practical scenario where the distribution of the QoI does not follow the model assumptions. Figure 8 shows a sample signal from each vehicle employed in this section. Just one signal is presented for the sake of clarity, since 50 signals are available for each vehicle. The whole dataset, including all the signals, is available in Gonçalves (2021).

Figure 8 – Example of simulated strains according to the simplified dynamic model for each analyzed vehicle.
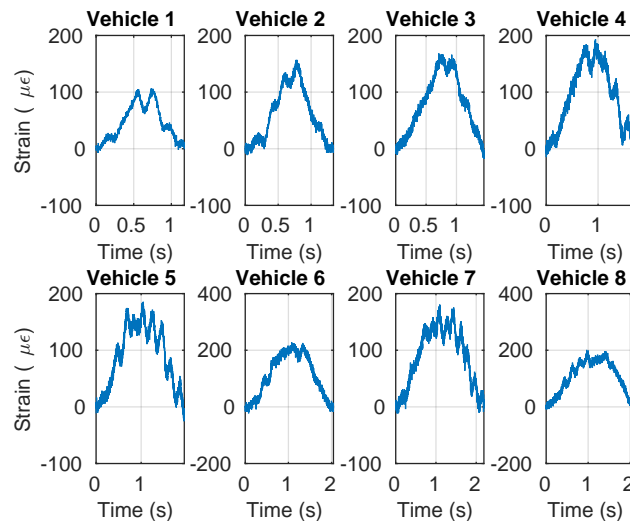
Another relevant aspect that should be discussed is related to the independence hypothesis stated in the derivation of the hierarchical approach, mainly considering the errors of successive measurements from the same vehicle. The information retrieved by B-WIM systems comprises a set of time series, sampled at a high sample rate. In this context, it is important to remark that, in many cases, observations related to adjacent instants of time present positively correlated errors (JAMES et al., 2013). Indeed, such kinds of serial correlation were also observed in other works regarding B-WIM systems (YOSHIDA; SEKIYA; MUSTAFA, 2021). The application of the independence assumption for a situation where the errors are actually correlated, without further action, could corrupt the overall results. This may occur because the presence of correlation typically leads Bayesian analyses to infer a false precision, since a sequence of correlated observations presents less information, compared with the same quantity of independent data (GELMAN et al., 2013). The following procedure is adopted in this study to mitigate the effect of serial correlation in hierarchical approach results. The idea is to perform a downsampling procedure to every signal. In this process, the effective sample rate is reduced by discarding some data points following a regular pattern. The idea in employing such a procedure is that the reduction in the effective dataset size decreases the false precision

induced by the serial correlation. In addition, as correlated observations can be understood to be redundant, this process can be conducted without major concerns. The factor of reduction is chosen based on a Durbin-Watson test (DURBIN; WATSON, 1950). Distinct effective sample rates are evaluated, keeping the same value for all vehicle runs. The value in which serial correlation could not be argued for the highest number of runs is chosen, based on the value of p of the Durbin-Watson test, whose threshold is set here as 0.05. In this work, a minimum effective sample rate of 10 Hz is adopted in order to avoid excessive modification of the signal by the downsampling procedure. It is worth mentioning that this is just a simplified procedure for assessing when the reduction in effective sample rate seems suitable. Studies for addressing the presence of serial correlation in a more efficient way are indicated as a promising future research subject, with more detailed suggestions discussed in further sections. To evaluate the impact of this procedure, the hierarchical approach is evaluated for two cases: without (Case 1) and with (Case 2) downsampling.

The first analysis performed is related to the suitability of the obtained results as a function of the number of signals employed. This is an important aspect when dealing with B-WIM systems, since calibration procedures are usually limited to dozens of runs. Figure 9 and Figure 10 present the influence of the number of runs on the suitability of the MCMC samples for Cases 1 and 2, respectively. It is worth pointing out that the same number of runs from each vehicle type is utilized and the speeds of these selected events follow the same proportion as in Table 3. The real values employed for μ_θ^* and σ_θ^* in the simulation of the signals are precisely known and, hence, are used as a comparison criterion. Conversely, as the error comprises all the issues not handled by the forward model, the exact value of σ_ε is not previously known.

When observing the reported results, it is noticed that the major distinction between both methods relies on the uncertainty regarding the estimates of σ_ε. The predictions provided by the hierarchical approach without downsampling (Case 1) are almost point estimates. In this case, the inclusion of more vehicle runs leads to new estimates of σ_ε that fall outside the range of the previous prediction, illustrating the false precision that serial correlation may induce. Conversely, the hierarchical approach with downsampling (Case 2) presents distributions where there is a clear overlap of posterior distributions of σ_ε from different dataset sizes, indicating that such results are more consistent. Although the differences are presented for σ_ε, it is clear that both approaches are able to predict both μ_θ^* and σ_θ^* properly. This indicates that the downsampling procedure is able to reduce the false precision due to the violation of the independence assumption without corrupting the main aspects of the signal. As already expected, the uncertainty decreases within the increasing of the number of datasets considered, where a good convergence to the real values is noticed.

Although better results are expected when employing more runs, the model updating results with fewer runs are already able to properly predict the uncertainties regarding the parameter of interest. To illustrate this last statement, Figure 11 depicts the uncertainties

Figure 9 – Estimates of analyzed parameters for the hierarchical model without downsampling applied to the simulated data.
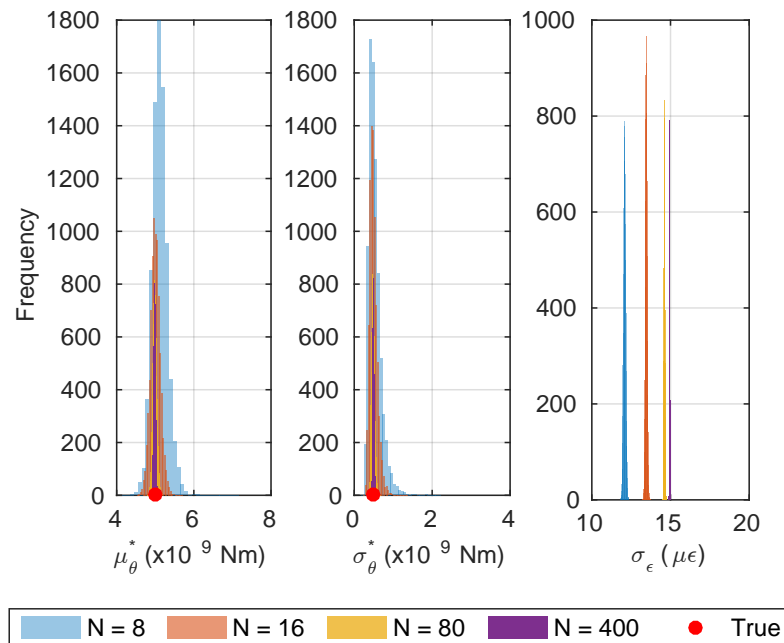

for the parameter θ considering both approaches, where each pdf is calculated based on the respective MAP estimate for μ_θ and σ_θ^2. It is noticed that, in both cases, the shape of the sampled distribution is quite similar to the real employed values for all numbers of runs considered. This is important since, from the B-WIM perspective, a number of the level of dozens of runs is of the same order of magnitude of current practical values for calibration procedures. This aspect indicates that the amount of data currently obtained for calibration procedures is able to provide reasonable information to assess the uncertainties in this QoI.

As already discussed, the calibration procedure is limited to just a few vehicles. As the forward model employed is not able to perfectly describe the real behavior of the vehicle-bridge system, it is already expected that model updating results will depend on the characteristics of the vehicles utilized for calibration. Although such a dependence is recognized, a proper model updating procedure should not be excessively affected by these characteristics. To assess the dependence of the model updating results within the configuration of the calibration vehicles, a comparative analysis is performed. This analysis relies on the comparison of resulting updated parameters for datasets considering just runs referred to each vehicle independently. In this case, just the hierarchical model with downsampling is analyzed, since such an approach presented more consistent results in the previous analysis. Figure 12 presents the updated values of μ_θ^*, σ_θ^*, and σ_ε for datasets referred to 50 signals from each vehicle ID. Only data regarding Vehicles 1, 3, 6, and 8 are shown, for the sake of clarity.

The general behavior for parameters μ_θ^* and σ_θ^*, independently of the vehicle employed, is quite similar, approaching well the known real values employed in the simulations. Such aspects

Figure 10 – Estimates of analyzed parameters for the hierarchical model with downsampling applied to the simulated data.
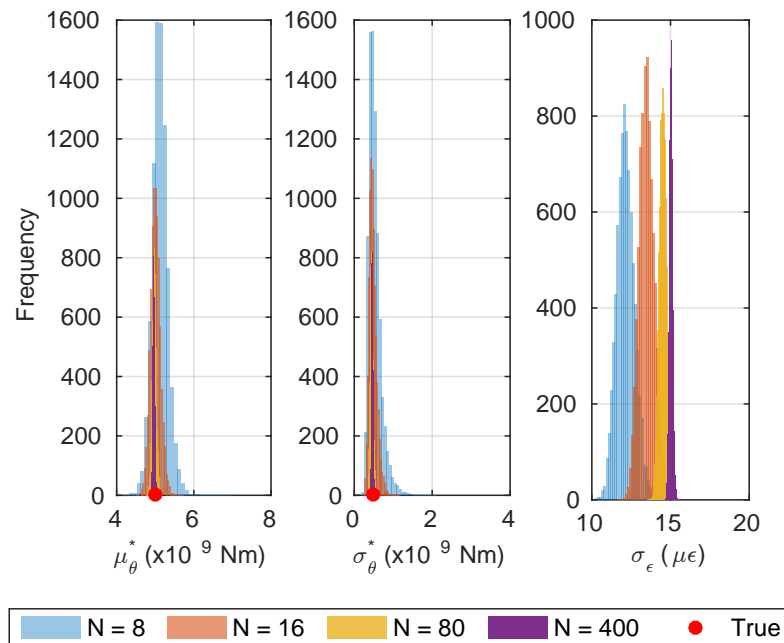

indicate that the updated results for both parameters are robust to the specific characteristics of the vehicles and, hence, the proposed approach is able to extract proper information for model updating of both parameters. For the parameter σ_ε, however, it is noticed that different vehicles generate estimates that are considerably different. In particular, the predictions for Vehicle 1 are significantly lower than for the remaining vehicles. This difference could be problematic, for instance, when the model is employed for propagating uncertainties and predicting the response of the vehicle-bridge system for an unseen vehicle. As previously discussed, the error is being utilized to represent all unmodeled aspects of the dynamic problem, in an additive way. Therefore, as the generated strains and, consequently, the differences between model and measurements are a direct function of the axle weights of a given vehicle, heavier vehicles will tend to present a high value for σ_ε. Recalling Table 2, it is noticed that the weight of Vehicle 1 is, at least, two times lower than any other vehicle employed in this comparison, which is in accordance with such a statement. Thus, proposing strategies for improving the estimates for σ_ε, allowing the error to better represent the behavior of the model for different vehicles, seems an interesting issue to be addressed in future studies.

5.4.3 Real-world B-WIM system calibration data

To exemplify the application of the proposed hierarchical Bayesian approach for a real B-WIM system calibration procedure, data collected for the Itinguijada bridge are employed. The Itinguijada bridge is located 147 km south from the border of the states of Goiás and Tocantins in the road BR-153, Brazil. The structure has a total length of 29.70 m and comprises

Figure 11 – The pdf of θ for the hierarchical approaches for the numerical simulations: (a) without downsampling; (b) with downsampling.
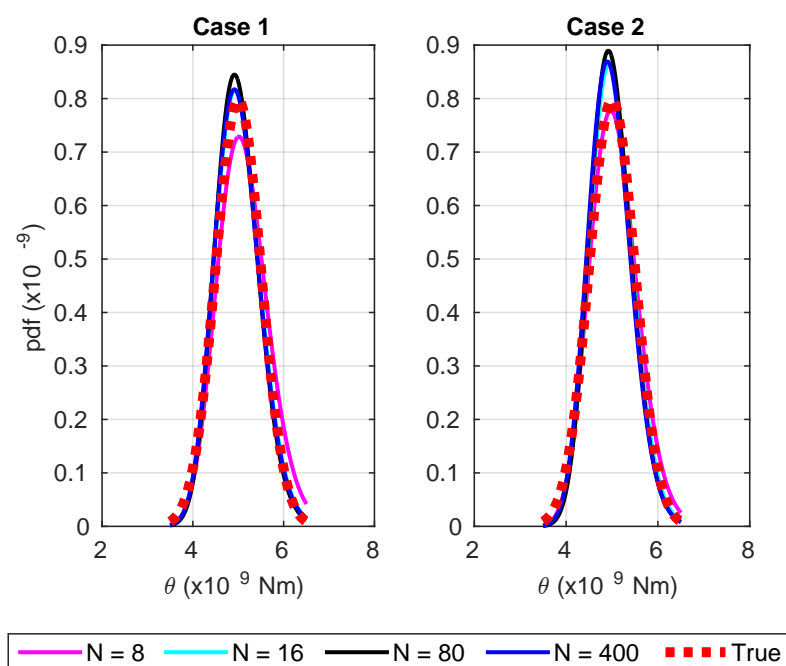
five cross beams and two girders. Figure 13, Figure 14 and Figure 15 show the analyzed bridge, the main dimensions of its cross section, and its lateral view, respectively. The theoretical response for a simply supported bridge model is adopted to define the shape of the influence line employed in the model updating procedure. Two sets of FADs are attached underneath the bridge slab, one per lane, with a longitudinal spacing of 4 meters between sensors in the same lane. In addition, for both lanes, one of these sensors is installed at the mid-span of the bridge. Each girder is equipped with two strain sensors at its mid-span, attached to the bottom of the girder. Therefore, the structural response for each girder is the average signal from these two sensors.

Two trucks, whose main characteristics are given in Table 4, were employed to calibrate the B-WIM system. The resulting dataset refers to strains and FAD signals collected for 49 runs, 29 for the three-axle vehicle and 20 for the five-axle one. This results in, at least, 10 runs per truck over each lane. The speed of the vehicle on each run is calculated from the information provided by the FADs. Furthermore, all runs are joined together, regardless of the lane along which the vehicle traveled. This could be done since the proposed forward model does not make any distinction between runs related to different lanes. Figure 16 shows four strain signals, accounting for the contribution of both girders, as utilized in the proposed method, from each vehicle employed in the calibration of the B-WIM system.

It is worth pointing out that the analyzed bridge is relatively old, around 50 years (JUNGES, 2017), and there is no reliable information regarding its structural properties for properly estimating a true QoI value. Even the bridge's exact age is not precisely known, which

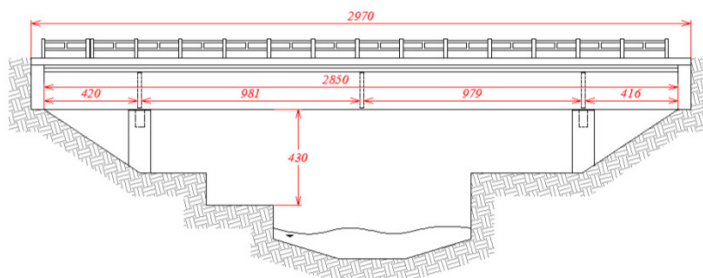Figure 12 – Estimates of analyzed parameters for the hierarchical model with downsampling, as a function of the vehicle whose signals were employed for performing the model updating.

Figure 13 – Itinguijada bridge

Figure 14 – Mid-span cross section dimensions (values in cm)

Figure 15 – Lateral view dimensions (values in cm)

Table 4 – Axle weights and spacing for calibration vehicles

| Vehicle	Axle mass (kg)				
	Axle 1	Axle 2	Axle 3	Axle 4	Axle 5
Three-axle vehicle	6,900	14,900	12,900	-	-
Five-axle vehicle	7,500	14,100	13,300	11,100	9,200
	Axle position (m)				
	Axle 1	Axle 2	Axle 3	Axle 4	Axle 5
Three-axle vehicle	0	4.78	6.07	-	-
Five-axle vehicle	0	3.57	9.16	10.43	11.66

Figure 16 – Example of measured strains from the B-WIM system calibration data. Vehicle 1 is the three-axle vehicle and Vehicle 2 is the five-axle vehicle.
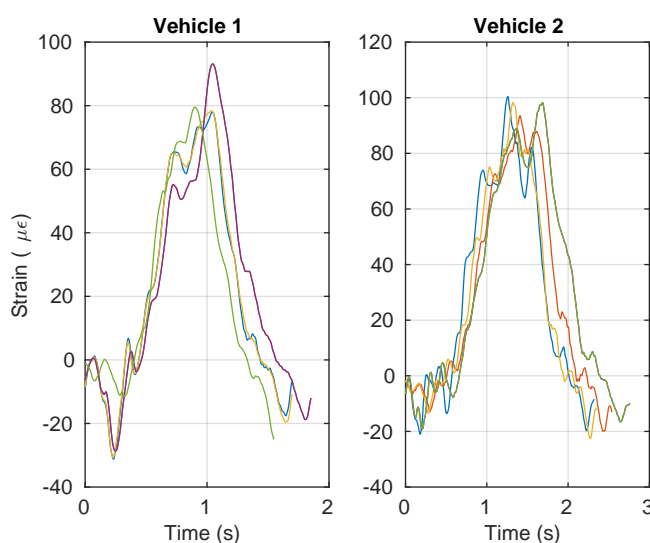
is a common scenario for Brazilian bridges (LIMA E OLIVEIRA; GRECO; BITTENCOURT, 2019). Thus, by contrast with the numerical simulations in which all bridge properties are exactly known, the real bridge calibration example does not present a target value for the QoI. The aim is to avoid inaccurate estimation of corrupt conclusions with respect to the QoI. Despite the absence of a real comparison criterion, this example illustrates, indeed, a situation in which the proposed approach is particularly useful. Even in this scenario, some analyses can still be conducted to evaluate the overall suitability of the proposed procedure. The agreement regarding model updating considering two disjoint datasets is the first one, as already performed

Figure 17 – Estimates of analyzed parameters for the hierarchical model with downsampling for the real calibration example.
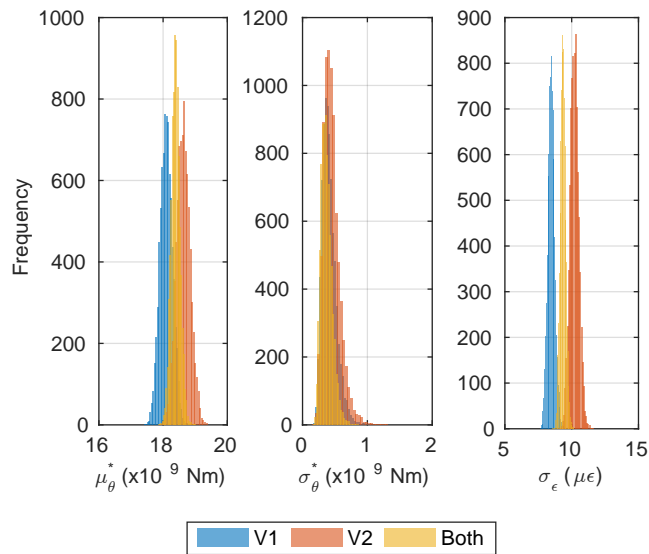

for the simulated signals case. Figure 17 shows the histograms for each variable, comparing the results for datasets referred to each vehicle individually, for the hierarchical model with downsampling. For all parameters, similar updated values are reported, since a considerable overlap between histograms obtained from different datasets is noticed. This indicates that the obtained sampled distribution for such parameters should be representative of the real behavior of the structure, with the modeling strategy adopted performing similarly for different vehicles. In this real data study, a slightly higher deviation between predictions using different vehicles is observed for μ_θ^*. This might be because there are more unmodeled issues present in the real data scenario than in simulated signals. For instance, vehicles are much more complex dynamic systems than the simple sprung mass systems employed for simulating signals; the exact transverse position of the vehicle at each run is variable and not precisely known and the bridge structure comprises many other components besides its girders. Although a larger deviation is present, it is remarked that such a difference does not reach 5% among the means of μ_θ^* calculated from both samples. Hence, it is considered that the model updating results are robust to different vehicles for μ_θ^* and σ_θ^*. This difference is somewhat noticeable for σ_ε when the dataset for each vehicle is employed independently. However, the distinction is not so remarkable as that observed for the simulated data, since the range of vehicle weights analyzed for this real data experiment is smaller. Again, the estimate of σ_ε is higher for the heavier vehicle, which is consistent with the previous discussion.

   Another procedure that might help in the process of assessment of the suitability of the model updating process is the uncertainty propagation of the system. The uncertainties calculated from the hierarchical procedure with downsampling and considering the dataset employing both vehicles for parameters μ_θ, σ_θ^2, and σ_ε^2 are employed for predicting the strains

generated by each vehicle. Figure 18 shows the 95% confidence bounds for the predicted strains induced, accounting for the contribution of both girders, together with one signal collected from each vehicle. Just one signal is employed for sake of clarity; however, results are similar for the remaining signals. It is noticed that the majority of the signals fall within the confidence bounds, indicating that the uncertainties quantified by the hierarchical approach are able to properly represent the signal of each vehicle independently, even though both vehicles are considerably different. This is another relevant result for indicating the robustness and suitability of the proposed hierarchical model.

Figure 18 – Uncertainty propagation for predicted strains for the real calibration example.
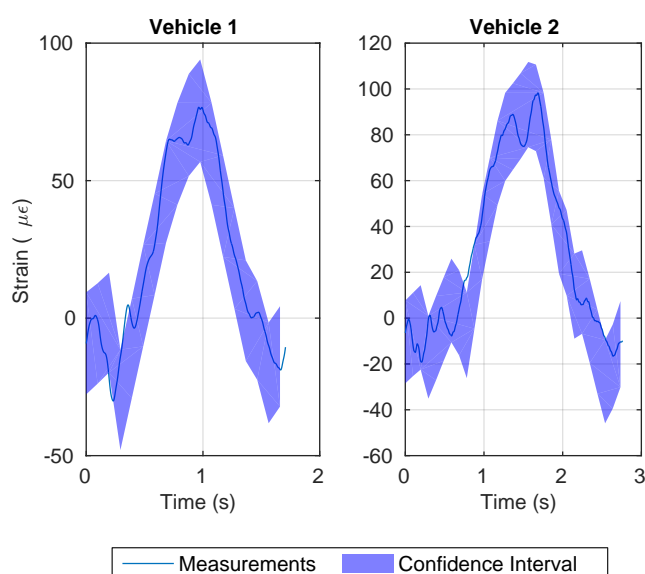
One of the main advantages of employing a hierarchical strategy is its capability of accurately predicting the total uncertainties regarding the QoI. This advantage is remarkable for systems where an inherent variability is present. The bridge structural response due to a moving vehicle is argued in this study to belong to this class. To evaluate the level of inherent uncertainty present in this problem, Figure 19 presents the estimated pdf of the QoI, as a function of the vehicles employed in the process. It is noticed that the hierarchical estimates present a reasonable dispersion, resulting in a coefficient of variation higher than 2%. Although this might not seem a noticeable value, it is preferable to consider this uncertainty for further analyses instead of employing an approach that completely disregards it. In addition, other bridge structures might present a different behavior. To ensure that a considerable uncertainty is not being disregarded, it is prudent to estimate it. The proposed hierarchical Bayesian model updating approach is able to take this uncertainty into account, regardless of its magnitude, ensuring a higher robustness to the provided estimates. Therefore, such an approach should be preferred, allowing a better estimate of total uncertainties.

Figure 19 – The pdf of θ for the hierarchical approach with downsampling for the real calibration example.
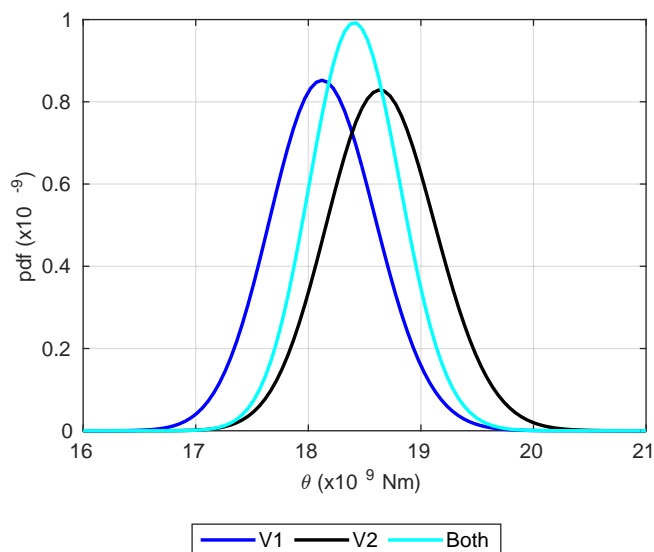
5.5 FURTHER REMARKS

Both numerically simulated signals and an example of B-WIM system calibration data were employed to assess the suitability of the proposed approach. The results indicate that the proposed hierarchical approach is promising for practical applications, mainly employing the downsampling procedure to mitigate the effects of serial correlation. This works has an even higher relevance when considering the situation where no previous knowledge is available, as, for instance, in the case of old bridges for which design plans (i.e., blueprints or structural specifications) are no longer available. Indeed, this is the scenario in which the updating process of the real B-WIM calibration data example was performed and corresponds to a common situation for Brazilian bridges. Although this might not be a problem for proper B-WIM system operation, further analyses, such as safety assessment, require additional information. Thus, the proposed model updating approach arises as an alternative to provide estimates regarding important parameters, including confidence bounds.

It is important to cite two relevant practical aspects on which such results are based. First, the road surface condition has an important role in the dynamic response of a bridge under a moving vehicle. When performing the numerical simulations, it was intended to use a road class that reflects what is expected in practical applications. According to the study of Múčka (2017), who performed a review of published works, Classes A and B are roughly recommended as representative of a typical road profile for many functional road categories. Indeed, many recent works adopted such road classes for numerical simulations. For instance, Cantero (2021) and He et al. (2019) employed Class A, Gonçalves et al. (2022) applied Class B, and He et al. (2021) and Gonçalves, Carraro, and Lopez (2021) utilized Classes A and B. Therefore, it is expected that, by applying the road Class B in this study, the results of the

method will be representative enough for practical purposes. The second relevant aspect to be addressed is related to the support conditions of the analyzed bridges. The shape of influence line employed in the model updating process is related to a simply supported bridge and works properly for such applications. However, if the support conditions of the bridge under analysis correspond to a different behavior, it might be necessary to employ an influence line shape corresponding to the support condition that better represents this behavior.

This study is a first attempt to link model updating through hierarchical models and B-WIM systems. With this point in mind, it was chosen to keep the model as simple as possible, but without losing its practical relevance. This context indicates that some points of the proposed methodology could be improved in future work. Furthermore, many different applications could be developed based on the ideas proposed in this study. Hence, as suggestions for future works, one could cite the following:

- more elaborate forward models: for this work, a simple forward model, based only on a theoretically calculated influence line for a simply supported bridge, was employed. However, different applications may require more complex forward models. For instance, one could employ a modeling strategy that takes into account the dynamic behavior of the vehicle-bridge system, such as in Gonçalves, Carraro, and Lopez (2021);

- allowing a number of QoI: for this study, a single QoI was utilized to represent the system. However, for more complex forward models, more variables might be necessary;

- a number of girders and a transverse load distribution: for real structures, mainly when the deterioration process is significant and many girders are available, modeling each girder independently should be a more suitable approach. Such a model should also take into account the inclusion of the vehicle transverse position into the forward model. This procedure could result in even more reliable safety assessment for bridge structures for known extreme events, such as overloaded vehicles;

- other applications related to structural safety: it is also possible to extend the proposed formulation in such a way that the updated parameters describe more complex processes, such as the stiffness degradation due to reinforcement corrosion, as in the work of Ma et al. (2014). In this case, the parameters that describe the process may be estimated by the hierarchical approach and the updated model could be employed to perform future resistance predictions in a more reliable manner. Another possibility is to apply the hierarchical model together with a simplified finite element model of the structure for damage identification, such as in Behmanesh and Moaveni (2016);

- influence line calculation: in this study, a theoretically calculated influence line was employed to predict the response of the structure to moving loads. An alternative is

to model the coefficients that define the influence line as the QoI in order to assess the related uncertainties. This influence line could have many further applications, including B-WIM purposes. For instance, such an approach is well suited for working with Bayesian B-WIM algorithms, such as those of Yoshida, Sekiya, and Mustafa (2021) and Gonçalves et al. (2022);

- a more complex covariance matrix structure for the error between measurements and theoretical model: in this work, the covariance matrix was assumed to represent independent measurements, although the presence of serial correlation in error terms was recognized and a downsampling procedure was proposed to mitigate the effect of such a correlation. However, this is a simplified approach that does not explicitly account for the serial correlation. For instance, a covariance matrix related to autoregressive models could be updated in the process. Furthermore, the error variance can be modeled as a function of the axle weights, similar to the approach taken by Mingming Song et al. (2019) in relating the effective stiffness and vibration level. This could be useful for improving the agreement among prediction for different sets of vehicles.

5.6   CONCLUSION

In this study, a hierarchical Bayesian approach is proposed to perform model updating of parameters related to the bending response of bridge structures. It employs a dataset generated during the calibration procedure for a B-WIM system, comprising a number of controlled runs of known vehicles. In addition, a downsampling procedure was performed to mitigate the effect of serial correlation among residuals. To assess the suitability of the proposed approach, both numerically simulated and real-world signals were applied. For the numerical simulations, where the true values employed for generating the signals were previously known, the updating process was able to properly estimate the uncertainties regarding the parameters of interest. For the real B-WIM calibration example, such a comparison was not possible. However, the estimates are consistent, even when comparing results obtained for datasets from different vehicles. Thus, the presented results indicate that the proposed approach is able to provide useful and robust information for helping in decision-making related to the safety of bridge structures.

ACKNOWLEDGMENTS

REFERENCES

BALLESTEROS, G. C.; ANGELIKOPOULOS, P.; PAPADIMITRIOU, C.; KOUMOUTSAKOS, P. Bayesian Hierarchical Models for Uncertainty Quantification in Structural Dynamics. In: VULNERABILITY, Uncertainty, and Risk: Quantification, Mitigation, and Management. [S.l.: s.n.], 2014. P. 1615–1624.

BEHMANESH, Iman; MOAVENI, Babak. Accounting for environmental variability, modeling errors, and parameter estimation uncertainties in structural identification. **Journal of Sound and Vibration**, v. 374, p. 92–110, 2016. ISSN 0022-460X.

BEHMANESH, Iman; MOAVENI, Babak; LOMBAERT, Geert; PAPADIMITRIOU, Costas. Hierarchical Bayesian model updating for structural identification. **Mechanical Systems and Signal Processing**, v. 64-65, p. 360–376, 2015. ISSN 0888-3270.

BROWNJOHN, James Mark William; MOYO, Pilate; OMENZETTER, Piotr; LU, Yong. Assessment of Highway Bridge Upgrading by Dynamic Testing and Finite-Element Model Updating. **Journal of Bridge Engineering**, v. 8, n. 3, p. 162–172, 2003.

CANTERO, Daniel. Moving point load approximation from bridge response signals and its application to bridge Weigh-in-Motion. **Engineering Structures**, v. 233, p. 111931, 2021. ISSN 0141-0296.

CANTERO, Daniel; GONZÁLEZ, Arturo. Bridge Damage Detection Using Weigh-in-Motion Technology. **Journal of Bridge Engineering**, v. 20, n. 5, p. 04014078, 2015.

CANTERO, Daniel; KAROUMI, Raid; GONZÁLEZ, Arturo. The Virtual Axle concept for detection of localised damage using Bridge Weigh-in-Motion data. **Engineering Structures**, v. 89, p. 26–36, 2015. ISSN 0141-0296.

CARRARO, Felipe; GONÇALVES, Matheus Silva; LOPEZ, Rafael Holdorf; MIGUEL, Leandro Fleck Fadel; VALENTE, Amir Mattar. Weight estimation on static B-WIM algorithms: A comparative study. **Engineering Structures**, v. 198, p. 109463, 2019. ISSN 0141-0296.

CATBAS, F. Necati; ZAURIN, Ricardo; GUL, Mustafa; GOKCE, Hasan Burak. Sensor Networks, Computer Imaging, and Unit Influence Lines for Structural Health Monitoring: Case Study for Bridge Load Rating. **Journal of Bridge Engineering**, v. 17, n. 4, p. 662–670, 2012.

DNIT, Departamento Nacional de Infraestrutura de Transportes. **Quadro de fabricantes de veículos**. Rio de Janeiro, Brazil, 2012. Available from: `https://www.gov.br/dnit/pt-br/rodovias/operacoes-rodoviarias/pesagem/QFV2012ABRIL.pdf`.

DURBIN, J.; WATSON, G. S. Testing for Serial Correlation in Least Squares Regression: I. **Biometrika**, v. 37, n. 3/4, p. 409–428, 1950. ISSN 00063444.

FRØSETH, Gunnstein T.; RØNNQUIST, Anders; CANTERO, Daniel; ØISETH, Ole. Influence line extraction by deconvolution in the frequency domain. **Computers & Structures**, v. 189, p. 21–30, 2017. ISSN 0045-7949.

GELMAN, Andrew; CARLIN, John B.; STERN, Hal S.; DUNSON, David B.; VEHTARI, Aki; RUBIN, Donald B. **Bayesian Data Analysis**. Third. [S.l.]: Chapman and Hall/CRC, 2013. ISBN 9781439840955.

GONÇALVES, Matheus Silva. **Vehicle-bridge dynamics simulation considering inherent variability in structural properties**. [S.l.: s.n.], 2021. Mendeley Data. v1. Available from: `http://dx.doi.org/10.17632/9j2wngpdg3.1`.

GONÇALVES, Matheus Silva; CARRARO, Felipe; LOPEZ, Rafael Holdorf. A B-WIM algorithm considering the modeling of the bridge dynamic response. **Engineering Structures**, v. 228, p. 111533, 2021. ISSN 0141-0296.

GONÇALVES, Matheus Silva; LOPEZ, Rafael Holdorf; OROSKI, Elder; VALENTE, Amir Mattar. A Bayesian algorithm with second order autoregressive errors for B-WIM weight estimation. **Engineering Structures**, v. 250, p. 113353, 2022. ISSN 0141-0296.

HE, Wei; LIANG, Xiaodong; DENG, Lu; KONG, Xuan; XIE, Hong. Axle Configuration and Weight Sensing for Moving Vehicles on Bridges Based on the Clustering and Gradient Method. **Remote Sensing**, v. 13, n. 17, p. 3477, 2021. ISSN 2072-4292.

HE, Wei; LING, Tianyang; O'BRIEN, Eugene J.; DENG, Lu. Virtual Axle Method for Bridge Weigh-in-Motion Systems Requiring No Axle Detector. **Journal of Bridge Engineering**, v. 24, n. 9, p. 04019086, 2019.

HEITNER, Barbara; SCHOEFS, Franck; O'BRIEN, Eugene J.; ŽNIDARIČ, Aleš; YALAMAS, Thierry. Using the unit influence line of a bridge to track changes in its condition. **Journal of Civil Structural Health Monitoring**, v. 10, n. 4, p. 667–678, 2020.

HELMI, Karim; TAYLOR, Todd; ANSARI, Farhad. Shear force–based method and application for real-time monitoring of moving vehicle weights on bridges. **Journal of Intelligent Material Systems and Structures**, v. 26, n. 5, p. 505–516, 2015.

IENG, Sio-Song. Bridge Influence Line Estimation for Bridge Weigh-in-Motion System. **Journal of Computing in Civil Engineering**, v. 29, n. 1, p. 06014006, 2015.

ISO 8606:1995. **Mechanical Vibration-Road Surface Profiles-Reporting of Measured Data**. [S.l.], 1995.

JACOB, Bernard; O'BRIEN, Eugene J.; JEHAES, Sophie. **Weigh-in-motion of road vehicles: final report of the COST 323 action**. Paris, 2002.

JAMES, Gareth; WITTEN, Daniela; HASTIE, Trevor; TIBSHIRANI, Robert. **An introduction to statistical learning**. [S.l.]: Springer, New York, NY, 2013.

JUNGES, Paulo. **Análise de fadiga em pontes curtas de concreto armado a partir de dados de sistemas B-WIM**. 2017. Ph.D. Thesis – Universidade Federal de Santa Catarina, Florianópolis, Brazil (in Portuguese).

KHAN, Mohammad Shihabuddin; CAPRANI, Colin; GHOSH, Siddhartha; GHOSH, Jayadipta. Value of strain-based structural health monitoring as decision support for heavy load access to bridges. **Structure and Infrastructure Engineering**, Taylor & Francis, v. 18, n. 4, p. 521–536, 2022.

KWAG, Shinyoung; JU, Bu Seog. Application of a Bayesian hierarchical model to system identification of structural parameters. **Engineering with Computers**, v. 36, n. 2, p. 455–474, 2020.

LANSDELL, Andrew; SONG, Wei; DIXON, Brandon. Development and testing of a bridge weigh-in-motion method considering nonconstant vehicle speed. **Engineering Structures**, Elsevier, v. 152, p. 709–726, 2017. ISSN 0141-0296.

LIMA E OLIVEIRA, Caroline Buratto de; GRECO, Marcelo; BITTENCOURT, Túlio N. Analysis of the Brazilian Federal Bridge Inventory. **Revista IBRACON de Estruturas e Materiais [online]**, v. 12, n. 1, p. 1–13, 2019.

LYDON, Myra; TAYLOR, Su E.; ROBINSON, D.; MUFTI, Aftab; O'BRIEN, Eugene J. Recent developments in bridge weigh in motion (B-WIM). **Journal of Civil Structural Health Monitoring**, Springer, v. 6, n. 1, p. 69–81, 2016.

MA, Yafei; WANG, Lei; ZHANG, Jianren; XIANG, Yibing; LIU, Yongming. Bridge Remaining Strength Prediction Integrated with Bayesian Network and In Situ Load Testing. **Journal of Bridge Engineering**, v. 19, n. 10, p. 04014037, 2014.

MANDIĆ IVANKOVIĆ, Ana; SKOKANDIĆ, Dominik; ŽNIDARIČ, Aleš; KRESLIN, Maja. Bridge performance indicators based on traffic load monitoring. **Structure and Infrastructure Engineering**, Taylor & Francis, v. 15, n. 7, p. 899–911, 2019.

MOSES, Fred. Weigh-in-Motion System Using Instrumented Bridges. **Transportation Engineering Journal of ASCE**, v. 105, n. 3, p. 233–249, 1979.

MÚČKA, Peter. Simulated Road Profiles According to ISO 8608 in Vibration Analysis. **Journal of Testing and Evaluation**, ASTM International, v. 46, n. 1, p. 405–418, 2017.

O'BRIEN, Eugene J.; BROWNJOHN, J. M. W.; HESTER, D.; HUSEYNOV, F.; CASERO, M. Identifying damage on a bridge using rotation-based Bridge Weigh-In-Motion. **Journal of Civil Structural Health Monitoring**, v. 11, n. 1, p. 175–188, 2021.

O'BRIEN, Eugene J.; QUILLIGAN, Michael J.; KAROUMI, Raid. Calculating an influence line from direct measurements. **Proceedings of the Institution of Civil Engineers - Bridge Engineering**, v. 159, n. 1, p. 31–34, 2006.

O'BRIEN, Eugene J.; ROWLEY, Cillian W.; GONZÁLEZ, Arturo; GREEN, Mark F. A regularised solution to the bridge weigh-in-motion equations. **International Journal of Heavy Vehicle Systems**, v. 16, n. 3, p. 310–327, 2009.

O'BRIEN, Eugene J.; ZHANG, Longwei; ZHAO, Hua; HAJIALIZADEH, Donya. Probabilistic bridge weigh-in-motion. **Canadian Journal of Civil Engineering**, v. 45, n. 8, p. 667–675, 2018.

OKASHA, Nader M.; FRANGOPOL, Dan M.; ORCESI, André D. Automated finite element updating using strain data for the lifetime reliability assessment of bridges. **Reliability Engineering & System Safety**, v. 99, p. 139–150, 2012. ISSN 0951-8320.

PRESS, S. James. **Subjective and Objective Bayesian Statistics: Principles, Models, and Applications**. Second. [S.l.]: John Wiley & Sons, 2002. ISBN 978-0-471-34843-6.

QUILLIGAN, Michael. **Bridge Weigh-in-Motion Development of a 2-D Multi-Vehicle Algorithm**. 2003. Licentiate Thesis – KTH Royal Institute of Technology, Stockholm, Sweden.

ROWLEY, Cillian; GONZÁLEZ, Arturo; O'BRIEN, Eugene J.; ŽNIDARIČ, Aleš. Comparison of conventional and regularized bridge weigh-in-motion algorithms. In: PROCEEDINGS of the international conference on heavy vehicles. [S.l.: s.n.], 2008. P. 221–230.

SCHLUNE, Hendrik; PLOS, Mario; GYLLTOFT, Kent. Improved bridge evaluation through finite element model updating using static and dynamic measurements. **Engineering Structures**, v. 31, n. 7, p. 1477–1485, 2009. ISSN 0141-0296.

SEDEHI, Omid; PAPADIMITRIOU, Costas; KATAFYGIOTIS, Lambros S. Data-driven uncertainty quantification and propagation in structural dynamics through a hierarchical Bayesian framework. **Probabilistic Engineering Mechanics**, v. 60, p. 103047, 2020. ISSN 0266-8920.

SEDEHI, Omid; PAPADIMITRIOU, Costas; KATAFYGIOTIS, Lambros S. Probabilistic hierarchical Bayesian framework for time-domain model updating and robust predictions. **Mechanical Systems and Signal Processing**, v. 123, p. 648–673, 2019. ISSN 0888-3270.

SIMOEN, Ellen; DE ROECK, Guido; LOMBAERT, Geert. Dealing with uncertainty in model updating for damage assessment: A review. **Mechanical Systems and Signal Processing**, v. 56-57, p. 123–149, 2015. ISSN 0888-3270.

SONG, Mingming; MOAVENI, Babak; PAPADIMITRIOU, Costas; STAVRIDIS, Andreas. Accounting for amplitude of excitation in model updating through a hierarchical Bayesian approach: Application to a two-story reinforced concrete building. **Mechanical Systems and Signal Processing**, v. 123, p. 68–83, 2019. ISSN 0888-3270.

YOSHIDA, Ikumasa; SEKIYA, Hidehiko; MUSTAFA, Samim. Bayesian Bridge Weigh-in-Motion and Uncertainty Estimation. **ASCE-ASME Journal of Risk and Uncertainty in Engineering Systems, Part A: Civil Engineering**, v. 7, n. 1, p. 04021001, 2021.

YU, Yang; CAI, C. S.; DENG, Lu. State-of-the-art review on bridge weigh-in-motion technology. **Advances in Structural Engineering**, SAGE Publications, v. 19, n. 9, p. 1514–1530, 2016.

YU, Yang; CAI, C.S.; DENG, Lu. Nothing-on-road bridge weigh-in-motion considering the transverse position of the vehicle. **Structure and Infrastructure Engineering**, Taylor & Francis, v. 14, n. 8, p. 1108–1122, 2018.

ŽNIDARIČ, Aleš; KALIN, Jan. Using bridge weigh-in-motion systems to monitor single-span bridge influence lines. **Journal of Civil Structural Health Monitoring**, v. 10, n. 5, p. 743–756, 2020.

Table 5 – Stiffness of each axle

Vehicle ID	Axle stiffness (kN/m^2)								
	Axle 1	Axle 2	Axle 3	Axle 4	Axle 5	Axle 6	Axle 7	Axle 8	Axle 9
1	400	1,000	-	-	-	-	-	-	-
2	400	1,000	1,000	-	-	-	-	-	-
3	400	1,000	750	750	-	-	-	-	-
4	400	1,000	1,000	750	750	-	-	-	-
5	400	1,000	1,000	750	750	750	-	-	-
6	400	1,000	1,000	750	750	750	750	-	-
7	400	1,000	1,000	750	750	750	750	750	-
8	400	1,000	1,000	750	750	750	750	750	750

Table 6 – Mass of each axle

Vehicle ID	Axle mass (kg)								
	Axle 1	Axle 2	Axle 3	Axle 4	Axle 5	Axle 6	Axle 7	Axle 8	Axle 9
1	6,000	10,000	-	-	-	-	-	-	-
2	6,000	8,500	8,500	-	-	-	-	-	-
3	6,000	10,000	8,500	8,500	-	-	-	-	-
4	6,000	8,500	8,500	10,000	10,000	-	-	-	-
5	6,000	8,500	8,500	10,000	10,000	10,000	-	-	-
6	6,000	8,500	8,500	8,500	8,500	8,500	8,500	-	-
7	6,000	8,500	8,500	8,500	8,500	8,500	8,500	10,000	-
8	6,000	8,500	8,500	8,500	8,500	8,500	8,500	8,500	8,500

.1 VEHICLE INFORMATION

All simulated signals are referred to the strains at the bottom of the bridge girder, at its mid-span. The damping coefficient for all vibration modes is defined as 0.05 and the mass per unity length of the beam is set to 10,000 kg/m. The simulations were carried out following a procedure analogous to that described by Carraro et al. (2019), considering a total of 15 vibration modes. To simplify the simulations, and without loss of generality, the cross section employed is such that the values of moment of inertia and section modulus are equal.

The vehicles are simulated as a sequence of moving sprung masses. The properties regarding the stiffness, mass, and position of each axle, respectively, of the simulated vehicles are given in Table 5, Table 6 and Table 7. For all simulations and axles, the damping is fixed at 10,000 Ns/m.

Table 7 – Longitudinal position of each axle

Vehicle ID	Axle position (m)								
	Axle 1	Axle 2	Axle 3	Axle 4	Axle 5	Axle 6	Axle 7	Axle 8	Axle 9
1	0	4.25	-	-	-	-	-	-	-
2	0	3.7	5.5	-	-	-	-	-	-
3	0	3.7	7.4	9.2	-	-	-	-	-
4	0	3.7	5.5	9.2	12.9	-	-	-	-
5	0	3.7	5.5	9.2	12.9	16.6	-	-	-
6	0	3.7	5.5	9.2	11	14.7	16.5	-	-
7	0	3.7	5.5	9.2	11	14.7	16.5	20.2	-
8	0	3.7	5.5	9.2	11	12.8	16.5	18.3	20.1

6 CONCLUDING REMARKS

The objective of the present thesis was to contribute to the development of more efficient B-WIM systems. For reaching this goal, both the improvement in accuracy of B-WIM weight estimates and the assessment of structural bridge properties by means of calibration data were addressed. The approaches adopted for providing better weight predictions were formulated after analyzing Carraro et al. (2019), who presented a big picture of the most promising issues in this regard. The present work addressed directly two of them: the consideration of dynamic response into B-WIM predictions (chapter 3) and the application of prior information for guiding the weight estimation (chapter 4). Regarding the assessment of bridge structural properties, this work presented a method that employs the data collected during the calibration of B-WIM systems to reach this goal (chapter 5). As each method was independently developed, it was opted to show conclusions individually for each of them. Moreover, despite the relevant contributions presented to the improvement of B-WIM system applications in general, there are some issues that should be addressed to expand the proposed approaches and proceed with the continuous evolution of B-WIM systems technology. Hence, some suggestions that are seen as the most promising ones are remarked when drawing conclusions for each method (for more comments, detailed suggestions related to each approach were drawn at the end of each chapter).

6.1 A B-WIM ALGORITHM CONSIDERING THE MODELING OF THE BRIDGE DYNAMIC RESPONSE

A B-WIM algorithm that includes a simplified dynamic model for the vehicle-bridge system was presented in Gonçalves, Carraro, and Lopez (2021a) (chapter 3). It is based on the work of Ning-Bo Wang et al. (2017), whose goal was to extract the static component of the bridge influence line from a single calibration run. In the present work, this method was extended for accounting to multiple calibration runs by the utilization of the maximum likelihood approach (IENG, 2015). In addition, the dynamic response of the structure was utilized to generate a parametric influence line that is a function of the vehicle speed and the equations needed to perform the weight prediction were derived. As a result, continuous functions are utilized as influence lines, which better reflects its expected behavior (ŽNIDARIČ; KALIN; KRESLIN, 2018). Moreover, as already discussed in the present study and also noticed in other works (O'BRIEN; GONZÁLEZ; DOWLING, 2010), the bridge response relies on the vehicle speed and introducing it as a parameter for creating the influence line seems a suitable option. In addition, just a small set of parameters is fitted by the calibration of the model. It avoids adjusting all the ordinates of the influence line, which likely introduces patterns that are due to the specific characteristics of calibration vehicles instead of reflecting the bridge behavior. Due to all discussed points, it was expected that the proposed approach provides better estimates for vehicles of the usual traffic flow (i.e., a higher generalization capacity).

Three distinct implementations were evaluated, according to the assumptions stated for the calculation of the model parameters: Standard (static approximation + fluctuation part, analogous to Ning-Bo Wang et al. (2017)), Analytical (quasi-static + fluctuation) and Static (static approximation alone). The numerical simulations included bridge lengths ranging from 10 to 30 m, different road profiles and test vehicles distinct from the calibration ones. The predictions of both Analytical and Static methods were able to overcome the mean absolute error reported by all the other evaluated methods (matrix method (O'BRIEN; QUILLIGAN, M. J.; KAROUMI, 2006), pBWIM (O'BRIEN et al., 2018) with the implementation proposed by Gonçalves, Carraro, and Lopez (2021b), maximum likelihood (IENG, 2015) and regularized approach (O'BRIEN et al., 2009)). The main difference occurs for the 30 m bridges, in which the Analytical method shows a remarkable performance. It is worth to notice that such results occurred even considering that bridge dynamic properties were not precisely known previously, indicating that the proposed approach is also robust. Another interesting aspect to observe is that the Analytical method removed a large amount of bias present in the mean absolute error due to the vehicle speed (i.e, estimates presented for distinct vehicles are scattered around a mean absolute error close to zero for the Analytical method, which is not achieved for other methods). This is a direct result of the inclusion of the vehicle speed as a model parameter, which allows that a same vehicle induces different structural responses according to its speed. The results for both Static and Analytical methods indicated that they reached their objectives, mainly for longer bridges. Although the results of the Analytical method presented robustness, such a method will not perform properly if no estimates for bridge properties are available at all. In this case, one could employ just the Static method which should still present better results for unseen vehicles.

In what follows some suggestions for future works in this matter are drawn. The first issue that seems interesting to be addressed is the validation of the method with experimental data. It was not performed yet since the dataset available was related to a bridge with characteristics that does not follow model assumptions. This point remarks other major contribution that should be performed: to extend the formulation to account for bridges with other boundary conditions than single-span simply supported ones, also allowing the possibility of analyzing continuous bridges.

6.2 A BAYESIAN ALGORITHM WITH SECOND ORDER AUTOREGRESSIVE ERRORS FOR B-WIM WEIGHT ESTIMATION

A common problem for B-WIM estimates is related to the lower accuracy for individual axle estimates when compared with GVW predictions (HE et al., 2019; O'BRIEN et al., 2018; RICHARDSON et al., 2014; O'BRIEN et al., 2009). In order to address this issue, a Bayesian strategy was proposed in Gonçalves et al. (2022) (chapter 4) to account to prior information regarding the expected values of axle weights in practice. As a consequence, it also intends to overcome spurious estimates that often arise in classical B-WIM methods (e.g., negative

estimates for closely spaced axle weights). The most common approach when utilizing Bayesian strategies is to assume that errors between theoretical and measured responses are independent, such as in the work of Yoshida, Sekiya, and Mustafa (2021). An important problematic issue detected during the derivation of the proposed procedure, however, was related to the presence of high serial correlation among residuals. It has an undesired impact into Bayesian predictions, since the importance of the likelihood is artificially increased, reducing the effect of the prior distribution. Then, in contrast to the usual strategy, in the present method the independence assumption was avoided by the utilization of a second order autoregressive (AR(2)) process for modeling the aforementioned error.

The suitability of the proposed approach was assessed by evaluating both simulated signals and an example of real B-WIM calibration data, analyzing also out-of-sample predictions (i.e., distinct vehicles for calibrating and testing the system). The results were compared to the least square solution and the regularized approach with near optimal parameters. The latter approach can be seen as an example of excellent performance, however the strategy to select the regularization parameter is not reproducible in practice. Then, its results are just for comparison purposes. In addition, four variants of the proposed strategy are tested, aiming to check the influence of both prior distribution and model for the error term into results. Finally, as the prior definition is somewhat subjective, sensitivity analyses are also performed by evaluating results for distinct combinations of prior parameters. The results indicated that the proposed approach was able to avoid spurious estimates such as negative axle weights, as intended. Furthermore, the accuracy reached outperformed those ones obtained by the other analyzed algorithms, even considering scenarios that do not fit the prior beliefs (e.g., axle weights clearly above the prior mean). The results are even better when considering the single axle predictions, which achieved an accuracy level similar to GVW predictions. Furthermore, the statements regarding the importance of modeling correlated errors were confirmed. The Bayesian estimates without the utilization of the AR(2) model were highly similar to the least squares solution, almost disregarding the prior distribution information. Then, the proposed prior distribution, based on the practical values for axle weights, needs to be utilized together with the AR(2) model to effectively improve results. The sensitivity analyses confirmed the robustness of the proposed approach to the definition of the prior distribution. It is an already expected result since the range of prior parameters that cover axle weights for usual vehicles is not so wide. It is, indeed, the higher practical advantage of the proposed method. The prior distribution has a clear correspondence with quantities that are usual for who operates a B-WIM system, which allows reliable guesses for the definition of such a distribution.

The strategy presented in chapter 4 was able to provide excellent point estimates for the axle weights. However, one could make use of the full posterior probability distribution of such quantities. It would allow many further analyses, such as the probability of overweight for a given vehicle axle, which would be useful for practical purposes. In addition, the same Bayesian ideas utilized for weight estimation would be utilized for calculating the bridge influence line.

It may allow a better understanding of the confidence in the calculated curve by means of confidence bounds. Furthermore, such uncertainties may be propagated for further probabilistic analyses.

6.3 MODEL UPDATING USING HIERARCHICAL BAYESIAN STRATEGY EMPLOYING B-WIM CALIBRATION DATA

The motivation for the third topic of the present work was the lack of information noticed for Brazilian bridges (LIMA E OLIVEIRA; GRECO; BITTENCOURT, 2019). Even some basic data, such as their exact age, may not be precisely known. Without reliable information, it is difficult to assess the real bridge safety, which ultimately may be converted into risk for bridge users. Then, instead of utilizing the dataset generated during the calibration of a B-WIM system for calculating the bridge influence line as usual, the approach proposed in Gonçalves, Lopez, and Valente (2022) (chapter 5) aims to utilize this information to improve the knowledge regarding bridge structural parameters. In this regard, it is important to notice that the dataset likely presents an inherent variability, i.e., the value of the QoI may change from one calibration event to another. This is due to the own nature of calibration events, which are not completely isolated experiments and, hence, no one has total control over all parameters that may affect the results (e.g., environmental conditions). In order to address this inherent variability, the proposed approach utilized a hierarchical Bayesian framework. Such strategies were previously applied for several structural systems (BEHMANESH; MOAVENI, 2016; KWAG; JU, 2020; SONG, M. et al., 2019), indicating that it is a promising technique for the present application.

The proposed method was also evaluated utilizing simulated signals, including simple examples to illustrate the advantages of the hierarchical strategy, and an example of real B-WIM calibration data. The estimates for simulated signals were close to the known true values for all the analyzed parameters. In particular, the method was able to properly estimate the uncertainties related to the QoI (i.e., the product between elastic modulus and section modulus of the bridge girders), which was the main goal of employing a hierarchical strategy. It is worth to remark that such results were confirmed utilizing a number of vehicle runs compatible with practical B-WIM calibrations and considering individually the data generated by each vehicle. The latter statement is important since just few vehicles are usually employed in calibration and it is important that results are not excessively dependent of specific properties of such vehicles. When evaluating the real calibration data example, results are also interesting. In this case, the differences between estimates from distinct vehicles are higher than for simulated signals, however results still are consistent. As real datasets are more complex, it was an already expected behavior. Furthermore, the uncertainty propagation analyses were able to properly predict the response for both vehicles. All analyses indicated that such an approach is promising and able to provide useful information, mainly in the context of lack of basic information. Despite the simplified model utilized, this work provides an initial framework to

help in the development of models that allow a better assessment of the safety of the structure.

The approach proposed in chapter 5 is a proof of concept. It showed that the data generated in calibration of B-WIM systems may be employed to estimate bridge structural properties, including uncertainty quantification. However, it is noticed that the model utilized is somewhat simplified. Although the limited information scenario for Brazilian bridges suggests that such added information is already useful, more complex models can be developed and provide more complete analyses. For instance, one could account for the transverse distribution of loads together with the consideration of distinct properties for each girder. Other example is the application of the same ideas to perform further analyses for structural safety assessment (e.g., prediction of stiffness degradation due to reinforcement corrosion as in the work of Ma et al. (2014) or the own calculation of influence line coefficients). In addition, a covariance matrix that relaxes the hypothesis of independence among error terms could be employed as in Gonçalves et al. (2022). Some corrective constant may also be applied to model the heteroscedasticity among datasets from distinct vehicles, following an approach analogous to Mingming Song et al. (2019).

6.4 FINAL REMARKS

The present work remarks the practical importance of B-WIM systems, indicating also a possible path to deal with the lack of information for Brazilian bridges. After a final discussion related to the proposed approaches, it is possible to affirm that the objective of this thesis was achieved. It has provided relevant contributions for the improvement of B-WIM system applications in general, being a piece in the continuous evolution of B-WIM systems technology.

REFERENCES

BARONE, Giorgio; FRANGOPOL, Dan M. Reliability, risk and lifetime distributions as performance indicators for life-cycle maintenance of deteriorating structures. **Reliability Engineering & System Safety**, v. 123, p. 21–37, 2014. ISSN 0951-8320.

BEHMANESH, Iman; MOAVENI, Babak. Accounting for environmental variability, modeling errors, and parameter estimation uncertainties in structural identification. **Journal of Sound and Vibration**, v. 374, p. 92–110, 2016. ISSN 0022-460X.

BLOWER, Daniel; WOODROOFFE, John. **Survey of the status of truck safety: Brazil, China, Australia, and the United States**. Ann Arbor, Michigan, 2012.

CANTERO, Daniel; GONZÁLEZ, Arturo. Bridge Damage Detection Using Weigh-in-Motion Technology. **Journal of Bridge Engineering**, v. 20, n. 5, p. 04014078, 2015.

CANTERO, Daniel; KAROUMI, Raid; GONZÁLEZ, Arturo. The Virtual Axle concept for detection of localised damage using Bridge Weigh-in-Motion data. **Engineering Structures**, v. 89, p. 26–36, 2015. ISSN 0141-0296.

CARRARO, Felipe; GONÇALVES, Matheus Silva; LOPEZ, Rafael Holdorf; MIGUEL, Leandro Fleck Fadel; VALENTE, Amir Mattar. Weight estimation on static B-WIM algorithms: A comparative study. **Engineering Structures**, v. 198, p. 109463, 2019. ISSN 0141-0296.

CESTEL. **SiWIM Bridge Weigh-in-Motion System**. [S.l.: s.n.], 2017. https://www.cestel.eu/.

CNT / SEST SENAT. **Pesquisa CNT de rodovias 2018 - Relatório gerencial**. Brasília, 2018.

DENG, Lu; WANG, Wei; YU, Yang. State-of-the-Art Review on the Causes and Mechanisms of Bridge Collapse. **Journal of Performance of Constructed Facilities**, v. 30, n. 2, p. 04015005, 2016.

FRANGOPOL, Dan M.; LIU, Min. Maintenance and management of civil infrastructure based on condition, safety, optimization, and life-cycle cost. **Structure and Infrastructure Engineering**, Taylor & Francis, v. 3, n. 1, p. 29–41, 2007.

FRØSETH, Gunnstein T.; RØNNQUIST, Anders; CANTERO, Daniel; ØISETH, Ole. Influence line extraction by deconvolution in the frequency domain. **Computers & Structures**, v. 189, p. 21–30, 2017. ISSN 0045-7949.

GONÇALVES, Matheus Silva; CARRARO, Felipe; LOPEZ, Rafael Holdorf. A B-WIM algorithm considering the modeling of the bridge dynamic response. **Engineering Structures**, v. 228, p. 111533, 2021. ISSN 0141-0296.

GONÇALVES, Matheus Silva; CARRARO, Felipe; LOPEZ, Rafael Holdorf. A gradient based optimization procedure for finding axle weights in probabilistic bridge weigh-in-motion method. **Canadian Journal of Civil Engineering**, v. 48, n. 5, p. 570–574, 2021.

GONÇALVES, Matheus Silva; LOPEZ, Rafael Holdorf; OROSKI, Elder; VALENTE, Amir Mattar. A Bayesian algorithm with second order autoregressive errors for B-WIM weight estimation. **Engineering Structures**, v. 250, p. 113353, 2022. ISSN 0141-0296.

GONÇALVES, Matheus Silva; LOPEZ, Rafael Holdorf; VALENTE, Amir Mattar. Model Updating Using Hierarchical Bayesian Strategy Employing B-WIM Calibration Data. **Journal of Bridge Engineering**, v. 27, n. 5, p. 04022023, 2022.

HE, Wei; LING, Tianyang; O'BRIEN, Eugene J.; DENG, Lu. Virtual Axle Method for Bridge Weigh-in-Motion Systems Requiring No Axle Detector. **Journal of Bridge Engineering**, v. 24, n. 9, p. 04019086, 2019.

HEINEN, Sabrina Kalise. **Efeito da distribuição transversal das cargas na obtenção de linhas de influência reais usando um sistema de pesagem em movimento em pontes**. 2016. Master Thesis – Universidade Federal de Santa Catarina, Florianópolis, Brazil (in Portuguese).

HELMI, Karim; TAYLOR, Todd; ANSARI, Farhad. Shear force–based method and application for real-time monitoring of moving vehicle weights on bridges. **Journal of Intelligent Material Systems and Structures**, v. 26, n. 5, p. 505–516, 2015.

IBGE, Instituto Brasileiro de Geografia e Estatística. **Frota de veículos**. [S.l.: s.n.], 2020. `https://cidades.ibge.gov.br/brasil/pesquisa/22/28120?indicador=28123&` `tipo=grafico`. Accessed: 2022-03-29.

IENG, Sio-Song. Bridge Influence Line Estimation for Bridge Weigh-in-Motion System. **Journal of Computing in Civil Engineering**, v. 29, n. 1, p. 06014006, 2015.

JACOB, Bernard; FEYPELL-DE LA BEAUMELLE, Véronique. Improving truck safety: Potential of weigh-in-motion technology. **IATSS Research**, v. 34, n. 1, p. 9–15, 2010. ISSN 0386-1112.

JACOB, Bernard; O'BRIEN, Eugene J.; JEHAES, Sophie. **Weigh-in-motion of road vehicles: final report of the COST 323 action**. Paris, 2002.

JUNGES, Paulo. **Análise de fadiga em pontes curtas de concreto armado a partir de dados de sistemas B-WIM**. 2017. Ph.D. Thesis – Universidade Federal de Santa Catarina, Florianópolis, Brazil (in Portuguese).

KWAG, Shinyoung; JU, Bu Seog. Application of a Bayesian hierarchical model to system identification of structural parameters. **Engineering with Computers**, v. 36, n. 2, p. 455–474, 2020.

LANSDELL, Andrew; SONG, Wei; DIXON, Brandon. Development and testing of a bridge weigh-in-motion method considering nonconstant vehicle speed. **Engineering Structures**, Elsevier, v. 152, p. 709–726, 2017. ISSN 0141-0296.

LANTSOGHT, Eva O. L.; VAN DER VEEN, Cor; DE BOER, Ane; HORDIJK, Dick A. State-of-the-art on load testing of concrete bridges. **Engineering Structures**, v. 150, p. 231–241, 2017. ISSN 0141-0296.

LIMA E OLIVEIRA, Caroline Buratto de; GRECO, Marcelo; BITTENCOURT, Túlio N. Analysis of the Brazilian Federal Bridge Inventory. **Revista IBRACON de Estruturas e Materiais [online]**, v. 12, n. 1, p. 1–13, 2019.

LYDON, Myra; TAYLOR, Su E.; ROBINSON, D.; MUFTI, Aftab; O'BRIEN, Eugene J. Recent developments in bridge weigh in motion (B-WIM). **Journal of Civil Structural Health Monitoring**, Springer, v. 6, n. 1, p. 69–81, 2016.

MA, Yafei; WANG, Lei; ZHANG, Jianren; XIANG, Yibing; LIU, Yongming. Bridge Remaining Strength Prediction Integrated with Bayesian Network and In Situ Load Testing. **Journal of Bridge Engineering**, v. 19, n. 10, p. 04014037, 2014.

MANDIĆ IVANKOVIĆ, Ana; SKOKANDIĆ, Dominik; ŽNIDARIČ, Aleš; KRESLIN, Maja. Bridge performance indicators based on traffic load monitoring. **Structure and Infrastructure Engineering**, Taylor & Francis, v. 15, n. 7, p. 899–911, 2019.

MOSES, Fred. Weigh-in-Motion System Using Instrumented Bridges. **Transportation Engineering Journal of ASCE**, v. 105, n. 3, p. 233–249, 1979.

O'BRIEN, Eugene J.; BROWNJOHN, J. M. W.; HESTER, D.; HUSEYNOV, F.; CASERO, M. Identifying damage on a bridge using rotation-based Bridge Weigh-In-Motion. **Journal of Civil Structural Health Monitoring**, v. 11, n. 1, p. 175–188, 2021.

O'BRIEN, Eugene J.; QUILLIGAN, Michael J.; KAROUMI, Raid. Calculating an influence line from direct measurements. **Proceedings of the Institution of Civil Engineers - Bridge Engineering**, v. 159, n. 1, p. 31–34, 2006.

O'BRIEN, Eugene J.; ROWLEY, Cillian W.; GONZÁLEZ, Arturo; GREEN, Mark F. A regularised solution to the bridge weigh-in-motion equations. **International Journal of Heavy Vehicle Systems**, v. 16, n. 3, p. 310–327, 2009.

O'BRIEN, Eugene J.; ZHANG, Longwei; ZHAO, Hua; HAJIALIZADEH, Donya. Probabilistic bridge weigh-in-motion. **Canadian Journal of Civil Engineering**, v. 45, n. 8, p. 667–675, 2018.

O'BRIEN, Eugene J.; GONZÁLEZ, Arturo; DOWLING, Jason. A filtered measured influence line approach to bridge weigh-in-motion. In: THE Fifth International IABMAS Conference: Bridge Maintenance, Safety Management and Life-Cycle Optimization. Philadelphia, USA: Taylor & Francis (Routledge), 2010.

OLASZEK, Piotr; ŁAGODA, Marek; CASAS, Joan Ramon. Diagnostic load testing and assessment of existing bridges: examples of application. **Structure and Infrastructure Engineering**, Taylor & Francis, v. 10, n. 6, p. 834–842, 2014.

OTTO, G. G.; FRANCESCHI, L.; DELLAROZA, L. F. G; TANI, V. Z.; VALENTE, A. M. Impacts of the Lack of Weight Enforcement on Maintenance Costs of the Brazilian Roadway Network. In: 8TH International Conference in Weigh-in-Motion. Prague, Czech Republic: International Society for Weigh-In-Motion (ISWIM) & Institut Français des Sciences et Technologies des Transports, de l'Aménagement et des Réseaux (IFSTTAR), 2019. P. 265–273.

QUILLIGAN, Michael. **Bridge Weigh-in-Motion Development of a 2-D Multi-Vehicle Algorithm**. 2003. Licentiate Thesis – KTH Royal Institute of Technology, Stockholm, Sweden.

RICHARDSON, Jim; JONES, Steven; BROWN, Alan; O'BRIEN, Eugene J.; HAJIALIZADEH, Donya. On the use of bridge weigh-in-motion for overweight truck enforcement. **International Journal of Heavy Vehicle Systems**, Inderscience, v. 21, n. 2, p. 83–104, 2014.

ROWLEY, Cillian; GONZÁLEZ, Arturo; O'BRIEN, Eugene J.; ŽNIDARIČ, Aleš. Comparison of conventional and regularized bridge weigh-in-motion algorithms. In: PROCEEDINGS of the international conference on heavy vehicles. [S.l.: s.n.], 2008. P. 221–230.

SCHLUNE, Hendrik; PLOS, Mario; GYLLTOFT, Kent. Improved bridge evaluation through finite element model updating using static and dynamic measurements. **Engineering Structures**, v. 31, n. 7, p. 1477–1485, 2009. ISSN 0141-0296.

SEDEHI, Omid; PAPADIMITRIOU, Costas; KATAFYGIOTIS, Lambros S. Probabilistic hierarchical Bayesian framework for time-domain model updating and robust predictions. **Mechanical Systems and Signal Processing**, v. 123, p. 648–673, 2019. ISSN 0888-3270.

SIMOEN, Ellen; DE ROECK, Guido; LOMBAERT, Geert. Dealing with uncertainty in model updating for damage assessment: A review. **Mechanical Systems and Signal Processing**, v. 56-57, p. 123–149, 2015. ISSN 0888-3270.

SONG, Mingming; MOAVENI, Babak; PAPADIMITRIOU, Costas; STAVRIDIS, Andreas. Accounting for amplitude of excitation in model updating through a hierarchical Bayesian approach: Application to a two-story reinforced concrete building. **Mechanical Systems and Signal Processing**, v. 123, p. 68–83, 2019. ISSN 0888-3270.

WANG, Ning-Bo; HE, Li-Xiang; REN, Wei-Xin; HUANG, Tian-Li. Extraction of influence line through a fitting method from bridge dynamic response induced by a passing vehicle. **Engineering Structures**, Elsevier, v. 151, p. 648–664, 2017. ISSN 0141-0296.

XU, Fu You; ZHANG, Ming Jie; WANG, Lei; ZHANG, Jian Ren. Recent Highway Bridge Collapses in China: Review and Discussion. **Journal of Performance of Constructed Facilities**, v. 30, n. 5, p. 04016030, 2016.

YOSHIDA, Ikumasa; SEKIYA, Hidehiko; MUSTAFA, Samim. Bayesian Bridge Weigh-in-Motion and Uncertainty Estimation. **ASCE-ASME Journal of Risk and Uncertainty in Engineering Systems, Part A: Civil Engineering**, v. 7, n. 1, p. 04021001, 2021.

YU, Yang; CAI, C.S.; DENG, Lu. Nothing-on-road bridge weigh-in-motion considering the transverse position of the vehicle. **Structure and Infrastructure Engineering**, Taylor & Francis, v. 14, n. 8, p. 1108–1122, 2018.

ZHAO, Hua; UDDIN, Nasim; O'BRIEN, Eugene J.; SHAO, Xudong; ZHU, Ping. Identification of Vehicular Axle Weights with a Bridge Weigh-in-Motion System Considering Transverse Distribution of Wheel Loads. **Journal of Bridge Engineering**, v. 19, n. 3, p. 04013008, 2014.

ZHAO, Zhisong; UDDIN, Nasim; O'BRIEN, Eugene J. Bridge Weigh-in-Motion Algorithms Based on the Field Calibrated Simulation Model. **Journal of Infrastructure Systems**, v. 23, n. 1, p. 04016021, 2017.

ŽNIDARIČ, Aleš; KALIN, Jan. Using bridge weigh-in-motion systems to monitor single-span bridge influence lines. **Journal of Civil Structural Health Monitoring**, v. 10, n. 5, p. 743–756, 2020.

ŽNIDARIČ, Aleš; KALIN, Jan; KRESLIN, Maja. Improved accuracy and robustness of bridge weigh-in-motion systems. **Structure and Infrastructure Engineering**, Taylor & Francis, v. 14, n. 4, p. 412–424, 2018.